Northern Gulf of Mexico

Chemosynthetic Ecosystems Study

Final Report

Volume II: Technical Report

Northern Gulf of Mexico

Chemosynthetic Ecosystems Study

Final Report

Volume II: Technical Report

Editors

Ian R. MacDonald
William W. Schroeder
and
James M. Brooks

DISCLAIMER

This report was prepared under contract between the Minerals Management Service (MMS) and Geochemical and Environmental Research Group. This report has been technically reviewed by the MMS and approved for publication. Approval does not signify that the contents necessarily reflect the views and policies of the Service, nor does mention of trade names or commercial products constitute endorsement or recommendation for use. It is, however, exempt from review and compliance with MMS editorial standards.

REPORT AVAILABILITY

Extra copies of the report may be obtained from the Public Information Unit (Mail Stop 5034) at the following address:

CITATION

Suggested citation:

COVER PHOTOGRAPH

The foreground photograph shows the submersible *Johnson Sea-Link I* preparing for one of its many dives to study chemosynthetic ecosystems. The map depicts the locations of known chemosynthetic ecosystems in the northern Gulf of Mexico.

PREFACE

The Chemosynthetic Ecosystems Study concerns the prominent biological communities of tube worms, mussels, and clams that occur at natural hydrocarbon seeps on the continental slope and that derive their food supply from chemicals associated with the seeps. This is the Technical Report (Volume II) of the Final Report that will be issued by the Study, which is sponsored by the U.S. Department of Interior Minerals Management Service (MMS), Gulf of Mexico Region OCS Office (Contract 14-35-0001-30555).

The Study is being conducted by ten principal investigators (PIs) and four associates under the overall management of the Geochemical and Environmental Research Group (GERG) of Texas A&M University (see next page). The Program has completed all of the three scheduled research cruises and has completed processing material collected on these cruises. The first report of the Study (MacDonald 1992) presented a review of published literature pertinent to the subject and a limited synthesis of data collected prior to commencement of the Program. An appendix volume to this report reproduced the core, peer-reviewed literature pertinent to Gulf of Mexico seep communities An interim report described the methods, techniques, and equipment used during the field program, outlined the data sets and collections obtained during the field study, and discussed the analyses and interpretations employed to treat these materials. This report comprises some of the introductory material from the two previous reports in order to provide unfamiliar readers with a context for Study findings. In keeping with MMS guidelines, these chapters are addressed to an audience of knowledgeable lay-people. To enhance readability, extended listings of materials and methods will be given in an appendix volume or by citation to previous reports or publications.

Principal Investigators (*) and Associates for the Chemosynthetic Ecosystems Study. Affiliation abbreviations are:

TAMU *Texas A&M University*
GERG *Geochemical and Environmental Research Group;*
TAMU
OCNG *Oceanography Department, Texas A&M University*
LSU *Louisiana State University*
PSU *Pennsylvania State University*
WHOI *Woods Hole Oceanographic Institution*
UA/DISL *University of Alabama, Dauphin Island Sea Lab*

Principal Investigator	Affiliation	Major Responsibility
Javier Alcala-Herrera	TAMU/GERG	Chemical Analyses
James M. Brooks*	TAMU/GERG	Project Director
Robert S. Carney*	LSU	Ecology
Charles R. Fisher*	PSU	Physiology
Norman L. Guinasso, Jr.*	TAMU/GERG	Data Analysis
Holgar W. Jannasch*	WHOI	Microbiology
Mahlon C. Kennicutt II*	TAMU/GERG	Geochemistry
Ian R. MacDonald*	TAMU/GERG	Ecology/Deputy Project Director
Eric N. Powell*	TAMU/OCNG	Taphonomy
William S. Sager*	TAMU/OCNG	Geology
William W. Schroeder*	UA/DISL	Geology/Ecology
Dan L. Wilkinson	TAMU/GERG	Field Logistics
Carl O. Wirsen	WHOI	Microbiology
Gary A. Wolff	TAMU/GERG	Data Management

TABLE OF CONTENTS

LIST OF FIGURES

LIST OF TABLES

1.0 Chemosynthetic Ecosystems Study: Overview

The chemosynthetic communities associated with hydrocarbon seeps on the Louisiana/Texas continental slope are one of a series of functionally and taxonomically related assemblages in the deep-sea. For the purposes of this report, we define a chemosynthetic community as *a persistent, largely sessile assemblage of marine organisms that depend upon the chemoautotrophic productivity of bacteria.* These communities are characteristically associated with sources of hydrogen sulfide and/or methane in an oxygenated environment. The underlying geological processes supplying these reduced compounds vary from site to site.

1.1 Chemosynthetic Communities in the Gulf of Mexico

The first discovery of chemosynthetic communities was made at hydrothermal vents in the eastern Pacific Ocean (Corliss et al. 1979). The principal components of these communities are tube worms, clams, and mytilids that derive their entire food supply from symbiotic bacteria, which were in turn supported by chemical components in the venting fluids and by the physiological mediations of their host organisms (Cavanaugh et al. 1981; Childress and Mickel 1985). This series of discoveries contributed to what became a fundamental reordering of theories regarding life in the deep sea (Tunnicliffe 1992). In 1984, a large quantity of bivalves and tube worms was recovered in a series of trawls that were pulled through oil and gas seeps on the northern Gulf of Mexico continental slope. It soon transpired that these then unfamiliar animals were close relatives of a fauna found in so-called "chemosynthetic communities" that had only recently been discovered at hydrothermal vents in the eastern Pacific Ocean (Kennicutt et al. 1985).

Previously, the general concept of the continental slope of the Gulf of Mexico, held that the sea floor comprised a vast extent of soft sediment, sparsely populated

by diverse, but tiny burrowing animals and an assortment of depth-adapted fishes and crustaceans. Occurrence of species that were taxonomically and functionally similar to vent fauna on a passive continental margin meant that the distribution of chemosynthetic fauna was much more wide-spread. Dependence on hydrocarbon seepage also placed the communities in the one deep-sea benthic zone that is certain to be subject to possible impact from human activities. Addressing these concerns, Minerals Management Service (MMS) issued guidelines designed to protect the biological communities at oil seeps from possible harm due to disturbance associated with the energy industry (MMS 1988). Simultaneously, a review by MMS of information needed for prudent management of the seep communities concluded that additional study was required. Several critical questions were identified, including the following:

1.   What are the specific geological, chemical, and ecological processes whereby seeping hydrocarbons support distinct communities?

2.   How do these communities persist, and to what degree do physical-chemical and biological factors interact on different spatial and temporal scales?

3.   How quickly and to what degree will chemosynthetic communities recover from mechanical damage?

4.   How rare or common are dense chemosynthetic communities across the Gulf of Mexico?

5.   How much biomass do these communities comprise on the continental slope and what is the contribution to slope ecosystems?

To evaluate possible impacts, it is important to determine how these communities persist in the natural environment and the extent to which they will be

resilient in the face of petroleum-related activities. In this regard, our overall goal is to determine to what extent the Gulf of Mexico deep water petroleum seeps fit into two possible categories: a robust or fragile community.

Determination of the extent to which the hydrocarbon seep communities are robust or fragile entails coordinated geological, geochemical, and ecological research efforts that will develop an understanding of the spatial and temporal linkage pattern between hydrocarbon seepage and the formation of chemosynthetic community development on the seafloor. These investigations must determine how communities are established and persist within the particular geological and geochemical environments that support them. As stated above, the key to understanding potential impacts lies in understanding how the processes of geology, geochemistry, and biology interact.

1.2   Summary of Study Accomplishments

The Study was initiated on 26 July 1991. The Principal Investigators (PIs) made substantial resources available to the Study at no cost to MMS. These resources included a large and diverse amount of data gathered during previous investigations of chemosynthetic ecosystems in the Gulf of Mexico. Additionally, the North Carolina National Oceanographic and Atmospheric Administration (NOAA) National Undersea Research Center had granted the PIs a series of submarine dives with the *Johnson Sea-Link* during 1991 and 1992. Consequently, the PIs were able to offer MMS a research program that was more extensive and which commenced field activities more expeditiously than anticipated in the Request for Proposal (RFP).

The first submarine cruise (JSL-91) on this project utilized the *Johnson Sea-Link I*, deployed from the support ship R/V *Seward Johnson* during 25, 26, and 31 August and 14-27 September 1991. The cruise occupied locations of known chemosynthetic communities in water depths of 500 to 750 m (Figure 2.1).

Collectively, these sites were judged by the PIs to represent the faunal and environmental diversity of the chemosynthetic communities on the mid- to upper continental slope. A base-line set of water column, sediment, carbonate, and tissue samples from chemosynthetic and heterotrophic fauna were collected at each site. Additionally, extensive photographic and video documentation was obtained, particularly from stations delineated with durable sea-floor markers and floats. At selected sites, collections of tube worms, mussels, or clams were measured, marked, and returned alive to their habitats to determine *in situ* growth rates for the species. Samples of *Beggiatoa* mats were collected for shipboard experiments and laboratory assay. Several deployments of two time-lapse camera systems were carried out to determine short and long-term activity patterns within clusters of tube worms and mussels. Various markers, shell collections, and cages were also deployed for retrieval during subsequent cruises.

The second submarine cruise (JSL-92) on this project utilized the *Johnson Sea-Link I,* deployed from the support ship R/V *Seward Johnson* during the period 3-31 August 1992. This cruise occupied the same sites as JSL-91 and successfully resampled many of the stations established previously. The long-term experiments were retrieved with uniform success, although there were some failures in performance. New techniques utilized during JSL-92 included an *in situ* pore-water sampling device and a small-diameter push-core array that made it possible to collect up to 15 sediment and bacteria samples from a 1 m^2 grid.

A limited cruise was recently completed using the R/V *Gyre* during 4-9 November 1992 (Gyre-92). This cruise collected sediment cores with a piston-corer specially designed for collecting intact shell samples from the surface strata ($\leq$ 3 m subbottom). Two of the sites occupied during JSL-91 and JSL-92 were successfully cored. A third non-study site was also cored and subbottom profile data were collected at two sites.

The first report was submitted in final form on 30 November 1992. For this report, each of the PIs wrote an independent overview of both the published literature in his topic area and of his unpublished results which are sufficiently advanced to release. In addition, a collection of the core literature pertinent to the Gulf of Mexico communities was assembled and reproduced in an appendix to this report. This collection included the discovery papers, review articles, and a series of papers entitled "Gulf of Mexico Hydrocarbon Seep Communities: I through VII," which has been dispersed among a variety of journals.

The Interim Report was submitted in final form on June 29, 1993. It described the methods, techniques, and equipment used during the field program. It also outlined the data sets and analyses used by the principal investigators (PIs).

The major findings of the individual PIs were presented to the public during the MMS Information Transfer Meeting held in New Orleans, Louisiana on 15 December 1993. This report closely follows the format of those presentations.

2.0 The Regional Distribution of Chemosynthetic Communities Across the Continental Slope in the Northern Gulf of Mexico
Ian R. MacDonald

2.1   Introduction

Hydrocarbon seepage is one of the major natural processes that shape the geological and geochemical characteristics of the Gulf of Mexico. Evidence for extensive natural hydrocarbon seepage in this region comes from historical records of floating and beached oil that predate modern offshore production and transport (Geyer and Giammona 1980), and from extensive collections of oil-stained marine sediments (Kennicutt et al. 1988b). Hydrocarbons migrate upward along faults from reservoirs situated at subbottom depths of 2000 m or greater (Kennicutt et al. 1988a; Cook and D'Onfro 1991); oil and gas escape the sediment column in discrete regions known as seeps (MacDonald et al. 1989; MacDonald et al. 1990b); within seeps, there are often highly localized vents where very active release of gas and oil takes place; finally, the released oil floats to the sea surface where it forms slicks that drift with wind and current until dispersed by evaporation, dissolution, and bacterial consumption (MacDonald et al. 1993). This overall sequence produces significant effects at length scales in the range of a few centimeters to a few kilometers.

Appropriate management of human activities that might affect the chemosynthetic communities that are supported by hydrocarbon seepage must refer to reliable estimates of the abundance and distribution of the communities. Collectively, the historical data indicate substantial seepage across most of continental slope in the Gulf of Mexico; but they do not give a repeatable measure of the distribution of seepage nor of the biological communities associated with seepage. The small size and extreme inaccessibility of seep communities makes it difficult to determine where they occur without direct observation. During the

course of the Study, satellite and airborne remote sensing were successfully employed as means for detecting seepage on a regional basis (MacDonald et al. 1993, in press). A newly developed optical sensor, the laser line scan system, was also evaluated in a demonstration deployment. Brief description of these results will be presented.

Subsequent chapters in this report will describe geological, geochemical, and ecological effects of hydrocarbon seepage based on detailed observations and collections at representative seep sites made during this Study. This section will place these sites in their regional context by documenting the geographic range, frequency and possible magnitude of seepage.

2.2   Types of Seep Communities

Four general community types were described by MacDonald et al. (1990b). Respectively, these were communities dominated by vestimentiferan tube worms (*Lamellibrachia* c.f. *barhami* and *Escarpia* n.sp.), mytilids (Seep Mytilid Ia, Ib, and III), epibenthic vesicomyid clams (*Vesicomya cordata* and *Calyptogena ponderosa*), or infaunal lucinid or thyasirid clams (*Lucinoma* sp. and *Thyasira* sp.). These faunal groups display distinctive characteristics in terms of how they aggregate, the size of the aggregations, the geological and chemical properties of the habitats in which they occur, and to some degree, the heterotrophic fauna that occur with them.

Tube worms form dense clusters that range in size from small tangles 20 cm in diameter to continuous bush-like stands tens of meters across. Tube worms are most often found in association with oil-laden sediment, which often contain up to 10% extractable oil by weight (MacDonald et al. 1989). The oil contributes directly or indirectly to high local concentrations of sulfide.

Mytilids generally occur in single- or double-layer beds that range in size from less than 0.5 m2 to 500 m2 (MacDonald et al. 1990a; 1990b). The beds are

restricted to the localized areas where methane and oxygen are simultaneously available. Oxygen is present in the ambient seawater, methane from either direct evolution of gas bubbles or dissolved in brine (MacDonald et al. 1989). Mytilid beds often define the distinct boundaries of this availability.

Living clams are either infaunal, in the case of the lucinaceans, or epibenthic, in the case of the vesicomyids. The latter often form distinctive furrow-like tracks as they plow through the surface sediment in search of sulfide (Fisher 1990). Areas which living vesicomyids occupy more or less continuously may be 100 to 150 m in width (Rosman et al. 1987). The dead shells of both groups, however, tend to accumulate on the surface sediment, sometimes producing shell "pavements" that cover more extensive areas (Callender et al. 1990). The shells of the two groups are often difficult to distinguish from each other visually and dead vesicomyids often occur in life position. Visual observations of shell beds may therefore indicate a community of living vesicomyids or an infaunal community of lucinaceans.

2.3 Zonal Distribution of Chemosynthetic Communities in the Northern Gulf of Mexico

2.3.1 Local Patterns

The best evidence for long-term seepage is presence of chemosynthetic fauna at specific sites. Figure 2.1 shows the locations where the major chemosynthetic fauna have been collected or unambiguously observed. Table 2.1 lists the groups of chemosynthetic fauna found, nominal locations, depths, collection method and the citation. Occurrence of a chemoautotrophic community can indicate a range of environmental conditions; in all cases, however, this fauna is an indicator of hydrocarbon seepage (Brooks et al. 1987; Kennicutt et al. 1988a). Reliability of information on the areal extent, density, and continuity of the individual communities shown in Figure 2.1 is uneven. Clearly, trawl samples will not provide

Table 2.1 Sites where chemosynthetic metazoans have been collected by trawl (Trl) or submarine (Sub), or definitively photographed by submarine, remotely operated vehicle (ROV), or photosled (Photosl). Fauna indicates the type of chemosynthetic fauna found: V=vestimentiferan tube worms, M=Seep Mytilids, C=vesicomyid or lucinid clams, PG=pogonophoran tube worms; codes in bold face followed by asterisk (e.g., 1* VM) are Sampling Sites for the present study. Lease block designators follow MMS standard abbreviations. Data sources give precedence to observations published in the open literature.

Fauna	Latitude (North)	Longitude (West)	MMS Lease Block	Depth (m)	Obs method	Data source
VM	26°21.20'	94°29.80'	AC0645	2200	Sub	1
M	27°23.50'	94°29.45'	EB0602	1111	Trl	2
PG	27°27.55'	93°08.60'	GB0500	734	Trl	2
VC	27°30.05'	93°02.01'	GB0458	757	Trl	2
M	27°31.50'	92°10.50'	GB0476	750	Sub	3
MC	27°33.40'	92°32.40'	GB0424	570	Sub	3
V	27°35.00'	92°30.00'	GB0425	600	Sub	3
VC	27°34.50'	92°55.95'	GB0416	580	Sub	3
VC	27°36.00'	94°46.00'	EB0376	776	Sub	3
PG	27°36.15'	94°35.40'	EB0380	793	Trl	2
MC	27°36.50'	92°28.94'	GB0382	570	Sub	3
VC	27°36.60'	94°47.35'	EB0375	773	Trl	2
VC	27°36.82'	92°15.25'	GB0386	585	Sub, Trl	2, 3
VC	27°37.15'	92°14.40'	GB0387	781	Sub, Trl	2, 3
V	27°37.75'	91°49.15'	GC0310	780	Trl	2
VC	27°38.00'	92°17.50'	GB0342	425	Trl	2
C	27°39.15'	94°24.30'	EB0339	780	Trl	2
VC	27°39.60'	90°48.90'	GC0287	994	Sub, Trl	2
C	27°40.45'	90°29.10'	GC0293	1042	Trl	2
VC	27°40.50'	92°18.00'	GB0297	589	Trl	2
VMC	27°40.88'	91°32.10'	GC0272	720	Sub, Trl	2, 3, 4
VC	27°42.65'	92°10.45'	GB0300	719	Trl	2
V	27°43.10'	91°30.15'	GC0229	825	Trl	2
VM	27°43.30'	91°16.30'	GC0233	650	Sub	5
VMC	27°43.70'	91°17.55'	GC0233	813	Trl	2
VM	27°44.08'	91°15.27'	GC0234	600	Sub	3, 6
VM	27°44.30'	91°19.10'	GC0232	807	Sub	3
VM	27°44.80'	91°13.30'	GC0234	550	Sub	3, 7
VC	27°45.00'	90°16.31'	GC0210	715	Sub	3
C	27°45.50'	89°58.30'	GC0216	963	Sub, Photosl	8, 2
VMC	27°46.33'	90°15.00'	GC0210	796	Sub	3
VM	27°46.65'	91°30.35'	GC0184/5	580	Sub, Trl	2, 3, 9
VM	27°46.75'	90°14.70'	GC0166	767	Sub, Trl	2, 3
VM	27°49.16'	91°31.95'	GC0140	290	Sub	10
V	27°50.00'	90°19.00'	GC0121	767	Sub	3
VM	27°53.56'	90°07.07'	GC0081	682	Photosl	11
VC	27°54.40'	90°11.90'	GC0079	685	Trl	2
VM	27°55.50'	90°27.50'	GC0030	504	Sub	3
VPG	27°56.65'	89°58.05'	GC0040	685	Trl	2
C	27°57.10'	89°54.30'	MC0969	658	Trl	2
V	27°57.25'	89°57.50'	EW1010	597	Sub, Trl	2, 3
V	27°58.70'	90°23.40'	EW1001	430	Sub, Trl	2, 3
VC	29°11.00'	88°00.00'	VK0826	545	Sub, ROV, Trl	3, 4, 12

Data sources: 1–Brooks et al.. (1989), 2–Kennicutt et al. (1988a,b), 3–GERG unpubl. data, 4-Callender et al. (1990), 5–MacDonald et al. (1990b), 6–MacDonald et al. (1990b), 7–MacDonald et al. (1990a), 8–Rosman et al. (1987), 9–MacDonald et al. (1989), 10–Roberts et al. (1990), 11–Boland 1986, 12–Boss (1968), Gallaway et al. (1990), Volkes (1963).
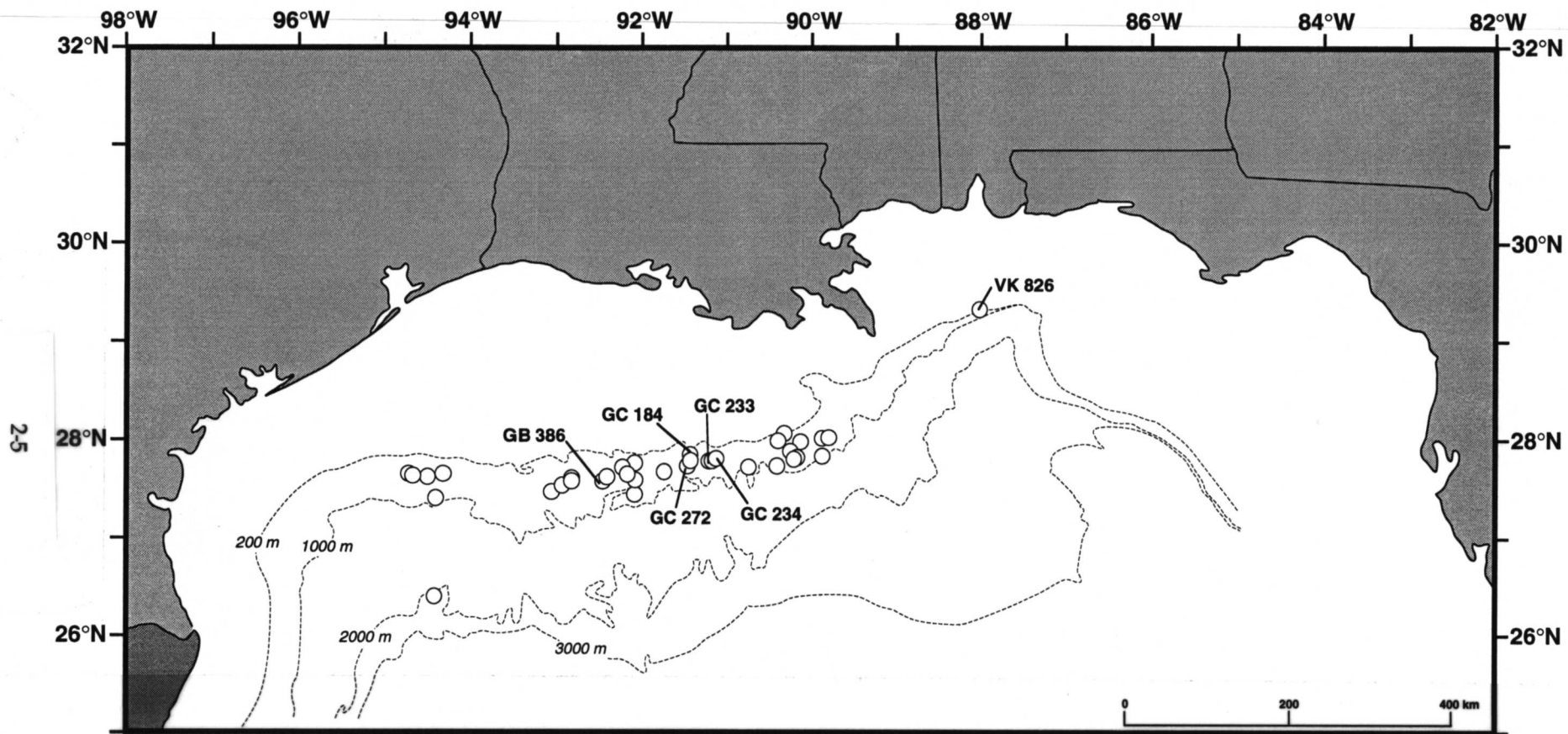
Figure 2.1   Locations where vestimentiferan tube worms, seep mytilids, or vesicomyid clams have been collected or photographed in the northern Gulf of Mexico. Observations separated by less than 1 NM have been pooled. Study sites are indicated by their MMS lease block number.

reliable data of this type; and photo surveys generally cannot provide an exhaustive mapping of individual communities. It is therefore difficult to determine what constitutes a chemosynthetic community in terms of management concerns. Does, for example, a single collection of clam shells signify a lush community? Likewise, in how much detail should offshore operators be required to search in order to certify that their operations will not impact a lush community? One approach to this issue is to examine the variable evidence for the typical length scales and geological dependency of well-documented chemosynthetic communities.

An analysis of clustering frequencies for tube worms at GC 234 found significant clustering at spatial scales of about 5, 20, and 75 m (MacDonald 1990a), which may be indicative of clustering due to formation of tube worm "bushes" at the smaller scale, and to the size and spacing of fault zones at the larger scales. A review of the occurrence of chemosynthetic fauna along the submarine track-lines tends to confirm a characteristic size of 10 to 100 m for vestimentiferan and mytilid communities and 100 to 300 m for clam communities. We therefore have support for speculation that communities separated by less than 300 m probably share a common hydrocarbon reservoir. Multi-channel seismic data from the GC 184/185 lease blocks (Cook and D'Onfro 1991) provided information on the spacing of reservoirs and migration pathways at this site. From these data, it appears that communities separated by distances of 1 km are not supported by seepage from a common reservoir.

2.3.2 Regional Patterns

Chemosynthetic fauna have been found in a 700 km-long corridor between 88°W and 95°W and between the 290 and 2200 m isobaths. Distribution is uniform; the greatest number of communities were found between 91°W and 93°W between the 500 and 700 m isobaths. These observations have been influenced by the limits

of exploration; the envelope of occurrence suggests that the potential number of communities is much larger than those found to date. There was a gap in occurrences where the Mississippi Canyon intersects the corridor. Although this area has not been exhaustively explored for communities, geochemical exploration shows a general absence of oil-stained sediments from the Canyon, which suggests that the hiatus in community occurrence may be real (GERG unpublished data).

The easternmost community, in the Viosca Knoll block 826, was found by investigations initiated by the Oryx Energy Company (Gallaway et al. 1990). Interestingly, this area was trawled in 1955 by the U.S. Fish and Wildlife Service's M/V Oregon. The resulting collections provided the holotype for the original description of Calyptogena cordata (Boss 1968) and a paratype for the original description of Acesta bullisi (Volkes 1963). The photograph of this paratype shows the unmistakable shell deformation that is caused by the commensal interaction with a vestimentiferan. The Viosca Knoll site represents early, unrecognized evidence for hydrocarbon seep communities in the northern Gulf, as well as a recent range extension.

Each chemosynthetic community supported by hydrocarbon seepage depends on a reservoir of hydrocarbon and a migration pathway or pathways through which these fluids reach the seafloor. Implicit in the distribution shown in Figure 2.1, or in a larger scale mapping of community distribution, is a determination of what spatial separation is required to consider two occurrences as distinct communities. The number of communities in a given area should be indicative of the number of hydrocarbon reservoirs, the number of migration pathways (i.e., faults), the characteristic size of the faults, and interaction of the unconsolidated sediments, hydrates, or carbonate with seepage. This determination is also important for estimating the numbers of the communities and for management concerns regarding the potential zone of impact for a seafloor activity.

2.4 Remote-Sensing Detection of Natural Oil Seepage

2.4.1 Use of Geophysical Methods for Indirect Detection of Chemosynthetic Communities

Our study suggests that geophysical techniques can be used to narrow the areas of detailed study needed to locate and classify chemosynthetic communities. Ultimately, no geophysical method will allow the reliable identification of such communities without in situ observation. However, by using known geophysical signatures and affinities, likely locations can be identified for more detailed study.

Seeps are located along faults and faults are usually identified in regional seismic exploration profiling surveys. Thus, the first step in locating chemosynthetic communities is to map the faults along which seeps could occur. The likeliest faults to harbor seeps are those that are active and thus extend to the surface and those that show a significant displacement.

Having found the faults, the next step would be to look for seep related topography and sediment disturbance. Topographic features would be mud mounds, carbonate mounds, and pock-marks. The mud mounds are typically more than 10 m in height and more than 100 m in diameter and would be evident on high-resolution bathymetry maps and side-scan sonar images. Carbonate mounds can be somewhat smaller, one to a few meters high and 10 m wide, or less. In addition, pock-marks are variable in size, from small, shallow craters a few meters across to large craters many meters deep and hundreds of meters wide.

Sediment disturbances can usually be found using acoustic profiling and imaging techniques. On side-scan sonar records, the disturbance can appear as an increase in backscatter, particularly in conjunction with small mounds. In 3.5 kHz and other echo sounder profiles, the disturbance may show up as an attenuation of signal reflections ("wipe out"), as an enhancement ("hardbottom"), or as

reverberation ("turbidity"). These are caused mostly by gas, carbonate layers or disseminated nodules, or hydrate layers. In addition, if the seepage is particularly strong and contains much gas, the gas bubbles may be detected within the water column by these acoustic methods (Anderson and Bryant 1990).

Having located areas of larger scale topographic features or sediment disturbances caused by seepage, a more detailed examination is necessary. To locate chemosynthetic communities, various ultra-high-resolution imaging methods are needed. Side-scan sonar images will show carbonate outcrops, and may even show tube worm bushes or bivalve clusters if the resolution is high enough and the organisms are dense enough. Typically, this will require a deep-towed sonar or sonar affixed to a submersible, so that the acoustic source and target are not greatly separated. However, many chemosynthetic organisms, such as bivalves, may be invisible. Underwater photography, such as with a camera sled or a laser line-scan device can provide visual sitings, as can submersible dives. Although these last are slow and painstaking techniques, presumably they can be directed, using a nested search technique employing increasingly higher resolution methods, so that the time consuming visual searches can be minimized. Likewise, new technologies, such as laser line-scanning imaging, may dramatically improve the search speed for visual survey. Another nesting procedure would combine geophysical methods with remote sensing of floating oil by use of airborne or satellite sensors.

2.4.2 Formation and Detection of Surface Oil Slicks

Oil, and other organic compounds, can be detected remotely in the ocean because they form a floating film that modifies the characteristics of the surface layer and locally increases specular reflection of radiant energy such as visible light or radar waves (Garrett 1986; Scott 1986; Stevenson et al. 1988). The phenomenon has been used to study small-scale oceanographic circulation (Cox and Munk 1954;

Soules 1970; La Violette and Arnone 1988), the effects of ship wakes (Peltzer et al. 1992), and the surface slicks formed by natural oil seepage (Estes et al. 1985). Micro-layer surfactants originate from at least two sources: petroleum oil and the biological activity of plankton and fish (Garrett 1986). Although biological surfactants are physically and chemically different from oil, and can be distinguished remotely by their wave damping properties under some circumstances (Huhnerfuss et al. 1989), confirming the source of a remotely detected micro-layer is often difficult or impossible. By comparing remote sensing images that show evident oil slicks with locations of chemosynthetic communities (Table 2.1) and surface observation of floating oil (MacDonald et al. 1993) made it possible to confirm the locations of perennial oil slicks from natural seepage.

2.4.3 Remote Sensing Methods

The remote sensing data base comprised images collected from three sensor systems on board three satellites:

1) European Radar Satellite (ERS-1, SAR image)

Orbit	Frame	Date
9518	3051	8 May 1993
9475	3051	8 May 1993
11250	3051	9 Sept. 1993

2) Landsat - (Landsat 5 , Thematic Mapper image)

Path, Row	Collection Time and Date	
22, 41	1105 CST	31 July 1991

3) Space Shuttle (Atlantis with 120 mm format photograph, hand-held)

Mission, Roll, and Frame	Collection Time and Date
STS-30, 151, 028	1535-1538 CST; 05 May 1989

The Space Shuttle photograph was scanned and digitally resampled to conform with the position of known coastal features and offshore installations. Suspected slicks in these images were outlined as closed polygons. The set of slick polygons for each image was then stored as a layer in a geographic information system (GIS) by use of MAPIX® software.

The objective of this exercise was to combine observations from the data sets described above, then to review these observations to identify probable sites for sea-floor seeps. This was accomplished in a 2-stage fashion: First, all possible image pairs were compared to determine co-locations of slick polygons. Overlapping polygons were classified according to the style of conjunction by use of the following ranking scheme:

Rank A: Overlap of the upwind ends of slicks in two or more images.

Rank B: Overlap of slick ends irrespective of wind direction.

Rank C: Ends of slicks within ≈2 km of each other.

Rank D: Overlap of any portion of slick polygons in two or more images.

Second, slick polygons were compared to locations of collections of floating, freshly surfaced oil and to locations of chemosynthetic communities. A location was considered to be a geochemical anomaly if a visibly oil-stained sediment sample was collected in the same lease block with a surface slick or community of chemosynthetic animals.

By analyzing the remote sensing and ancillary data, we found 63 locations where multiple data sets indicated presence of perennial oil slicks (Table 2.2, Figure 2.2). At six of these sites, we report collection of freshly surfaced oil from the surface at locations that coincide with a target in one of the remote sensing images. Oil-stained sediments and chemosynthetic fauna were also present in five and three

Table 2.2   Oil slicks detected in one or more remote sensing images from the northern Gulf of Mexico. Latitude and longitude are for point of overlap. Lease block designators follow standard MMS format. Depths given are mean depths for lease block. Slicks listed as having no overlap were confirmed by coincidence with sea truth collections or observation from submarine.

ID	Latitude	Longitude	Lease Block	Depth (m)	Remote Sensing Overlap	Seafloor Manifestation	Geochemical Anomaly	Floating Oil Collected
1	27°44.83' N	91°13.33' W	GC0234	831	no overlap	Chemo fauna	Oily core	Floating oil
2	27°43.71' N	91°36.57' W	GC0226	825	no overlap	-	Oily core	Floating oil
3	27°40.53' N	92°18.00' W	GB0297	589	no overlap	Chemo fauna	Oily core	Floating oil
4	27°31.55' N	92°10.58' W	GB0476	891	no overlap	Chemo fauna	-	Floating oil
5	27°21.99' N	92°23.01' W	GB0648	1058	no overlap	-	Oily core	Floating oil
6	27°13.02' N	91°03.12' W	GC0766	1523	no overlap	-	Oily core	Floating oil
7	27°57.88' N	90°43.23' W	EW0995	281	upwind ends	-	-	-
8	27°55.63' N	91°52.86' W	SM0205	184	upwind ends	-	Oily core	-
9	27°48.73' N	90°51.03' W	GC0154	715	upwind ends	-	Oily core	-
10	27°48.65' N	91°07.20' W	GC0148	551	upwind ends	-	-	-
11	27°45.04' N	91°29.48' W	GC0229	825	upwind ends	-	-	-
12	27°42.74' N	91°19.14' W	GC0232	807	upwind ends	-	Oily core	-
13	27°40.52' N	90°49.46' W	GC0287	994	upwind ends	Chemo fauna*	-	-
14	27°38.93' N	90°48.39' W	GC0331	1037	upwind ends	-	-	-
15	27°37.26' N	91°17.38' W	GC0321	881	upwind ends	-	Oily core	-
16	27°33.29' N	90°58.55' W	GC0415	1049	upwind ends	-	-	-
17	27°32.55' N	90°60.00' W	GC0415	1049	upwind ends	-	-	-
18	27°32.10' N	90°59.75' W	GC0415	1049	upwind ends	-	-	-
19	27°32.04' N	91°24.65' W	GC0451	1027	upwind ends	-	-	-
20	27°31.96' N	91°23.18' W	GC0451	1027	upwind ends	-	Oily core	-
21	27°31.41' N	91°22.31' W	GC0451	1027	upwind ends	-	-	-
22	27°27.12' N	90°55.64' W	GC0504	1181	upwind ends	-	-	-
23	27°24.89' N	91°22.67' W	GC0539	1288	upwind ends	-	-	-
24	27°24.53' N	91°21.86' W	GC0540	1307	upwind ends	-	-	-
25	27°24.12' N	91°39.70' W	GC0577	1274	upwind ends	-	-	-
26	27°23.88' N	91°21.05' W	GC0584	1375	upwind ends	-	-	-
27	27°22.70' N	91°45.02' W	GC0576	1302	upwind ends	-	-	-
28	27°22.56' N	91°10.25' W	GC0588	1502	upwind ends	-	-	Floating oil
29	27°22.32' N	91°10.45' W	GC0587	1558	upwind ends	-	-	-
30	27°21.39' N	91°03.09' W	GC0590	1404	upwind ends	-	Oily core	-
31	27°21.31' N	90°02.97' W	GC0611	1341	upwind ends	-	Oily core	-
32	27°17.97' N	91°11.95' W	GC0675	1622	upwind ends	-	-	-
33	27°14.35' N	91°36.36' W	GC0711	1412	upwind ends	-	-	-
34	27°13.98' N	90°54.12' W	GC0725	1455	upwind ends	-	-	-
35	27°13.62' N	91°01.21' W	GC0723	1421	upwind ends	-	Oily core	-
36	27°13.56' N	90°47.80' W	GC0727	1374	upwind ends	-	Oily core	-
37	27°12.41' N	91°02.04' W	GC0766	1523	upwind ends	-	Oily core	-
38	27°05.60' N	91°21.69' W	GC0892	1999	upwind ends	-	-	Floating oil
39	27°05.09' N	91°23.75' W	GC0891	2006	upwind ends	-	-	-
40	27°44.24' N	91°18.83' W	GC0232	807	ends undeter.	Oil seep obs.	Oily core	Floating oil
41	27°42.74' N	91°19.14' W	GC0232	807	ends undeter.	Chemo fauna	Oily core	-
42	27°31.35' N	91°24.25' W	GC0451	1027	ends undeter.	-	-	-
43	27°15.05' N	91°35.83' W	GC0711	1412	ends undeter.	-	-	-
44	27°13.76' N	91°02.02' W	GC0722	1414	ends undeter.	-	Oily core	Floating oil
45	27°13.57' N	90°48.89' W	GC0727	1374	ends undeter.	-	Oily core	-
46	27°48.51' N	90°51.07' W	GC0154	715	ends < 2km	-	-	-
47	27°39.64' N	91°22.03' W	GC0319	909	ends < 2km	-	-	-
48	27°24.73' N	91°18.44' W	GC0541	1374	ends < 2km	-	-	-
49	27°10.42' N	91°12.36' W	GC0807	1676	ends < 2km	-	Oily core	-
50	27°47.63' N	91°07.23' W	GC0148	551	random overlap	-	-	-
51	27°46.67' N	91°30.39' W	GC0185	718	random overlap	Oil seep obs.	Oily core	Floating oil
52	27°44.47' N	91°12.75' W	GC0235	841	random overlap	-	Oily core	-

2-12

53	27°43.62' N	91°25.19' W	GC0230	825	random overlap	-	-	-
54	27°40.93' N	91°36.46' W	GC0271	851	random overlap	-	Oily core	-
55	27°32.79' N	90°58.34' W	GC0416	1072	random overlap	-	-	-
56	27°32.60' N	91°32.57' W	GC0404	947	random overlap	-	Oily core	-
57	27°28.39' N	90°56.73' W	GC0504	1181	random overlap	-	-	-
58	27°27.09' N	90°54.70' W	GC0505	1172	random overlap	-	-	-
59	27°26.18' N	91°50.52' W	GC0530	1176	random overlap	-	-	-
60	27°22.43' N	91°21.62' W	GC0584	1375	random overlap	-	-	-
61	27°20.55' N	91°23.44' W	GC0627	1395	random overlap	-	-	-
62	27°18.90' N	91°38.93' W	GC0666	1323	random overlap	-	-	-
63	27°18.13' N	91°10.80' W	GC0675	1622	random overlap	-	-	-

cases, respectively. At 39 sites listed in Table 2.2, we make our primary determination based on overlap of the evident upwind ends of slicks in two or more of the remote sensing images . Floating oil was collected at two of these sites and oil-stained sediments were collected at an additional ten sites within this group. Among the remaining 23 locations listed in Table 2.2, four are distinguished as particularly strong candidates for perennial seeps because of positive indicators among the supporting data sets. The remaining sites fit into our scheme of overlapping targets in multiple remote sensing images, but they lack supporting evidence.

Three locations were selected for dives with the research submarine *Johnson Sea-Link* because they coincided with remotely detected oil slicks. The dives had the objective of trying to locate a chemosynthetic community or other definitive evidence for long term seepage on the sea floor below each surface target. In particular, the concern was to explore potential new sites that were in greater water depths than previously known sites. All dives were made with the research submarine *Johnson Sea-Link*, which has a maximum depth rating of 1000 m. *Johnson Sea-Link* was supported by the mother ships R/V Seward Johnson and R/V Edwin Link. Dives consisted of approximately 2 h of bottom time; during which, the submarine was first directed to the appropriate location by a surface ship, then carried out autonomous exploration based on what was visible to scientists in the submarine.
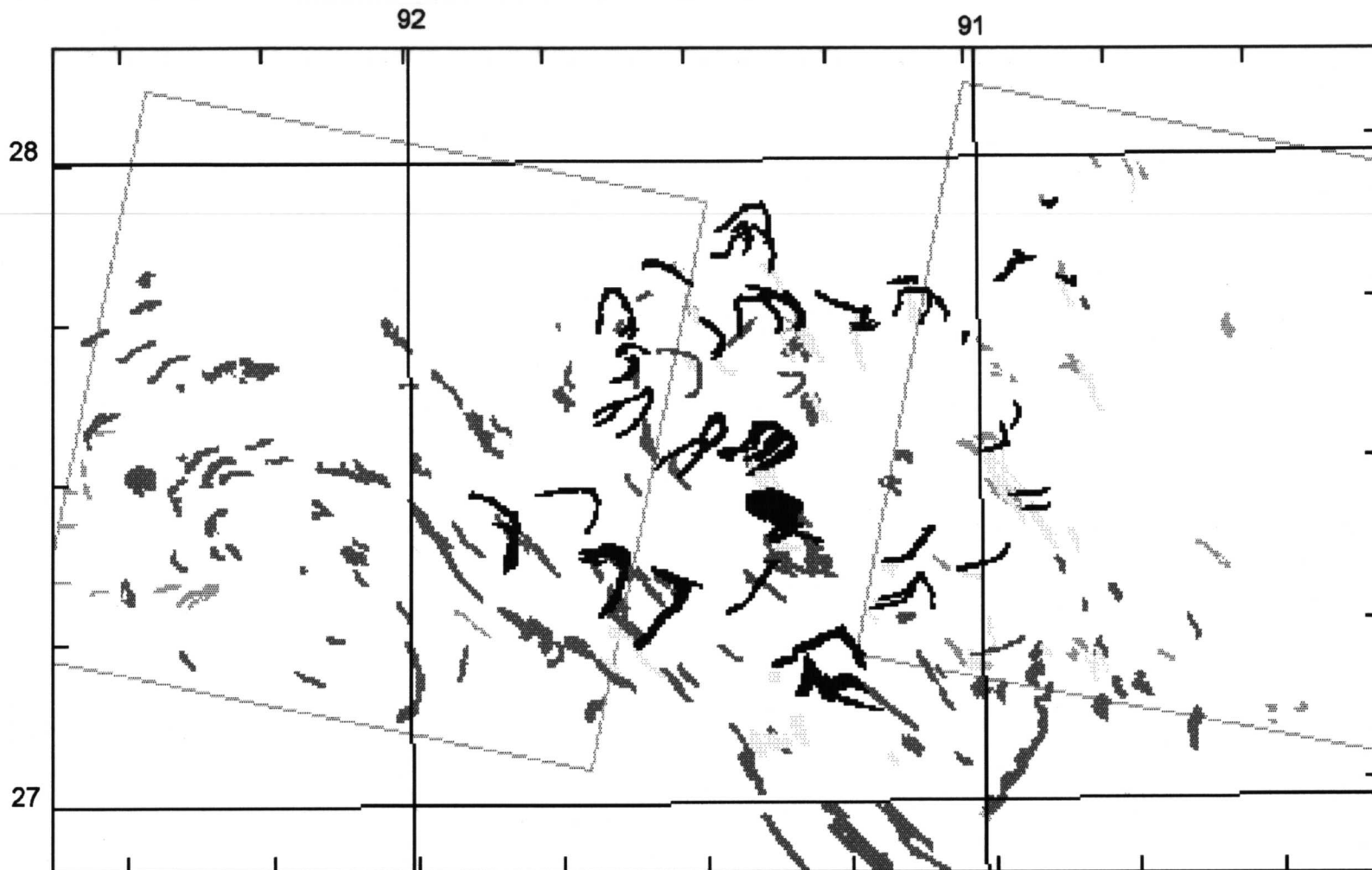
Figure 2.2   Overlap between oil slicks detected in remote sensing images from different dates reveals the locations of perennial oil seeps. (Rectangular outlines show coverage for individual remote sensing images.) ERS-1: European Radar Satellite 1, TM: Thematic Mapper, LFC: Linhoff Frame Camera.

Sites selected for dives were located in the Green Canyon 232, 287 and 321 lease blocks (Table 2.2). We were able to find chemosynthetic fauna at the first two of these sites, but not at the third. The surface slick in Green Canyon 232 was spotted from an airplane and was clearly visible to ship-board observers before it was noted in the satellite data. During two dives to depths of 700 m, we noted dense aggregations of tube worms and seep mussels similar to assemblages at the Bush Hill site (MacDonald et al., 1989). One of us (Guinasso) inadvertently caused a copious discharge of oil and gas from the sea floor by attempting to collect some of the mussels. The mussels were clustered within a field of authigenic carbonate rubble. Probing the mussel cluster with a scoop sampler disturbed the carbonate substratum and initiated a burst of gas bubbles followed by a flow of oil droplets that continued unabated for over 30 min. Arrival of the oil droplets at the surface was noted by the shipboard observers at a location about 100 m from the submarine's sea floor position.

The surface slick at Green Canyon 287 was noted in the LandSat TM and ERS-1 data sets. The site is the location is on a plateau that rises from a base depth of 1500 m to a crest depth of 760 m. A salt body has intruded to the near seafloor and salt movement has produced a series of shallow faults trending northwest-southeast normal to the salt (see Reilly et al., this volume). The *Johnson Sea-Link* bottomed at a depth of 800 m and followed a southern course across the flank of the uplift block. This track took the submarine across a series of northwest-southeast trending valleys. Clam shells, carbonate outcrops encrusted with tube worms, and occasional gas seeps were observed in the floors of these valleys. Although clam shells were broadly distributed, the abundance of chemosynthetic fauna in the communities at this site was much less than at the Green Canyon 232 site. Although gas venting was evident at several locations, macro-seepage of oil was not

observed. Extractable hydrocarbons from sediment samples at the site were heavily biodegraded (MacDonald, unpubl. data).

Surface slicks at the Green Canyon 321 site were evident in all of the remote sensing data sets. We traversed the sea floor below these slicks repeatedly during more than 6 hours of submarine exploration that covered depths from 750 to 900 m. Occasional indications of oil seepage, i.e. mats of Beggiatoa bacteria and outcrops of authigenic carbonate, were observed, but neither significant aggregations of chemosynthetic fauna nor other definitive sea floor indications of macro-seepage were observed.

2.4.4 Estimates of Total Seepage

Estimating the magnitude of seepage required to produce slicks of a given length requires knowledge of the detectable thickness of the visible oil slick, the rate at which it advects away from the point at which the oil arrives at the surface, and the rate of disappearance due to evaporation and dissolution. Direct measurement of slicks over oil seeps suggests slick thicknesses of 0.1 to 1.0 μm (Allen et al. 1970). Duckworth (personal communication 1993) dispensed a variety of crude oils on seawater and observed the coverage. Although results depended upon oil type, water cleanliness, and evaporation, generally 1 ml of oil will spread to produce a stable silver-gray film that covers 10 sq m, which corresponds to a mean thickness of 0.1 μm. The stable film degraded to an invisible film that suppressed capillary waves and enhanced reflectivity, and that occupied an area consistent with a thickness of approximately 0.01 μm. Slick thicknesses required to produce the rainbow sheen and mousse reported during the sea-truth trials probably exceeded 1 μm; however, these observations were restricted to small areas within the overall slicks, and the slicks themselves contained patches of un-oiled water. A thickness of 0.01 μm is therefore a reasonable lower limit for a detectable slick.

Oil floating on the sea degrades as a result of evaporation and dissolution. As a slick disperses from its point of origin, these effects will compound progressive thinning of the slick due to spreading until the slick is no longer detectable (Hollinger and Mennella 1973). A slick formed by an instantaneous release of oil will therefore have a set detectable life span. A persistent slick represents a continuous flux of oil to the surface (Fallah and Stark 1976). Oil coming to the surface continuously into an advective regime caused by current or wind forms a plume. An advective velocity of 20 cm sec-1 would move oil downstream from a point at about 17.2 km day-1. Plumes with lengths of the order of 5 km contain oil that has been on the surface for less than 1 day. Hollinger and Mennella (1973) noted that the oil slicks are thickest along a central axis and suggested that most of the oil in a slick is confined to a small fraction of its total area.

More about the nature of these plumes can be learned by proposing a simple dispersion model of a plume. We posit a Gaussian distribution of oil thickness in the transverse cross-section of a plume because this is consistent with previous findings and because analytical solutions to Gaussian functions are well-described. A three-dimensional Gaussian plume can be described by

$$c = \frac{q}{\sqrt{2\pi}u\sigma} \exp\left(\frac{-rx}{u} - \frac{y^2}{2\sigma^2}\right) \tag{1}$$

where c is the thickness of the oil on the surface, cm; q is the seafloor seepage rate, cm3 sec-1; u is the advection velocity, cm sec-1; x is the downwind distance, cm; r is a degradation coefficient for the oil, sec-1; y is the cross plume distance, cm; and s is the cross plume standard deviation. The standard deviation is given by assuming diffusion-like spreading so that

$$\sigma = \sqrt{2\,dx\,/u} \tag{2}$$

where x is downwind distance, cm; and d is a dispersion coefficient, cm2 sec-1. Similar models are described by Csandy (1972) to describe a plume resulting from a continuous oil spill.

The x,y points that lie on the boundary of the detectable plume satisfy the equation

$$\frac{q}{\sqrt{2\pi u}\sigma}\exp\left(\frac{-rx}{u} - \frac{y^2}{2\sigma^2}\right) - c_d = 0 \tag{3}$$

where cd is the minimum detectable thickness of oil, cm; r is the e-folding time or degradation constant (r = 0.693/(86,400T), sec-1; T is a degradation half life, days; and s is given by (2). The model requires that the size and shape of the detectable plume is dependent on the parameters q, cd, u, r, and d, which we will refer to as the parameters. Some insight can be gained into these equations by scaling them in terms of some simple dimensionless variables. A natural scale length for the problem is given by

$$L = \frac{d}{u} \tag{4}$$

Substituting the dimensionless variables Y=y/L, X=x/L, R=rd/u2, and Q=q/(dcd) into (1) gives

$$C = \frac{1}{2}\frac{Q}{\sqrt{\pi X}}\exp(-RX - \frac{Y^2}{4X}) \tag{5}$$

When Y, the dimensionless crossplume distance equals zero, then

$$C = \frac{1}{2}\frac{Q}{\sqrt{\pi X}}\exp(-RX)$$

(6)

The length of the plume is that value of X defined by (6) when $C=c/cd = 1$. Substituting $C=1$ into (6) we can solve for Q as a function of the overall length of the plume XL

$$Q = 2\sqrt{\pi}\sqrt{X_L}\exp(RX_L)$$

(7)

The shape of the plume is given by solving (5) for Y with $C=1$. This gives

$$Y = 2\sqrt{X}\sqrt{-\ln\left(\frac{2\sqrt{\pi X}}{Q\exp(-RX)}\right)}$$

(8)

We estimated the range of possible seepage rates required to produce the slicks in the two images by solving (7) for the lengths of slicks measured in the Shuttle and TM images. We used an advection rate, $u = 20$ cm s-1, which we estimate from the recorded wind speeds, and threshold thicknesses, $cd = 0.01$ and 0.1 μm, and degradation half-life, $T = 0.25$ and 1 day, which we regard as a reasonable range for these parameters. This exercise suggests that natural seepage is on the order of 4.3 x 103 to 7.8 x 104 m3 y-1 in the 8,200 sq km area imaged in the TM scene and 1.1 x 104 to 4.8 x 105 m3 y-1 in the 15,000 sq km area imaged in the 1989 Atlantis photograph.

2.4.5 Trial of the Laser Line Scan System

At present there are two means for sea-floor imaging: seismic and optical. Seismic imaging, such as side-scan sonar or active sonar, is distinctly limited in resolution. Optical imaging, such as underwater photography, has long been limited in scope because of backscatter. The Laser Line Scan System (LLSS) is a state-of-the-art optical imaging system that overcomes the back-scatter problems plaguing underwater photography. Very recent design improvements by Westinghouse Electric Corp., Underwater Laser Systems have produced a new LLSS, Model SM2000S, that reduced power requirements to under 200 watt and reduced size and weight by roughly half. This improvement makes this LLSS a potential tool for much of the research submersible fleet including ROV's and towed fish, but as yet, the submarine user community has not undertaken any detailed scientific or engineering tasks with the system. In its current configuration, the LLSS provides high-resolution pictures of the seafloor along swaths up to 40 m wide. Despite the promise of this technology, it was unclear whether it could be used to image chemosynthetic fauna in adequate detail.

A modification to the Study program was made to facilitate a trial with a laser system over Bush Hill. In this trial, the ART laser system, operated by SAIC, diverted from another mission and spent 12 hr surveying the GC 184 study site. This laser system was deployed in a towed fish by the R/V Gyre. The laser produced excellent images in shallow water, but was severely limited by tow-fish stability in deeper waters. The results over Bush Hill were, therefore, disappointing in terms of providing a detailed map of the community. The effort did produce several quite satisfactory images of tube worm clusters and bacterial mats (Figure 2.3). This demonstrates that the technique can work, provided the stability problem is solved.
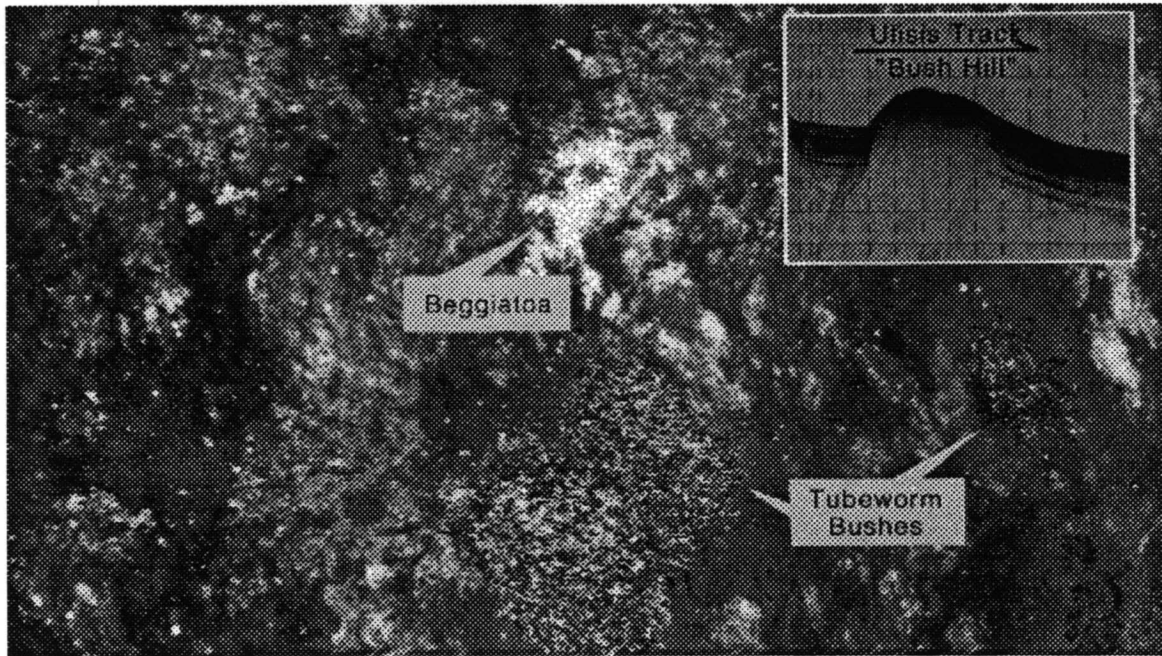
Figure 2.3   Laser line scan image collected over Bush Hill during the June 1993 trials. Note the extreme image distortion caused by the roll, pitch and yaw in the towed vehicle. During a brief intervals of relative stability, the instrument captured a very clear image of several tube worm colonies. The largest colony is probably 1 to 2 m in diameter. Note the very abundant white patches of bacterial mats.

2.5   Summary

Chemosynthetic fauna occur across most of the continental slope in the northern Gulf of Mexico. Their distribution is more homogeneous over larger geographic and depth ranges than is the case for hydrothermal vent communities. Seep communities tend to be dominated by vestimentiferans, seep mytilids, or vesicomyid and lucinid clams, but intergradations among these community types are the rule, particularly between vestimentiferans and mytilids. The MMS Chemosynthetic Ecosystems Study encompasses a series of study sites which were

selected from the known list of communities on the basis of community type and geographic location.

Methods for the remote sensing of chemosynthetic communities, many of which were developed or refined during this Study, can be applied to improve understanding of the distribution of hydrocarbon seepage. The distribution of macro oil seepage revealed by satellite remote sensing demonstrates that the conditions required for formation of hydrocarbon seep communities extend well beyond the artificial limits imposed by the exploration tools previously used. It is quite defensible to assume that hydrocarbon seep communities occur to depths of 2000 m or greater across much of the northern Gulf of Mexico slope.

3.0 Geological and Geophysical Characterization of Hydrocarbons
William W. Sager, Changshik Lee, and William W. Schroeder

3.1   Introduction

Hydrocarbon seeps have been routinely studied by the oil industry using geophysical techniques. Often the deep subsurface structure is known through multichannel seismic reflection profiles acquired to find oil. Also, in areas where drilling rigs or pipelines are to be located, the oil industry has often acquired high-resolution geophysical data for a "hazard" survey. Even the most precise of high-resolution surveys, however, has insufficient resolution to image objects on scales of a few meters because of the separation of the observer at the sea surface from the target on the seafloor. Thus, small features and biologic communities at seeps are not routinely imaged by traditional sea surface geophysical techniques.

In contrast, much of our knowledge of the biology or geochemistry of hydrocarbon seep communities comes from either dredge or trawl samples, or submersible viewing and sampling. Dredges and trawls provide spot samples, but are often difficult to relate to the seafloor in detail because they are typically dragged over the seafloor. Submersible studies provide a detailed view of the community inhabitants, relations, and small scale distribution, but are limited in scope by visibility and the slow speed at which observers can traverse the seafloor in a submersible.

What is missing in this spectrum of studies is a link from the broad scale of geophysical sounding to the ultra small scale of the submersible viewport. In this report we examine the use of a hybrid technique, geophysical data collected from a submarine, as the basis of a study of the geological and geophysical characteristics of hydrocarbon seeps in the Gulf of Mexico. These geophysical data provide a synoptic

view on the scale of hundreds of meters, but with a resolution of less than a meter and this allows us to compare viewport-scale observations with broad scale seismic data.

Our primary observations were made with two acoustic tools, a 25 kHz echo-sounder and a 77 kHz side-scan sonar. Both were used aboard the U.S. Navy nuclear submarine *NR-1* to collect profile data in grids over four hydrocarbon seeps known to be inhabited by chemosynthetic communities. We chose these particular seeps because they have been the subject of intensive interdisciplinary studies and industry geophysical data are also available for all to some degree. This situation allowed us to examine the middle scale geologic characteristics and to link the ultra small and broad scale data sets. In this report, we attempt to synthesize the geological and geophysical characteristics of each of these four sites and then extrapolate this information to the broader population of chemosynthetic community sites.

3.1.1 Study Locations

The four seep sites examined in the geological/geophysical study are all located on the Louisiana continental slope in the Green Canyon (GC) and Garden Banks (GB) lease blocks areas (Figure 3.1). From east to west, the sites are GC234, GC 184/185, GB 386/387, and GB 424/425 (for brevity, we henceforth refer to the last three sites as GC1 184, GB 386, and GB 425). GC 234 is located along a portion of a tensional fault between salt diapir ridges (Behrens 1988). The other sites are all mounds located either on the flank of a salt diapir (GC 386, GB 425) or on a fault radiating from a salt diapir (GC 184). The deepest seep site is GB 425 at 575 m, next is GB 386 at 585 m, GC 184 at 540 m, and the shallowest is GC 234 at depth of 530 m.

3.1.2 Geologic Causes and Symptoms of Hydrocarbon Seeps in the Gulf of Mexico

Hydrocarbon seeps are widely scattered throughout the ocean basins because the two main ingredients that give rise to seeps, hydrocarbon source sediments and
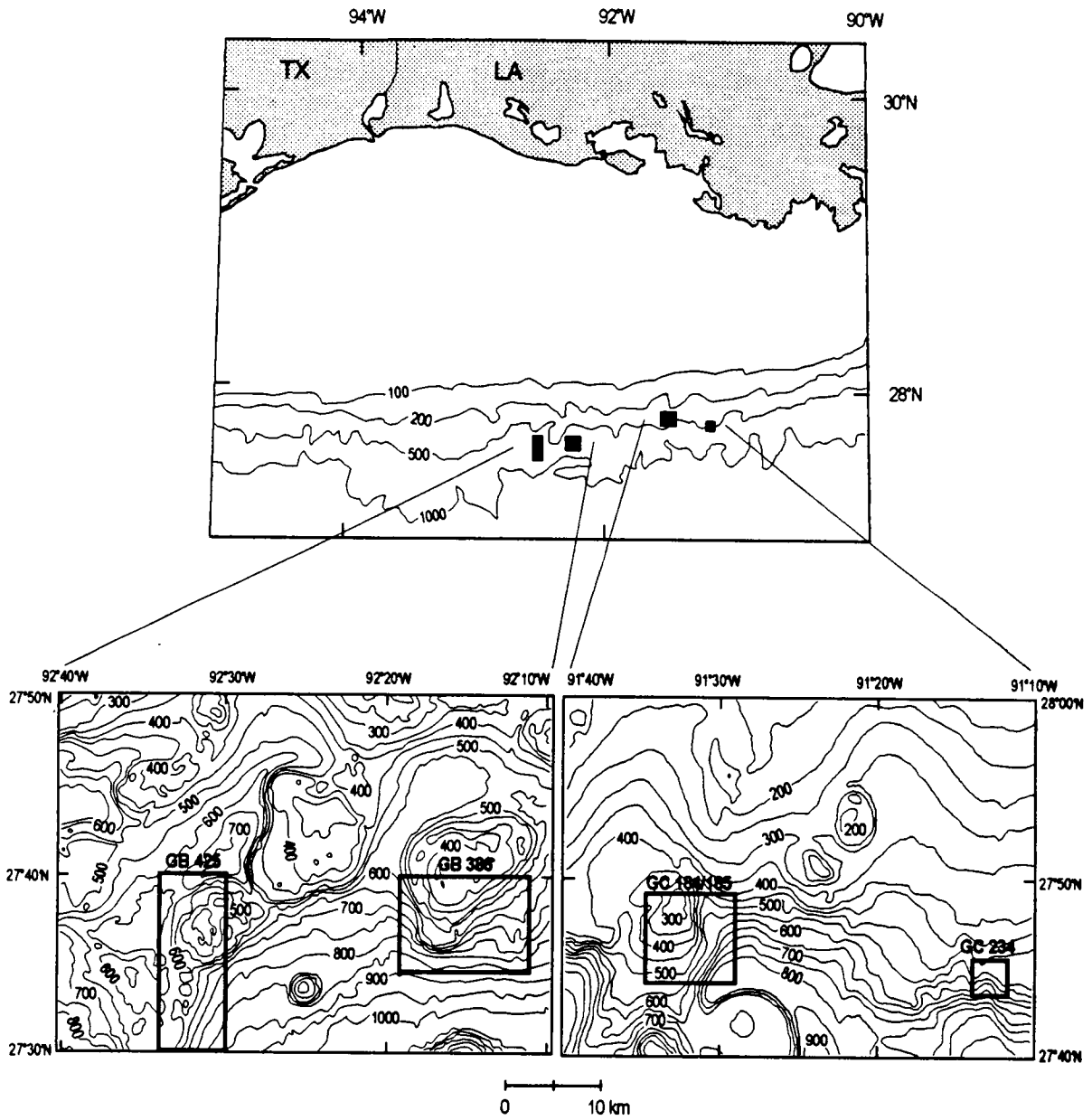
Figure 3.1   Location of study areas.

tectonic fracturing, are relatively common (Hovland and Judd 1988). In the Gulf of Mexico, the source layers are Cretaceous carbonate sediments and Cenozoic terrigenous sediments, both of which have layers containing abundant organic matter that can form hydrocarbons.

Early in its history, during the Jurassic Period, the Gulf of Mexico was a shallow, periodically desiccated basin in which an extensive evaporite layer (the Louann Salt), up to several kilometers in thickness, was deposited (Buffler et al. 1980; Worrall and Snelson 1989). Many additional kilometers of sediment, first carbonate and then terrigenous were piled atop the evaporites, as the basin margins aged and subsided (Worrall and Snelson 1989; Wu et al. 1990a). The organic material in these sediments was compressed and heated to form gas and oil. Salt is the main constituent of the evaporites. Because it is nearly incompressible, its density changes little with burial whereas the overlying sediments become denser through compaction. Moreover, under differential stress, salt deforms plastically on geologic time scales. The end result is that with continuing burial, the Louann Salt became mobile beneath the Gulf of Mexico shelf and slope during the Cenozoic Era.

The mobile salt has greatly affected the physiography of the northern Gulf of Mexico (Jackson and Seni 1983; Jackson and Galloway 1984; Jackson and Talbot 1986; Wu et al. 1990b; Simmons 1991). It has moved vertically to form diapirs and ridges, only some of which have reached the surface. It has moved laterally to form salt nappes and intraslope salt-withdrawal basins. Of greatest significance for chemosynthetic ecosystems, the movements have caused faulting, which is active today at many locations. The faults are typically tensional, listric, growth faults, often with parasitic antithetic faults (Worrall and Snelson 1989; Seni and Jackson 1992). These faults frequently tap reservoirs of hydrocarbons deep within the sediment column. Not only to they break the reservoir seal, but they also provide a conduit for upward hydrocarbon migration. Thus, hydrocarbon seeps are associated

with active salt movement and active faulting. Because the hydrocarbons cannot penetrate impermeable hemipelagic muds to any great degree, seeps are found along the faults that liberated the hydrocarbons (Roberts et al. 1990). Moreover, because it is the salt movement that causes the faults, usually seepage is on faults near salt bodies (Behrens 1988; Roberts et al. 1990; Kennicutt and Brooks 1990).

3.1.3 Geophysical Signatures of Seeps

For some time it has been realized that hydrocarbon seepage at the seafloor has effects that can be recognized by acoustic profiling and imaging methods (Hovland and Judd 1988). The effects can be generally broken into two categories: those that cause some sort of topographic feature and those which change the acoustic reflection characteristics of the sediments.

Seep-related topographic features range from depression to uplift. The latter include mounds of authigenic (i.e., formed *in situ*) carbonate (Roberts et al. 1990) or mud mounds (Hovland and Judd 1988; Neurauter and Bryant 1990). Authigenic carbonate mounds are formed by precipitation of carbonate during microbial degradation of hydrocarbons, whereas the mud mounds were probably formed by fluid mud entrained by the ascending hydrocarbons (e.g., Figure 3.2). The negative topographic features are pockmarks (small, subcircular, shallow craters) or blow-out craters, probably formed by escaping gas (Hovland and Judd 1988).

The acoustic effects of hydrocarbon seeps are several. Gas bubbles within the sediment column can attenuate the acoustic signal, preventing further penetration and causing a "wipe out" zone in which deeper layers are hidden (Behrens 1988; Anderson and Bryant 1990). This signature can also be caused by near-surface biogenic gas, so it is not necessarily a sign of deep-rooted seepage. Authigenic carbonates change the reflection characteristics of the sediments, causing a reverberation or "turbidity" owing to the scattering of sound energy by disseminated
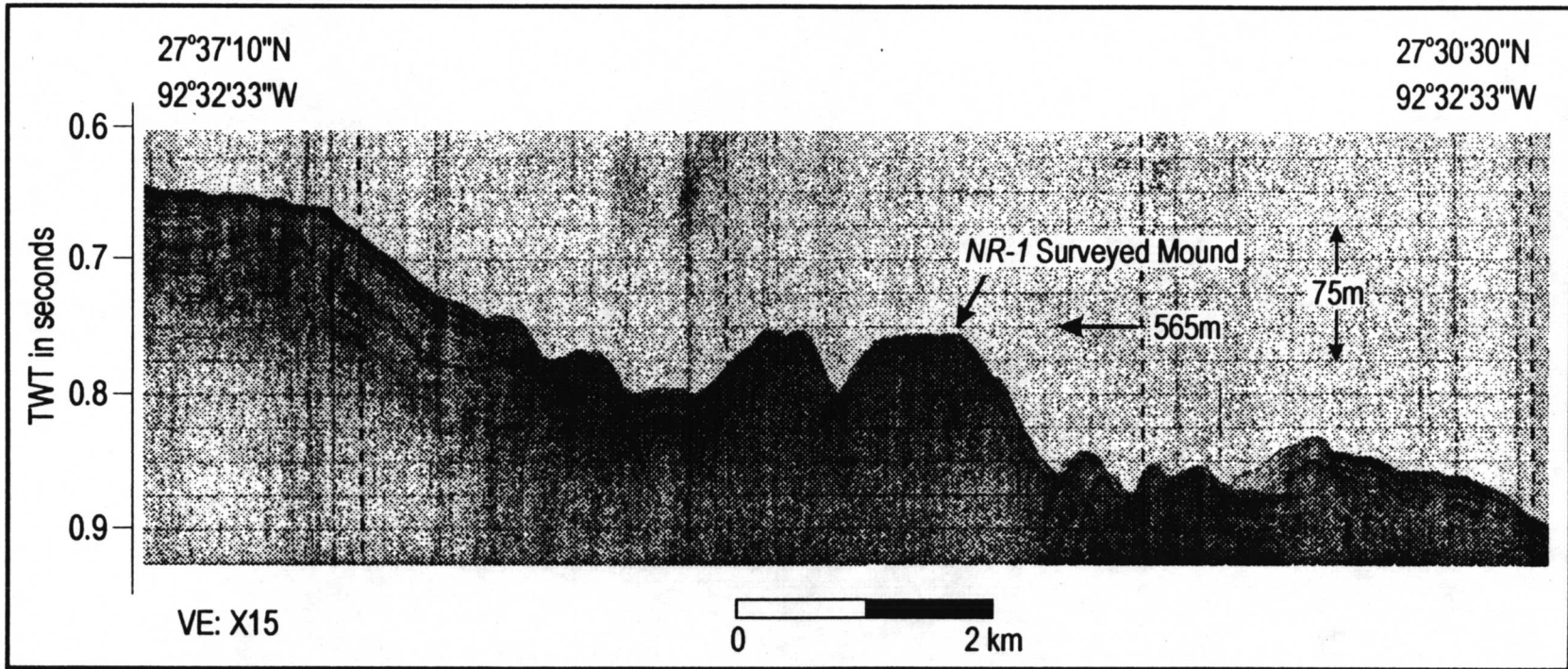
Figure 3.2   3.5 kHz echo sounder profile over the flat-topped mud mound in GB 425.

nodules (Behrens 1988). This may also be the source of strong acoustic backscattering sometimes seen around seeps using side-scan sonars. Gas hydrates within the sediment column also change the reflection characteristics. A hydrate layer may attenuate penetrating acoustic waves and it may also cause bottom simulating reflectors (BSRs) owing to the acoustic impedance contrasts at its edges Hovland and Judd 1988).

3.2   Data

As stated above, the primary data for this study were 25 kHz echo sounder profiles, 77 kHz side-scan sonar images, and bathymetry data acquired with the submersible *NR-1* during surveys in 1991-1992 (GC 184/194, GC 234, GB 386) and 1993 (GC 425). Both the echo-sounder and side-scan sonar were mounted on the lower hull of the submarine, which was sailed at an a more-or-less constant altitude of 3 to 10 meters above the seafloor, typically at a velocity of 1 to 2 knots. The echo sounder records were recorded in analog fashion on videotape and have a vertical resolution of less than 10 cm. Side-scan sonar records were also recorded in analog, on paper records 20 inches wide. The sonar swath width was set at 100 m, and the images have a resolution of about 0.5 m. Most surveys consisted of lines spaced 30 to 100 m apart, giving more than 100% overlap of the side scan images from adjacent tracks.

Although they are related, the side-scan sonar and echo sounder data show somewhat different aspects of the seafloor characteristics. The echo-sounder sends an acoustic wave to the seafloor at vertical incidence, so the received energy is proportional to the reflection coefficient of the seafloor and other interfaces (Urick 1975; Dobrin and Savit 1988). Some of the acoustic energy bounces back, but the rest penetrates into the seafloor, to be reflected by subsurface interfaces (e.g., sediment layers) or dissipated. Thus, a plot of received energy versus time gives a

picture of the interfaces at which significant acoustic impedance contrasts occur and these are interpreted as having geologic significance. Many investigators have employed the technique known as "seismic stratigraphy", using external and internal reflection characteristics as a scheme for the classification and interpretation sediment layers (Damuth 1975; Damuth and Hayes 1977). Our purpose for the echo sounder data was similar. Except at the nadir, acoustic waves from a side-scan sonar strike the seafloor obliquely, so the energy that returns to the instrument is not reflected, but is "backscattered" (Urick 1975). Backscattering depends on many factors and chief among them are topography, seafloor roughness, and sediment texture (Johnson and Helferty 1990).

Bathymetry data were also collected along submarine tracks, using a high-frequency echo sounder on the bottom of *NR-1*. Bathymetric depths were determined from the two-way travel time of acoustic waves emitted and received by the echo sounder. Because the distance from the transceiver and seafloor was small, the separation was calculated using a constant sound velocity. This distance was added to the submarine depth, determined by pressure sensor, to arrive at total depth.

Some *NR-1* cruises produced data in the form of audio and video records of objects and organisms on the seafloor. These records were of from visual observations of features seen out the small forward viewing ports on the submarine.

Positioning of the *NR-1* was accomplished by inertial navigation between acoustic fixes from the mothership at the sea surface. Although the surface ship was positioned with the military Global Positioning System (GPS) satellite navigation, there are unknown errors in the acoustic ranging position of the submarine at fix locations. Furthermore, currents or inaccurate drift corrections can lead to significant horizontal positioning errors between fixes, depending on the frequency and quality of fixes. However, comparison of side-scan sonar record overlaps on adjacent

tracks suggests that for most of the data, the navigation for any given survey is internally consistent on the order of 5 m or less.

Geologic ground truth data were provided by 0.5-m push cores, visual observations, and video photography obtained with the submersible *Johnson Sea-Link* as well as 3-m piston cores acquired aboard the R/V *Gyre*. Both the *Gyre* and the motherships for the *Johnson Sea -Link* (R/V *Seward Johnson* and R/V *Edwin Link*), were positioned by civilian GPS satellite navigation, with an accuracy of about 30 m. The submersible was positioned relative to the ship by an acoustic ranging system, which was repeatable to a few tens of meters. Although the *Gyre*'s position was typically well determined, during coring both the ship's drift and currents pushing the coring wire off vertical can lead to errors in positioning the cores.

Sea surface geophysical data were available for all four sites, but these data were diverse in type and parameters because most were borrowed from industry sources. For GC 184, GC 234, and GB 386, a few industry multichannel seismic reflection profiles were available. Likewise a variable number of hazard survey profiles, typically either run with a 3.5 kHz or similar echo-sounder or a high resolution multichannel seismic system, were also obtained. The navigation methods used for these surveys were typically unknown, since the data are proprietary, but industry standards are such that these data probably have navigation accuracies of less than 10 m. A more serious problem was offsets between different navigation data sets; these offsets were sometimes found to be on the order of a few hundred meters. In such instances, we had to resort to feature-matching to align submarine and sea surface data. We did not acquire industry data for GB 425, but instead carried out a 3.5 kHz and 12 kHz echo sounder survey with the R/V *Gyre*.

3.3 Objectives

The objective of this study was to use maps of geophysical (mainly acoustic) characteristics of the seafloor and shallow subbottom at hydrocarbon seep sites to provide a framework for assessing the effects of the seeps on the seafloor and the relationship to chemosynthetic communities. Using the principles of seismic stratigraphy, we wished to classify and map the extent of sediments affected by seepage. Our goal was to ground truth these classifications with geologic data (cores and submersible observations) and to correlate these characteristics with other geophysical and geologic data. A major objective of this task was to compare the geophysical framework with locations of chemosynthetic communities, surface features, and subsurface structures, such as faults. In addition, we wished to use the observational framework developed in this study for implications about the geologic formation and evolution of hydrocarbon seeps.

3.4 Methods

For each survey, the geophysical data were plotted at the same scale so that maps could be made for comparison of features. Bathymetric data were determined as described above and contoured at 5-m intervals. Where other sources of bathymetry data were available, the different data sets were compared to quantify and correct navigation offsets. The additional data were used to fill gaps or extend bathymetry contours outside the submarine survey area.

Side-scan sonar records from *NR-1* were automatically slant-range and speed corrected to produce deskewed images in which the along track and cross track dimensions are nearly the same. The slant-range correction method is internal to the sonar electronics and assumes a flat seafloor. Consequently, significant deviations from horizontal can cause errors in the plotting of features in the images. Sonar records were combined to make a mosaic of the acoustic backscatter variations over

each site. The paper side-scan records were electronically scanned as 8-bit gray scale images and were manipulated with a computer program (*Photo Styler*) to match common features on adjacent sonar swaths. This typically required some small adjustments of line navigation. The resultant image was a mosaic of the backscatter variations for each site. Some of the mosaics have gaps where it was impossible to manipulate the side-scan records to be consistent with adjacent tracks. This usually occurred at turns and where the submarine stopped or changed velocity in a manner that produced inaccurate speed corrections in the records.

The 25 kHz echo sounder data were recorded with a video camera on 8-mm videotape. These images were played on a videotape player and a Macintosh computer with video frame grabbing board was used to capture the images digitally. Each image represented only about 2 minutes of data, so longer records were constructed by electronically mosaicking adjacent images. As described below, the echo sounder records were classified by reflection characteristics and these characteristics were plotted along navigation tracks and then contoured to fill in the gaps between lines. Where possible, the side-scan images were used to help the interpolation between lines.

For ground truthing, piston cores and push cores (see Tables 3.1 and 3.2) were used along with visual observations and video data from submarine *NR-1* and the *Johnson Sea-Link* submersible. The piston cores were obtained from a surface ship and examined for geologic features; samples were also taken for porosity and carbonate percentage analysis. Push cores were taken using the manipulator arm of the *Johnson Sea-Link* submersible. They were typically 30 to 50 cm in length, if full, and were extruded and examined visually. Video and voice records were used to identify the locations of chemosynthetic organisms for some surveys. The time of an observation was noted, so the observation could be plotted versus the submarine navigation and thus correlated to sediment acoustic character.

Table 3.1 Description of piston cores.

Core ID	Description	Echo Type	Core length (cm)
GB 386-A	Compact carbonate rock layer at the top of the core	I	225
GB 386-B1	Empty	I	0
GB 386-B2	Empty	I	0
GB 386-C	Homogenous mud (no carbonate)	VI	230
GB 386-D	Homogenous mud (no carbonate)	VI	230
GB 386-S5	Carbonate rock layer in the top 50 cm Cracks filled with oil	I	182
GB 425-A	10 cm gas expansion void Numerous vesicles and black-stained mud above the void	II	215
GB 425-B	Homogenous mud Vesicles in the top 50 cm	II	230
GB 425-C	Homogenous mud with frequent empty spaces Vesicles between empty spaces	II	235
GB 425-D	Carbonate nodules in the top 35 cm Shell fragments and oil stains throughout the core	IV	212
GB 425-E	Homogenous mud Vesicles in the top 70 cm	II	240

Table 3.2   Description of push cores.

Core ID	Echo Type	Gas	Oil	Carbonate	Shell	Bacterial Mat
GC 184-a	II	P	tr	-	-	-
GC 184-b	II	P	P	P	P	-
GC 184-c	II	P	P	P	-	-
GC 184-d	II	P	-	-	P	-
GC 184-e	VI	-	-	-	-	P
GC 184-f	II	P	-	-	P	-
GC 184-g	II	P	-	P	P	-
GC 234-a	VI	-	-	-	-	P
GC 234-b	VI	-	-	-	-	-
GC 234-c	III	P	tr	tr	-	-
GC 234-d	VI	-	-	-	-	P
GC 234-e	III	P	P	tr	-	-
GC 234-f	III	P	tr	-	-	-
GC 234-g	VI	-	-	-	-	P
GC 234-h	VI	-	-	-	-	-
GB 386-a	II	-	-	-	-	P
GB 386-b	VI	-	-	-	-	P
GB 386-c	VI	-	-	-	-	P

(P = present, tr= trace)

To determine the interrelation of deep and shallow structure, faults and deep structure were interpreted on select multichannel seismic lines and extrapolated to the near surface. Structure maps were then compared with the side-scan sonar, bathymetry, and acoustic character maps.

3.5 Results

3.5.1 Acoustic Echo Types

Echo sounder records were divided into six classes (Figure 3.3) based on the amount and type of apparent disturbance of the sediment layers. Descriptions of these classifications are as follows:

Type 1: Characterized by a strong reflector at the seafloor and no evident acoustic penetration into the subbottom. The strong reflector is probably carbonate or gas hydrate at or near the seafloor and has a high reflection coefficient, causing much of the acoustic energy to be reflected or attenuated near the seafloor.

Type 2: Shallow penetration with an abrupt termination of acoustic penetration. This signature probably represents a thin layer of mud overlying a hardbottom, such as carbonate or hydrate. It may show areas in which recent mud flows have covered a pre-existing hardbottom.

Type 3. Scattered subbottom echoes without continuous horizontal internal reflectors. Such a pattern probably shows non-layered sediments disturbed by oil, gas, or disseminated carbonate precipitates.

Type 4. Scattered subbottom echoes with indistinct, horizontally-continuous reflectors. This signature probably represents layered sediments disturbed by gas, oil, or carbonate precipitates.

Type 5. Zones in which acoustic energy is abruptly attenuated; typically laterally-continuous features disappear within these zones. Such zones are widely
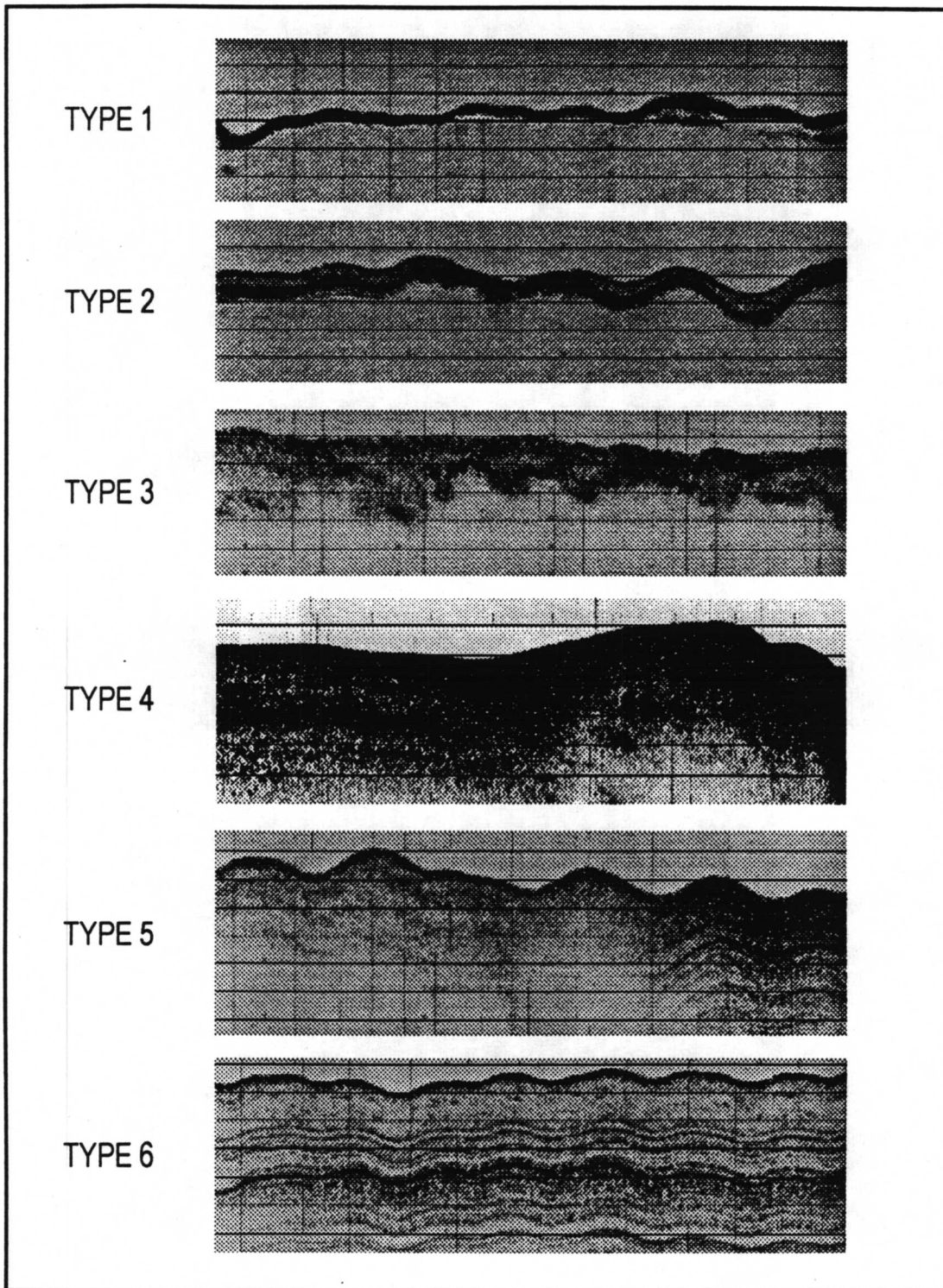
Figure 3.3   Examples of acoustic echo types seen in 25kHz subbottom reflection profiles.

recognized as the result of acoustic attenuation owing to scattering or absorption by gas bubbles within the sediments (Hovland and Judd, 1988).

Type 6. Parallel, continuous subbottom reflectors. These characteristics denote normal, undisturbed hemipelagic sediments.

3.5.2 Ground Truth

In this section we describe the implications of our ground truth data for the interpretations of acoustic facies. Our interpretation of the Type 1 hardbottom zones is based on cores, side-scan images, and submersible observations. Cores within these zones were typically short and contained carbonate rocks, usually within the upper 20 cm, as seen for example in core GB 386-A from the seep mound in GB 386 (Figure 3.4). Side-scan mosaics often showed rough topography in these regions and when viewed by submersible, carbonate outcrops were often seen.

Type 2 is similar to Type 1, but is a hardbottom covered with a thin sediment layer. Such zones usually appeared no different from surrounding sediments when seen in side-scan images or from a submersible, because of the covering of sediment. Cores taken in these areas, however, showed similar features to Type 1 area cores, but the hard layers were buried below the surface. Push cores from a Type 2 area on the seep mound in GC 184 typically contained mud with disseminated carbonate, but one had nodular carbonate at its bottom. About half of these push cores showed traces of oil. Core GC 425-A, from a similar zone on the mound in GB 425, retrieved muds of two different colors, separated by an expansion void above which were small vesicles and a band of dark mud (Figure 3.5). This core seems to show the boundary between two layers, presumably that seen in the echo sounder records. However, the two muds do not have sufficiently different properties to cause a strong reflection at their interface. Instead, the gas expansion features suggest that gas hydrate may have existed at the interface, but it evaporated when the core was raised. Thus, the
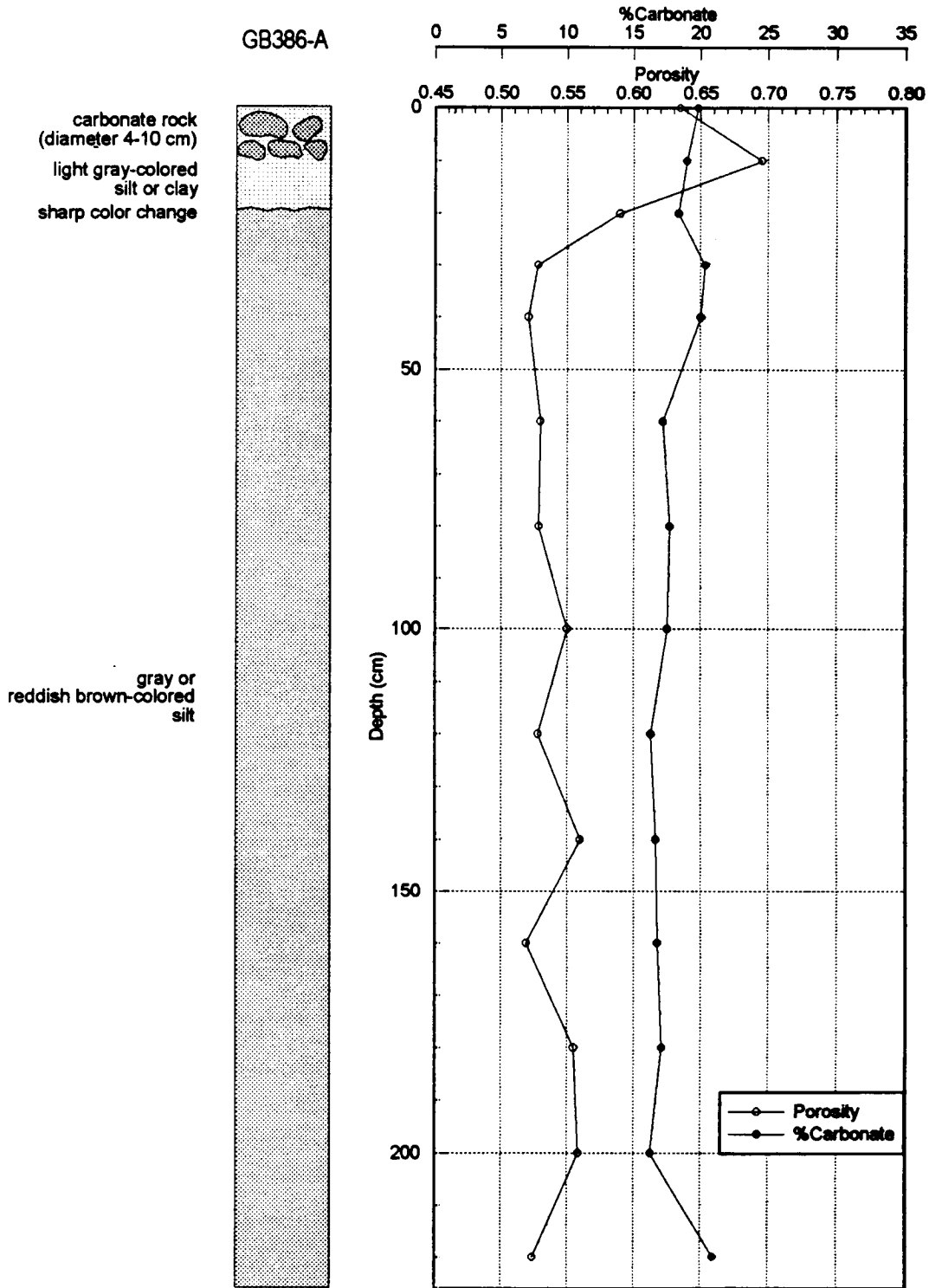
Figure 3.4   Description of Core GB386-A, from a Type 1 (hard substrate) echo character zone. At right are trends in carbonate percentage and porosity.
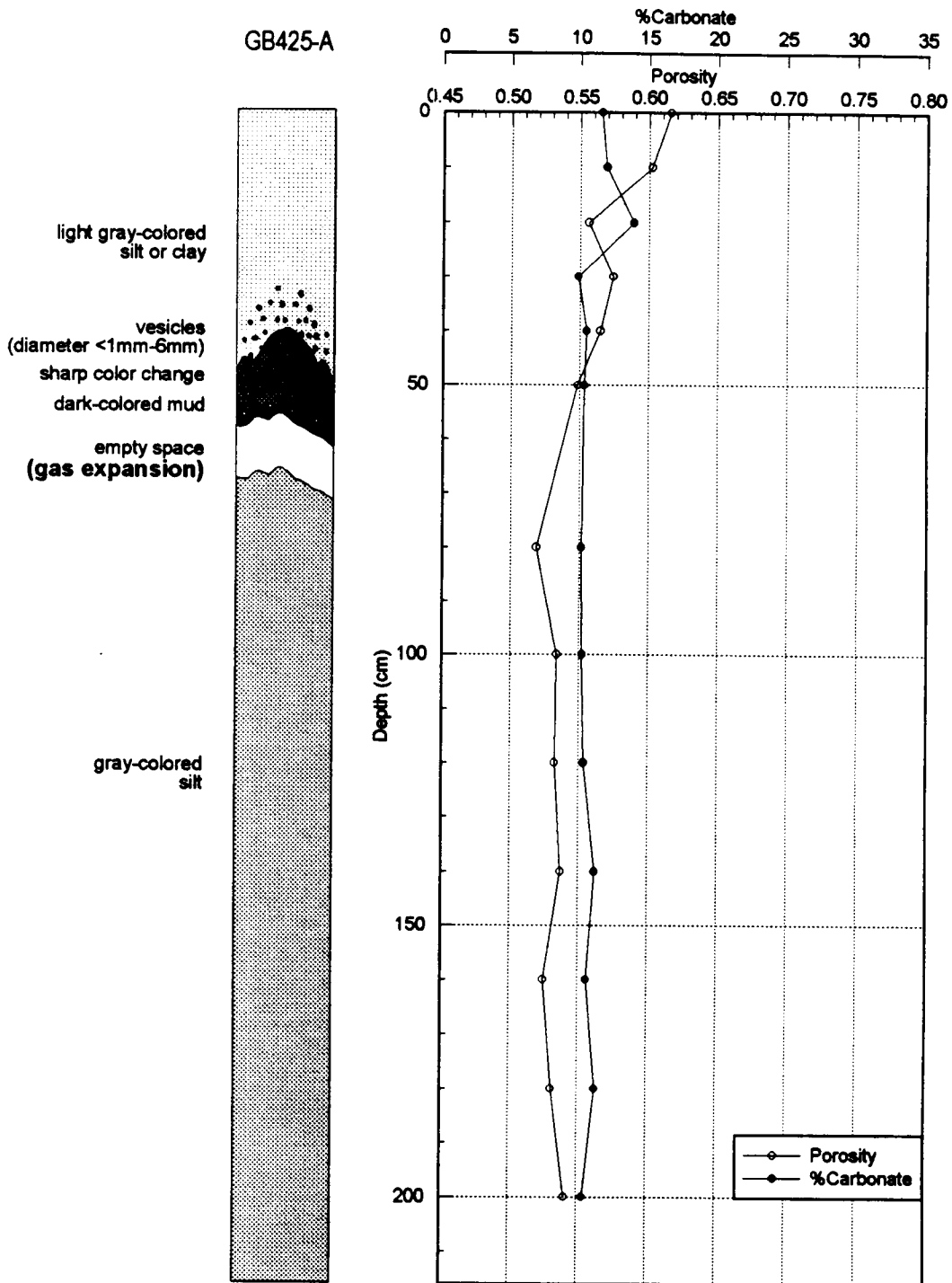
Figure 3.5 Description of Core GB 425-A, from a Type 2 (buried hard substrate) echo character zone. At right are trends in carbonate percentage and porosity.

reflector at this location may have been hydrate. The Type 2 geometry suggests a hardbottom buried by a thin layer of sediment and may indicate recent seep-related sedimentation. We base this interpretation in part on observations of mudflows and active mud expulsion from seep vents on the mound in GB 425, where Type 2 sediments cover much of the surface.

Types 3 and 4 are similar, except for the existence of internal reflectors, which are likely related to the original deposition of the sediments. Core GC 425-D (Figure 3.6) was recovered from a Type 4 zone (Figure 3.7) and it yielded mud permeated with carbonate nodules, oil stains, and shell fragments. All three components are potential scatterers of acoustic waves (particularly if the oil is accompanied by gas) and may therefore be the source of the apparent disturbance of the sediments noted in reflection profiles.

We had no core samples of Type 5 acoustic wipeout zones because they
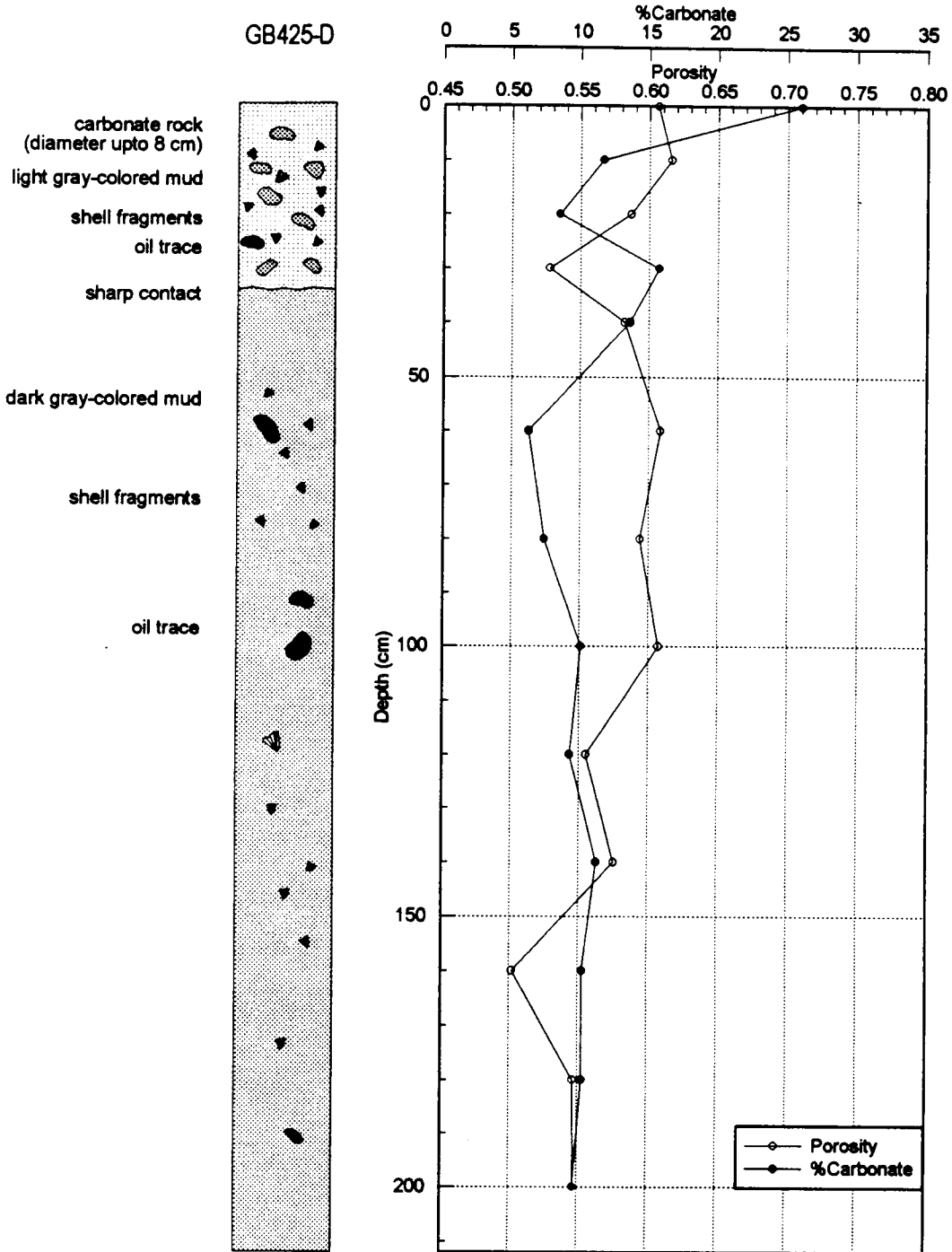
Figure 3.6   Description of Core GB 425-D, from a Type IV (disseminated disturbance) echo character zone.   At right are trends in carbonate percentage and porosity.
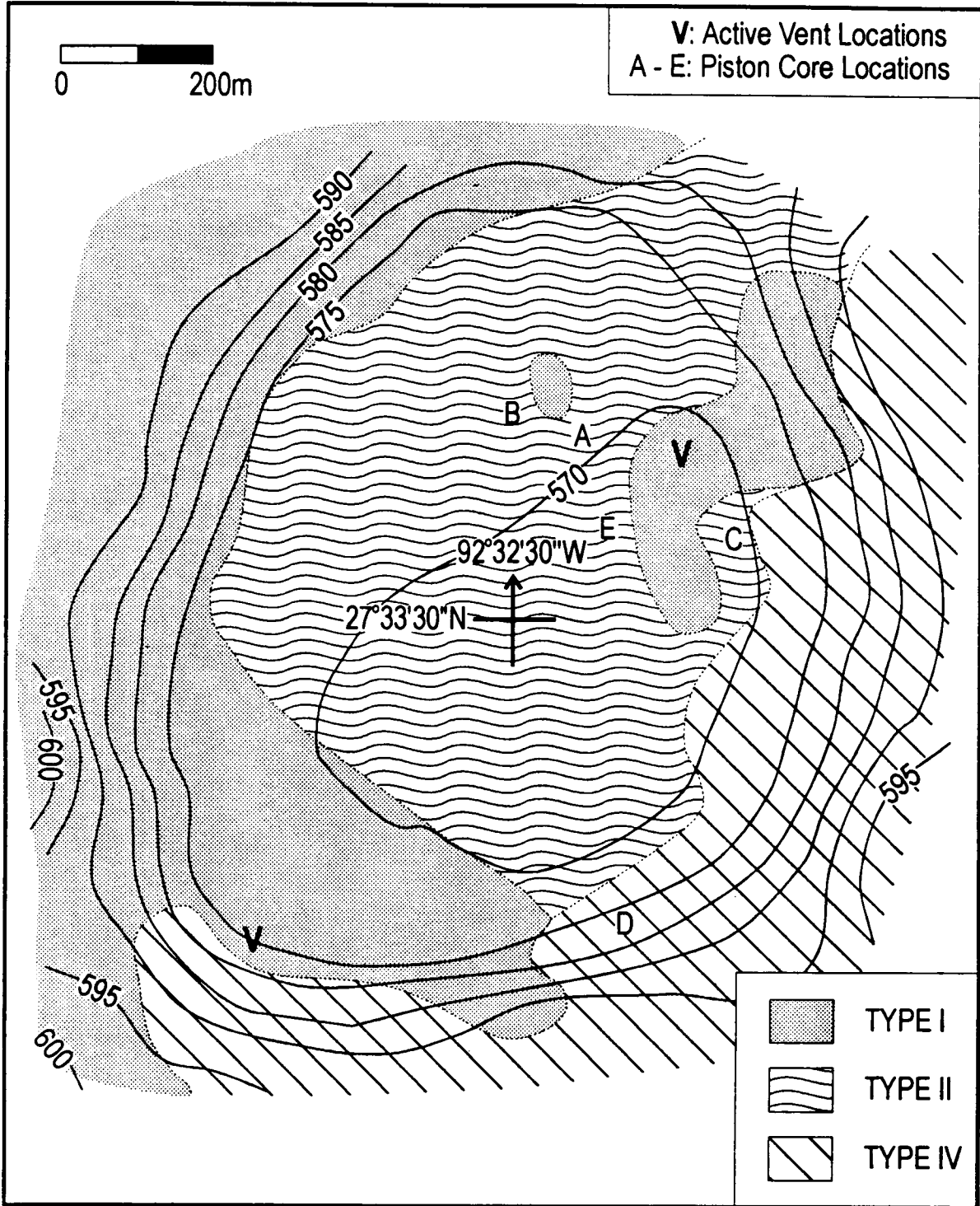
Figure 3.7. Patterns of acoustic echo types in the GB 425 survey area. Bathymetry contours shown at 5-m intervals. Echo types are explained in Figure 3.3. Letters A- D show piston core locations (see Tables 3.1 and 3.2); the letter V shows active vent locations.
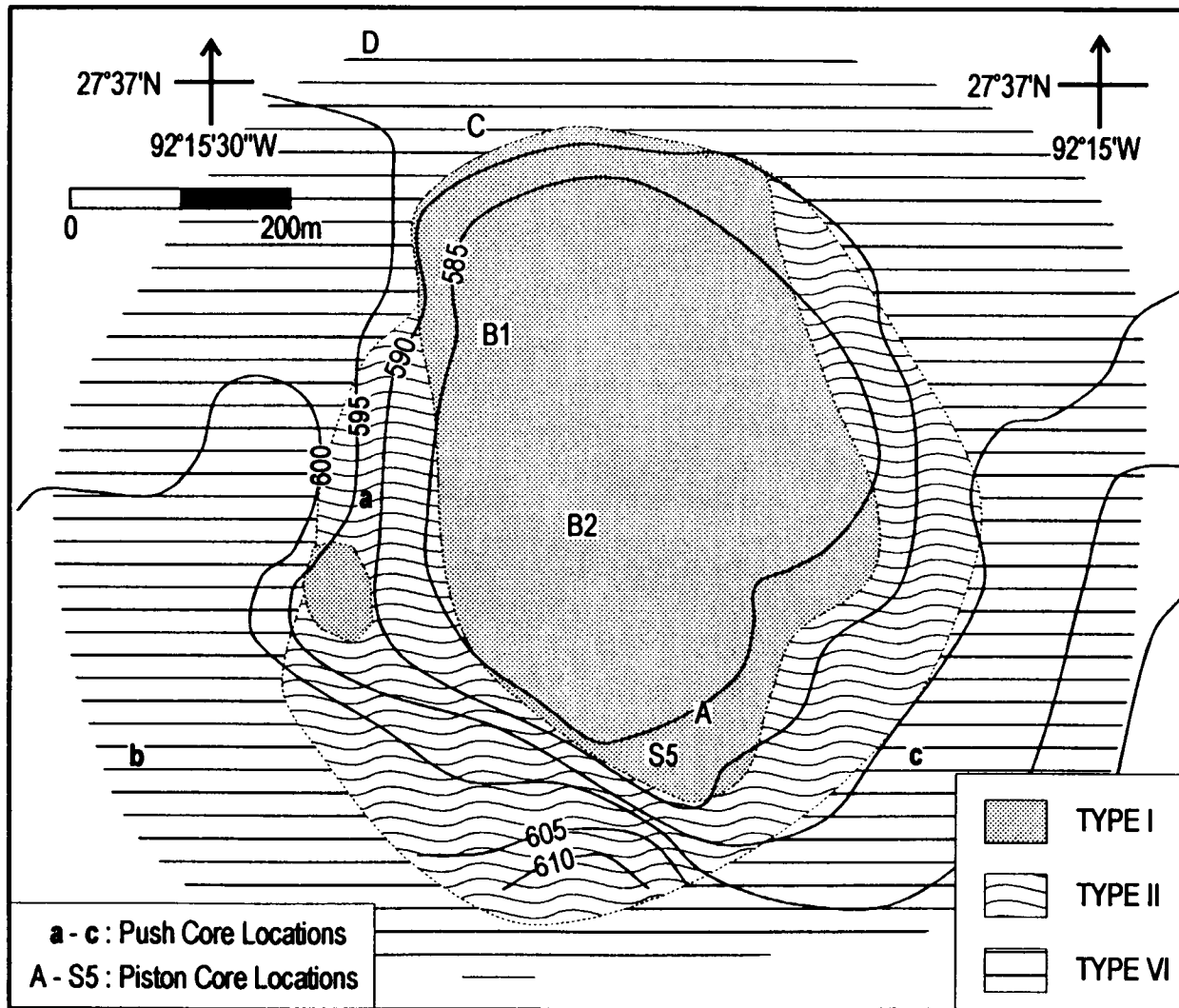
Figure 3.8   Patterns of acoustic echo types in the GB 386 survey area. Bathymetry contours shown at 5-m intervals. Echo types are explained in Figure 3.3. Captial letters show piston core locations; small letter show push core locations (see Tables 3.1 and 3.2).
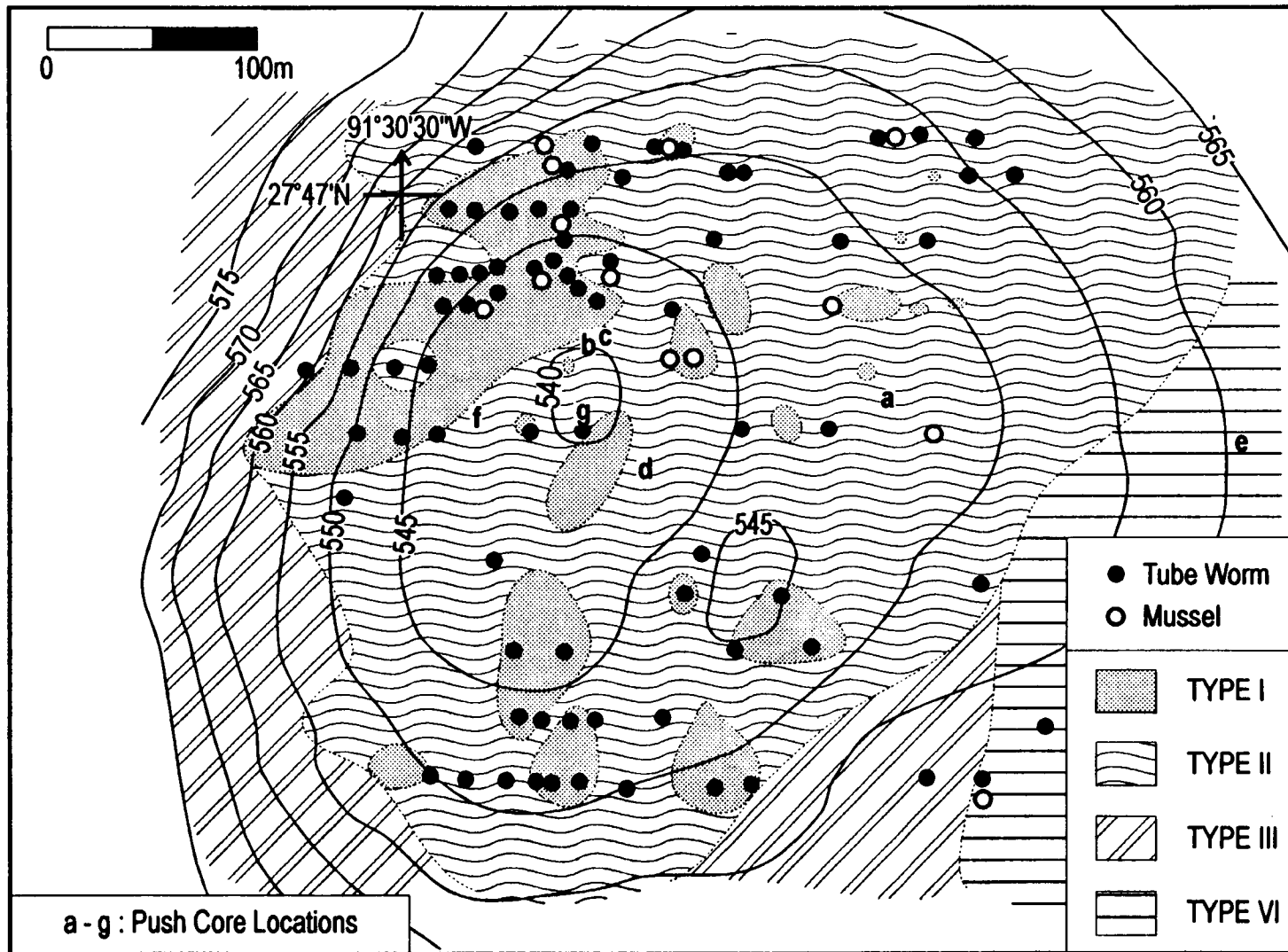
Figure 3.9 Patterns of acoustic echo types in the GC 184 survey area. Bathymetry contours shown at 5-m intervals. Echo types are explained in Figure 3. Also shown are locations of tube worm bushes and bivalve shells, denoted by filled and open circles, respectively. Lower case letters show the locations of push cores (see Tables 3.1 and 3.2).

types show that hardbottoms are at or near the surface, owing to active or recently active carbonate precipitation or hydrate formation. The Type 2 signatures may indicate recent mudflows that have buried a previous hardbottom, as interpreted from submersible observations at GB 425. The typical nearness of the hard substrate to the seafloor suggests that with time, the covering of sediments is probably incorporated into the hard substrate, so that the hard reflector moves upward through the sediment column. Alternatively, erosion may uncover some hard substrate. Given the uniformity of the burial or exposure of most hard substrate reflections, it seems that the upward movement is probably the most likely occurrence.

Interestingly, patterns of Type 1 and Type 2 occurrence are slightly different at each site. GB 386 has Type 1 over the mound summit and Type 2 around its edges (Figure 3.8), whereas the distribution on the GB 425 mound is almost opposite (Figure 3.7). GC 184 appears different from the other two because the areas of Type 1 returns are patchy and scattered (Figure 3.9). These differences probably reflect a variability in the occurrence of carbonate or hydrate, which in turn may signify variability in the structure of the mounds and hence the geometry of hydrocarbon seepage.

Around the mounds, the acoustic facies are variable, apparently dependent on the areal extent of the seepage zone. GB 386, seems to be an isolated seep mound, as it is surrounded by undisturbed, Type 6, sediments. Both GB 425 and GC 184 are evidently part of zones of seep disturbance that are larger than the survey areas. In GB 425 Type 1 and Type 4 sediments surround the mound (Figure 3.8), whereas in GC 184, Type 3 sediments surround the mound (Figure 3.9). In both cases, sea surface geophysical survey data indicate that the study areas are only small parts of larger zones of seepage.

GC 234, which has no large mound structure, has acoustic facies patterns that are clearly different from the other sites (Figure 3.10). Here, the distribution is complex, but mainly consists of small patches of Type 1 (hard substrate), Type 3 (disturbed sediments), and Type 5 (acoustic wipe out) within an area of Type 6 (undisturbed) sediments. The occurrence of Type 1 and Type 5 reflections, scattered in patches throughout the survey area, seems to indicate that carbonate or hydrate formation and gas seepage are widespread along the fault scarp and not as localized as at the mound sites.

3.5.4 Backscatter Mosaics

Acoustic backscatter patterns in the side-scan sonar records seem to mainly show the effects of small scale topography and this topography is extremely variable in its appearance at the sites we studied. In some instances, the topography is apparently related to mound structure or formation because the topographic features follow the bathymetric contours, such as curved ridges at the edges of the mounds in GB 386 (Figure 3.11) and GB 425.

In some locations, the topography appears to be rock outcrop. In the images, such features appear as small scale roughness or clusters of mounds (Figure 3.12). The roughness, blockiness, and clear acoustic shadows cast by these features suggests they are outcrops. Probably these outcrops consist mainly of authigenic carbonate; however, in some areas it is possible that the small scale roughness is actually caused by clusters of tube worms (e.g., at GC 234) or even by hydrate mounds (MacDonald et al. 1990a). Our study indicates that these outcrop zones are often correlated with Type 1 acoustic facies reflection patterns (compare Figs. 3.10 and 3.12). Because the Type 1 character is a hard substrate, this is not surprising. Furthermore, at GC 234, at least, many of the "outcrops" are more-or-less linear and seem to be correlated with faults mapped in multichannel seismic data (Figure 3.13).
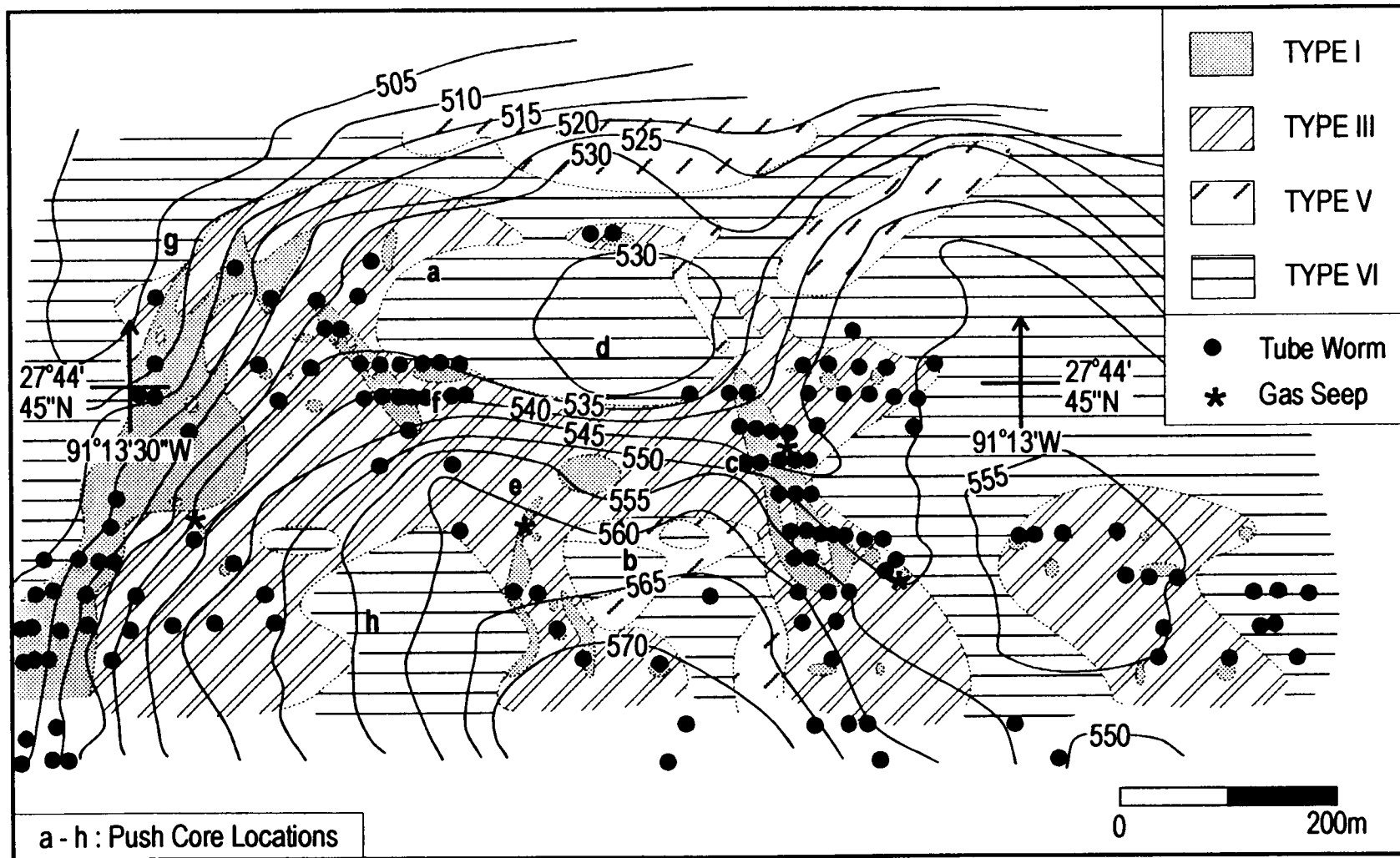
Figure 3.10 Patterns of acoustic echo types in the GC 234 survey area. Bathymetry contours shown at 5-m intervals. Echo types are explained in Figure 3.3. Also shown are locations of tube worm bushes, denoted by filled circles, and gas seeps, shown by an asterisk. Lower case letters show the locations of push cores (see Tables 3.1 and 3.2).
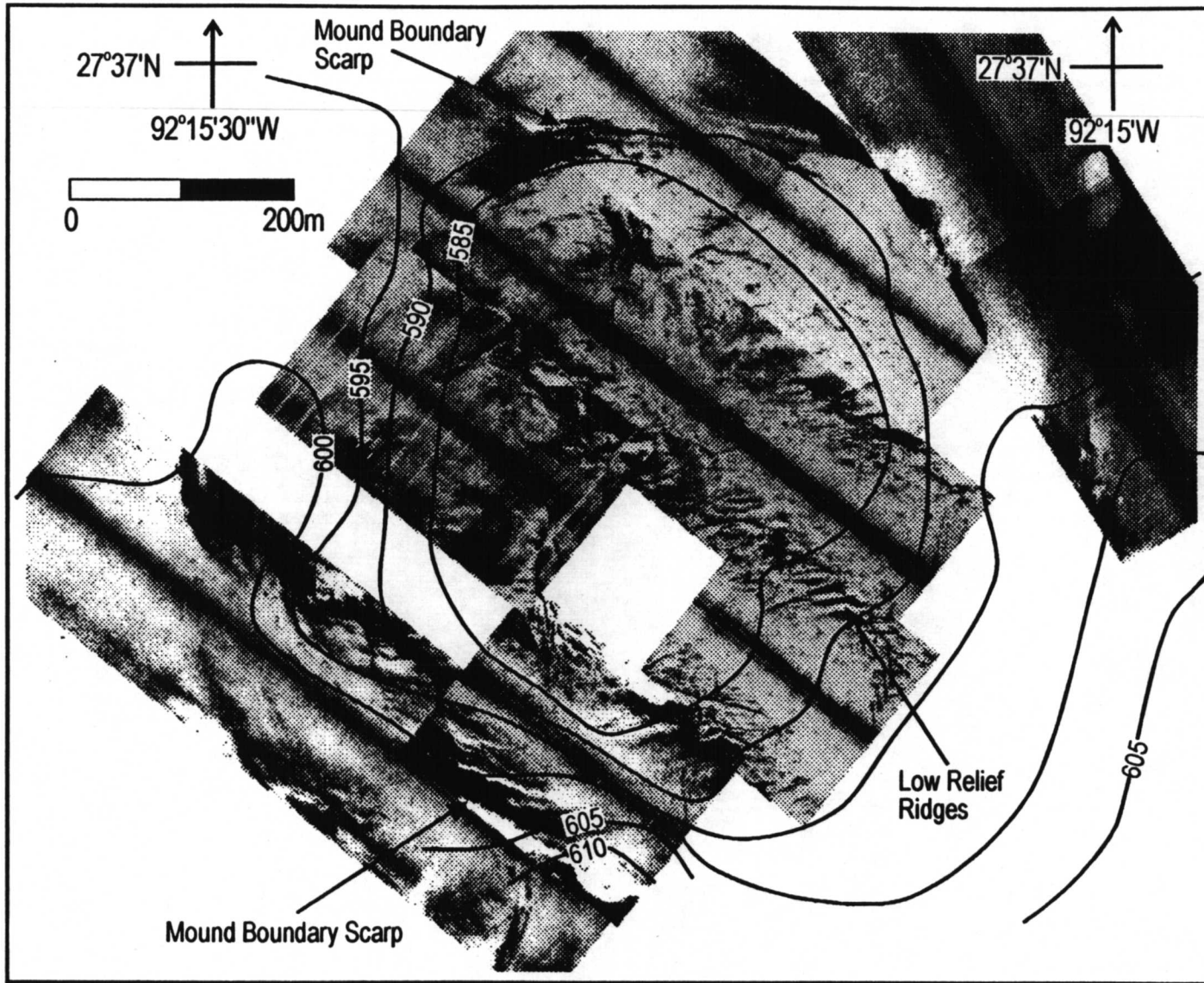
Figure 3.11 Side scan sonar mosaic of the GB 386 survey site. Bathymetry contours shown at 5-m intervals. Dark areas represent strong acoustic backscatter.
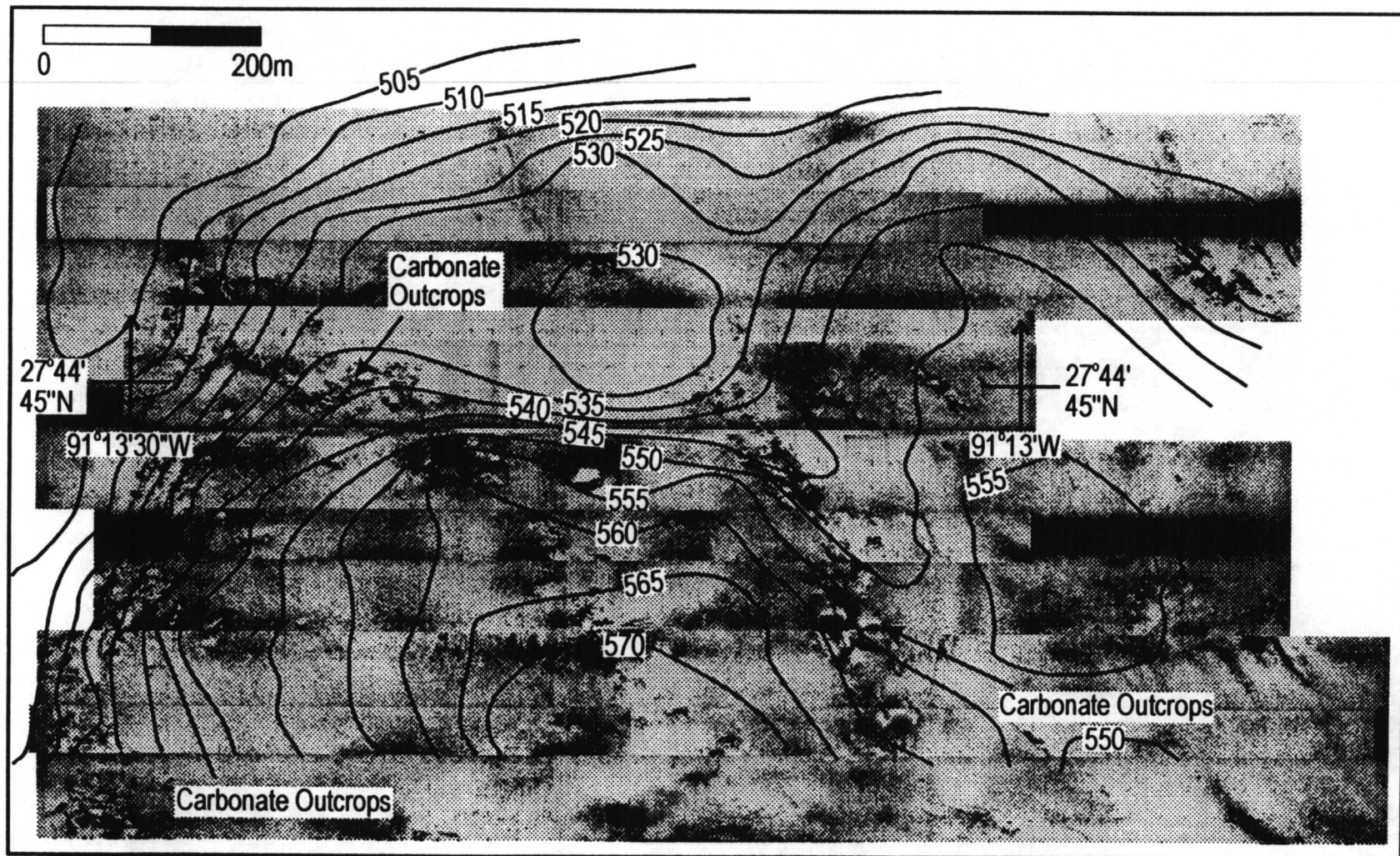
Figure 3.12 Side scan sonar mosaic of the GC 234 survey site. Bathymetry contours shown at 5-m intervals. Dark areas represent strong acoustic backscatter.
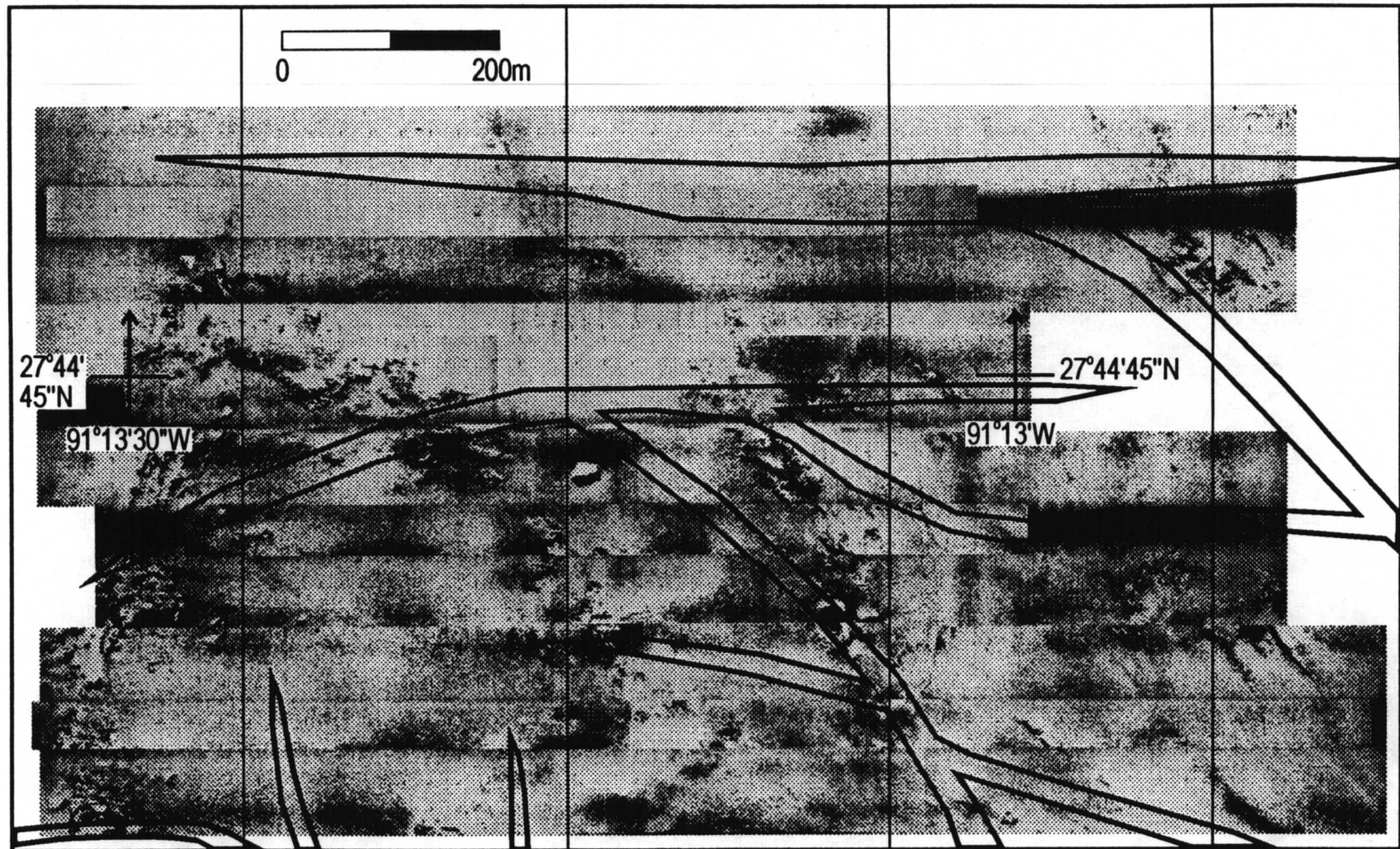
Figure 3.13 Comparison of GC 234 side scan sonar mosaic and fault traces (heavy black lines) mapped with multichannel seismic data (J. Reilly, in preparation).

Thus, the "outcrops" may represent the effects of seepage along the fault traces at the seafloor.

The background acoustic backscatter from the seafloor appears remarkably constant on most of the side-scan mosaics. From experience in other areas with carbonate mounds (e.g., Laswell et al. 1990; 1994), we expected the sedimentary surface to show greater backscatter in disturbed areas where such factors as carbonate precipitation or shell deposits might increase the backscatter. In general, we did not find this to be true, perhaps because several of the survey areas were virtually entirely affected by seepage. Notably, in the survey area with the greatest acoustic facies variability (GC 234), it is clear that Type 1 outcrop features are generally surrounded by patches of seafloor with greater backscatter (darker in the mosaics; Figure 3.12).

Some of the features in the mosaics have origins that are unclear. This is true of linear and curved ridges atop the two flat-topped mounds, GB 386 and GB 425. As seen from submersibles, such ridges are usually low (<1 m in height) and rounded. One possibility is that they are related to deformation of the mud in the mound; although, another is that they are formed by carbonate precipitation. The latter hypothesis arises from submersible observations in which some of these ridges were seen to be crusted with carbonate.

At one site, GC 184, mysterious linear troughs, a few meters in width, were noted criss-crossing the mound. From submersible observations the troughs are seen to be shallow and smooth. Furthermore, available seismic data do not apparently show any structure beneath the troughs, such as fault offets. Consequently, we think these features are probably some type of drag or trawl marks.

3.5.5 Connections to Deep Faults

In most of our study areas, it is still difficult to make detailed connections to deep faults. The faults are usually imaged with low-frequency multichannel seismic profiles, whose horizontal resolution is limited. In contrast, high-frequency, high-resolution data, both 3.5 kHz echo sounder profiles taken at the sea surface and 25 kHz profiles taken at depth, are unable to penetrate the Type 1 and Type 2 zones that characterize most of the seeps, so the near surface traces of the faults are unclear. Nevertheless, some relationships are clear. In each study, the seep is situated along the trace of a major fault, either caused by the uplift of a nearby salt diapir (GB 386, GB 425, and GC 184) or by faults between subsurface salt ridges (GC 234). In GC 184, for example, the mound known as "Bush Hill" occurs on a fault that is active, as shown by the offset of near surface sediment layers (Figure 3.14). The exact location of the fault beneath the mound is unclear because of the lack of acoustic penetration, but the geometry to the north and south of the feature suggest it is located near the steeper, western side of the mound where most of the Type 1 reflection areas are located. GC 234 has no large mound, so there it is possible to map the traces of several faults that comprise the fault zone which crosses the study area. An excellent correlation is found among fault traces, carbonate outcrops, and chemosynthetic community locations (Figures 3.10, 3.12, and 3.13). These observations suggest that Type 1 and Type 2 reflection zones in some cases show the seafloor traces of faults, where seepage causes the precipitation of authigenic carbonate and supports chemosynthetic communities.

3.5.6 Relationship of Geophysical Signatures and Seep Organisms

Within the limitations of our data set, we see a good correlation among hard substrate reflections, wipe out zones, "outcrops" on side-scan sonar images, and the locations of chemosynthetic organism clusters. One must remember that most of
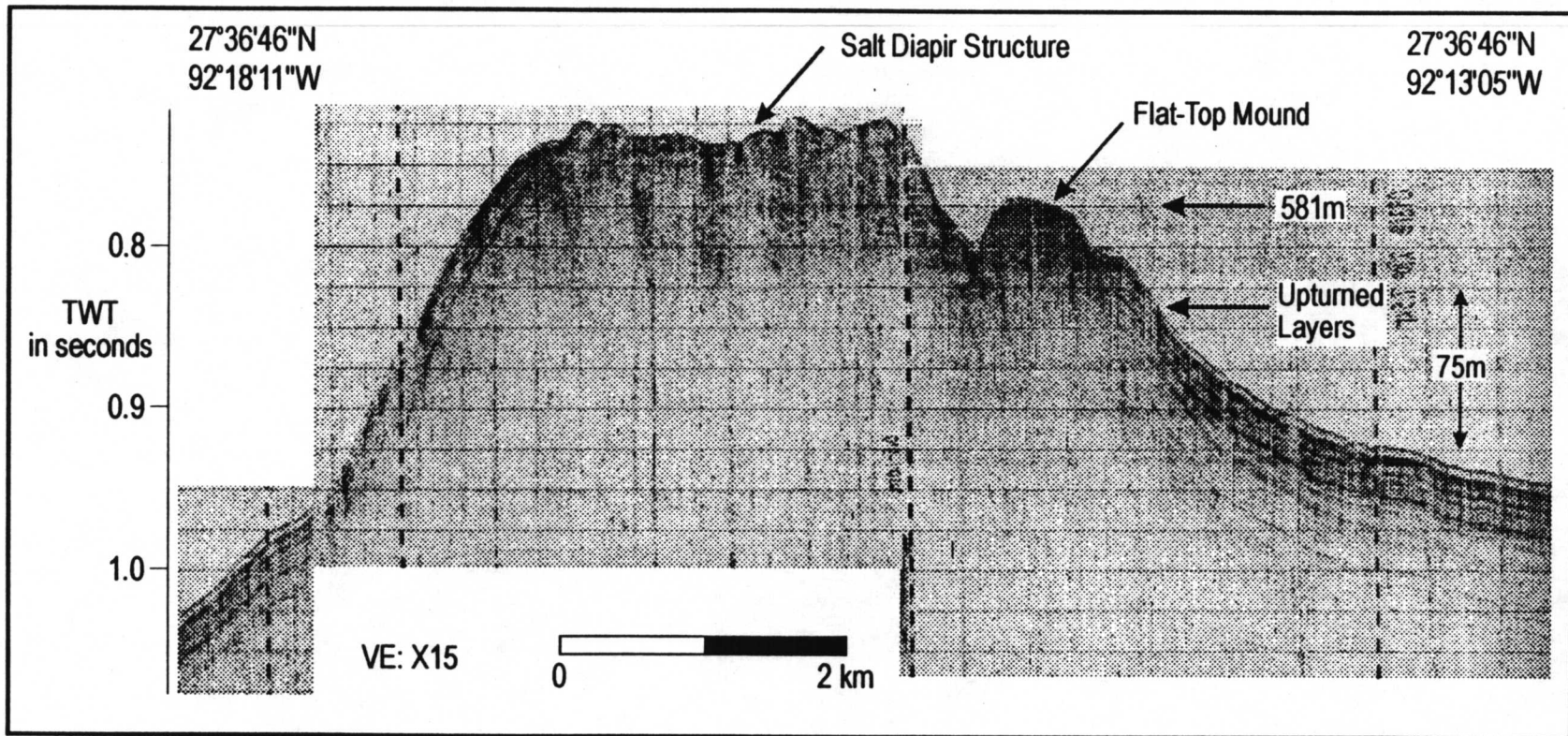
Figure 3.14 East-west 3.5kHz echo sounder profile across the GB 386 mud mound (right of center), on the flank of a large salt diapir.

our data on the locations of chemosynthetic organisms comes from verbal observations recorded on tape during *NR-1* cruises, so they record only the presence or absence of organisms that caused the observers, looking out the submarine portholes, to comment. Because tracks are located 30 to 100 m apart, the observations relate only the few tens of meters near the track line in which objects on the sea floor are visible. In addition, we cannot account for observer bias or variations in attention during the survey. Nevertheless, we were able to extract a large number of sitings, mainly of tube worm bushes, in the GB 184 and GC 234 survey areas (Figures 3.9 and 3.10).

Comparison of acoustic facies and chemosynthetic organism sitings shows that at GC 184, 97% of tube worm bush locations and 92% of bivalve sitings are within areas classified as having Type 1 or Type 2 reflection characteristics (Figure 3.9). At this site, almost all of the seep mound shows these two reflection types, so we could also say that 96% of all chemosynthetic organisms are on the mound. The lack of organisms off the mound, even within the small survey area, is striking. At the site in GC 234, the situation is slightly different. No Type 2 reflections were noted, but much of the seep zone is characterized by Type 1 or Type 3. Here there is a clear clustering of organisms near zones characterized by these two reflection types (Figure 3.10). Although 86% of the organisms are located on Type 1 or Type 3 reflection zones, only 46% are located on Type 1 hard substrate reflectors, implying Type 1 areas are not required as community sites.

These observations indicate a clear preference of chemosynthetic organisms for sediments showing Type 1, Type 2 (both hard substrates), and Type 3 (shallow disseminated seep products) characteristics. This is probably the result of two factors. First, these are areas where there has been a significant precipitation of authigenic carbonate, which may form a solid substrate to which organisms, such as tube worms, can attach themselves. Second, such areas also have high

concentrations of seeping hydrocarbons, hence the massive carbonate precipitation, so the organisms find at such locations the hydrocarbons needed to produce food.

3.6 Discussion

Tensional faults are one of the primary effects of deep salt movement on the sediment column of the Gulf of Mexico continental shelf and slope. These faults may dissect hydrocarbon reservoirs within the sediment column, allowing gas and oil to escape by providing both a break in the reservoir seal and an upward pathway. In order that the hydrocarbons reach the sea floor, it is probably necessary that the faults are large, or genetically related to one that is large, and also active. Only large faults will usually penetrate sufficiently deep to tap a mature reservoir and also provide sufficient offset to break through impermeable formations. Likewise, only active or recently active faults will break through to the seafloor, and this is probably necessary to let the hydrocarbons escape.

Many faults that fit these qualifications exist within the Gulf of Mexico because salt body movements are ongoing. In our study areas, which are limited in geographic extent, all of the seeps occur either on the flanks of salt diapirs or along a fault system formed between two diapirs. This implies that the diapirs are the locus of most intense deformation and hence the most likely locations for seeps to occur.

When hydrocarbons reach the seafloor, they have several geologic effects. The hydrocarbons change the characteristics of the sediments, causing disturbances that can be imaged by acoustical methods. They may also entrain sediments, causing the formation of seep mounds.

The effects that perturb acoustic signals can be divided into two classes: the results of gas within the sediments and the results of materials precipitated within the sediments. The gas causes attenuation of the acoustic waves and the result is usually a zone of acoustic wipe out (signal loss) where subsurface reflections are not

seen or turbidity (reverberation) where reflectors may be masked (Hovland and Judd, 1988; Anderson and Bryant, 1990). This former is the Type 5 reflection character noted in our study. Precipitates either cause acoustic turbidity, the scattered, amorphous reflections within the sediment column, or a hard substrate that reflects most of the acoustic energy. Hard substrates may be caused by the precipitation of massive carbonate layers and blocks (Roberts et al. 1990) or by the formation of gas hydrate layers. We see these as the Type 1 and Type 2 reflections within our surveys. Carbonates can also be disseminated as macro- or micronodules (Behrens 1988; Roberts et al. 1990) and thus cause acoustic turbidity by the diffraction of acoustic energy throughout the affected sediment column. These effects cause Type 3 and Type 4 reflection characters in our study areas.

The formation of a seep mound implies the localization of the seep to nearly a point source. Interestingly, the three mounds we studied are all located on the flanks of salt diapirs (Figure 3.14), whereas the one site without a significant mound is along a fault system between diapirs. This may indicate that seeps next to diapirs are more likely to be localized, perhaps within a narrow fault, whereas those between are along wider fault zones are less likely to be constrained and localized.

Our observations suggest that the mounds are formed by flows of low viscosity mud, like a "mud volcano," rather than by the diapiric rise of a mud body (Figure 3.15). Evidence in favor of this hypothesis is as follows. Low viscosity, fluidized sediments are inferred from observations of fresh mud flows and the active eruption of gas and oil-charged mud from vents on the summit of the mound in GB 425. In addition, a layer of fresh, buried mussel shells in a core from near GC 234 indicate that the shells were quickly buried by a mud flow, before the shells could be degraded by post-mortem contact with sea water. That these mounds are not diapiric is inferred from industry multichannel seismic reflection profiles that appear to show
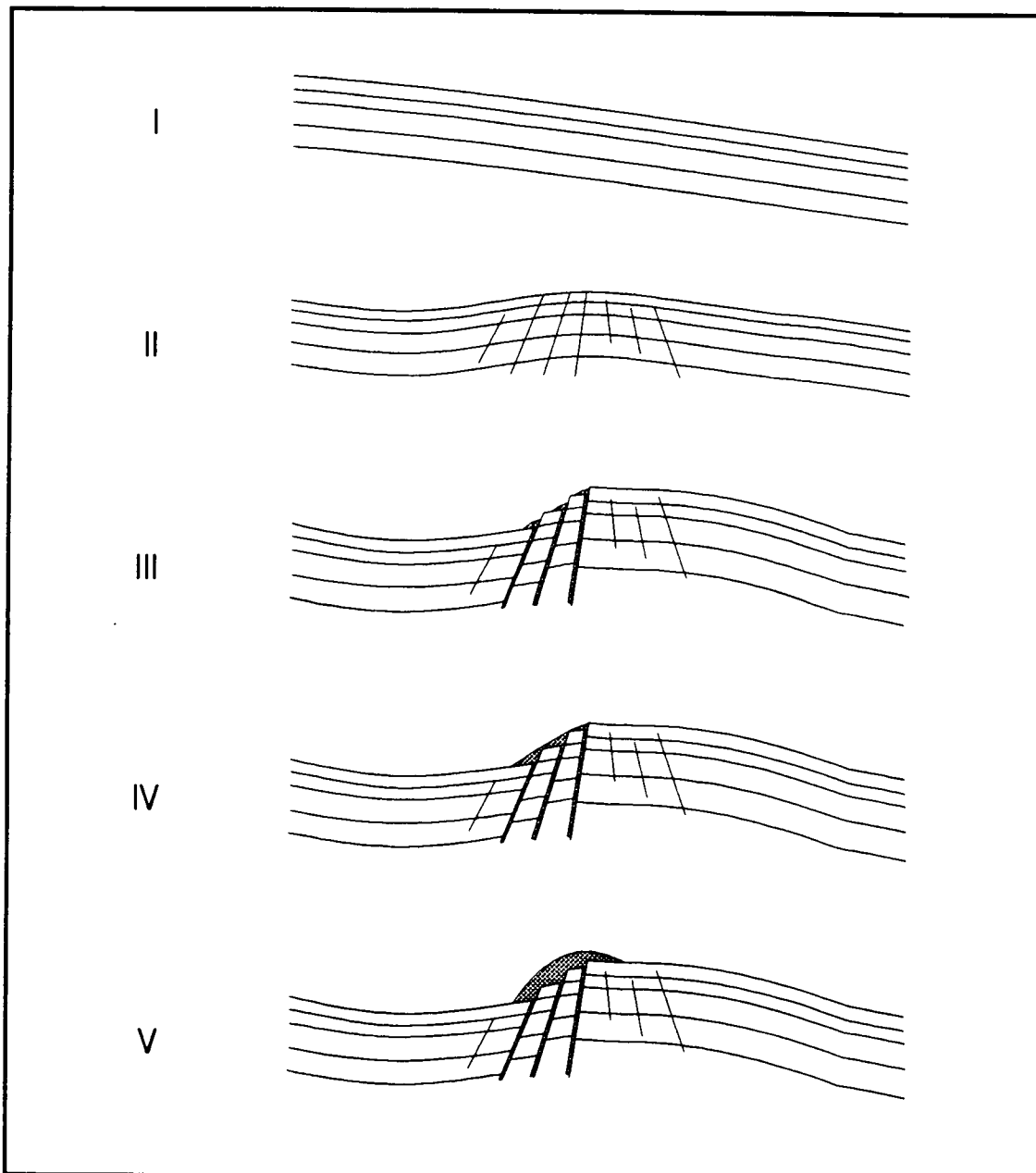
Figure 3.15 Model of the formation of the GC 184 mud mound. Faulting provided a conduit for fluid mud (top) which formed mound on fault scarp (middle). Asymmetry of fault scarp may have caused mound asymmetry (bottom).

3-36

continuous layers beneath the GB 386 and GC 184 mounds. This observation implies that the sediments were not deformed by diapiric action.

Our observations also suggest that there are at least two types of mounds: those with rounded summits and those with flat-topped summits (Figures 3.2 and 3.16). The one rounded-summit mound we studied, in GC 184, is asymmetric and has Type 1 reflections and chemosynthetic organisms occurring mainly on one side of the mound. These asymmetries suggest that the source of the hydrocarbons, probably the fault beneath the mound, lies under the west side of the mound (Figure 3.9). The flat-topped mounds appear more symmetric in cross-section. In addition, observed hydrocarbon venting on the GB 425 mound was observed only at locations along the edge of the summit platform. We suggest that the middle of the summit, which shows mostly Type 2 hardbottom reflections, is impermeable to hydrocarbon migration, perhaps because it is capped by hydrate or carbonate, and this causes the hydrocarbons to vent around the edges of the summit.

Interestingly, the flat-topped mound in GB 386, which has hardbottom at the surface (Figure 3.8), is not a site of abundant and varied chemosynthetic communities, whereas GB 425, which has a thin sediment covering atop hardbottom (Figure 3.7), is inhabited by many different species of chemosynthetic organisms. This difference may indicate that the GB 425 mound is more active, expelling more mud, gas, and oil, and this is the reason for the greater numbers and variety of chemosynthetic organisms.
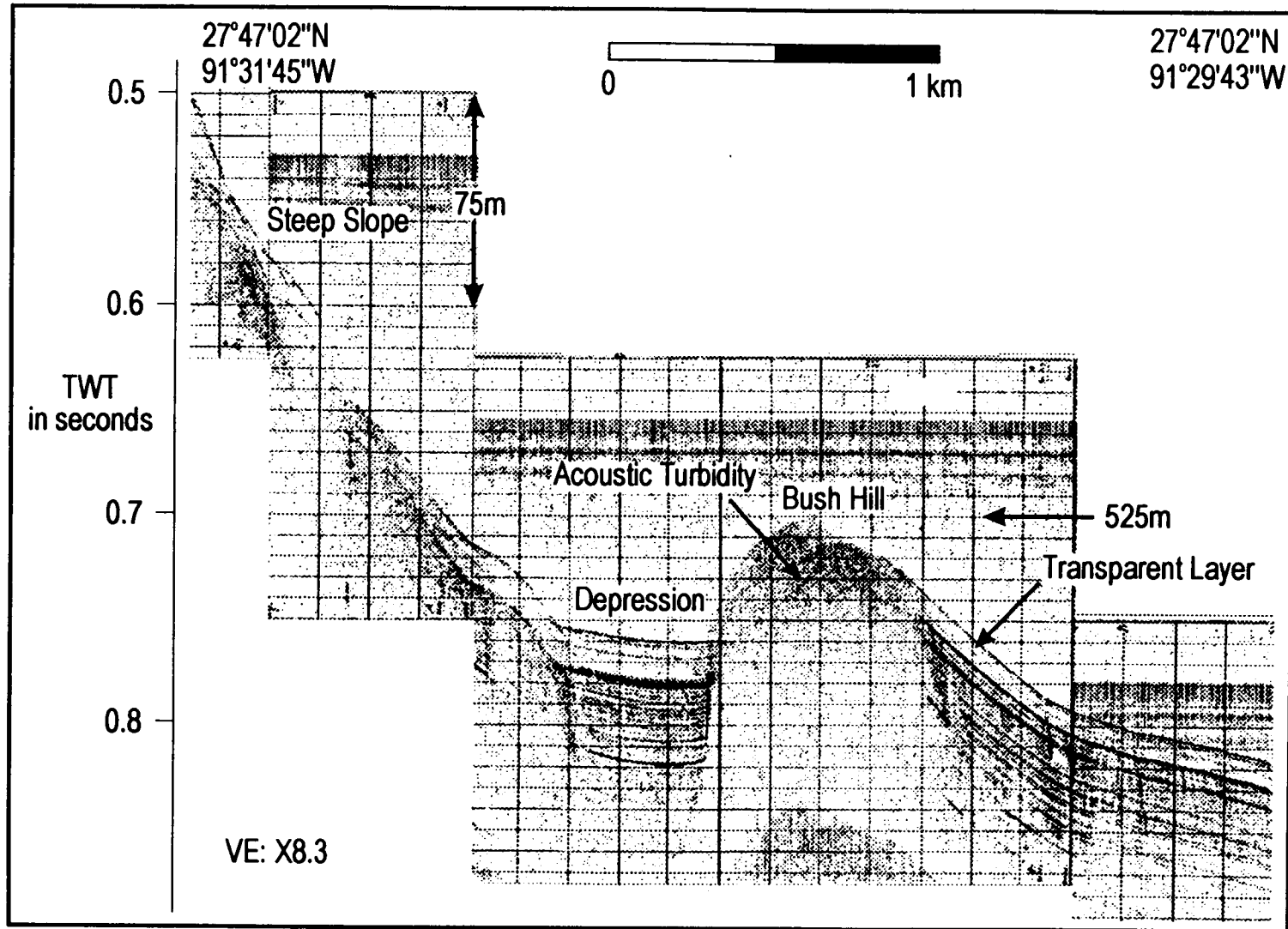
Figure 3.16 East-west 3.5kHz echo sounder profile across the GC 184 mud mound. Note offset of sedimentary layers on either side, indicating fault offset.

4.0 Geochemical Alteration of Hydrocarbons in Seep Systems
M.C. Kennicut II and Roger Sassen

4.1 Introduction: A Descriptive Model of the Geochemical Setting of Seep Communities

All chemosynthetic locations studied to date have a number of common geochemical features. These include oil seepage; gas charged sediments; hydrates; authigenic carbonate; active hydrocarbon oxidation; chemosynthetic biomass; elevated EOM, TOC, and salinity; and biodegraded oil (Figure 4.1). While it is still not clear which features are essential, it is clear that these attributes are closely related. The general model describing geochemical settings that characterize seep communities was documented with collections made during the 1991 and 1992 cruises.

The management relevance of this portion of the program can be summarized as follows:

1. Future releases of petroleum due to anthropogenic activities will be difficult to document because (a) ambient petroleum levels are high and heterogeneous and, (b) the most likely fluid to be spilled is the same as that which is naturally leaking.

2. The issue of depletion or reduction of the hydrocarbon seepage due to extraction of petroleum reserves is still an unresolved question, however the potential does exist.

3. Due to chronic exposure to petroleum, as a result of fundamental life style, additional insults due to anthropogenic inputs may have little detrimental effect. However, if certain communities are perceived to already be in poor condition an additional insult could cause catastrophic failure of the ecosystem.

Parameter	GC-272 CF	GC-234	BH	BP (historical)	GB-386 (single sample)	Indicates
Elevated TOC	X	X	X	X	X	Oil Seepage
Elevated $CaCO_3$	X	X	X	X	X	Authigenic CO_3
H_2S	X	O	X	X	O	Anoxia
Light P.W. CO_2	X	X	X	X	X	Methane/Oil Oxidation
Elevated ΣCO_2	X	X	X	X	O	Hydrocarbon Oxidation
Saline Waters	O	X	O	X	O	Brine Seepage
Fresh Water	X	X	X	X	O	Hydrate Decomposition
Light Tissue $\delta^{13}C$	X	X	X	X	X	Chemo Autotrophy

Figure 4.1   Summary of seep site processes and indicators. (Note, site descriptions refer to locations given in Figure 2.1 and Table 2.1 – except BH stands for Bush Hill, GC-184 and BP stands for Brine Pool Nr-1, GC-233. Light P.W. CO_2 indicates pore water $CO_2 S^{13}C$ values.)

4-2

A fundamental feature of the chemical setting of chemosynthetic communities dominated by tube worms is the presence of oil seepage (Kennicutt et al. 1988b; MacDonald et al. 1989). Oil seepage is a source of labile carbon (Figure 4.2). This labile carbon can be oxidized by bacteria, most likely in conjunction with the reduction of seawater sulfate to H_2S. This process leads to anoxic conditions through consumption of O_2. The production of sulfide also fulfills the energy needs of the dominant symbiont bacteria, sulfide oxidizers. Due to the ^{13}C-depleted nature of the carbon in oil, a lowering of the sedimentary organic carbon stable isotopic compositions can be observed as the amount of organic matter increases (Figure 4.2). The introduction of oil to the system can increase the available organic carbon by several orders of magnitude (Figure 4.3). This latent source of both carbon and energy may provide the initial conditions that fuel the enhanced biomass.

Production of large amounts of CO_2 during hydrocarbon oxidation leads to precipitation of authigenic carbonate (Figure 4.4). The rapid microbial cycling of labile carbon allows for large increases in CO_2 in interstitial water. ^{13}C-depleted carbonate, which ultimately forms if CO_2 is produced in excess of its solubility, is a pervasive feature at seep sites. The precipitation of carbonate is an important event for the ecology of an area since hard substrate appears to be essential to the establishment of some of the characteristic megafauna (i.e., tube worms). The presence of ^{13}C-depleted carbonate represents an accumulation of materials over time (Figure 4.5). Once formed, the carbonate will remain in place unless a dissolution or erosional event occurs. The presence of hard substrate is an important control on the expression of community structure at chemosynthetic sites.

A review of the stable isotopic compositions of both organic and inorganic pools of carbon at seep sites reveals the pervasive presence of ^{13}C-depleted carbon due both to the infusion of ^{13}C-depleted carbon into the system and preferential
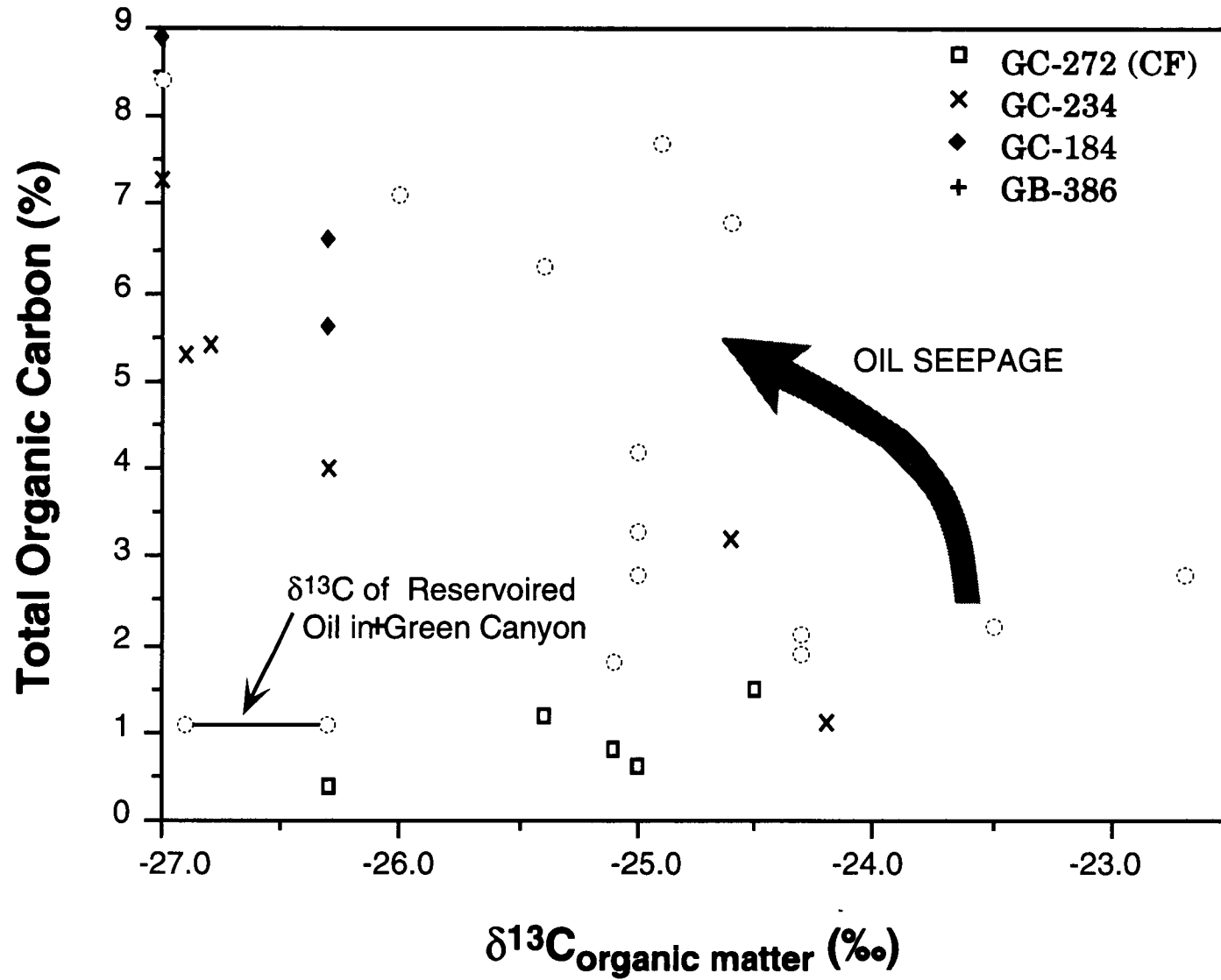
Figure 4.2   Oil seepage adds ^{13}C-depleted organic carbon.
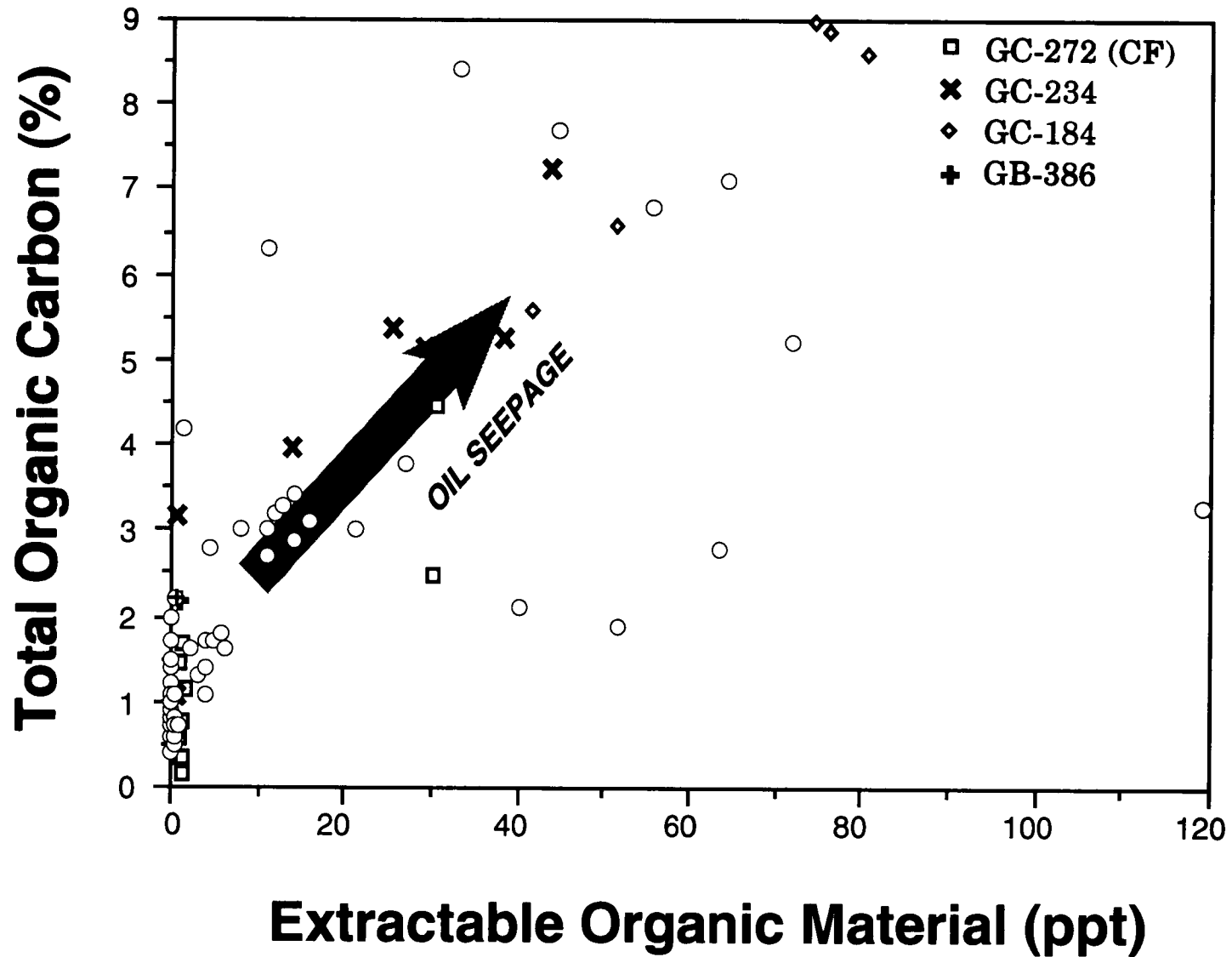
Figure 4.3   Oil seepage adds organic carbon at seep sites.
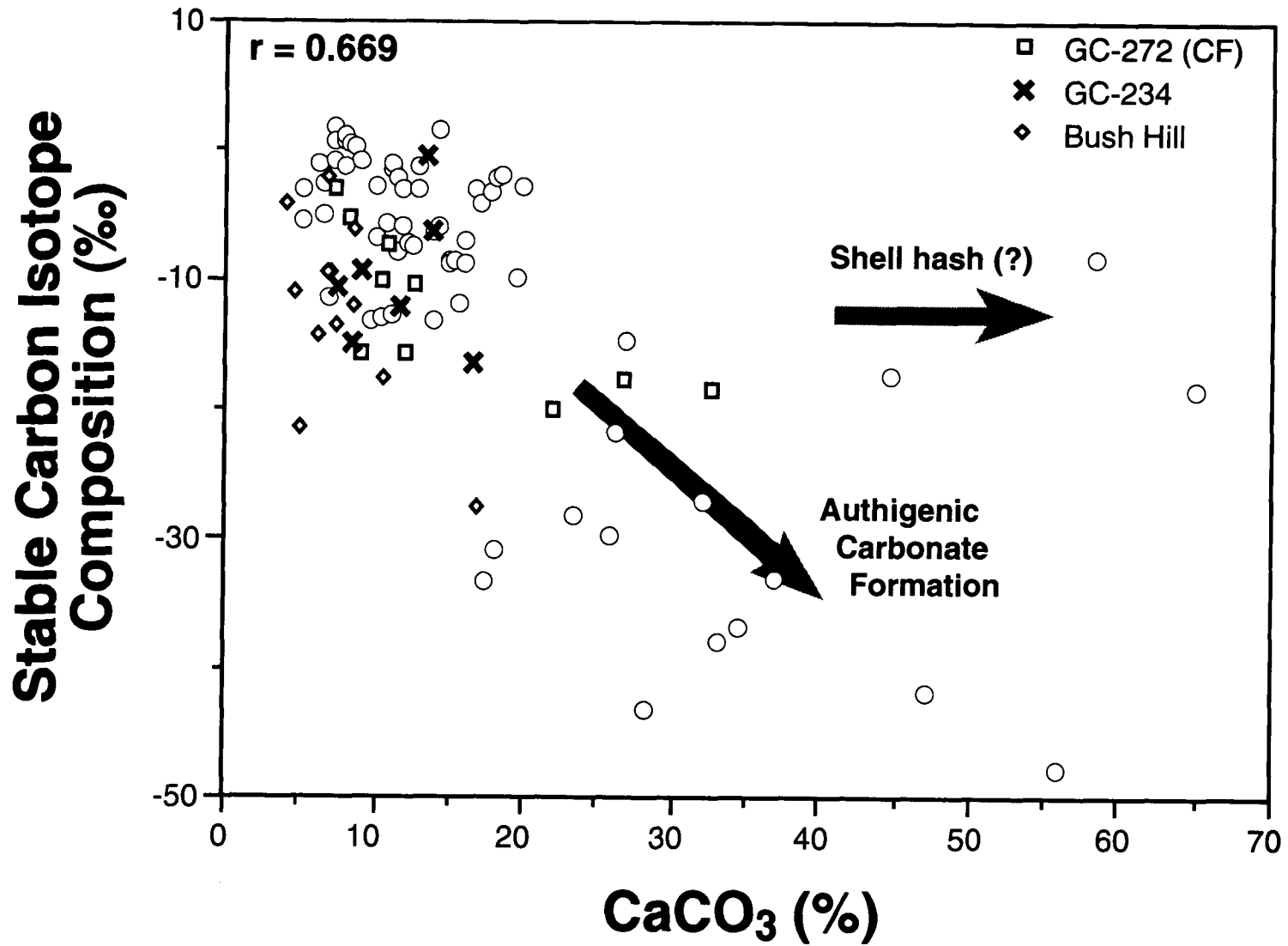
Figure 4.4   Sources of carbonate at seeps. Stable carbon isotope values are expressed in $S^{13}C$ notation.
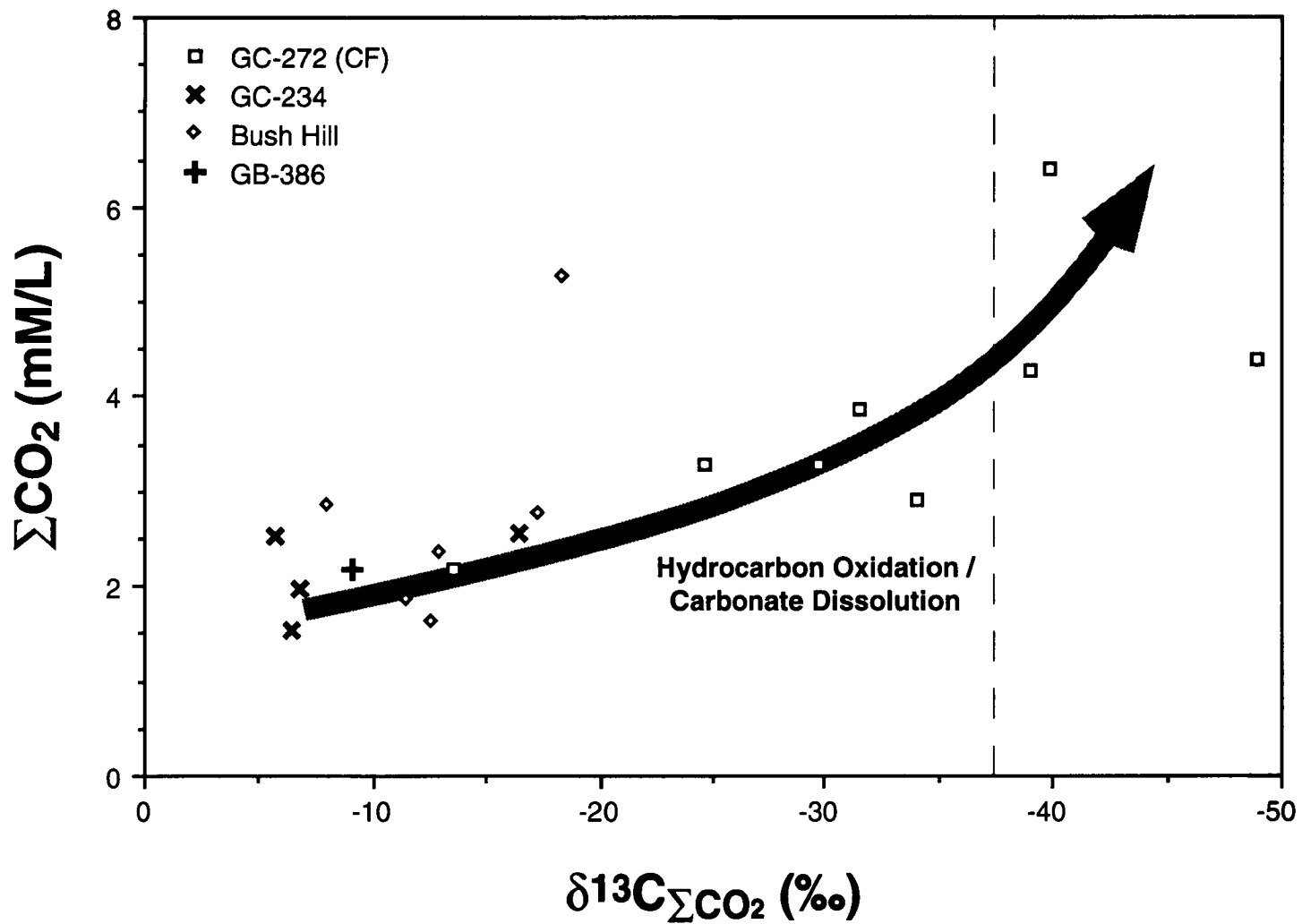
Figure 4.5   Evidence of microbial hydrocarbon oxidation.

fixation of ^{12}C carbon during chemosynthesis (Figure 4.4). A closer examination of these data indicates the importance of various biogeochemical processes at these sites both now and in the past.

One feature of chemosynthetic seep sites that make them difficult to describe in a quantitative manner are steep gradients in the concentrations of chemicals. Seep sites are characterized by a heterogeneous distribution of chemicals. This heterogeneity allows for incompatible elements essential to chemosynthesis to occur in close proximity, i.e., reduced and oxidized compounds. Small scale studies (~1 m^2), which were first undertaken in 1992 at several sites, demonstrated this heterogeneity (Figures 4.6 to 4.9). Methane concentrations can vary by orders of magnitude over just a few centimeters. Hydrates are restricted in areal extent and can occur at or near the sediment/water interface. It is also apparent that heterogeneity occurs in three dimensions. These distributions suggest that relatively small scale microenvironments are pervasive and that individual organismal requirements can be satisfied by transport of chemicals over relatively short distances. Strong elemental gradients appear to determine the biotic and geological heterogeneity of seep communities.

To test our model for geochemical control of community formation we undertook an intensive program of resampling of four of the main study sites during dives in 1993. Our main objectives were (1) to document the processes that affect hydrocarbon composition and modify the seafloor, and (2) to establish the extent to which these processes impact the development of specific components of seep communities.

0 – 5 cm

1.0 m

1.0 m

$C_1 / C_2 \sim 50–100$

n-C_4 / i-C_4 variable 0.5–1.0

200

400

600

800

1000

3 – 15 cm

200

1000

800

600

400

12,152 ppm

2,293 ppm
oil seepage noted

● **Pushcore Locations**   ⊗ **Possible Hydrate**

⊙ **Bacterial Mat**
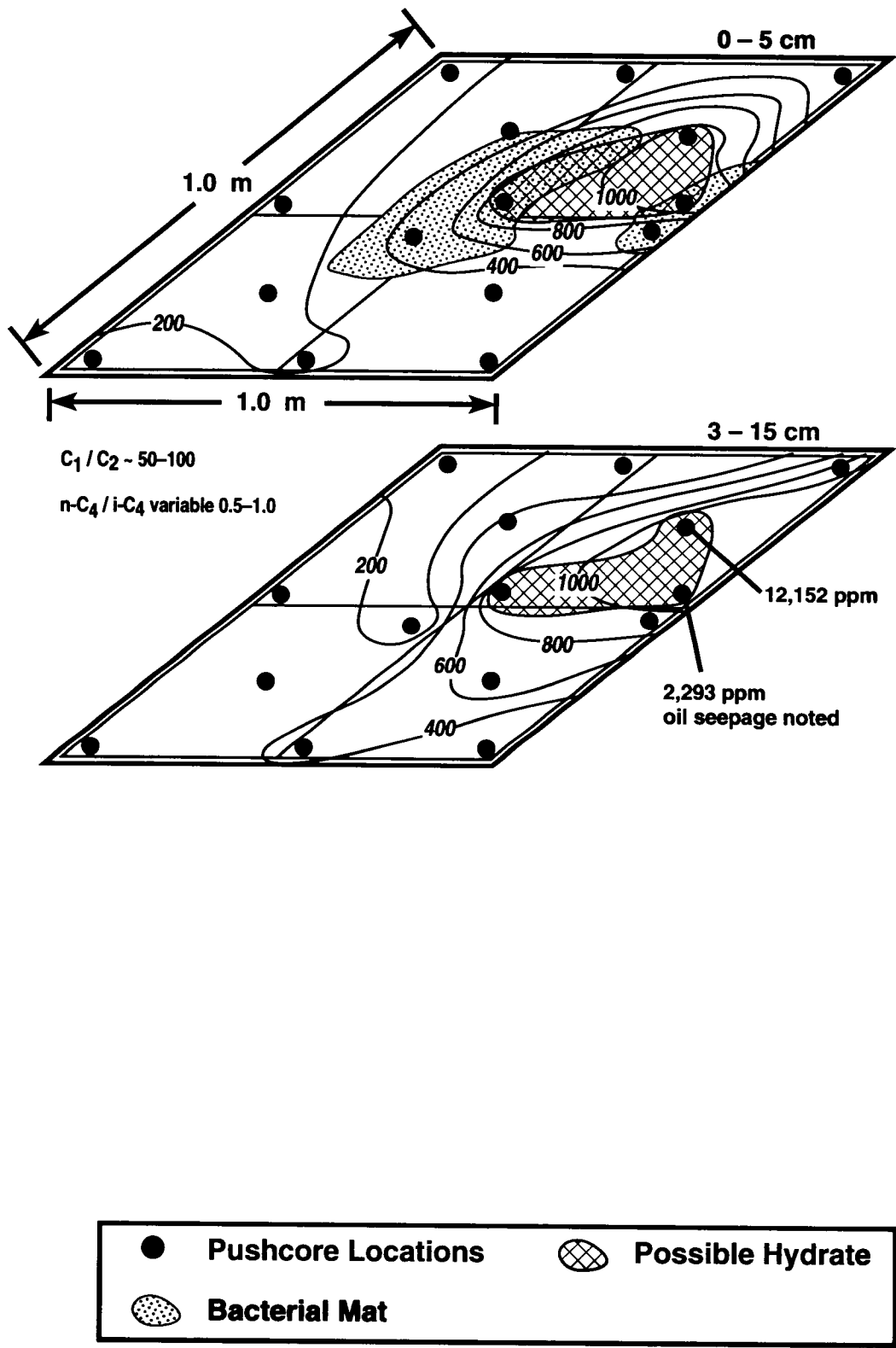
Figure 4.6   GC 184 (Dive 3269) methane concentrations (ppm). Contour intervals
in ppm.

0 – 10 cm

1.0 m

100

200 400

200 100

400 200

100

~1000

37,178 ppm

1.0 m

$C_1 / C_2 \sim 100$

$n\text{-}C_4 / i\text{-}C_4 \sim 0.2\text{--}0.3$

> 10 cm

100 200

400

1000

400 200

100

33,250 ppm

● Pushcore Locations   ⊗ Possible Hydrate

⊙ Orange Mat with White Fringe
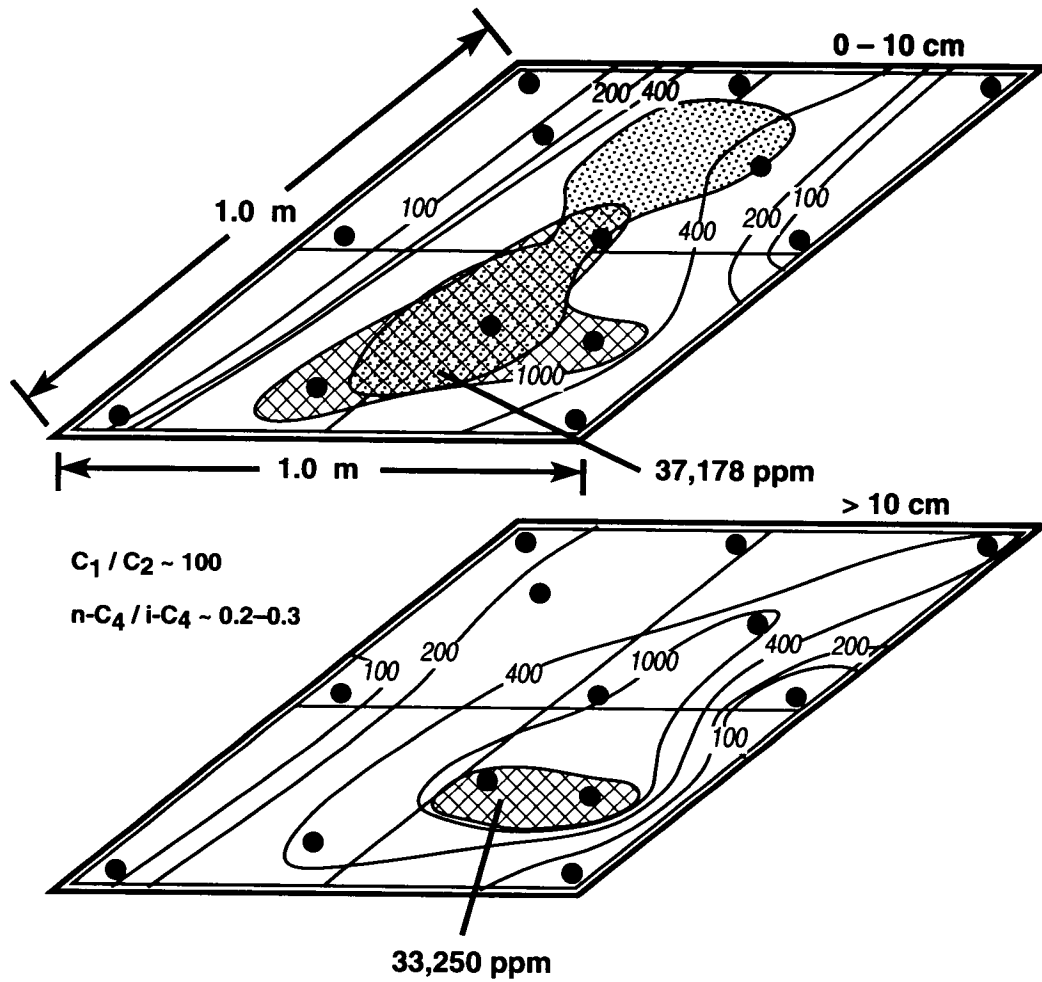
Figure 4.7   GC 234 (Dive 3265) methane concentrations (ppm). Contour intervals in ppm.

4-10

0 – 3 cm

1.0 m

1.0 m

200

100

100

200

$C_1 / C_2 \sim 50$–100

n-C_4 / i-C_4 variable 0.5–1.0

3 – 11 cm

200 400 600 800 1000

400

600 800

1000

11 – 25 cm

● Pushcore Locations   ⊗ Possible Hydrate
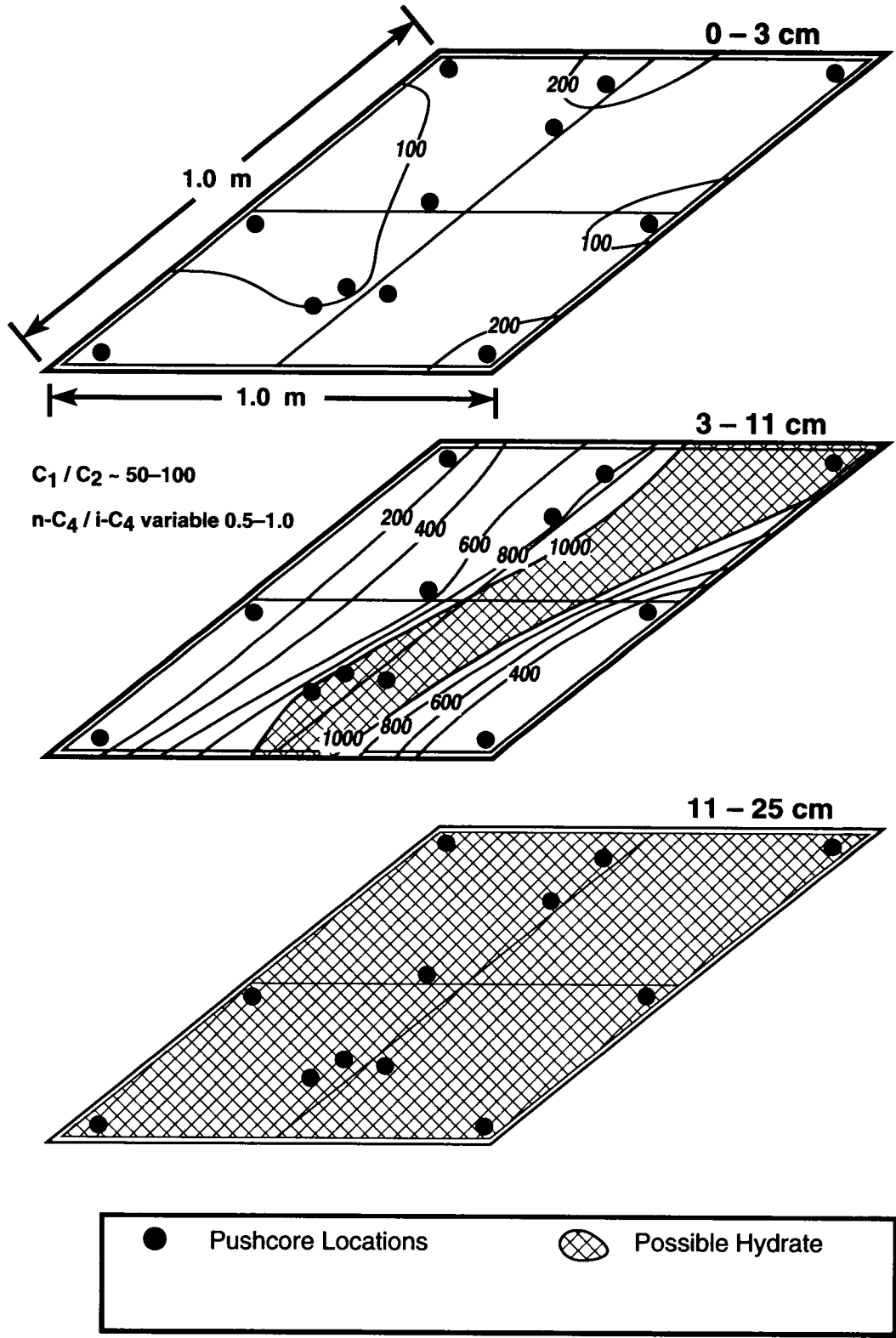
Figure 4.8   GC 272 (Dive 3280) methane concentrations (ppm). Contour intervals in ppm.

0 – 3 cm

100

1.0 m

1.0 m

$C_1 / C_2 \sim 50$

$n\text{-}C_4 / i\text{-}C_4 \sim 2\text{–}3$

100

3 – 9 cm

100

200

200

9 – 15 cm

8,754 ppm

500

400

300

200

100

400

100

200

300

300

200

100

● Pushcore Locations

⬭ Orange Bacterial Mat   ● White Bacterial Mat
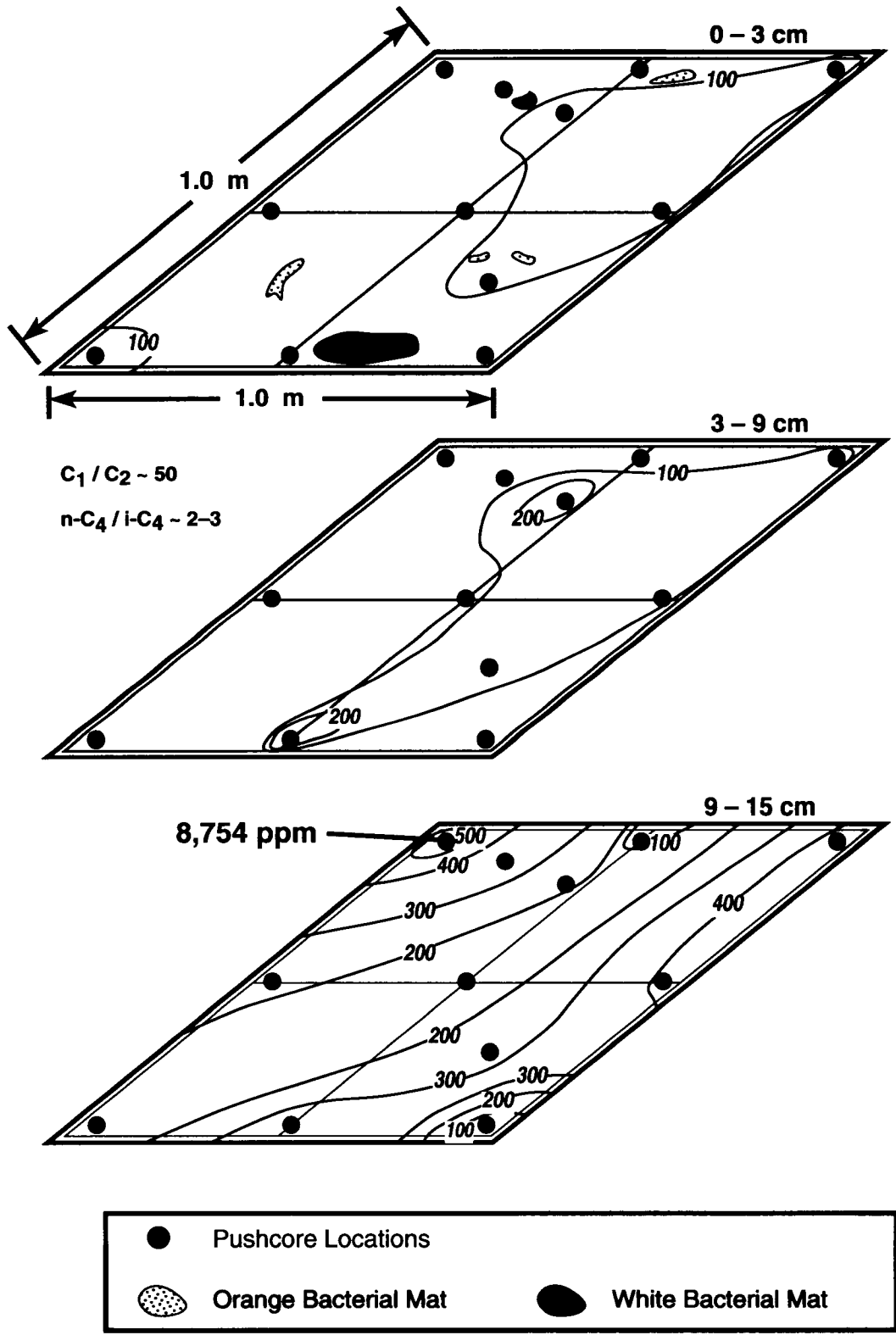
Figure 4.9   GC 272 (Dive 3279) methane concentrations (ppm). Contour intervals
in ppm.

4.2 Experimental

4.2.1 <u>Samples</u>

Samples of sediments (45 cm push-cores) were acquired in 1993 at four of the Study sampling sites (GC 234, 185, 272, 233) in the Green Canyon area of the Gulf slope by the *Johnson Sea-Link* (JSL) research submarine. Samples were transferred to cans after collection, sodium azide bactericide was added, and the cans were then sealed under N_2. Samples were frozen until analysis.

Sediment samples were obtained from specific areas within chemosynthetic communities to document differences in hydrocarbon concentration and composition. Samples GC 234-1 through -12 were acquired during JSL dive 3525 (27° 44.77'N, 91° 13.34'W) at a water depth of about 543 m. Small diameter core tubes (2 cm i.d.) were used to collect densely spaced samples within a 1 m^2 grid straddling an isolated orange and white *Beggiatoa* mat (Figure 4.10). *Beggiatoa* are H_2S-oxidizing bacteria that are widely distributed at seep localities (Sassen et al. 1993b). The larger GC 234 locality is described by MacDonald et al. (1990a).

Samples GC 185-1 through -12 were acquired during JSL dive 3529 at Bush Hill (27° 46.92' N, 91° 30.46' W). Small diameter core tubes (2 cm i.d.) were used to collect sediment samples within a 1 m^2 area beneath part of a *Beggiatoa* mat adjacent to a vestimentiferan tube worm cluster. Water depth at the sample site was approximately 541 m. The tube worms (*Lamelliabrachia* n. sp.) contained bacterial symbionts that oxidize H_2S (MacDonald et al. 1989). Sample GC 185-13 was acquired from a gas hydrate that breached the sea floor nearby on Bush Hill (MacDonald et al. 1994). No other samples of "outcropping" hydrates had been analyzed previously.

Samples GC 272-1 through -7 were acquired using large diameter core tubes (6.5 cm i.d.) during JSL dive 3535 in an area (27°41.28'N, 91°32.45'W) characterized by anoxic sediments with epifaunal vesicomyid clams. Water depth at the site was
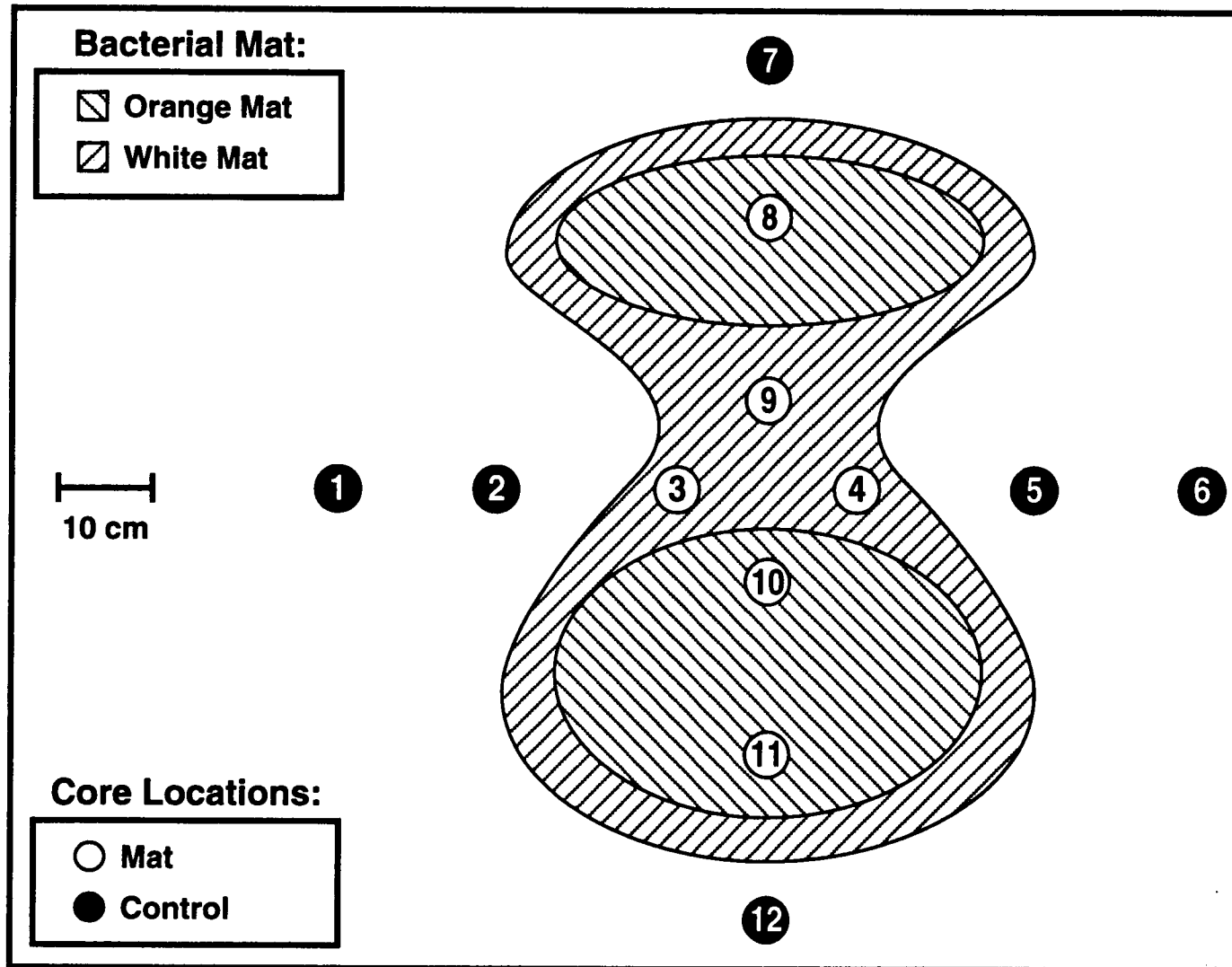
Figure 4.10 Detailed locations of core samples taken from a zoned orange and white *Beggiatoa* mat at the GC 234 locality. Numbers refer to Table 4.1 and 4.2.

approximately 575 m. The clams contained bacterial symbionts that oxidize H_2S (MacDonald et al. 1990a).

Sample GC 233-1 was acquired using a large diameter core tube (6.5 cm i.d.) during JSL dive 3539 (27°43.43'N, 91°16.78'W) adjacent to an anoxic brine pool rimmed with methanotrophic mussels (Seep Mytilid I) at a water depth of about 650 m. The brine pool site is described by MacDonald et al. (1990b).

4.2.2 <u>Methods</u>

We have relied on basic geochemical measurements to provide preliminary insight to oil and C_1-C_5 hydrocarbons of sediments in this reconnaissance study. Methods used for geochemical analysis are similar to those described by Kennicutt et al. (1988a).

Dried and powdered sediment samples were Soxhlet-extracted with hexane for 24 hours, and after reduction in volume, extracts were subjected to C_{15+} gas chromatography using a Hewlett-Packard 5880 chromatograph equipped with a 30 m DB-5 capillary column. This approach yields the total hydrocarbon concentration in sediments. Chromatograms of recent sediments that do not contain oil typically consist of n-alkanes with strong odd-carbon predominance, and a flat baseline because the hydrocarbons that characterize oil tend to be absent or in low abundance. If oil is present, chromatograms typically show an elevated baseline.

The area beneath the elevated baseline is called the unresolved complex mixture (UCM) because naphthenes and other compounds that are difficult to resolve by gas chromatography are present. The n-alkanes and isoprenoids, normally prominent in unaltered oils, were absent or in low abundance in our samples because these compounds had been altered by microbial oxidation. Moreover, oil was present in such great concentration as to generally overprint any higher-plant waxes co-extracted from the sediments. For these reasons, no data on

n-alkanes or isoprenoids are presented. The concentrations of UCM are expressed as ppm by sediment weight.

We analyzed the free C_1-C_5 hydrocarbons in the headspace of canned samples to define hydrocarbon types, and because they are sensitive indicators of bacterial oxidation (James and Burns 1984; Sassen et al. 1988). The C_1-C_5 hydrocarbon gases were separated using a Hewlett-Packard 5710 chromatograph equipped with a 2 m packed alumina column. The concentrations of individual C_1-C_5 hydrocarbons are expressed as ppm by volume.

4.3 Results

Results of analysis of 33 sediment samples from the four chemosynthetic communities sampled in Green Canyon are shown in Table 4.1 (UCM, total C_1-C_5, gas ratios) and Table 4.2 (C_1-C_5 compositions).

4.3.1 Isolated Bacterial Mat at GC 234

The C_{15+} chromatograms of hexane extracts from GC 234 showed a broad UCM characterized by the absence of n-alkanes and isoprenoids (Figure 4.11). UCM concentrations were in the 2,226-7,809 ppm range (mean = 4,039 ppm). Concentrations were highest beneath the mat (mean = 5,650 ppm), and decreased away from the mat (mean = 2,966 ppm).

Total concentrations of C_1-C_5 hydrocarbons were in the 11.5 to 52,926 ppm range (mean = 6,531 ppm). The total C_1-C_5 concentrations were highest beneath the mat (mean = 12,979 ppm), whereas concentrations decreased away from the mat (mean = 83.6 ppm). Gas compositions were dominated by C_1 (predominantly methane), as indicated by gas wetness in the 0.1 to 11.7% range. The lowest gas wetness occurred beneath the orange mat. The i-C_4/n-C_4 ratios

Table 4.1   Concentrations of UCM (ppm by weight) and total C_1-C_5 hydrocarbons (ppm by volume) in sediment samples. Gas wetness - $(C_2$-C_4/C_1-$C_4)$ X 100. (Dashed numbers, e.g. GC 234-1, refer to core locations, see Figure 4.1 for example.)

Sample	UCM	Total C_1-C_5	Gas Wetness	i-C_4/n-C_4
Green Canyon 234				
GC 234-1	2380	11.5	11.7	0.52
GC 234-2	2684	20.1	10.8	0.51
GC 234-3*	ND	169.6	9.8	0.52
GC 234-4*	3928	104.1	14.7	0.58
GC 234-5	2226	45.9	2.7	0.56
GC 234-6	3393	165.2	1.7	1.77
GC 234-7	4513	128.7	2.6	0.66
GC 234-8*	7809	1257.9	2.9	0.34
GC 234-9*	ND	97.6	3.0	0.48
GC 234-10*	4168	23316.1	0.1	0.59
GC 234-11*	6693	52925.9	0.4	37.49
GC 234-12	2597	130.1	2.6	2.04
Green Canyon 185				
GC 185-1	35209	33035.2	1.8	39.02
GC 185-2	38992	300.8	15.1	ND
GC 185-3	23519	363.4	26.5	15.32
GC 185-4	18702	2486.1	1.5	ND
GC 185-5	35938	6780.2	69.4	585.62
GC 185-6	21667	7180.7	0.5	ND
GC 185-7	25802	10643.3	0.8	37.14
GC 185-8	21587	12602.4	1.9	1.14
GC 185-9	23145	31136.8	3.4	55.86
GC 185-10	14849	8723.9	1.0	2.92
GC 185-11	20312	18057.6	7.0	121.75
GC 185-12	17583	1138.1	17.1	92.50
GC 185-13	ND	153566	73.3	0.18
Green Canyon 272				
GC 272-1	1060	47436.9	8.5	0.20
GC 272-2	1464	26398.1	0.2	8.47
GC 272-3	3294	39682.7	0.1	8.51
GC 272-4	3312	38951.3	0.3	30.88
GC 272-5	1089	23986.8	0.3	5.53
GC 272-6	328	7426.7	5.6	3.76
GC 272-7	1463	17476.5	0.3	5.25
Green Canyon 233				
GC 233-1	82	8834.2	0.1	1.88

* = mat samples

Table 4.2   Concentrations of individual C$_1$-C$_5$ hydrocarbons (ppm by volume) in sediment samples.

Sample	Methane	Ethane	Ethylene	Propane	Propylene	i-Butane	n-Butane	i-Pentane	n-Pentane
Green Canyon 234									
GC 234-1	10.1	0.5	0.1	0.4	0.0	0.2	0.3	0.0	0.0
GC 234-2	17.7	0.8	0.2	0.6	0.1	0.2	0.5	0.0	0.0
GC 234-3*	149.6	6.7	2.6	4.3	1.0	1.8	3.5	0.0	0.0
GC 234-4*	82.7	5.4	1.7	3.7	5.4	1.9	3.3	0.0	0.0
GC 234-5	44.5	0.9	0.1	0.2	0.1	0.0	0.1	0.0	0.0
GC 234-6	162.3	2.5	0.1	0.2	0.0	0.0	0.0	0.0	0.0
GC 234-7	125.1	2.7	0.2	0.3	0.1	0.1	0.2	0.0	0.0
GC 234-8*	1218.7	19.5	1.9	6.1	0.9	2.8	8.1	0.0	0.0
GC 234-9*	92.9	1.6	1.1	0.7	0.7	0.2	0.4	0.0	0.0
GC 234-10*	23289.5	23.7	0.6	1.0	0.3	0.4	0.6	0.0	0.0
GC 234-11*	52702.7	187.7	0.4	7.2	0.2	26.9	0.7	0.0	0.0
GC 234-12	124.4	1.8	1.4	0.6	0.9	0.7	0.3	0.0	0.0
Green Canyon 185									
GC 185-1	31504.9	170.0	0.2	157.2	0.1	235.1	6.0	961.6	0.0
GC 185-2	225.0	8.9	0.2	10.1	35.7	20.8	0.0	0.0	0.0
GC 185-3	266.9	43.8	0.1	26.7	0.0	24.3	1.6	0.0	0.0
GC 185-4	2449.0	13.7	0.3	4.0	0.1	18.9	0.0	0.0	0.0
GC 185-5	485.6	104.5	0.6	74.7	0.3	920.5	1.6	5192.4	0.0
GC 185-6	7143.5	34.6	0.3	2.3	0.0	0.0	0.0	0.0	0.0
GC 185-7	10554.2	59.7	0.3	8.5	0.1	19.9	0.5	0.0	0.0
GC 185-8	12362.9	97.9	0.0	36.7	0.0	56.0	48.9	0.0	0.0
GC 185-9	28783.5	307.4	0.2	223.8	0.0	460.9	8.3	1352.7	0.0
GC 185-10	8631.9	81.3	0.6	8.0	0.2	1.4	0.5	0.0	0.0
GC 185-11	14631.6	198.4	0.6	173.6	0.4	715.6	5.9	2331.7	0.0
GC 185-12	942.6	92.7	0.5	45.0	0.2	56.6	0.6	0.0	0.0
GC 185-13	24132.9	13011.4	0.0	15634.3	0.0	6210.0	35074.3	57870.0	1632.9
Green Canyon 272									
GC 272-1	40594.9	2252.5	0.0	607.4	0.2	151.9	759.3	2218.7	852.1
GC 272-2	26347.0	44.8	0.2	3.0	0.2	2.6	0.3	0.0	0.0
GC 272-3	39626.4	49.1	0.1	4.2	0.1	2.5	0.3	0.0	0.0
GC 272-4	38846.6	78.3	0.1	6.4	0.2	19.0	0.6	0.0	0.0
GC 272-5	23909.4	68.1	0.2	5.1	0.2	3.3	0.6	0.0	0.0
GC 272-6	7013.2	105.8	0.6	149.3	0.4	124.4	33.1	0.0	0.0
GC 272-7	17424.3	46.5	0.2	3.2	0.2	1.7	0.3	0.0	0.0
Green Canyon 233									
GC 233-1	8829.1	4.7	0.1	0.2	0.0	0.0	0.0	0.0	0.0

* = mat samples
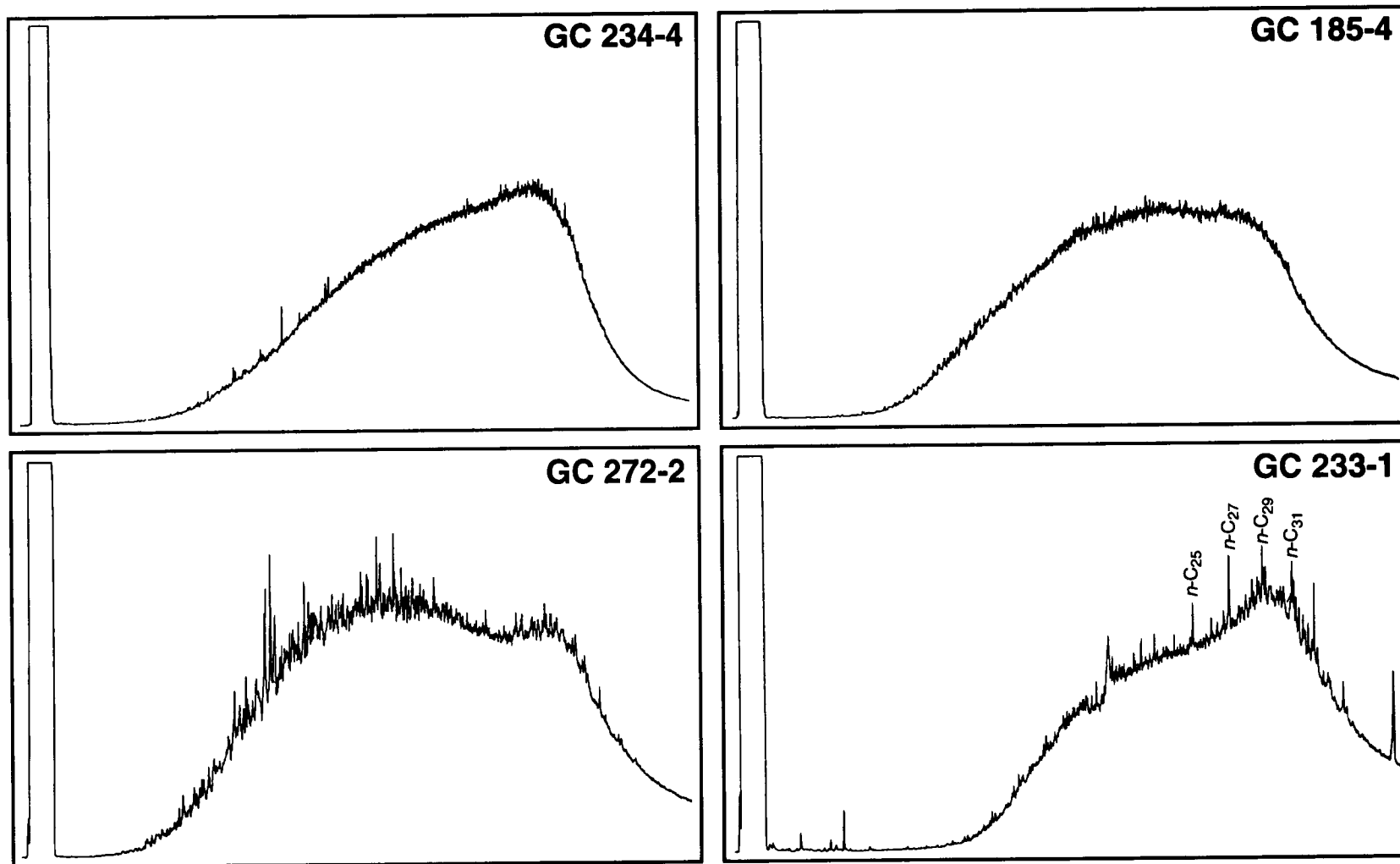
Figure 4.11   Examples of C_{15+} chromatograms of hexane extracts from the GC 234, GC 185, GC 272, and GC 233 areas. All chromatograms from these areas show an UCM feature, and the absence of the n-alkanes and isoprenoids present in oil.

the 0.3-2.0 range, with the exception of a single orange mat sample (37.5). C_5 hydrocarbons were absent or below detection limits.

4.3.2 Bacterial Mat and Tube Worms at GC 185 (Bush Hill)

C_{15+} chromatograms from samples GC 185-1 through -12 exhibit an UCM characterized by the absence of n-alkanes and isoprenoids (Figure 4.11). The UCM concentrations were in the 17,583 to 38,992 ppm range (mean = 24,775 ppm).

Total concentrations of C_1-C_5 hydrocarbons were in the 301-33,035 ppm range (mean = 11,037 ppm). Gas compositions were generally dominated by C_1, but there were exceptions. The range of gas wetness was wide (0.5-69.4%). In three samples, n-C_4 was absent or below detection limits. i-C_4/n-C_4 ratios in nine samples were in a wide range, 1.1-586. Although n-C_5 was below detection limits in these samples, i-C_5 was a significant component in four samples (961-5,192 ppm).

4.3.3 Gas Hydrate at GC 185 (Bush Hill)

Total C_1-C_5 concentration of the hydrate sample (GC 185-13) was 153,567 ppm. The C_2-C_4 hydrocarbons were major components of the hydrate, as reflected by a gas wetness of 73.3%. In contrast to other samples, i-C_5 and n-C_5 were significant components. The i-C_4/n-C_4 ratio was 0.18 and the i-C_5/n-C_5 ratio was 35.4.

4.3.4 Chemosynthetic Clams at GC 272

C_{15+} chromatograms of samples from an area characterized by vesicomyid clams only exhibited UCMs (Figure 4.11). The UCM concentrations were in the 328-3,312 ppm range (mean = 1,716 ppm). Total concentrations of C_1-C_5 hydrocarbons were in the 7,427-47,437 ppm range (mean = 28,766 ppm). Gas compositions were dominated by C_1, as indicated by gas wetness in the 0.1-8.5%

range. The i-C_4/n-C_4 ratios varied in the 0.2-30.9 range. The C_5 hydrocarbons were either absent or below detection limits in all but one sample.

4.3.5 Chemosynthetic Mussels at GC 233

The C_{15+} chromatogram of sediment from the brine pool (Seep Mytilid I) only exhibited UCMs with slight overprinting from the co-extraction of higher-plant waxes from recent sediments (Figure 4.11). The UCM concentration was 82 ppm. The total concentration of C_1-C_5 hydrocarbons was 4,903 ppm. C_1 dominated, as indicated by a gas wetness of about 0.1%. The C_4 and C_5 hydrocarbons were either absent or below detection limits.

4.4 Discussion

4.4.1 Hydrocarbons

Hydrocarbon compositions at chemosynthetic communities appeared to be effected by multiple processes including (1) rates of migration of thermogenic hydrocarbons to sediments, (2) differing levels of bacterial oxidation, and (3) exclusions related to hydrate formation. The presence and type of hydrocarbon alteration appeared to strongly influence the chemoautotrophic fauna. We emphasize that large differences may occur within spatial scales of less than 1 m, helping to explain the great heterogeneity observed *between* and *within* chemosynthetic communities.

The most basic observation concerning the *Beggiatoa* mat at the GC 234 sampling locality is that concentrations of UCM (Figure 4.12) and C_1-C_5 hydrocarbons (Figure 4.13) were higher beneath the mat than in control cores near the mat. It should be stressed that the concentrations of C_1-C_5 hydrocarbons beneath the mat were an order of magnitude higher than in control samples only 10 cm from mat margins (Table 4.1 and Figure 4.10). The result is consistent with the
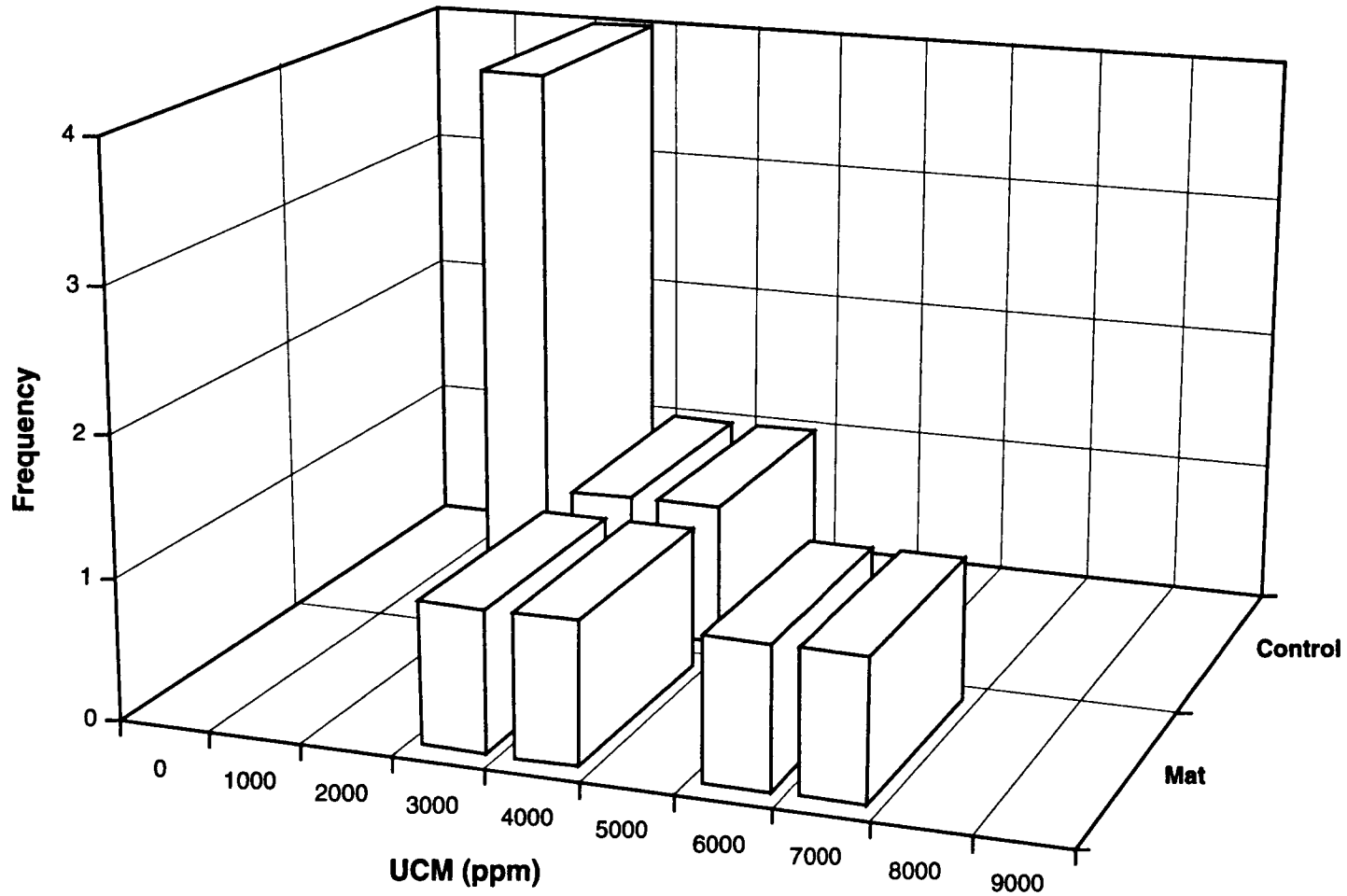
Figure 4.12 Histograms illustrating that the concentrations of UCM in core samples of the GC 234 *Beggiatoa* mat are higher beneath the mat than in control cores away from the mat.
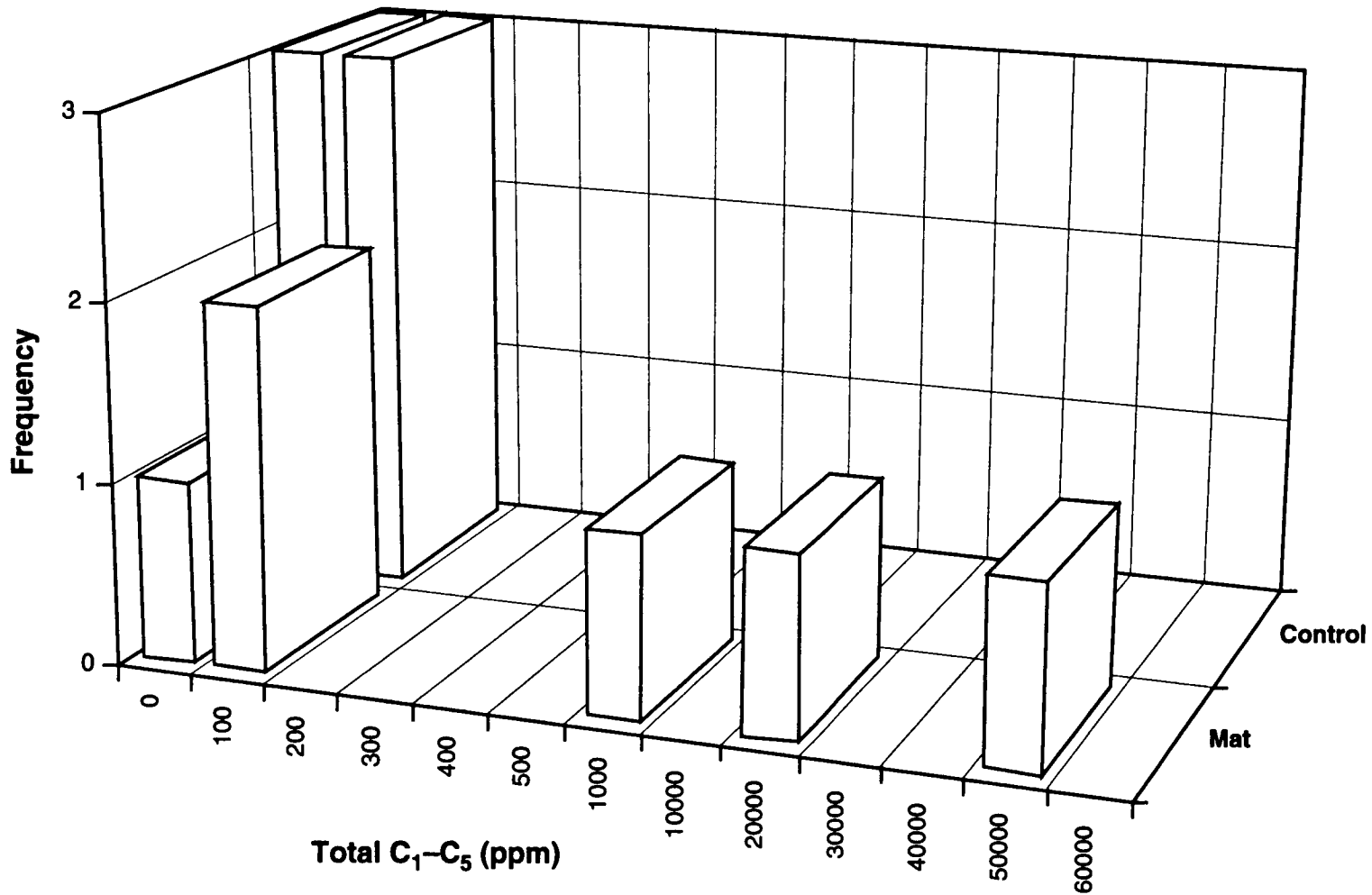
Figure 4.13 Histograms illustrating that the concentrations of total C_1-C_5 hydrocarbons in core samples of the GC 234 *Beggiatoaa* mat are higher beneath the mat than in control cores away from the mat.

tight coupling between mats and hydrocarbon gradients suggested by Sassen et al. (1993b).

The effects of aerobic microbial oxidation can be recognized since the prominent n-alkanes and the branched-chain isoprenoids originally present in crude oil are preferentially degraded, leaving a residue of UCM (Sassen et al. 1993b). This sequence is illustrated in Figure 4.14 by comparison of an unaltered oil from a subsurface reservoir and an degraded seep extract. The C_{15+} chromatograms of extracts from the GC 234 sampling area were altered by bacterial oxidation, as shown by the example in Figure 4.11.

The i-C_4/n-C_4 ratios of low molecular weight hydrocarbons can provide a sensitive index of the degree of bacterial oxidation (Sassen et al. 1988). Since n-C_4 is preferentially oxidized by bacteria, i-C_4 tends to become more significant as this process advances (Winters and Williams 1969). The lowest gas wetness values and highest i-C_4/n-C_4 ratio were from samples acquired from directly beneath the mat (Table 4.1). Bacterial oxidation effects (as indicated by the C_1-C_5 hydrocarbons) thus appeared more advanced beneath the mat than away from the mat.

It should be emphasized that the highest hydrocarbon concentrations, as well as the most advanced bacterial oxidation, occurred beneath the mat we sampled rather than away from the mat. Hydrocarbons set into motion complex bacterial interactions within sediments (Sassen et al. 1993b). Hydrocarbon-oxidizing bacteria produce CO_2. When O_2 is depleted, sulfate-reducing bacteria become active and produce H_2S. *Beggiatoa* mats occupy the interface between anoxic sediments and the oxic water column. The mats oxidize H_2S to first form granules of elemental sulfur within cells, and ultimately oxidize the elemental sulfur to form sulfate.

The *Beggiatoa* mat adjacent to the tube worm cluster at GC 185 and the mat on GC 234 were similar in that thermogenic hydrocarbons altered by bacterial oxidation were present at both localities. However, the mean concentration of UCM
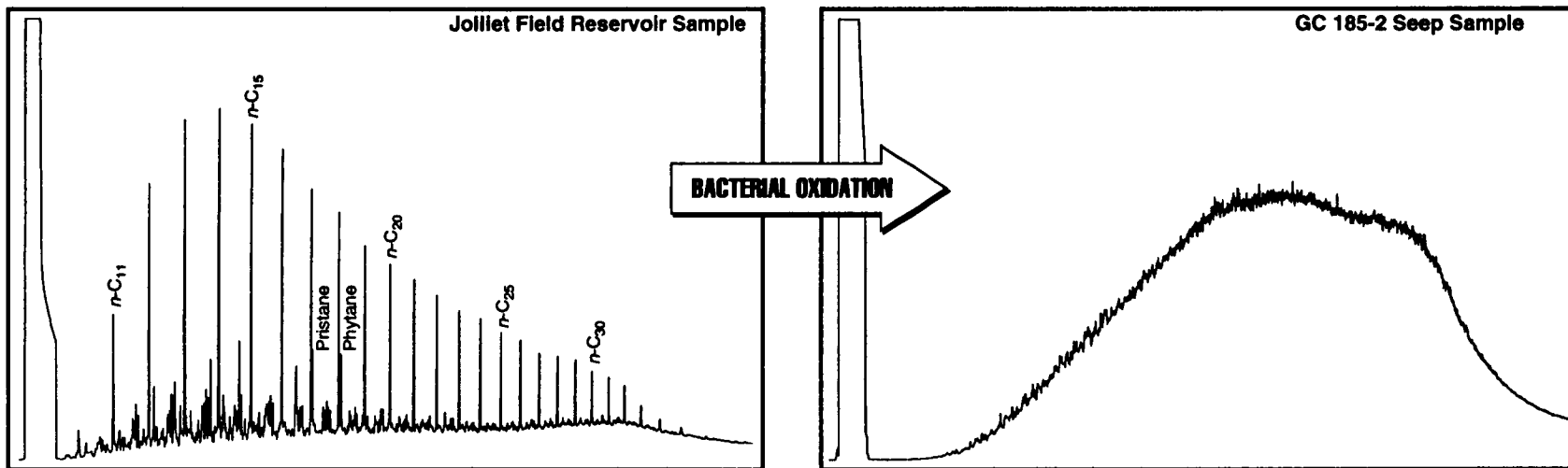
Figure 4.14 Comparison of C_{15+} chromatographs of a subsurface reservoir sample of oil from Jolliet Field in GC 184 and a seep sample from GC 185 (Bush Hill) illustrates the effects of bacterial oxidation.
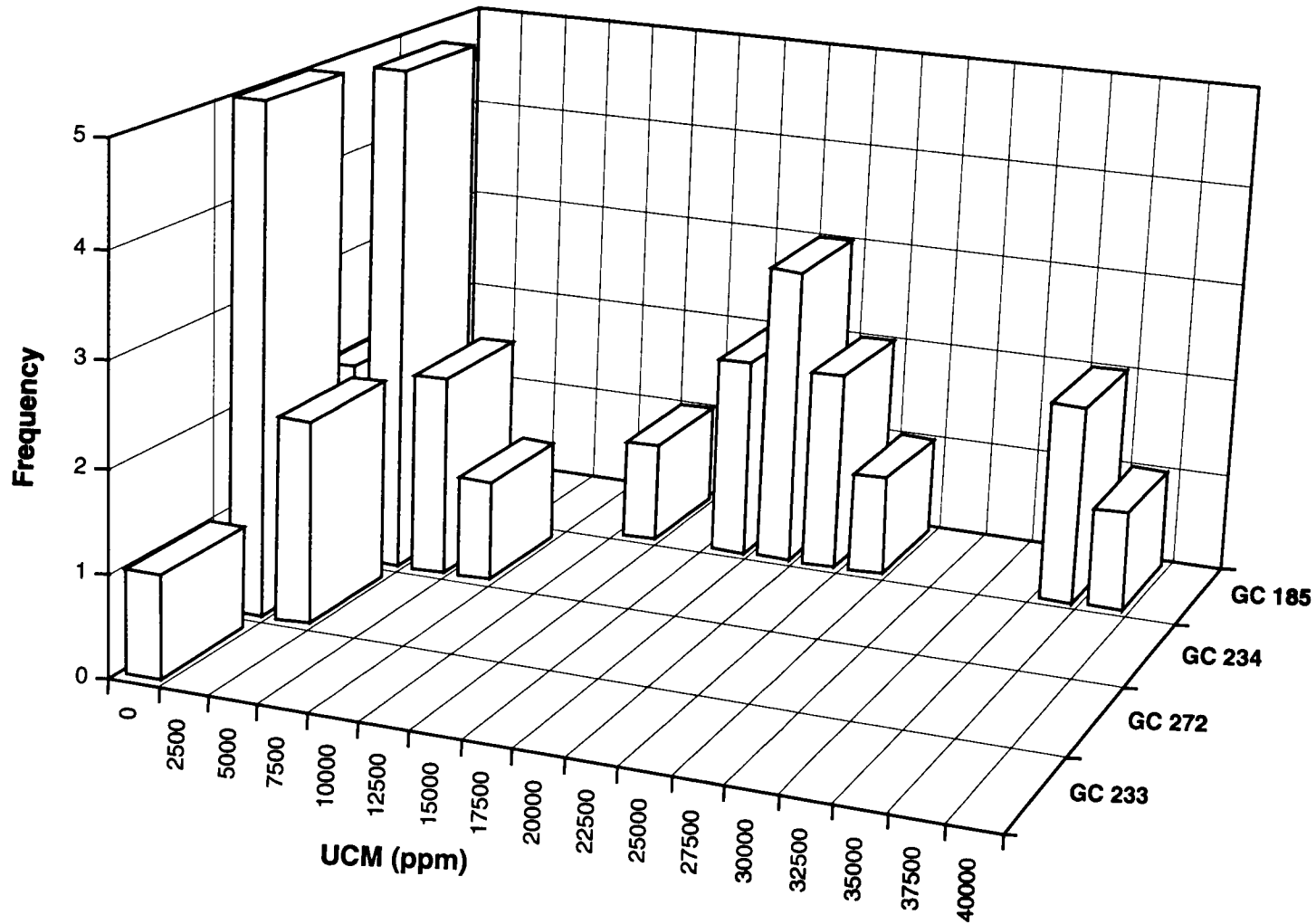
Figure 4.15   Histograms of illustrating differences in UCM concentrations between the four study areas. Note the relatively high UCM concentrations measured in samples from GC 185 (Bush Hill).

at GC 185 was higher (24,775 ppm) than at GC 234 (4,039 ppm) (Figure 4.15). Mean concentrations of C_1-C_5 hydrocarbons at GC 185 are also higher (11,037 ppm) than at GC 234 (6,531 ppm) (Figure 4.16).

Bacterial oxidation decreases gas wetness by degrading the thermogenic C_2-C_4 hydrocarbons, a process accentuated in natural systems by addition of biogenic C_1 (James and Burns 1984; Sassen et al. 1988). GC 185 samples showed a much wider range of gas wetness (0.5-69.4%) than noted at GC 234 (0.1-14.7%). Unusually high gas wetness in some GC 185 samples argue that another process affected our results. The i-C_4/n-C_4 ratios at GC 185 were quite variable (1.1-586). Many of the i-C_4/n-C_4 ratios at GC 185 were high enough to imply more advanced bacterial oxidation effects than at the GC 234 area, where values were lower (0.3-37.5). However, unusually low i-C_4/n-C_4 ratios in a few GC 185 samples also suggest that a process other than microbial oxidation affected our results. Relatively high concentrations of the i-C_5 hydrocarbon in four GC 185 samples also needs to be explained.

A core sample of gas hydrate that breached the seafloor (GC 185-13) was obtained near our other Bush Hill sample site. The abundant C_2-C_5 hydrocarbons (gas wetness = 74.3%) contrasted with previously analyzed hydrate from the Gulf slope in which C_1 is the dominant component (Brooks et al. 1984; 1986). The i-C_4/n-C_4 ratio of the hydrate is quite low (0.18), whereas the i-C_5/n-C_5 ratio was high (35.4). It should be emphasized that the n-C_4 and i-C_5 hydrocarbons were strongly favored as guest molecules in Structure II hydrate (Ripmeester and Ratcliffe 1991). Thus, there is a straightforward explanation for our data on GC 185 sediments. Since the GC 185 area contained abundant hydrate (Sassen et al. 1993a), it is likely that a number of sediment samples contained small amounts of Structure II hydrate.
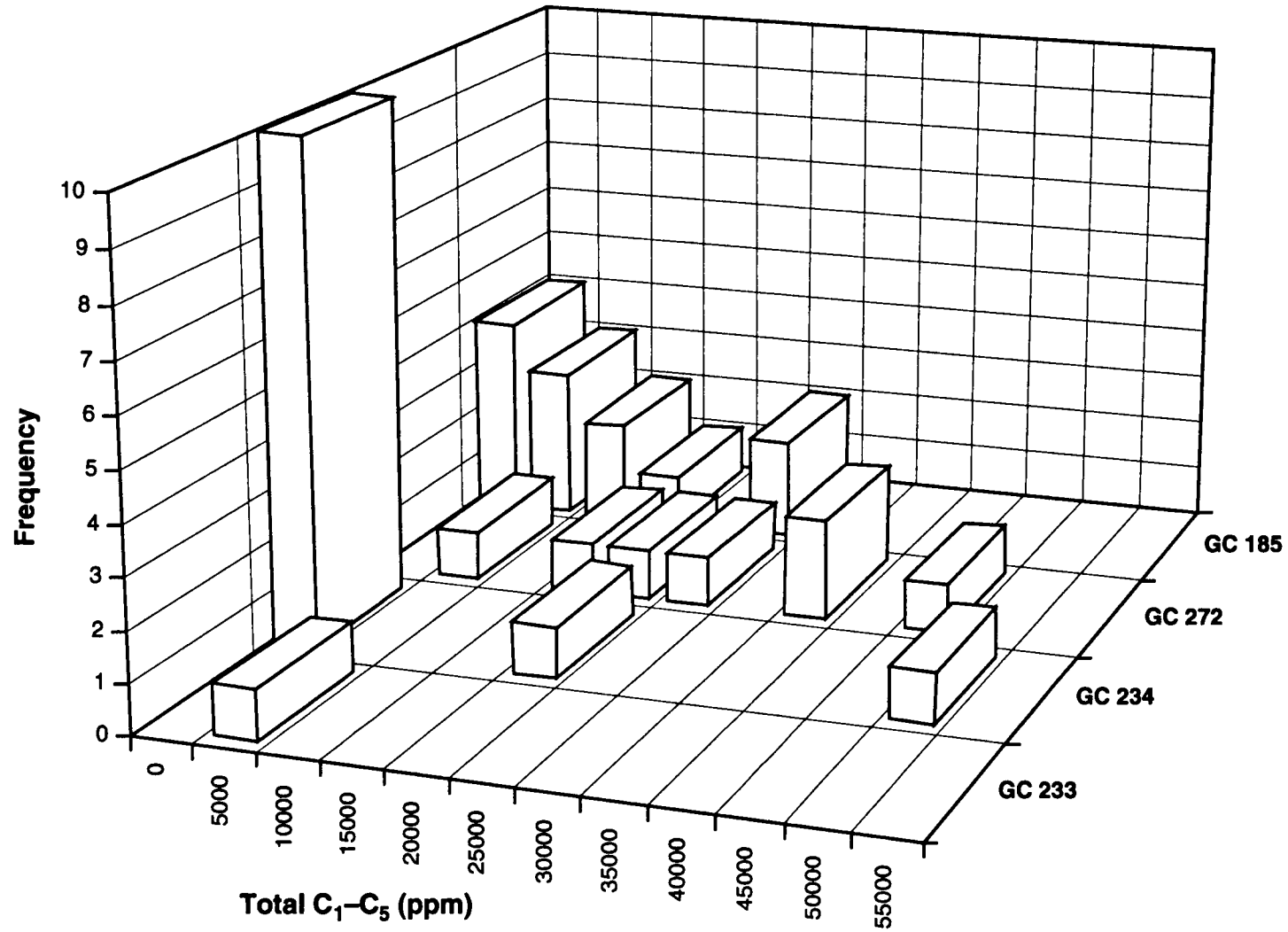
Figure 4.16. Histograms illustrating differences in total C_1–C_5 hydrocarbon concentrations between the four study areas.

The C_{15+} chromatograms of sediment extracts from a vesicomyid clam environment on GC 272 showed that oil has been affected by bacterial oxidation (Figure 4.10). The concentration of UCM was lower (mean = 1,716 ppm) than noted at GC 234 or GC 185 (Figure 4.15). C_1-C_5 concentrations (mean = 28,766 ppm), however, were higher than at other sites (Figure 4.16). C_1 dominated the compositions. The i-C_4/n-C_4 ratios tended to be lower than noted in samples adjacent to tube worm clusters at GC 185, suggesting that bacterial oxidation effects are less advanced.

The sample of sediment from the anoxic brine pool on GC 233 colonized by the Seep Mytilid I was characterized by low UCM (82 ppm). The dominant lower molecular weight hydrocarbon was C_1 (8,829 ppm). The low gas wetness (0.1%), and the absence of C_4 and C_5 hydrocarbons in our sediment sample, suggest a dominantly biogenic origin. This is consistent with the carbon isotopic composition of C_1 ($S^{13}C$ = -63.8‰) reported at the site (MacDonald et al. 1990b). The brine pool thus differs in that thermogenic hydrocarbons appear to be less significant than at other sites.

4.4.2 Seeps and Vents

Differences between seeps and vents need to be emphasized. Seeps are defined as areas where hydrocarbons accumulate in sediments and do not enter the water column in large volumes; vents are specific sea-floor features where hydrocarbons and other fluids bypass the sediments and enter the water column, creating gas bubble trains and natural oil slicks. There is geochemical evidence suggesting that, at least in some cases, the geochemistry of hydrocarbons can differentiate seeps from vents. Our data showed that complex chemosynthetic communities were associated with sea-floor seeps where high concentrations of oil and gas altered by bacterial oxidation occurred in sediments. In contrast,

chemoautotrophic fauna other than *Beggiatoa* mats were not observed near a mud volcano on GC 143 where an oil and gas episodically vented to the water column (Roberts and Neurauter 1990). Since abundant hydrocarbons were present at both seeps and vents, it is surprising that we did not see complex communities in both situations.

A C_{15+} chromatogram of oil-stained sediments from the active GC 143 mud volcano is shown in Figure 4.17. The chromatogram has unusual features including (1) a strongly elevated baseline (UCM) consistent with intense bacterial oxidation of oil, and (2) an envelope of *n*-alkanes and isoprenoids from oil that has not been significantly impacted by bacterial oxidation. This is consistent with episodic rather than continuous venting at the GC 143 mud volcano. Bacterial oxidation, at least at present, appears unable to keep pace with high rates of hydrocarbon venting.

4.4.3 Sea-Floor Modification at Seeps

Understanding why oil composition at seafloor seeps differs from that at vents could shed new light of the early development of complex chemosynthetic communities, particularly at GC 185 (Bush Hill). From the standpoint of the H_2S requirements of chemosynthetic communities, venting is negative since hydrocarbons needed to promote bacterial processes in sediments are lost to the water column. Unless hydrocarbons are retained in sediments, hydrocarbon-oxidizing bacteria will not deplete O_2, and bacterial sulfate reduction will be inhibited.

Beggiatoa mats appear to be so widely distributed because they are well adapted to rapid colonization of the many small or transient seep sites that provide energy and carbon sources on the Gulf slope (Sassen et al. 1993b). Our data showed a clear link to concentration gradients of thermogenic hydrocarbons, but mats also occurred at seeps of purely biogenic C_1 where UCM was present in low abundance
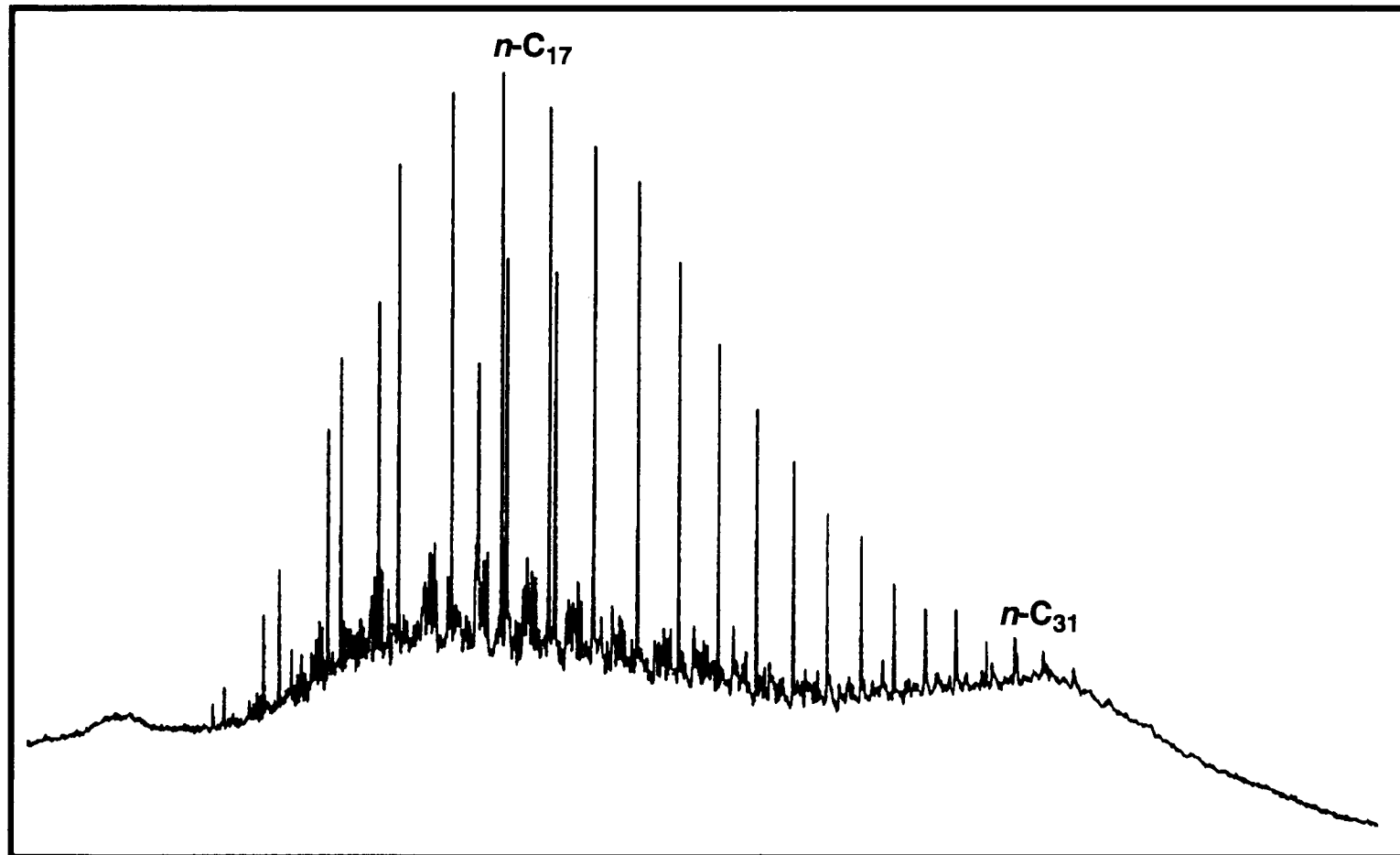
Figure 4.17. A C_{15}^+ chromatogram of sediments from a mud volcano on GC 143. Unusual features include a strongly elevated baseline (UCM) consistent with the effects of bacterial oxication that is overprinted by the n-alkanes and isoprenoids characteristic of unaltered oil from recent venting.

(Sassen et al. 1993b). Bacterial oxidation of any hydrocarbon type depletes O_2 in sediments, permitting the bacterial sulfate reduction that provides the mats with H_2S.

We propose that *Beggiatoa* mats and other bacteria play a role in starting a process of seafloor modification in areas of long term thermogenic seepage. *Beggiatoa* mats are thought to retard hydrocarbon loss to the water column, a function that would enhance production of the H_2S needed by the mats. This "biologic barrier" at the interface between sediments and the water column could also enhance precipitation of authigenic carbonate rock to further seal the seafloor (Sassen et al. 1993b).

Tube worms, in contrast, appear to occupy environments that have been modified by thermogenic seepage effects over a long span of time. The GC 185 (Bush Hill) site, for example, is associated with active faults that serve as conduits for vertical migration of oil and associated gas from subsurface reservoirs of nearby Jolliet Field (Sassen et al. 1993a). Since subsurface reservoirs of Jolliet Field were charged with oil and gas during the Pleistocene, hydrocarbons probably began to impact the seafloor at that time (Sassen et al. 1993a). The abundant authigenic carbonate rock that accumulated at our tube worm site (MacDonald et al. 1989), as well as over shallow salt and faults north of Jolliet Field (Roberts et al. 1989), provides conclusive evidence of seepage over a long span of time.

The highest UCM concentrations measured in the present study were adjacent to a vestimentiferan tube worm cluster on Bush Hill (GC 185). An empirical association of tube worms with oily sediments at GC 185 has been documented previously (MacDonald et al. 1989). Based on our new data, however, we can move further towards understanding why this relationship exists. Both migration and bacterial oxidation of hydrocarbons are rapid at this site. C_{15+} chromatograms only showed a UCM residue because the *n*-alkanes and isoprenoids

were destroyed by bacterial oxidation. The C_1-C_5 hydrocarbons from this site were particularly impacted by bacterial oxidation since the highest i-C_4/n-C_4 ratios were measured there (Table 4.1). Furthermore, n-C_4, i-C_5, and n-C_5 were absent or below detection limits in some samples (Table 4.2).

We suggest that the vestimentiferan tube worms were so abundant at GC 185 because modification of the site by seep-related bacterial processes was advanced. Relatively rapid seepage has occurred there since the Pleistocene, creating biologic barriers and relatively impermeable seals of authigenic carbonate rock and gas hydrate that retain hydrocarbons within sediments. Moreover, hydrate bodies could serve as buffers to maintain hydrocarbons in sediments for bacterial activity should hydrocarbon migration rates fluctuate over time. The intense bacterial oxidation of abundant hydrocarbons at GC 185 triggers the rapid production of the H_2S required by the tube worms, favoring their proliferation.

Another requirement of tube worms could help explain why they need a more specialized habitat than, for example, the adventitious *Beggiatoa* mats. Tube worms appear to need a hard substratum as a point of attachment (H.H. Roberts personal communication), and authigenic carbonate rock provides that in an otherwise unfavorable mud-dominated environment. A long span of time is required to precipitate enough carbonate rock to serve large populations of tube worms.

Results from the GC 272 site move us closer to understanding the relation of hydrocarbons to the vesicomyid clam environment. The C_{15+} chromatograms showed evidence of bacterial oxidation, but UCM concentrations were low (1,716 ppm) in comparison to GC 185 or GC 234. The C_1-C_5 hydrocarbon concentrations were high (mean = 28,766 ppm), but showed low gas wetness values consistent with both bacterial oxidation and strong dilution by biogenic C_1 (Table 4.1). It could be that the clams persist in a relict oil seep environment where the rate of oil seepage

has declined from higher levels in the past, or perhaps gas seepage triggers H_2S production instead of oil.

The composition of hydrocarbons sampled in association with the Seep Mytilid I (GC 233) was distinct since these organisms are methanotrophic. UCM was not present in significant concentration in sediments, and the main type of low molecular hydrocarbon was biogenic C_1. This does not imply a negative correlation between the Seep Mytilid I and other environments where thermogenic methane predominates, however, since this organism is known to utilize either biogenic and thermogenic C_1 as available (MacDonald et al. 1990a).

4.5   Conclusions

1.   Sediment samples from beneath an isolated mat of H_2S-oxidizing bacteria at GC 234 contained oil (mean = 5,650 ppm) and C_1-C_5 hydrocarbons (mean = 12,979 ppm) that are altered by bacterial oxidation. Control cores away from the mat contained lower concentrations of oil (mean = 2,966 ppm) and C_1-C_5 hydrocarbons (mean = 83.6 ppm). Bacterial oxidation of hydrocarbons depletes O_2, triggering bacterial sulfate reduction to produce the H_2S needed for mat development.   Moreover, CO_2 from the bacterial oxidation precipitates as authigenic carbonate rock, beginning a process that modifies the seafloor.

2.   Sediments at GC 185 (Bush Hill) contained high concentrations of UCM (mean = 24,775 ppm) and C_1-C_5 hydrocarbons (mean = 11,037 ppm).   Tube worm communities requiring H_2S occurred at GC 185 where the seafloor has already been greatly modified since the Pleistocene by accumulation of oil, gas hydrate, and authigenic carbonate rock in sediments. Venting is thus suppressed over time, favoring slow development of complex communities that depend on abundant hydrocarbons in sediments.

3. Sediment samples from an area with vesicomyid clams (GC 272) contained lower UCM (mean = 1,716 ppm) but C_1-C_5 concentrations were high (mean = 28,766 ppm). The clams appeared to persist at relict thermogenic seeps where the rate of seepage had declined from past highs, or H_2S production was triggered by gas instead of oil.

4. The sediment we sampled in association with the methanotrophic Seep Mytilid I was characterized by low UCM (82 ppm) and by dominance of biogenic C_1 (8,829 ppm).

5.0 Characterization of Habitats and Determination of Growth Rate and Approximate Ages of the Chemosynthetic Symbiont-Containing Fauna
Charles R. Fisher

One of the major factors that determines the ability of a species to recover from damage is the rate at which it grows. Growth and recovery in chemosynthetic fauna have been studied at hydrothermal vents (Hessler et al. 1988 #150), where they inhabit an environment subject to rapid and often catastrophic changes. Consequently, growth rates are high in these groups. Hydrocarbon seeps are believed to be geologically more stable; the chemosynthetic fauna dependent on these seeps would have less requirement for rapid growth. If true, recovery from damage would take longer. Direct measurements of growth rates in seep fauna were undertaken to increase understanding of this issue. Growth also depends on supply of nutrients, which can be quite heterogeneous in seeps; so it is necessary to combine the growth measurements with a characterization of the seep micro-habitats. The materials and methods section below will explain how all major work was carried out. The results section will present findings for each faunal group studied.

The five dominant species of chemoautotrophic-symbiont containing animals fall into three taxonomic categories that have distinct metabolic requirements and physiological strategies for exploitation of their chemoautotrophic lifestyle (see Fisher 1990 for review). Because of the differences in their lifestyles and their requirements (both from each other and especially from other non-symbiotic species), we devised unique methods to characterize their chemical habitat and measure growth and estimate age for each group. These animals live in a unique and dynamic environment that is virtually impossible to duplicate in the laboratory. In order to obtain meaningful growth rates for these animals, it was necessary to develop new techniques to measure their growth rates *in situ*, in their natural environment, using methods that were specifically adapted to each group's life styles. To characterize

their chemical habitats, we also developed new sampling apparatus and analysis methods which have provided the most comprehensive and biologically relevant data ever on the chemical microhabitats required by the symbiont-containing seep fauna.

5.1   Mussel Methods

Mussels used in this study were collected, from depths of 540 - 800 m, in September 1991, August 1992, and June 1993, using the deep-sea submersible *Johnson Sea Link* (Harbor Branch Oceanographic Institution). They were placed in a temperature-insulated retrieval box mounted on the front of the submersible. On the deck of the ship, the mussels were immediately transferred to buckets of 8°C sea water and placed in a cold room (8°C) for all subsequent handling. Shell length and width of all mussels were measured with calipers to the nearest 0.1 mm.

A subset of each collection (6-20 mussels, depending on the purpose) were processed for determination of morphometric relations and condition indices. Following shell measurements, the shells were drained of sea water by prying them open a few mm. The adductor muscles were then severed over an open, pre-weighed, specimen bag, so that all internal fluid was collected. Gill, mantle, and foot tissue subsamples were taken, placed in pre-weighed cryovials, and immediately frozen in liquid nitrogen. The remaining tissue (= "bulk tissue") was removed from the shell, added to the specimen bag, and stored at -20°C. The shells were cleaned, dried and marked for future shell volume measurements. Tissue samples were transported to Pennsylvania State University in liquid nitrogen or on dry ice and upon arrival stored in a -70°C freezer.

Mussel densities and size distributions were determined from collections made from within a 0.5 m diameter ring placed firmly in a bed of mussels. The ring consisted of a 20 cm high band of 2 mm thick stainless steel, with three 15 cm spikes protruding below the ring to anchor it in place, and a handle for manipulation by the

submersible. Mussels had been collected from the beds used for the growth studies several times in the years previous to the ring collections. To avoid making quantitative collections from impacted beds, the ring collections at GC 184 and GC 234 were made from nearby, undisturbed beds, which were visually similar. The similarity in water samples and size ranges of mussels collected from the beds within each site support the linked interpretation of the sites as presented here. In the case of the bed at GC 272, the ring collection was made from a relatively inaccessible and therefore undisturbed portion of the same bed as that used for the growth study. Again the similarity in water samples, and size ranges support the joint interpretation of the two data sets. Placement of the collection ring was not random within the patchy, small mussel beds, but efforts were made to sample "typical" areas within each bed (the extreme periphery, obvious areas of dead shells, and mounds of mussels were avoided). After placement of the ring, essentially all mussels within the ring were collected (first by grab sampler, then with a suction sampler) and a video record was made of the ring to document the occasional mussel not collected. The mussels from each collection were placed in separate sections of the temperature insulated collection box and processed as described below. Between 0.7 and 16% of the mussels were damaged during a given collection. These were counted and measured with as much accuracy as possible.

5.2   Water Sampling and Analysis

Water samples were collected using specially designed samplers which allowed collection of undiluted, small volume (1-5 ml) samples from specific areas above, within, or below the mussel beds. Samples were taken from three levels within the mussel beds; at the top of the shells near the siphons, 5 cm below that level, and 10 cm below that level. The three water samplers used were constructed of 316 stainless steel. Water was drawn through 2 μm fritted filters (the interstitial

samplers employ stainless steel filters and the "wand" sampler a plastic filter). The "wand" sampler consisted of a filter mounted on the end of a 70 cm tube fitted with a handle for the submersible. The interstitial water samplers were essentially large thumbtacks with the filters mounted below 14 cm diameter plates, above a sharpened point, and isolated from internal dead spaces by O-rings. The water was collected from a 1 cm length of filter centered either 5 or 10 cm below the plates with a flow rate of about 2 ml min^{-1}.

The filters were connected to 7 m of 0.025 cm ID polyetheretherketone tubing using low dead volume fittings, and plumbed into the rear compartment of the submersible through stainless steel swagelock fittings (and a stainless ball valve), such that the tubing completely penetrates the hull of the submersible and is connected to a plastic 0.15 cm diameter valve and leur lock (syringe) fitting on the inside of the compartment. The entire sampling apparatus, from filter to syringe fitting, had a dead volume of < 1.8 ml. Tubing from all three water samplers entered the rear compartment through the same ball valve which serves as an emergency cut off should an inner valve fail. All three samplers were carried in quivers mounted on the work platform of the submersible and could be picked up by the submersible manipulator and used at will.

The samplers were positioned by the submersible pilots, the lines bled (2 mls) and the samples collected in 1 ml glass syringes fitted with low volume gas-tight valves. After collection of an 0.5 ml sample, the sample was stored on ice until analyzed. To minimize the spontaneous oxidation of sulfide in the water samples before analysis, the sampling syringes were primed with 0.1 ml of a degassed pickling solution. In 1992 a solution of 1M Na$_4$EDTA in 1N HCl was used, which inhibited the initial rate of the oxidation reaction by 65%. In 1993 this solution was replaced with a basic zinc acetate solution (5:1, 2.6% ZnAcetate (W/V):6% NaOH (W/V)), which precipitated the sulfide and inhibited the oxidation reaction

much more effectively (> 90% of the initial sulfide and oxygen were recovered after 20 h of refrigerated storage in laboratory tests). Therefore, only the 1993 environmental sulfide data are presented here. Methane data from both years are given, as these data were not affected by the change in protocol. All water samples were analyzed on board ship for ΣCO_2, CH_4, O_2, ΣH_2S, and N_2 by gas chromatography (Childress et al. 1984) within 10 h of collection.

5.3   Growth Studies

Mussels were collected as previously described and the collection location was marked with a numbered float. A representative size range (~150 mussels) from each location was set aside for marking and an additional 20 were sampled as controls. In 1991, 3 different marking methods were tested; (1) notching the outer margin of the shell with a file, (2) gluing a commercial color-coded, numbered larval fish tag (6.9 mm x 3.2 mm), near the umbo of the shell, and (3) gluing a hand-made color-coded polypaper tag (9.8 mm x 3.3 mm), near the umbo. Before attaching the tags, shell length and width were measured. A small area of the shell was quickly dried and lightly abraded with #220 sand paper. The tags were attached with cyanoacrylate glue (Loctite #447 and/or #401), allowed to dry for 60 seconds, and rinsed in 2 changes of cold seawater. This entire procedure required the mussels to be removed from sea water for less than 2 min. All manipulations were conducted in the cold room (8°C). Both types of tags persisted until 1992. Only the larval fish tags were used in subsequent years. Notching was found to be unnecessarily invasive and was also discontinued after 1991. The mussels used in this study were never kept on board ship for more than 15 h.

For deployment, the mussels were placed in insulated acrylic containers filled with chilled sea water, returned to the site of collection, and released within 0.5 m of the marker float.

Marked mussels were retrieved in August 1992 and in June 1993. Twenty marked mussels and 20 unmarked mussels from each collection were processed as described above, with tissue subsamples removed from the first six. All other marked mussels were measured and re-released with additional newly marked mussels from the same collections (only the latter are presented in the growth analysis).

5.4 Transplant Experiment

A transplant experiment (with two treatment levels, transplant 1 and transplant 2) was conducted at GC 184. Mussels were collected in September 1991 and marked as described above. For deployment, 20 mussels were placed in each of two 42 cm x 19 cm coated wire cages and placed in the insulated collection box, in chilled 8°C sea water. The transplant cages were returned to the area of collection and deployed approximately 2 m (transplant 2) and 3-4 m (transplant 1) away from the collection (control) bed (the same bed used for the in situ growth study). Cages were retrieved in August 1992 and the mussels were treated as described for the growth studies. The twenty unmarked mussels from their original collection site (GC 184 growth site, 1991 and 1992 collections) served as controls for the transplant experiment.

5.4.1 Measures of Condition

Bulk tissue was thawed and homogenized in a 10x dilution of distilled, deionized water using a Brinkman PT 3000 Polytron with a PT-DA 3020/2TM generator. Replicate samples (10 ml) were taken from this primary homogenate for determination of ash-free dry weight. A 1 ml aliquot was removed and further homogenized, in a hand held glass tissue grinder, then diluted an additional 50x for glycogen determination. This glycogen assay is a modification of several previous protocols. Briefly, glycogen was degraded to glucose by amyloglucosidase and glucose

was quantified spectro-photometrically following a dye-linked enzymatic oxidation (Sigma Diagnostics kit #510). Modifications included the use of phosphate buffer (0.067 M , pH 5.8), which was found to be conducive to the action of all enzymatic steps, and a 2-h pre-incubation with amyloglucosidase (0.5 unit activity ml^{-1}). This protocol yielded > 90% recovery of spikes and allowed quantification in tissue homogenates so that prior isolation of glycogen was not needed. Free glucose concentrations in the tissue were determined in separate aliquots (without the addition of amyloglucosidase) and were subtracted for determination of tissue glycogen levels. Replicate glycogen and glucose standards were run with each assay and the standard curves used to calculate the tissue glycogen levels.

Condition index (CI), the ratio of the ash-free, dry mass of soft tissue to internal shell volume, is a commonly used measure of relative condition in bivalves and is a sensitive indicator of condition in related deep-sea mussels (Fisher et al. 1988). Soft-tissue dry weight was determined after drying replicate 10 ml samples of the homogenate described above to constant weight at 60°C. Ash weight was determined after ashing these samples in a muffle furnace, at 500°C, for 12 h. Internal shell volume was calculated based on the weight of sand contained in each valve. Each shell valve was filled with sand, leveled off across the open edge, and the weight of sand recorded, 3 times per valve. Sand weight was converted to volume based on the empirically determined relation between the two. Tissue water content was also calculated from the ash-free dry weights. It provides an easily obtained measure of condition but, unlike CI, it is sensitive to residual mantle cavity water.

5.5 Statistical Methods

Due to the nature of the condition indices data (percentages and ratios), an arcsine transformation ($y' = 2$ arcsine$\sqrt{y}$) was applied to all three condition parameters before testing for significant differences between sites and years. The parameters were normally distributed (Shapiro-Wilks test) and the variability of the condition parameters was analyzed with respect to site, year, and length by ANCOVA using a General Linear Model (GLM) procedure (SAS program, version 607). If significant differences ($p < 0.01$) in condition index, water content, glycogen content, or length were supported by one-way analysis of variance, then multiple comparison tests (Fisher PLSD and Scheff tests, Statview II) were used to demonstrate significant differences between specific sites and years.

Since the growth rate varied with initial length, statistical comparisons between sites and years were conducted on the size specific growth rates ($\Delta L/L_i$, where ΔL = final length - initial length and L_i = initial length (Bayne et al. 1982; Wootton 1991) and were compared by ANCOVA using a reduced model GLM procedure. Ages were estimated using the von Bertalanffy growth model and the variance of the age estimates were calculated using the following formula:

$$[=\partial g/\partial K]^2 var(K) + 2cov(K, L_{max})[\partial g/\partial K][\partial g/\partial L_{max}] + [\partial g/\partial L_{max}]^2 var (L_{max})$$

where g = age, L_{max} = the extrapolated point of no growth , K = the rate at which L_{max} is approached, L_i = initial length and $[\partial g/\partial K] = (1/K^2)[\ln(1-L_i/L_{max})]$ and $[\partial g/\partial L_{max}] = -L_i/(K*L_{max}*(L_{max}-L_i))$.

This formula was derived by M. Ghosh-Dastidar (Pennsylvania State University) using point estimates and standard errors for both K and L_{max} and the results from an asymptotic Kramer-delta procedure.

5.6   Growth Methods

To determine growth rates for these species a device was constructed which deployed bands (tie-wraps) around the anterior end of the tubes. The hydraulically actuated device is positioned by a submersible and deploys up to eight individualized bands per dive, with adjustable, preset, tension for each band. Tension was adjusted to assure a tight fit, without crushing the worms' tubes. The position of the band with respect to the growing end of the worm is then documented by video. Two features of the bands are used for scale in the images. The most precise is the width of the outer surface of the band itself, which can be used to compensate for the angle of documentation, because the band lies flat on the surface of the tube and is approximately perpendicular to the long axis of the tube. Spherical stone beads were also attached to the bands for absolute scale from any angle. Re-video or collection of the banded worms in subsequent years was used to determine the yearly in situ growth rates of the tubes of individual animals.

5.7   Results for Vestimentiferans: *Escarpia* sp. and *Lamellibrachia* sp.

The two species of tube-worms present at these sites are in two different families (Escarpidae and Lamellibrachidae) but have similar gross anatomy, physiology, and lifestyles (Jones 1985). The vestimentiferan larvae attach to hard substrate (including adult worm tubes in some species) when they settle and are immobile after metamorphosis to the adult form. The adults have no mouth, gut, or anus and apparently depend entirely on their symbionts to meet their nutritional needs. The symbionts constitute a significant proportion of their body mass (about

6% with another 40% accounted for by blood) and are housed in an internal organ inside the trunk of the animal with no direct connection to the outside environment (Childress et al. 1984; Jones 1985; Powell and Somero 1986). The symbionts require sulfide, oxygen, and inorganic carbon as chemoautotrophic substrates (Fisher et al. 1988) and the immobile host must live in an environment with a constantly replenished supply of these nutrients. We measured sulfide and oxygen concentrations in the pools of water around their plumes and in the sediments around their tubes. Since the tissue of these tube-worms extends all the way to the base of the tubes and they grow from their anterior end, we measured growth in these animals by measuring tube growth over two one-year periods. Tube growth is related to tissue growth through the empirically determined relation between the two (Figure 5.1).

5.7.1 Vestimentiferan Growth Rates

The Vestimentiferan bander has been used successfully on over 100 individuals. However, the limiting factor in our analyses turned out to be the quality of the video documentation obtained by the scientist in the sphere during the dive. Over the course of the past two years, we have obtained 28 measures of yearly growth increments (on 20 different individuals). At the suggestion of the scientific review panel, most of the banded animals are still *in situ*, so their growth can be monitored into the indefinite future. At least one more year's data will be collected in September 1994 during a cruise supported by NOAA.

The relatively small number of measurements made at each site, and the relatively large percent error associated with measurements of very small growth increments precludes statistical comparisons between sites. However, the data set is clearly sufficient for general conclusions concerning these species (Table 5.1) No growth was detected in any individual between 1992 and 1993 (five
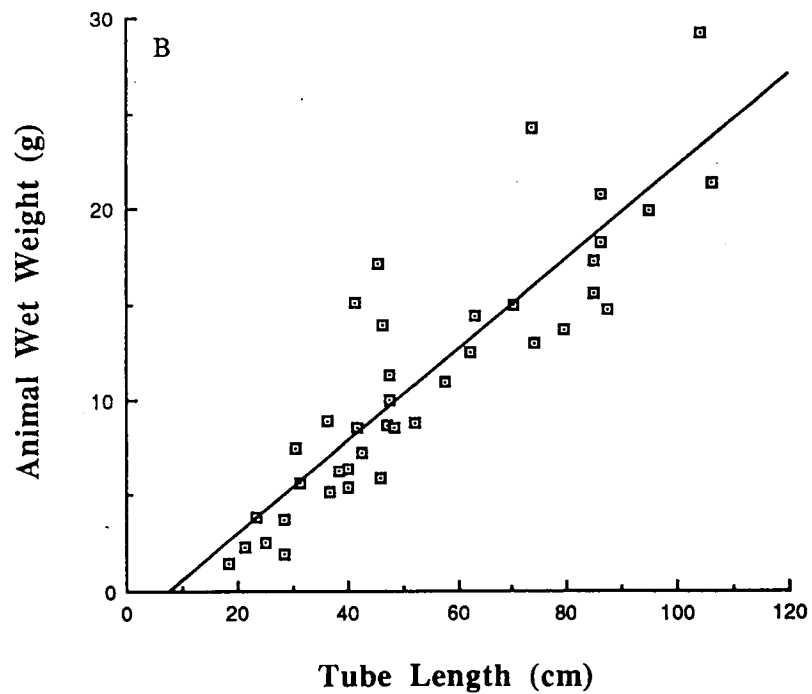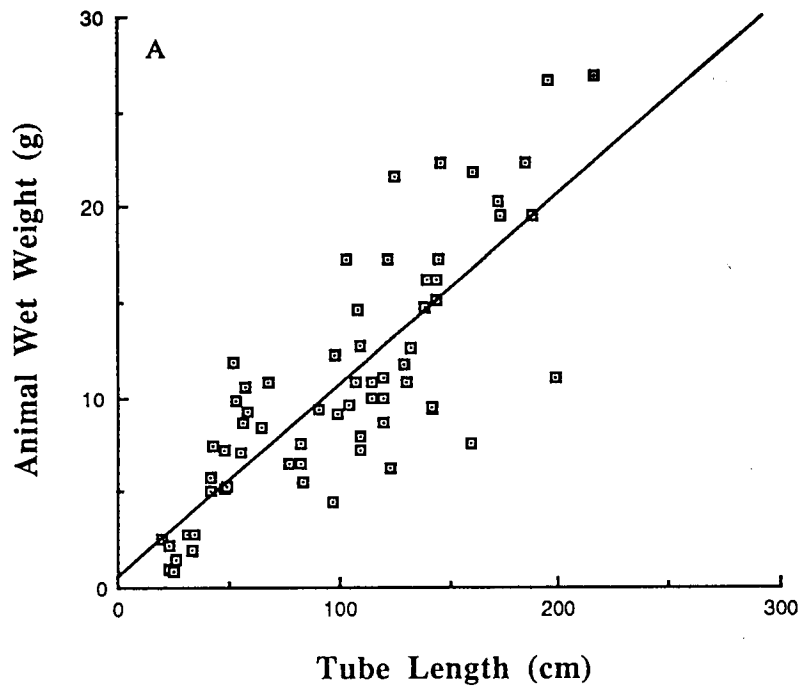
Figure 5.1   Relation between tube length and wet weight for hydrocarbon seep vestimentiferans. a) *Escarpia* sp., y = -1.931 + 0.241x, R^2 = 0.78. b) *Lamellibrachia* sp., y = 0.523 +0.101x, R^2 = 0.67.

lamellibrachids and eight escarpids), although growth was documented in one of these individuals of each species in the previous year. It is possible that for some unknown reason, this was a "bad year" for the Louisiana Slope vestimentiferans, and the following calculations do not include data from that year (the averages for both years combined for each species are given in Table 5.1). Direct measures of tube growth from digitized images over the first year, were 0 mm for the escarpid and 0, 3.1, 16.4, and 17.9 mm (0 to 3 rings, n = 4) for lamellibrachids. Of three additional escarpids monitored that year, one produced a single growth ring and the rest did not produce new tube material. Of the additional seven lamellibrachids monitored that year, one laid down three, one laid down two, and one laid down a single ring (the rest did not extend their tube that year). Thus, the average growth rate between 1991 and 1992 (based on data from measured individuals and using the average between-ring increments for the other monitored individuals) was 2.5 mm (n = 4, SD = 5.7 mm) for the escarpids and 7.1 mm (n = 11, SD = 8.3 mm) for the lamellibrachids. This represents an average increase in soft tissue biomass of 0.61% for the escarpids and 0.51% for the lamellibrachids.

Table 5.1   Vestimentiferan tube growth. Elongation rates of vestimentiferan tubes are shown. Since growth was determined to occur by secretion of new rings, only sample sizes (n) are shown for individuals which secreted no new rings (all determined rates for these individuals were 0 ± 1 mm/year). "*" indicates rates determined by measurement of digitized images; all other rates are based on calculations from increment counts.

New Increments (new rings)	*Lamellibrachia sp.* Elongation (mm/year)		*Escarpia sp.* Elongation (mm/year)	
	1991-1992	1992-1993	1991-1992	1992-1993
0	0 (n = 5)	0 (n = 5)	0 (n = 3)	0 (n = 8)
1	7, 3*		11	
2	13			
3	16*, 18*, 20			

Based on the full data set of 20 individuals at six different sites over 2 years (Table 5.1), it is apparent that these cold-seep vestimentiferans grow at a much

slower rate than their hydrothermal vent relatives. However, ultimately they can reach lengths two to three times that of the largest known hydrothermal vent species. The total lengths of most of the banded worms is unknown because they are still *in situ*, partly buried with sediment. Lengths determined for the banded vestimentiferans collected to date and other vestimentiferans collected from the same aggregations are shown in Table 5.1. Insufficient numbers of banded animals have been collected for statistical analysis of the relation between size and growth rate, but it should be noted that the largest banded individual collected (216 cm) deposited three growth rings between 1991 and 1992, and was thus among the fastest growing animals in this study. These collections are generally biased towards the smaller individuals in the aggregations because efforts were made to avoid collecting very large tube worms due to difficulties associated with handling the largest individuals in the submersible's insulated collection box. Individuals of *Lamellibrachia* sp. in excess of 3 m in length have been collected several times in the past, and one individual had the posterior 2 m of its tube stained from burial in the sediment documented photographically (personal observation CRF). The very slow growth rates and total lengths of these vestimentiferans indicate that they are a long-lived species. Based on these considerations, we suggest that the larger aggregations contain individuals in excess of 200 years old, perhaps greatly in excess of 200 years old. The current lack of growth data on smaller individuals precludes construction of allometric growth curves, which would allow more exact age determination of the adults at the sites studied.

Both species of seep vestimentiferan deposit external rings on their tubes as they grow, the temporal meaning of which is unknown. The length of the increment between rings was measured on all visible rings on the anterior end of the tubes (the rings disappear towards the posterior, older, portion of the tubes) of 14 escarpids and 20 lamellibrachids (a total of 411 rings were measured). The spacing between rings

varied from extremes of 1.4 to 22.6 mm on escarpids and 0.9 to 17.2 mm on lamellibrachids. However, the spacing of the rings was much less variable on a given individual, and the average ring spacing was 11.4 (SD = 4.3, n = 172) for the escarpids and 6.7 mm (SD = 3.0, n = 239) for the lamellibrachids. Based on examination of collected specimens and review of video footage, it appears that the rings mark the increment of tube deposited in a single growth "spurt", as suggested by Gardiner and Jones (1993). The terminal increment in all measured escarpids was within the 95% confidence interval of the mean of the adjacent 10 increments, suggesting that the increment had reached its full length. Based on the same criteria (95% confidence interval of the mean), the terminal increment of three out of 13 lamellibrachids measured was in the process of extension. The terminal tube increment of most of the individuals collected was noticeably thinner walled than adjacent sections of the tube, indicating that the second step in the deposition of a new tube increment is thickening the wall. We suggest that the rings are the relic of the flared tube ends, which strengthen the terminus of the tube and allows the worm to extend and retract without fouling the end of the tube, that the entire increment is deposited over a relatively short period of time, and then strengthened over an additional, longer period. This is also supported by the fact that no increases (±1 mm) in any pre-existing ring increments (including the original terminal increment) were detected on any of the animals measured *in situ*. We also conclude that there is no direct temporal significance to the rings, and they cannot be used to age the worms.

The low growth rates and longevity of the cold seep vestimentiferans imply life history strategies very different from their hydrothermal vent relatives. The deep sea in general is a relatively stable environment (Gage and Tyler 1991). In the case of the seep vestimentiferans and their source of nutrition (sulfide-based autotrophy) the environment may be even more stable as it is not tightly tied to vagaries in primary production on the ocean surface. At the other extreme are the hydrothermal

vent species whose habitats and source of reduced chemicals are ephemeral on time scales as short as years. Thus, the small phylum Vestimentifera, contains species that are among both the fastest growing and the longest lived deep-sea creatures.

5.7.2 Vestimentiferan Habitat Characterization

A second aspect of this study was to characterize chemically the vestimentiferan habitat, specifically with respect to their energy source, hydrogen sulfide. Dissolved gas concentrations (ΣCO_2, H_2S, O_2, N_2, and CH_4) were measured in samples of blood from individuals of both *Lamellibrachia* sp. and *Escarpia* sp., as well as in water samples from four different levels in the water column surrounding vestimentiferan bushes: plume level, midway between the plume level and the sediment surface, and 5 cm and 10 cm below the sediment surface. Blood levels of hydrogen sulfide have been shown to reflect exposure to sulfide in hydrothermal vent vestimentiferans (Childress et al. 1991). One water sample with unrealistically high N_2 and O_2 concentrations was not included in the analysis because experience indicates that this is caused by introduction of a small air bubble during handling of the sample.

Replicate samples of each type within two bushes were compared to determine the heterogeneity of the microhabitat within bushes (Table 5.2). Although seep environments are generally more stable than either hydrothermal vents or wood islands, the chemical environment at vestimentiferan bushes, as characterized by analysis of the precise water samples of this study, is quite patchy. A wide range of conditions are present at individual bushes. This unexpected variability most likely results from channeling of water flow in the vicinity of the vestimentiferan tubes, creating a patchy environment throughout and around each bush.

Table 5.2   Variability in replicate water samples. Ranges in dissolved gas concentrations (in
μM) are shown for plume level, midway between plume level and sediment surface,
and 10 cm interstitial water samples for two representative seep vestimentiferan
bushes. All values expressed here as "0" indicate the gases were not detectable, and
where no gases were detected within a sample type, the range is expressed simply
as "0." The detection limit of the procedure used to analyze these gases was
approximately 3 μM, although occasionally the gas chromatograph could detect
gases down to 1 μM in concentration.

Type	n	CO_2	H_2S	O_2	N_2	CH_4
			Site 1, Bush D			
Plume level	2	2784, 2828	0	152, 166	564, 660	0, 2
Midway	2	2722, 2762	0	80, 172	258, 660	0
10 cm	2	3284, 4950	0, 942	12, 140	644, 734	6, 734
			Site 2, Bush D			
Plume level	2	2600, 2952	0, 15	5, 148	602, 700	0
Midway	2	2496, 2552	0	33, 153	598, 629	0
10 cm	3	2776 - 3436	0 - 100	0 - 58	655 - 1167	0 - 20

Because of the extremes within site variability of interstitial water chemistry,
and the relatively low number of samples of each type taken at each site, no
statistically valid comparisons of water chemistry between sites could be made.
However, analysis of the full data set of water samples from the vestimentiferan
habitats and blood samples of the vestimentiferans provide considerably new insight
into the physiological ecology of the seep vestimentiferans and corroborate the
conclusions of low growth rates in these animals. Sulfide was rarely detected at the
plume level among the vestimentiferans (which is where hydrothermal vent
vestimentiferans take up sulfide) (Table 5.3). Thus, it seems likely that they access
a different pool of H_2S. The presence of H_2S in over half of the 10 cm interstitial
water samples suggests that these animals take up interstitial H_2S across the
buried posterior portion of their tubes, as had previously been suggested (Childress
1987). Since the base of a seep vestimentiferan tube can be buried by up to a meter

of sediment, the H2S pool available for uptake across the thin tube posterior portion of the tube is likely much higher.

Table 5.3   Localization of H2S at seep vestimentiferan bushes. Numbers of samples in which dissolved H2S was detectable and not detectable are shown for each sample type. *The detection limit of the procedure used to analyze these gases was approximately 3 μM, although occasionally the gas chromatograph could detect gases down to 1 μM in concentration.

Sample Type	Not Detectable (< 3μM*)	Detectable (> 3μM*)
Plume level	8	1
Midway	15	1
5 cm Interstitial	9	1
10 cm Interstitial	14	11
Lamellibrachia sp. Blood	13	2
Escarpia sp. Blood	4	2

The H2S concentration in blood samples of freshly collected vestimentiferans also provides insight into their physiological ecology. These animals have sulfide-binding hemoglobins that bind H2S with very high affinity in equilibrium with environmental H2S concentrations (Childress and Mickel 1985). In the seep vestimentiferans of this study, only four of 21 blood samples contained detectable H2S (Table 5.3). The maximum concentration found in any of these samples was 32 μM (*Escarpia sp.* = 1 and 15 μM, *Lamellibrachia sp.* = 16 and 32 μM). An average of 27μM sulfide was found in the blood of seven individuals collected by trawling in a previous study (Childress et al. 1986). All of this data implies equilibrium with a very low sulfide pool. For a full discussion of the implications of this data the reader is referred to Scott and Fisher (Submitted) and Simpkins (1994). In brief, we conclude that it is possible that the sulfide pool is around the plume but below our limits of detection, but more likely that it is an interstitial sulfide source in dynamic equilibrium with the vestimentiferan blood, limited by diffusional constraints.

5.7.3 Vestimentiferan Condition at Different Sites

A final aspect of this study was to compare the condition of individuals from a variety of environments. To do this, we used several different condition indicators and analyzed individuals of *Lamellibrachia* sp. in nine different bushes, and *Escarpia* sp. in seven different bushes, at four distinct hydrocarbon seep sites. Overall ranges in condition indicators were determined for each species and compared to means and standard deviations within bushes to ascertain the scale of variability within bushes (Table 5.4). This variability was analyzed following a General Linear Models procedure (SAS program, version 6.07) for each condition indicator to determine if it could be explained by variables measured in this study. Specifically, the GLM procedure was used to determine if the variability in each condition indicator (lipid content, water content, ash-free dry weight to tube-volume ratio, and RNA to DNA ratio) could be explained by the bush an individual was collected from (bush of origin), and/or the size of the individual (as reflected in wet weight, ash-free dry weight, or tube volume).

The variability in RNA/DNA ratios was not significantly explained by General Linear Models including all independent variables at $\alpha = 0.05$, although a model with bush of origin alone explained the RNA/DNA variability in escarpids significantly at p = 0.065 ($r^2 = 0.391$). We believe that this is likely due to the temporal sensitivity of this analysis as compared to the other condition indices used, which reflect longer term, cumulative effects. In other words, short-term transient fluctuations in exposure to sulfide would likely be reflected in RNA/DNA ratios, where tissue lipid or water levels would change over longer time intervals and reflect conditions averaged over a longer time period.

Table 5.4   Means, standard deviations, and sample sizes are shown for condition indicators in *Escarpia sp.* (a) and *Lamellibrachia sp.* (b) populations (non-summarized data is presented for sample sizes of 2). The total ranges for all indicators in individuals sampled from all populations are shown for comparison.

a: Condition indicators in *Escarpia sp.* populations.

	Water Content (% Wet Weight) mean ± sd (n)	AFDW/Vol. (g/ml) mean ± sd (n)	Lipid Content (% Wet Weight) mean ± sd (n)	RNA/DNA (g/g) mean ± sd (n)
Site 1, Bush A	83.2 ± 2.9 (4)	0.141 ± 0.027 (4)	2.1 ± 0.4 (4)	nd
Site 1, Bush B	76.6 ± 3.4 (3)	0.223 ± 0.060 (3)	2.5 ± 5.6 (3)	nd
Site 1, Bush C	78.5 ± 4.4 (6)	0.141 ± 0.035 (6)	3.6 ± 1.3 (4)	2.55 ± 0.47 (6)
Site 1, Bush D	75.4 ± 2.4 (6)	0.219 ± 0.054 (5)	1.8, 4.2 (2)	2.16 ± 0.32 (6)
Site 2, Bush D	69.5, 75.0 (2)	0.217, 0.305 (2)	4.7, 5.1 (2)	1.68, 1.86 (2)
Site 3, Bush A	79.7 ± 2.4 (5)	0.339 ± 0.106 (6)	4.8 ± 1.2 (5)	nd
Site 4, Bush A	72.8 ± 3.2 (13)	0.271 ± 0.052 (13)	4.8 ± 1.9 (11)	nd
Total Range	66.3-85.4 (39)	0.084-0.553 (39)	1.6-7.8 (31)	1.67-3.07 (14)

b: Condition indicators in *Lamellibrachia sp.* populations

	Water Content (% Wet Weight) mean ± sd (n)	AFDW/Vol. (g/ml) mean ± sd (n)	Lipid Content (% Wet Weight) mean ± sd (n)	RNA/DNA (g/g) mean ± sd (n)
Site 1, Bush B	78.9 ± 0.8 (3)	0.232 ± 0.027 (3)	2.0 ± 0.1 (3)	nd
Site 1, Bush C	85.0 ± 2.6 (6)	0.092 ± 0.030 (5)	1.7 ± 0.3 (4)	3.12 ± 0.49 (6)
Site 1, Bush D	76.8 ± 1.6 (6)	0.170 ± 0.072 (6)	2.7, 2.8 (2)	3.17 ± 0.65 (4)
Site 2, Bush A	85.6 ± 3.4 (17)	0.105 ± 0.047 (14)	1.6 ± 0.8 (17)	3.30 ± 0.53 (8)
Site 2, Bush B	83.1 ± 4.5 (7)	0.181 ± 0.036 (6)	2.1 ± 0.7 (7)	nd
Site 2, Bush C	86.6 ± 1.5 (10)	0.107 ± 0.023 (10)	1.3 ± 0.3 (4)	3.06 ± 0.54 (6)
Site 2, Bush D	72.4 ± 1.8 (4)	0.201 ± 0.033 (4)	4.7, 5.2 (2)	3.32 ± 0.62 (4)
Site 3, Bush A	80.1 ± 4.1 (6)	0.154 ± 0.037 (6)	2.4 ± 1.2 (6)	nd
Site 3, Bush B	78.3 ± 1.0 (8)	0.216 ± 0.042 (8)	2.8 ± 0.8 (7)	3.35 ± 0.80 (6)
Total Range	70.4-91.3 (68)	0.047-0.324 (63)	0.4-5.2 (53)	2.14-4.24 (35)

For each of the other three condition indicators analyzed (water content, ash-free dry weight/volume, and lipid content), bush of origin was found to explain 42 to 71% of the variation in the indicator for both species (Table 5.5), and size alone was found to explain between 0 and 30%. The combined models with the most explanatory power were determined by following stepwise GLM procedures (SAS version 6.07; Table 5.5). The bush an individual was collected from explains more about its condition than any single size variable, and only slightly less than a model that includes a size variable along with bush of origin (Table 5.5). Thus, although some of the variation in the condition indicators in the vestimentiferans may be due to the size (and possibly age) of the animals, most of the variation is a reflection of the collection site and presumably the microhabitat conditions experienced by the animals. This implies that there are significant differences in the average environmental conditions experienced by vestimentiferans at different sites and that future work with a more intense water sampling program would provide valuable data that would directly relate environmental chemistry to vestimentiferan condition.

Finally, all condition and size data were analyzed to determine if a size or condition indicator differential existed between the two seep vestimentiferan species. Using t-tests to compare all collected individuals of both species, *Escarpia* sp. were found to be significantly shorter in tube length (55.7 ± 25.2 cm vs. 99.8 ± 50.7 cm for *Lamellibrachia* sp., p≤0.0001), heavier in ash-free dry weight (2.28 ± 1.26 g vs. 1.51 ± 1.13 g for *Lamellibrachia sp.*, p = 0.0014), and wider in anterior opening interior diameter (8.24 ± 1.55 mm vs. 6.34 ± 1.42 mm for *Lamellibrachia* sp., p≤0.0001). Comparing condition variables between the two species with t-tests (Table 5.4), *Escarpia* sp. was found to have significantly (p≤0.0001) lower water content, higher ash-free dry weight/volume, and higher lipid content. Comparisons of escarpids and lamellibrachids collected from the same bushes corroborated these findings for individuals from the same site.

Table 5. 5   Condition indicator models for seep vestimentiferans. The explanatory power of the best statistical model*, determined using the stepwise General Linear Models procedures outlined in the text, as well as a single-variable General Linear Model of Bush of origin alone for each condition indicator for each species is indicated here by the expressed r^2 values and associated p-values (Table 5.5a: *Lamellibrachia sp.*, Table 5.5b: *Escarpia sp.*). The variables included in each model are abbreviated as follows: Bush of origin = Bush; Inner diameter of anterior increment = ID; and Tube volume = Volume.

a. *Lamellibrachia sp.*

Water Content	AFDW/Volume	Lipid Content
Variables in Model	Variables in Model	Variables in Model
Model r^2 (p-value)	Model r^2 (p-value)	Model r^2 (p-value)
Bush	Bush	Bush
0.717 ($\leq$ 0.0001)	0.664 ($\leq$ 0.0001)	0.536 ($\leq$ 0.0001)
Bush, ID*	Bush, Wet Weight, Volume*	Bush, Volume*
0.778 ($\leq$ 0.0001)	0.782 ($\leq$ 0.0001)	0.666 ($\leq$ 0.0001)

b. *Escarpia sp.*

Water Content	AFDW/Volume	Lipid Content
Variables in Model	Variables in Model	Variables in Model
Model r^2 (p-value)	Model r^2 (p-value)	Model r^2 (p-value)
Bush*	Bush	Bush
0.552 ($\leq$ 0.0001)	0.655 ($\leq$ 0.0001)	0.425 (0.0265)
	Bush, Wet Weight, Volume*	Bush, ID*
	0.739 ($\leq$ 0.0001)	0.521 (0.0096)

5.8   Results for Vesicomyid Clams: *Vesicomya chordata* and *Calyptogena ponderosa*

The two species of vesicomyid clams associated with the hydrocarbon seeps contain abundant symbiotic chemoautotrophic bacteria in their gills (Brooks et al. 1987). These bacteria use the same substrates as the symbionts of the tube worms — sulfide, oxygen, and dissolved inorganic carbon. The clams, however, are mobile

(Rosman et al. 1987) and while they acquire oxygen and CO_2 by normal means (across their gills), they apparently take up sulfide across the surface of their highly extensible and well vascularized foot (Arp et al. 1984; Fisher 1990). This is possible because their blood contains a sulfide binding protein, which has both a high affinity and capacity for sulfide (vesicomyids are able to concentrate sulfide by almost three orders of magnitude over environmental concentrations and the blood can bind sulfide to concentrations of 10 mM) (Arp et al. 1984). Based on our knowledge of these animals' physiology and ecology, we built and deployed clam corrals to contain marked clams in a 100 sq. foot area that we could characterize and return to in order to conduct growth experiments under a variety of environmentally relevant conditions. However, most clams did not survive the treatment (collection, recovery, marking, and redeployment). Only one experimental clam survived the treatment, and it did not grow a measurable amount in the following year. A second try in the subsequent year yielded similar results, with some indications of collection methods with better survival rate. This approach is still under study, however, for the purposes of this project we elected to apply our efforts to analyzing the microhabitat required by these clams by analysis of interstitial water from their habitat and analysis of the blood of freshly collected clams.

In areas where vesicomyids are found on the Louisiana slope, they are distributed in patches and present in relatively low density, compared to tube worms and mussels on the Louisiana slope or vesicomyids at hydrothermal vents. Therefore, a study of this type consumes a substantial quantity of submersible time. Over the two years of the study, approximately 12 dives were made to collect clams and/or water samples from the vicinity of living clams. On some dives, only one or

two living clams were collected, which again emphasizes the patchy and low density distribution of these clams. Additional data on the chemistry of water around the clams can be found in the section on the mini push core arrays. One qualitative observation made by several observers was that *V. chordata* is most often found singly, leaving long trails in the sediment as it moves, and that *C. ponderosa* is often found is small aggregations of a few individuals near small carbonate outcrops with no significant trails around them. This would suggest that *C. ponderosa* is associated with more active seep environments than *V. chordata*. We were unable to confirm this with the small number of water samples analyzed in 1992 and 1993. However, it is clear that both species live in relatively benign environments where sulfide distribution is patchy and concentrations are low, even in water from 10 cm depth (Table 5.6). Sulfide was never detectable around the siphons of the clams (1-2 cm above the sediment), which also suggests that seepage is slow in these areas and that the clams are obtaining their sulfide through their vascularized feet, as has been proposed for their hydrothermal vent relatives. Analysis of the blood of the freshly collected clams supports the suggestion that *C. ponderosa* lives in an environment of higher sulfide concentrations than does *V. chordata*. The blood of eight of nine specimens of *V. chordata* analyzed contained no detectable sulfide and the other contained 59 μm sulfide. One of the two *C. ponderosa* had 322 μm sulfide in its blood and sulfide was undetectable in the blood of the other. These data also support the general conclusions concerning the vesicomyid environments given above. For a full discussion of interpretation of vesicomyid blood sulfide levels and comparisons of seep and vent species, the reader is referred to Childress and Fisher (1992) and Scott and Fisher (submitted).

Table 5.6   Sulfide levels in Louisiana slope clam habitats and freshly collected blood.

Sample type	Mean (μM)	Range (μM)	n(UD)	n(total)
Sediment surface	UD		2	2
5 cm interstitial	2	UD-15	6	7
10 cm interstitial	36	14, 58	0	2
Vesicomya chordate blood	107	UD-322	2	3
Calyptogena ponderosa blood	7	UD-59	8	9

UD=undetected; detection limits for dissolved sulfide analyzed by gas chromatography were 1-3 μM depending somewhat on sample size.

5.9   Results for the Methane Mussel: Seep Mytilid Ia (SM Ia)

There are apparently at least 5 different species of symbiont-containing mytilids present associated with cold seeps in the Gulf of Mexico (Craddock et al., in press, Fisher 1993). None of these has yet been formally described, but their differences are apparent from physiological and molecular investigations (Fisher 1993, Craddock et al., in press). Two of these species are present at the shallow seep sites, SM Ia and SM 3. SM 3 is very rare, has sulfur-oxidizing symbionts, and has never constituted more than about 0.1% of the mussels collected from any station. The work presented here and most previous work has been on SM Ia.

Seep Mytilid Ia contains methane oxidizing symbiotic bacteria in its gills; the symbionts apparently provide the bulk of the animals' nutrition (Childress et al. 1986; Fisher et al. 1987). Because of the relative ease in handling methane (as compared to hydrogen sulfide), this species has proven relatively amenable to laboratory maintenance and study, and we have a lot of information on the physiology of both the intact mussel and the isolated symbionts. None-the-less the slow decline in the symbiont population in the laboratory, the sensitivity of the animals' growth and metabolism to methane and oxygen concentrations, and our

uncertainty of the microhabitat conditions the mussels are actually exposed to *in situ* required that growth rates be determined in the field. We used the quantitative collection rings (designed and built for this study), a variety of new water sampling apparatus (built for this study), unique marking methods (developed, tested, and employed for this study), and special temperature insulated deployment containers (designed for this study), which are described in a previous section. The mussels proved to be the most amenable to study of any of the symbiont-containing fauna, and we were able to characterize the population structure, growth rates, physiological condition, and microhabitats of three different areas with mussel communities (with data from a total of five mussel beds).

5.9.1 The Mussel Beds

5.9.1.1 GC 184 Mussel Beds

Sulfide was undetectable in the water samples from both experimental mussel beds in 1993. Methane levels in the samples from the two beds spanned a similar, relatively low range of undetectable to <60 μM, in both 1992 and 1993 (Table 5.7). Streams of bubbles (presumably methane) as well as large globules of oil were observed within both beds during the mussel collections. The retrieval container mounted on the sub, as well as the personnel handling the organisms, were always covered in an oil residue after recovery of mussels.

Larger mussels predominated at this site, with the majority >55 mm in length and none <9 mm (Figure 5.2a). Mussel density in the GC 184 bed was calculated to dbe 881 mussels m^{-2} based on the ring collection. Using the density and size frequency data from the ring collection, and the allometric equation derived from the logarithmic regression of tissue wet weight and shell length in 120 mussels between 12 and 110 mm shell length [Figure 5.3: Tissue wet weight (g) = 2.88 x 10^{-5} (shell length (mm))$^{3.162}$], the soft tissue biomass for this bed was calculated to be 11.3 kg

Table 5.7   Methane concentrations in water samples from mussel beds.

Mussel Bed	Sampling Depth (cm)	Methane Concentration (µM) 1992	1993
GC 184: ring	0	56	ND
	5	ND	22
	10	–	–
GC 184: growth	0	–	20
	5	ND	ND
	10	10	–
GC 272: ring	0	–	2
	5	–	4
	10	–	–
GC 272: growth	0	–	2
	5	35, 141, 290	4
	10	822, 27	–
GC 234	0	–	72, 832
	5	15, 16, 772, 869, 75	802, 10744, 9466
	10	ND, 986	–

ND = > non-detectable
- - = > not sampled
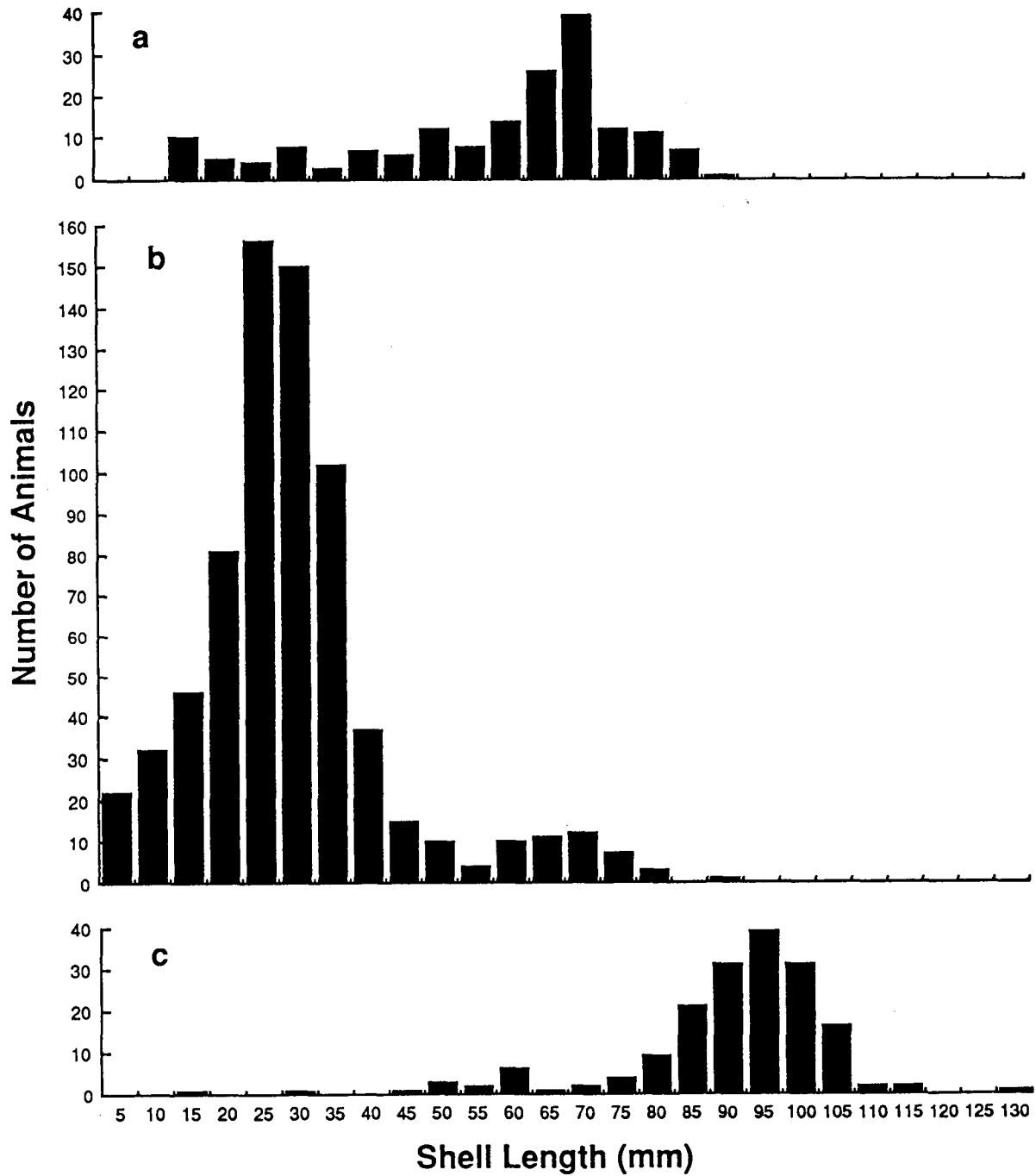
Figure 5.2 Size frequency distributions for SM Ia at three hydrocarbon seep sites. a) GC 184 (in 1992), b) GC 234 (in 1992), and c) GC 272 (in 1993). Total numbers from are ~0.5 m ring, densities are given in the text.
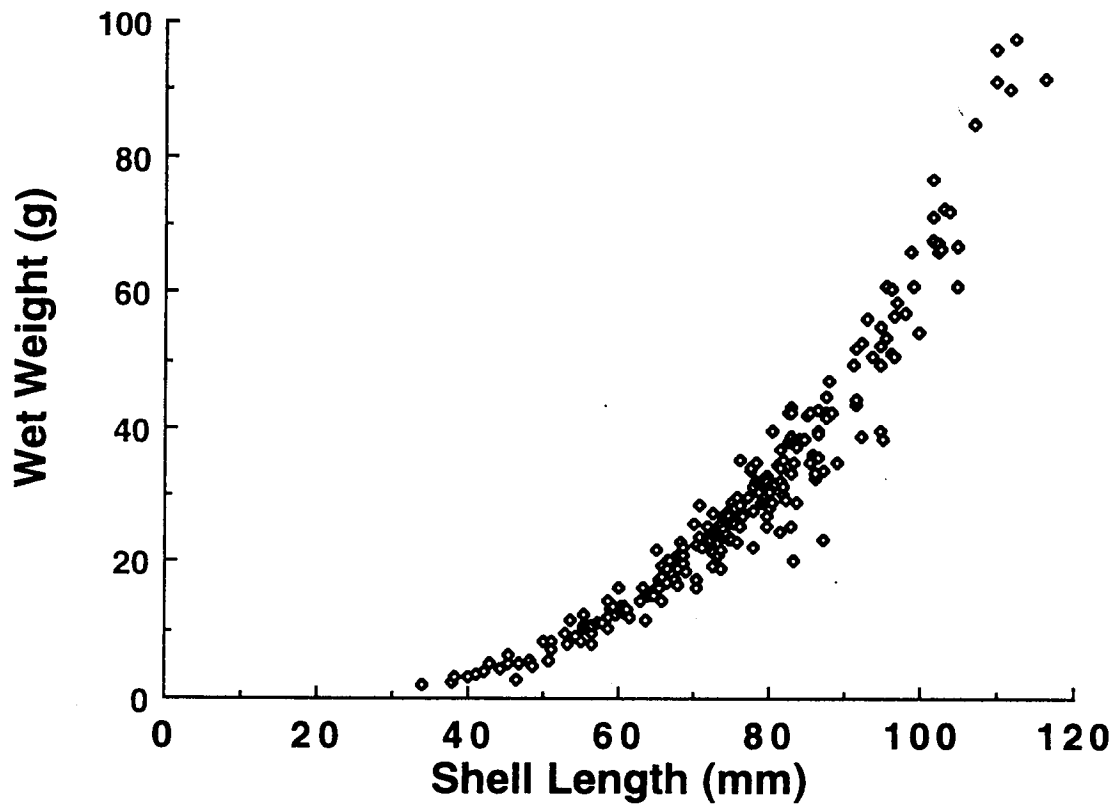
Figure 5.3   Relation between wet weight and shell length of SM Ia. The equation that best describes the relation is:

Tissue wet weight (g) = 2.28 x 10^{-5} [shell length (mm)]$^{3.162}$

m^{-2}. Since the dissolved gas concentrations, and size ranges and distributions of mussels from both beds were similar, the beds are considered together in the discussion of "GC 184" mussels.

5.9.1.2 GC 234 Mussel Beds

Both sulfide and methane levels in the water samples from the GC 234 beds were relatively high, especially in the samples taken 5 cm below the top of the mussels (between and below the shells), where sulfide and methane concentrations approached 8 and 11 mM, respectively (Table 5.7). Oil globules and streams of bubbles were also observed within these beds during sampling. The size distribution for the two beds sampled at GC 234 was dramatically different from the other two sites in that most of the mussels here were 15 to 40 mm long, with only a few larger mussels (Figure 5.2b). Mussel density for the bed sampled at GC 234 was calculated to be 3560 mussels m^{-2}, with living biomass calculated to be 7.3 kg m^{-2}. Since the dissolved gas concentrations, and size ranges and distributions of mussels from both beds were similar, the beds are considered together in the discussion of mussels from GC 234.

5.9.1.3 GC 272 Mussel Bed

Sulfide was not detected in any water samples from this mussel bed and methane levels decreased dramatically from 1992 (35 to 822 μM) to 1993 (2 - 4 μM). In contrast to the other two sites, no oil globules were released while collecting and neither the submersible or investigators were oil stained after handling the mussels. Gas bubbles were not observed in this mussel bed. This bed is dominated by large mussels, 78 - 105 mm long, which likely represent the last major settlement period at this site (Figure 5.2c). Mussel density in the bed was calculated to be 876 mussels m^{-2}, with calculated mussel biomass of 37.7 kg m^{-2}.

5.9.2 SM Ia Population Structure

The population structure of mussels from the three sites was strikingly different (Figure 5.2). Clearly the beds sampled at GC 234 are in an active settlement phase, and the bed at GC 272 has not seen successful recruitment in many years (the GC 184 beds show an intermediate pattern). It is not clear why there would not have been recruitment to GC 272 prior to 1992 as all measurements there (chemistry, growth rates, and condition indices) suggest that this was an excellent habitat at that time. The mussels there are currently relatively isolated from the rest of the population and larval supply there may have been limiting. Alternatively, if the variation in conditions documented during this study are characteristic of the recent history of this bed, this may explain the lack of juveniles there as they would be much more sensitive to significant perturbations in nutrient supply due to their higher metabolic demands. When one considers the spatial and temporal variation in seepage and the reliance of the mussels on methane in the seeping fluid, even large differences in population structure of mussel beds, which are only meters apart, is not surprising (MacDonald et al. 1990a).

5.9.3 SM Ia Chemical Microhabitat

The use of the new water sampling tools described here allowed collection of discrete water samples from specific points in and over the mussel beds, without the extensive dilution by ambient water, which had plagued previous efforts of this sort (personal observation; Fisher 1993). One fact that became abundantly clear in evaluation of the present data set (and confirmed by subsequent data sets) is that the presence of "seep fluid" is patchy. Even on scales of 0.1 m within a mussel bed, there are substantial vertical gradients on scales of centimeters as well. Because it is not known whether the mussels are able to acquire dissolved methane from their

siphons only or through their pedal gape as well, it is not clear exactly what methane concentrations they are actually exposed to. However, clear differences in methane and sulfide levels among the mussels at the different sites were evident, as was a change in conditions at GC 272 between 1992 and 1993.

Methane concentrations measured in the two experimental beds at GC 184 were consistently in the range 0 - 56 μM over both years (Table 5.7). Based on the laboratory studies of Kochevar et al. (1992), methane concentrations between 20 and 60 μM are barely adequate for growth of this mussel, with methane as the major carbon and energy source. Although growth was easily detectable in the population as a whole (Table 5.8), the lack of detectable growth in over 1/3 of the mussels less than 60 mm in shell length (Figure 5.4a) supports the suggestion that nutrient levels (mainly methane) were barely sufficient for maintenance of this population. The low environmental methane levels are also reflected in the physiological condition of the mussels from GC 184. Although the only year in which they were significantly different from the other sites was in 1991, the average values for the GC 184 collections indicated that those mussels were on the bottom of the condition scale every year.

At the other end of the spectrum, methane concentrations in 5 cm interstitial water from the GC 234 beds were as high as 10744 μM, and a concentration of 832 μM was documented around the siphons of mussels in 1993 (Table 5.7). The highest specific growth rates and average adult growth rates were found in the GC 234 mussels for the 1992-1993 period (Tables 5.9 and 5.10). The average values of the condition parameters were in general intermediate between those of the GC 184 and GC 272 mussels, with the GC 272 mussels having significantly higher condition index, lipid content, and significantly lower water content in both 1991 and 1992. This data implies that factors other than methane may be affecting the health of the mussels.

Table 5.8   Average growth rate of SMIa in size range 60 - 90 mm shell length from 3 hydrocarbon seep sites and 2 transplant experiments. Rates were determined two ways: absolute growth, the measured change in length per time (between 340 and 320 days) and normalized to a per year basis, and the specific growth rate, the measured change in length per time per unit length (calculated as a percent increase), also normalized to a per year basis. Standard deviation of the mean given in parenthesis. Values that are underlined are significantly different from the other two sites (p < 0.05). Sites marked with an asterisk are significantly different between years (p < 0.05). ‡Growth at transplant I was significantly different from GC 184 over the same time period (p < 0.01).

Site	1991 - 1992 Growth		n	1992 - 1993 Growth		n
	Absolute (mm/yr.)	Specific (%/yr.)		Absolute (mm/yr.)	Specific (%/yr.)	
GC 184	0.1 (0.9)	0.2 (1.4)	31	0.4 (0.4)	0.6 (0.6)	31
*GC 234	0.4 (1.4)	0.4 (1.9)	21	<u>1.9 (1.2)</u>	<u>2.9 (1.9)</u>	21
*GC 272	<u>1.7 (1.2)</u>	<u>1.9 (1.7)</u>	9	0.5 (0.6)	0.6 (1.2)	2
‡Transplant I	1.1 (1.0)	1.6 (1.4)	16	----------	-----------	—
Transplant II	-0.2 (0.4)	-0.3 (0.7)	14	----------	-----------	—

Table 5.9   Growth parameters of SMIa derived from Ford-Walford plots.

Site	K		L_{Max}	
	1992	1993	1992	1993
GC 234	0.205	0.210	74.37	74.26
GC 184	0.016	0.016	103.14	104.4
GC 184 Transplant I	0.108	--------	83.74	--------

Table 5.10   Condition indices and size range for SMIa at three hydrocarbon seep sites and two transplant experiments. Values for each site and year are averages (±SD). Underlined values were significantly different (p < 0.005) from collections at the same site in other years. Values marked with an asterisk are significantly different from values at the other sites in the same year (p < 0.01). The set of values underlined with a dashed line (% water in GC 234 in 1991 and 1992) were significantly different from each other (p < 0.01). Transplant values marked with a + were significantly different (p < 0.05) from GC 184 values in the same year. ‡ Lengths between sites were significantly different every year (p < 0.01 between GC 272 and the other two sites and p < 0.05 between GC 184 and GC 234). Lengths were not significantly different within the sites between years. TP = Transplant, WW = wet weight.

Collection Site Year	Glycogen (% WW)	Condition Index (g / ml)	Water (% WW)	Length (mm)‡ Range	Average	n
GC 184 - 1991	0.88 (0.63)	*0.037 (0.014)	*90.4 (2.03)	58 - 83	73 (8.3)	17
GC 184 - 1992	1.13 (0.88)	0.053 (0.018)	90.8 (2.28)	27 - 93	68 (15.7)	32
GC 184 - 1993	0.73 (0.44)	0.051 (0.010)	90.5 (1.25)	59 - 92	74 (10.5)	12
GC 234 - 1991	1.55 (0.82)	*0.061 (0.018)	*88.1 (1.84)	47 - 75	67 (7.9)	20
CG 234 - 1992	1.50 (0.96)	0.062 (0.019)	90.3 (1.92)	36 - 81	60 (13.9)	29
GC 234 - 1993	1.33 (0.73)	0.062 (0.020)	89.3 (2.84)	45 - 83	63 (12.1)	12
GC 272 - 1991	*2.94 (1.19)	*0.079 (0.024)	*86.0 (2.61)	72 - 105	90 (9.6)	20
GC 272 - 1992	*3.58 (1.24)	*0.105 (0.025)	*85.3 (2.43)	53 - 116	91 (15.3)	30
GC 272 -1993	1.07 (0.66)	0.056 (0.011)	90.0 (1.45)	64 - 110	92 (11.5)	11
TP I -1992	1.47 (0.73)	0.061 (0.13)	89.9 (1.6)	52 - 92	70 (10.6)	6
TP II -1992	0.41 (0.31)	+0.036 (0.012)	+93.3 (1.28)	50 - 94	68 (11.1)	6
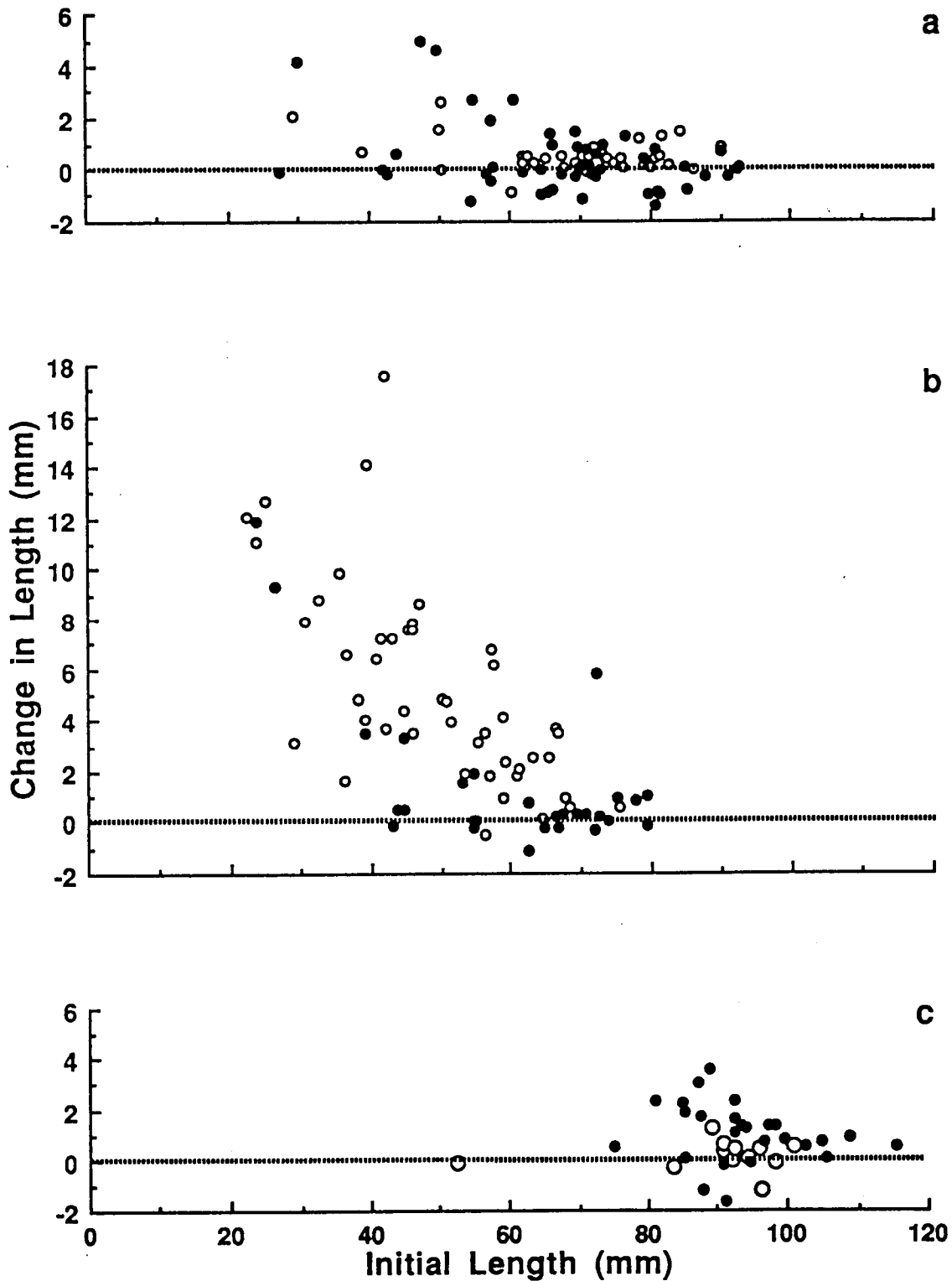
Figure 5.4   Change in length as a function of initial shell length for SM Ia from three hydrocarbon seep sites. Solid circles = change in length from 1991 to 1992 (~365 days) as a function of 1991 length, Open circles = change in length from 1992 to 1993 (~321 days) as a function of 1992 length, a) GC 184, b) GC 234, and c) GC 272.

Certainly the sulfide levels measured in these beds were the highest measured in this study, and all collections from this site were oil stained.

At the single bed investigated at GC 272, the five water samples taken in 1992 ranged from 27 to 822 μM CH_4 and the four taken in 1993 from 2 to 4 μM CH_4. This indicates a substantial change in the microhabitat of the mussel bed, from sufficient to marginal methane concentrations. This was strongly reflected in the reduced growth rates and significant drop in the physiological condition of the population in 1993 (Figure 5.4c, Tables 5.9 and 5.10). In 1991 and 1992, all three condition indices indicated that the mussels from GC 272 were in the best condition of any of the collections, although methane levels were higher at GC 234 in 1992. No crude hydrocarbon seepage associated with the GC 272 bed was apparent. The bioaccumulation of hydrocarbons in mussel tissue is known to adversely affect growth rates, reproductive processes, and nutritive storage capabilities (Bayne et al. 1982; Lowe and Pipe 1986; Stromgren and Nielsen 1991; Stromgren et al. 1986). As previously mentioned, crude hydrocarbons are abundant in both the GC 234 and GC 184 mussel beds. Wade et al. (1989) found that hydrocarbon loading (mostly polycyclic aromatics) of animals at the seeps is high, especially for the sessile organisms. Among mussels examined from several beds in all three sites, McDonald (1990) found that the tissue hydrocarbon concentrations were highest at the GC 234 site. Although McDonald (1990) demonstrated a cytochrome P450-dependent enzymatic detoxification mechanism at relatively high activities in SMIa (McDonald 1990), this adaptation to their potentially toxic environment is likely to exert a substantial metabolic cost on seep mussels inhabiting areas with high hydrocarbon levels, and may explain the better condition of the GC 272 mussels.

5.9.4 Growth Rates and Ages of SM Ia

The average growth rates, measured as increments in shell length, for adult SM Ia are roughly equal to growth rates reported for healthy mussels from littoral environments at similar temperatures (5-8°C) (Forster 1981; Sukhotin and Kulakowski 1992; Theisen 1973). These rates (Table 5.8) are over an order of magnitude higher than rates reported for a small deposit-feeding deep-sea bivalve (0.084 mm yr^{-1}; Turekian et al. 1975), but are lower than those of the related vent mytilid, *Bathymodiolus thermophilus*, which grows at rates similar to littoral mytilids from similar temperatures (about 1 cm yr^{-1} at 10-20°C) (Lutz et al. 1985; Rhoads et al. 1981; Stromgren and Cary 1984). Unlike most deep-sea environments, vents and seeps are very productive (as a result of chemoautotrophy and methanotrophy) and thus, as long as the sites remain active, the fauna are less limited by nutrient supply than the surrounding slope benthos (see reviews by Fisher 1990; Lutz and Kennish 1993; Tunnicliffe 1991).

Like most animals, the juveniles grow much more rapidly, although mussels over a year old are still growing at rates over 1 cm yr^{-1} at some sites (Figures 5.4b and 5.5b). This is likely driven by allometric changes in size specific respiration rates and resource allocation to reproductive effort (Reiss 1989; Seed and Suchanek 1992; Thompson 1984). The fast growth rates of juveniles may also be of ecological importance to the species. There are several possible predators at the seeps, including several decapods, starfish, and fish (Carney et al. submitted). These types of predators forage selectively on a size range of mussels in temperate habitats (Seed and Suchanek 1992), and likely behave similarly at seeps. The shells of these mytilids are relatively delicate (especially those below ~15 mm shell length) and are, therefore, potentially easy prey. Rapid growth of the juveniles will shorten the time period of maximum vulnerability to selective predation (Seed and Suchanek 1992). On the other hand, the slow growth rates of adults suggests that these bivalves may
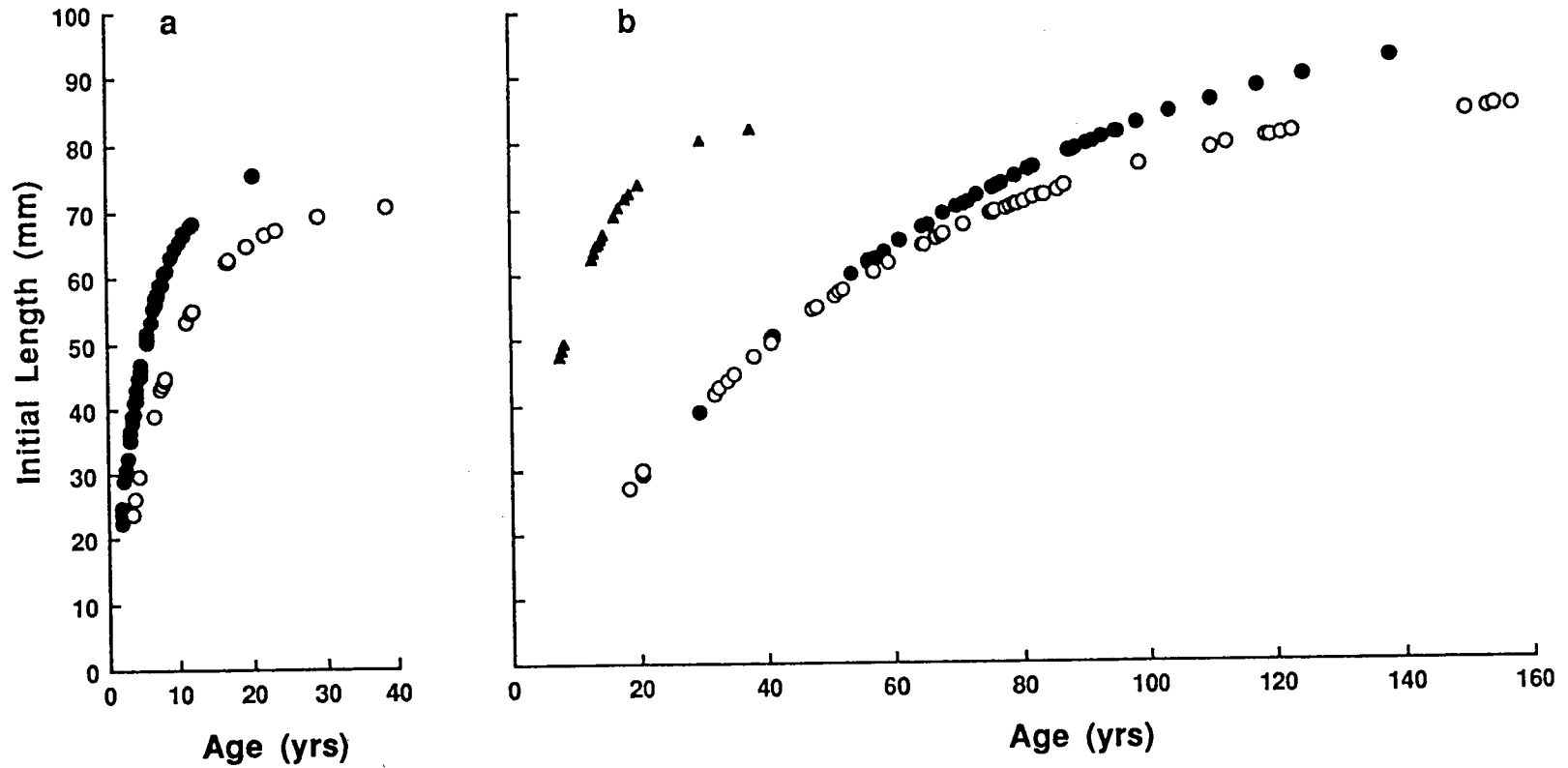
Figure 5.5 Age estimations for SM Ia from a) GC 234 (open circles = 1991, solid circles = 1992) and b) GC 184 (open circles =- 1991, solid circles = 1992, solid triangles = transplant I). Estimates were calculated using the von Bertalanffy growth equation, $L_t - L_{max} [1-e^{-kt-t_0}]$. Parameters for the equation, derived from a Ford-Walford plot, are given in Table 5.3.

live a long time after reaching reproductive competence, even under sub-optimal conditions.

Since the growth rate varied with initial length, statistical comparisons between sites were limited to the mature mussels between 60 and 90 mm in shell length (mussels in this size range were found at all sites and growth rate does not vary significantly as a function of shell length for mussels in this range). Both the average absolute growth rates and the average size specific growth rates ($\Delta L \cdot T^{-1} \cdot L^{-1}$; Almada-Villela 1984; Wootton 1991) were compared using one-way analysis of variance. Statistical differences and trends between sites and years were the same for both methods and only absolute growth rates are discussed.

No significant difference was found between the average growth rates of mature mussels at GC 184 and GC 234 in the 1991 to 1992 interval, but the average rate in GC 234 was higher in the 1992 to 1993 interval ($p<0.01$). Comparisons of GC 272 to GC 184 and GC 234 indicated a faster average rate at GC 272 ($p<0.01$) in 1991/1992; however, in 1992/1993, the average growth rate at GC 272 fell sharply and was significantly lower than GC 234 ($p<0.05$) yet not significantly different from GC 184.

Bivalve ages are commonly estimated by means of either the von Bertalanffy or the Gompertz growth equations (Bayne and Worrall 1980; Craeymeersch et al. 1986; Rhoads et al. 1981). The von Bertalanffy equation, ($L_t = L_{max} [1-e^{-k(t-t_0)}]$, where L_t is the shell length at the beginning of the experiment, L_{max} is the extrapolated point of no growth, k is the rate at which L_{max} is approached and t is time), provides a better description of growth for a population of more mature animals (Powell and Somero 1986; Seed and Richardson 1990) and the Gompertz equation, ($\log_{10} L_t = \log_{10} L_{max} [1-e^{-k(t-t_0)}]$), gives better descriptions of growth of juveniles (Theisen 1973). Due to the size disparity between the sites, ages were estimated for each population using both techniques. The age estimates from these

two equations were not notably different at GC 234. However, at GC 184, the Gompertz equation yielded much greater ages (up to 350 years old) than did the von Bertalanffy equation. This is likely a reflection of poor representation of smaller mussels at this site. Therefore, the results shown in Figure 5.5 are age estimations based on the von Bertalanffy growth equation. The parameters, L_{max} and k, are estimated from a Ford-Walford plot (Craeymeersch et al. 1986; Seed and Richardson 1990) and are given in Table 5.9. These parameters are obtained by plotting the length at a given time against the length a year before (Bayne and Worrall 1980). Age estimations for GC 234 and GC 184 are shown in Figures 5.5a and 5.5b, respectively, and were not calculated for GC 272 due to the complete lack of mussels below 50 mm in length (Figure 5.4c).

The variable nature of methane seepage (Behrens 1988; Roberts et al. 1990) makes evaluation of the calculated ages problematic. Although this variability is on much longer scales than that documented around hydrothermal vent fauna (where significant differences in the chemical environment around animals can occur on scales of seconds to minutes, Johnson et al. 1988), it can certainly be significant on scales relevant to age calculations. For example, if one assumes that conditions have been constant at the GC 184 site for the past 160 years, then there are likely mussels present there at least that old. However, the strong possibility of changing conditions within a bed (as clearly documented for GC 272 within 3 years) suggests that the mussels there may have reached a significant portion of their present size under different (more favorable) environmental conditions, and that the calculated ages are, therefore, an overestimation. This possibility was empirically demonstrated by one of the transplant experiments where mussels from the GC 184 site were moved <3 meters and left for one year (transplant I, see section 5.4.6). Maximum ages calculated from the shell growth of the transplanted GC 184 mussels (Figure 5.6) dropped to 40 years (from 160 years for the source population) (Figure 5.5a).
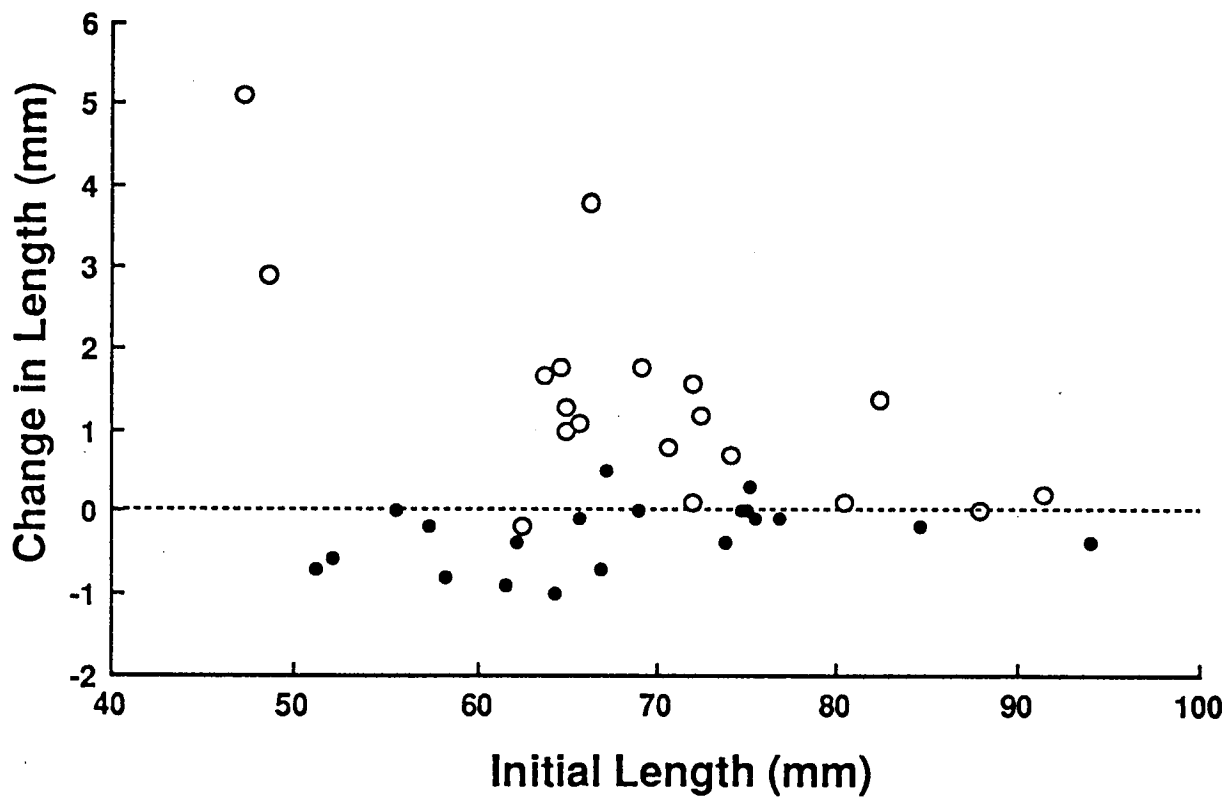
Figure 5.6   Change in length as a function of initial shell length for two GC 184
transplant experiments, open circles = transplant I, located 3 m away
from the original GC 184 mussel bed, solid circles = transplant II,
located 2 m away from the original GC 184 mussel bed. Duration of this
study was 325 days.

Thus, the age calculations assume growth over the entire life span of the organism under the current conditions, which is unlikely. However, these calculations do provide information on growth capabilities. Data from GC 234 in 1992 (Figure 5b) indicates that SM Ia can grow quite rapidly, and data from GC 184 in 1992 suggests they can also grow quite slowly without significant effects on condition. Based on these considerations and the fact that mussels up to 105 mm were collected at GC 272, it is reasonable to conclude that SM Ia can live for at least 50 years, and perhaps much longer.

5.9.5 Measures of Condition of SM Ia

No significant differences were found between marked and unmarked mussels in terms of glycogen, water content, and condition index in any collection from any site during the duration of the study. We conclude that any differences between sites or years are site specific and not the result of the marking procedure.

Due to the wide size range of mussels at GC 234 (and not at the other two sites), data from this site was used to check possible effects of size on the variation in the condition parameters (data from the three years was combined in order to achieve a more representative size range). Regression analyses indicated no significant relationship between shell length and condition index, water content, or glycogen.

Table 5.10 shows the mean values (±SD) of each of the condition parameters in each year for the three growth sites. Significant differences were demonstrated between GC 234 and GC 184 for water content and condition index in 1991 ($p<0.01$). No significant differences were found, for these parameters, between the sites in 1992 and 1993 or in glycogen content in any year. GC 272 mussels had significantly higher glycogen contents ($p<0.05$), higher condition indices ($p<0.01$), and lower water contents ($p<0.01$) than the other two sites in both 1991 and 1992, but not in 1993.

Mean shell lengths of mussels from all sites were significantly different in each year (p<0.05), but mean lengths within a site were not significantly different among years.

Two lines of reasoning support the utility of the condition indices. First, all significant differences in pairwise comparisons (between sites in a given year, or among years at a single site) were corroborated by all three indices, with one exception: GC 184 and GC 234 in 1991, where a significant difference was not demonstrated in glycogen content but was for the other two parameters. Thus, the three indices are internally consistent. Secondly, all three parameters were significantly correlated with growth rates measured in adults at GC 272 (Figure 5.7). This data set was chosen because of the range in growth rates among adults there and to avoid a data set with a large size range of individuals (because of the allometric effects on growth rate and not the other parameters). The largest r^2 and smallest relative 95% confidence interval on the slopes of these regressions was that relating growth and CI. This is likely due to the fact that determination of tissue water content is sensitive to residual mantle water and, therefore, draining technique (which is accomplished in a cold van on board ship), whereas CI is not, and the fact that glycogen content may be more sensitive to reproductive state and hydrocarbon exposure (Bayne 1976; De Zwaan and Mathieu 1992; Hummel et al. 1989; Lowe and Pipe 1986). The significant correlation between the growth rates recorded for individual mussels, and their condition as assayed by
our indices, corroborates the efficacy of our measures of physiological condition: the mussels with high condition indices are growing faster.

5.9.6 Transplant Studies with SM Ia

The transplant experiments provided additional insight into to the ecology of the mussels. The initial purpose of these experiments was to deprive the mussels of methane by placing them away from their food source in unoccupied mud, and follow
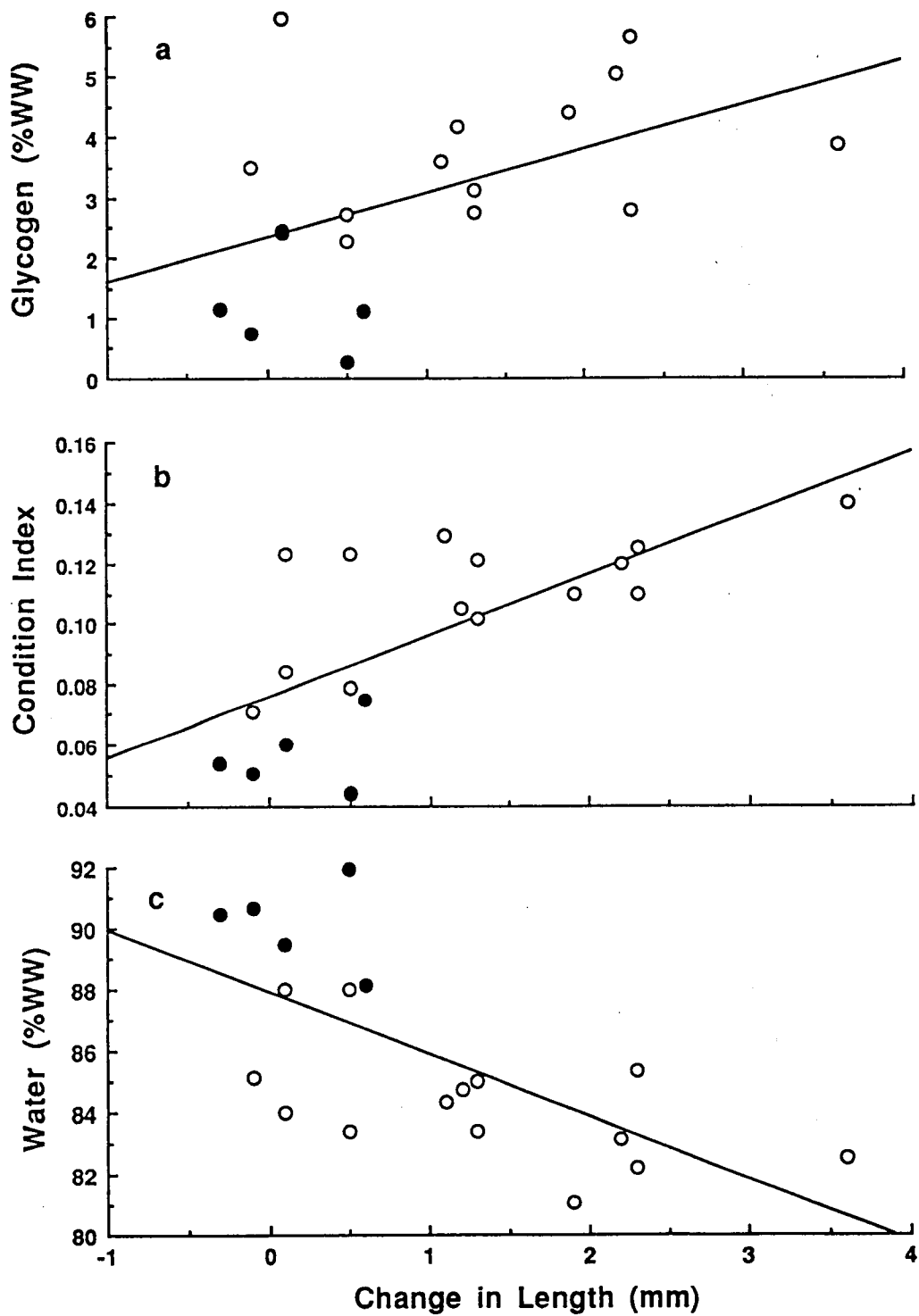
Figure 5.7   Relation between growth rate and condition indices in SM Ia from GC 272; data for 1992 (open circles) and 1993 (solid circles) are combined for the linear regression. a) Glycogen as a function of change in length, regression equation: $y = 0.73x + 2.313$ ($p<0.05$), 95% CI on slope is ±0.67, b) Condition index as a function of change in length, regression equation: $y = 0.020x + 0.076$ ($p<0.001$), 95% CI on the slope is ±0.01, c) Water content vs. change in length (mm), regression equation: $y = -2.03x + 87.88$ ($p<0.005$) 95% CI on slope is ±1.15. The slopes for each parameter were also significant ($p<0.05$) when tested with the 1992 data alone.

the effects on condition and growth. The results from transplant II (2 m from the original GC 184 site) were as expected. The average growth was -0.22 mm yr^{-1} (but was not significantly different from zero, $p > 0.3$), all condition indices fell dramatically (from the already low levels at GC 184), and in fact six of the 20 mussels were dead upon recovery. However, the mussels from transplant I, (located a little further away from the original bed and about 2 m from transplant II), were in better condition and grew at a faster rate (Figure 5.6, Table 5.8) than mussels from their bed of origin, and none of the 20 mussels died. The differences in growth rates in mussels that were only 2 m apart indicate that very localized effects are responsible. These differences are most likely differences in exposure to seeping fluid and since the transplant I mussels fared better than in their bed of origin, site chemistry alone is insufficient for establishment of a bed. As with intertidal mussels, another essential factor for the establishment of a bed is apparently substrate upon which to settle. Thus, the production of authigenic carbonates, which is often associated with seepage in the Gulf of Mexico (Brooks et al. 1990), can contribute to the production of habitats suitable for colonization by mussels.

5.9.7 Site Synopsis for SM Ia beds

When all data and observations are considered together, one can make some general conclusions concerning each site. The GC 184 beds have been active for at least 40 years, with appropriate conditions for larval settlement over most of that period. However, methane concentrations are currently low in the bed (although a stream of methane bubbles issue from one point in the bed), growth rates were low, and the population was dominated by large mussels, with a calculated mussel biomass of 11.3 kg m^{-2}. A plausible explanation is that there has been a recent decline in the quality of the habitat within this particular bed, which is supported by the mussel condition indices. At the beds in GC 234, there was a preponderance of

young mussels, indicating a recent active settlement period, and methane concentrations were high, as were growth rates. The mussel biomass in this bed was only 7.3 kg m^{-2}. However, the condition indices were significantly higher than for GC 184 mussels only in 1991 and significantly lower than GC 272 in both 1991 and 1992. Thus, although there were plenty of young, rapidly growing mussels, there may be some factor detrimental to condition. We suggest that may be due to exposure to high hydrocarbon levels and this may exert a considerable cost to the seep mussels. At GC 272 on the other hand, oil was never apparent during the collections. The mussels here were growing at appreciable rates in 1992 and were exposed to moderate to high levels of methane and the mussel biomass in this bed (37.7 kg m^{-2}) was considerably higher than in the other beds. Condition of animals in both 1991 and 1992 was excellent by all criteria. However in 1993, growth rates, condition, and methane concentrations in the bed had all decreased. The almost complete absence of juveniles here cannot be explained by the environmental measurements. We conclude that none of the beds studied here are providing "perfect" conditions for the mussels, and that sites with higher growth rates and productivity are likely present elsewhere.

Community methane oxidation rates were determined for each of the ring collection beds. According to the model of Kochevar et al. (1992), the seep mussels have a basal metabolic rate of 1 µmol O_2 g^{-1}hr^{-1} and methane oxidation rates between 4 and 10 µmol g^{-1}hr^{-1} for freshly collected mussels with non-limiting methane. It should be noted that these rate determinations were made on mussels with an average wet weight of 23 g. Since metabolic rate varies allometrically with wet weight in *Mytilus edulis* (Bayne 1976; Reiss 1989), the allometric equation BMR = aW^b (Reiss 1989) [where BMR = basal metabolic rate, W= wet weight, and a and b are derived parameters taken from literature on intertidal mussels; a=0.102, b=0.71 (Bayne and Newell 1983)] was applied to the above rates and the minimum mussel

bed oxidation rates necessary to sustain basal metabolism, and mussel bed methane consumption rates under optimal conditions, were estimated for each site using the quantitative ring collection data (the allometric relationship between length and wet weight from Figure 5.3 was used to determine wet weights for individual mussels in each ring collection). Minimum calculated mussel bed oxidation rates range from 2.9 $g\,d^{-1}m^{-2}$ at GC 234 to 49.4 $g\,d^{-1}m^{-2}$ at GC 272 (GC 184 = 7.2 $g\,d^{-1}m^{-2}$). Under optimal conditions (of O_2 and CH_4 concentrations), maximal methane consumption rates range from 14.6 $g\,d^{-1}\,m^{-2}$ at GC 234 to 197.7 $g\,d^{-1}\,m^{-2}$ at GC 272 (GC 184 = 36.2 $g\,d^{-1}\,m^{-2}$). These values are in the same range as those calculated by Fisher (1993) and are several orders of magnitude higher than any other aquatic system (Fisher 1993; Frenzel et al. 1990; Kuivila et al. 1988).

5.10 Implications of Growth Experiments and Habitat Characterizations on MMS Management Concerns

One of the main purposes of the studies described above was to address MMS management concerns on the robustness of these various communities. The very slow growth rates and long lives of the vestimentiferans indicates that a community destroyed by a physical disturbance would not recover in 100 years. In fact, as these animals require a hard exposed substrate to settle on, and very active seepage at that point in space, sedimented communities that are physically damaged would likely never recover.

The vesicomyid clams, on the other hand, are sparsely distributed and mobile. It is unlikely that a physical disturbance would impact either the population in the area or the habitat they require.

The bathymodiolid mussels, which use methane as a carbon source (seep mytilid Ia), have strict chemical requirements that tie them tightly to areas of the most active seepage in the Gulf of Mexico. Where conditions are right, they consume

methane at very high rates and produce biomass at rates that could be significant to the surrounding deep-sea fauna. Both individual mussels and communities appear to be relatively long lived, although the mussels are also capable of growing to reproductive size very quickly. Physical disturbance of an active mussel bed is unlikely to have a long lasting effect on the community due to the high growth rates of the individuals. Furthermore, the unexpected results of the transplant experiments suggests that the mussel distribution is limited by hard substrate and these animals may even increase in number if that substrate is supplied on the ocean floor.

6.0 Sessile Macrofauna and Megafauna at Mussel Beds
Robert S. Carney

6.1　Introduction

Prior to initiation of systematic sampling, it was generally expected that the fauna associated with the upper continental slope seeps off Louisiana would show some difference in composition between sites, among mussel beds within a single site, and even between the outer and inner portions of individual beds. These expectations can be developed both from succession and from island zoogeographic theory. If there is a succession in the fauna of mussel beds, then beds and positions of beds at different ages should also have a distinctive fauna. Alternately, if there is only random immigration from the normal background or distant seeps, then different mats and sites should show a faunal difference. The results of 61 *Johnson Sea-Link* grabs, detailed below, support neither succession nor island zoogeographic models. Edge to inner, bed to bed, and site to site, there is a monotonous consistency in the species compliment of the seeps.

Originally intended as an analysis of variance exercise looking at substrate, site, individual bed, and edge versus interior of the bed differences, in practice this study of the larger bed fauna ended as a general descriptive effort. Several aspects of the seep environment contributed to this. First, it is not feasible to target the substrate type during sampling. Except for the Brine Pool area, all beds proved to be underlain by rock, even if hidden by a thin veneer of mud. Second, it proved very difficult to locate patches suitable for sampling. Only a single mussel area was located at GC 272, and it was too small to sustain repeated sampling for a variety of purposes. Even at Bush Hill and GC 234, where beds seem to be abundant, finding a bed more than a few centimeters across accessible to the submersible was difficult.

Finally, even locating a definitive edge and inner area was difficult. However, these sampling problems did not mask the basic finding of a monotonous fauna.

6.2 Methods and Design

As originally envisioned and designed, megafaunal sampling would take the form of an analysis of variance allowing conclusions to be drawn about composition and abundance differences within/between seep sites, within/between different types of patches (mussel beds and tube worm clumps), and within/between the interior portions of a bed and the outer edge. The underlying questions all addressed the issue of how variable seep community composition was in space and, to some degree, in time. Unfortunately, we encountered three major problems in sampling for differences between types of patches. First, we could not devise a means of sampling either tubeworm clumps or clam beds that would assure capture of associated organisms. The worm clumps proved too large and well anchored for the methods available to us, while finding live clam beds suitable for sampling proved an elusive task. Second, my preliminary classification of mussel beds as being on rock or on sediment proved to be useless in the field; beds that appeared to be on mud usually proved to be on rock. Third, there was insufficient bottom time to search for appropriate bed types for sampling. As a result, this final report is restricted to the fauna of the mussel beds, which were well sampled. With the exception of the Brine Pool bed, all samples came from rock based mats.

6.2.1 Sampling Methods

All megafaunal sampling used the grab of the *Johnson Sea-Link* (JSL) submersible. The JSL grab is an integral part of the hydraulic manipulator on the *Johnson Sea-Link*. It consists of two semi-cylindrical jaws 19.2 cm long and 17.8 cm (T. Askew, personal communication) wide when open, which rotate closed about a

common axis. Under ideal conditions, the bite of the JSL grab samples 341 cm2 square meters of bottom. The JSL grab is powerful, extremely easy to use and can take repeated samples in just a few minutes. The real problem with the grab is that samples must be transferred into the "critter gitter" of the submersible. This is done by positioning the closed grab over a collection chamber and opening the grab so that the sample falls into the chamber. It is obvious that large amounts of sediment are lost during this transfer, and it is to be suspected that much of the smaller fauna is also lost. However, shelled and less mobile megafauna are successfully transferred.

6.2.2 Sampling Design

Due to the limitations of submersible sampling, the final sampling reflected opportunities that arose at the moment rather than prior planning. A total of 61 JSL grabs suitable for analysis were taken at four sites, Bush Hill, Green Canyon 272, Green Canyon 234, and Brine Pool NR-1 (Table 6.1). Sampling two different beds at each site proved impractical due to long search times, therefore all grabs were taken either from the same large bed at intervals separated by at least two meters or at adjacent small beds. In most instances, the planned sampling at the interior and at the edge was carried out, while at other sites bed geometry prevented this. All sampling was paired with two grabs being taken less than 50 cm. apart.

For data management, samples were designated by the dive number, a decimal point, and the chamber receiving the sample. Samples were classified as to site, bed 1 or 2, and replicate. A total of 63 samples were taken and logged, but two were rejected as having missed the mussel mat or lost material during transfer. Sample Analysis

Table 6.1   Sample collection for infaunal material.

Sample Dive/ Chamber	Date m/d/y	Latitude	Longitude	Depth feet	Site Block	Bed Location & Replicate
2598.02	09/14/89	27°43.38	91° 16.64	2149	GC-233	S outh End Pool 1
2598.03	09/14/89	27°43.38	91° 16.64	2149	GC-233	South End Pool 2
2598.04	09/14/89	27°43.38	91° 16.64	2149	GC-233	South End Pool 3
2598.05	09/14/89	27°43.38	91° 16.64	2149	GC-233	South End Pool 4
2598.07	09/14/89	27°43.38	91° 16.64	2149	GC-233	South End Pool 5
2598.08	09/14/89	27°43.38	91° 16.64	2149	GC-233	South End Pool 6
2598.09	09/14/89	27°43.38	91° 16.64	2149	GC-233	North End Pool 1
2598.10	09/14/89	27°43.38	91° 16.64	2149	GC-233	North End Pool 2
2598.11	09/14/89	27°43.38	91° 16.64	2149	GC-233	North End Pool 3
2598.12	09/14/89	27°43.38	91° 16.64	2149	GC-233	North End Pool 4
3137.11	09/19/91	27°41.27	91° 32.35	2372	GC-272	Bed 1 Interior Rep. 1
3137.12	09/19/91	27°41.27	91° 32.35	2372	GC-272	Bed 1 I nterior Rep. 2
3137.01	09/19/91	27°41.27	91° 32.35	2372	GC-272	Bed 1 Edge Rep. 1
3137.02	09/19/91	27°41.27	91° 32.35	2372	GC-272	Bed 1 Edge Rep.2
3137.03	09/19/91	27°41.27	91° 32.35	2372	GC-272	Bed 2 Edge Rep. 1
3137.04	09/19/91	27°41.27	91° 32.35	2372	GC-272	Bed 2 Edge Rep. 2
3137.05	09/19/91	27°41.27	91° 32.35	2372	GC-272	Bed 2 Interior Rep. 1
3137.06	09/19/91	27°41.27	91° 32.35	2372	GC-272	Bed 2 Interior Rep. 2
3139.12	09/21/91	27°46.92	91° 30.46	1790	CG-184	Bed 1 Edge Rep 1
3139.01	09/21/91	27°46.92	91° 30.46	1790	CG-184	Bed 1 Edge Rep. 2
3139.02	09/21/91	27°46.92	91° 30.46	1790	CG-184	Bed 1 Interior Rep. 1
3139.03	09/21/91	27°46.92	91° 30.46	1790	CG-184	Bed 1 Interior Rep. 2
3139.04	09/21/91	27°46.92	91° 30.46	1790	CG-184	Bed 2 Interior Rep. 1
3139.05	09/21/91	27°46.92	91° 30.46	1790	CG-184	Bed 2 Interior Rep. 2
3139.06	09/21/91	27°46.92	91° 30.46	1790	CG-184	Bed 2 Edge Rep. 1
3139.07	09/21/91	27°46.92	91° 30.46	1790	CG-184	Bed 2 Edge Rep. 1
3142.08*	09/25/91	27°44.72	91° 13.21	1787	CG-234	Bed 1 Interior Rep. 1
3142.09	09/25/91	27°44.72	91° 13.21	1787	CG-234	Bed 1 Interior Rep. 2
3142.10	09/25/91	27°44.72	91° 13.21	1787	CG-234	Bed 1 Interior Rep. 3
3142.11	09/25/91	27°44.72	91° 13.21	1787	CG-234	Bed 1 Edge Rep. 1
3142.12	09/25/91	27°44.72	91° 13.21	1787	CG-234	Bed 1 Edge Rep. 2
3142.01	09/25/91	27°44.72	91° 13.21	1787	CG-234	Bed 2 Interior Rep. 1
3142.02	09/25/91	27°44.72	91° 13.21	1787	CG-234	Bed 2 Interior Rep. 2
3142.03	09/25/91	27°44.72	91° 13.21	1787	CG-234	Bed 2 Edge Rep. 1
3142.04	09/25/91	27°44.72	91° 13.21	1787	CG-234	Bed 2 Edge Rep. 2
3145.12*	09/24/91	27°43.38	91° 16.63	2149	GC-233	Bed South Edge Rep. 1
3145.01	09/24/91	27°43.38	91° 16.63	2149	GC-233	Bed South Edge Rep. 2
3145.02	09/24/91	27°43.38	91° 16.63	2149	GC-233	Bed South Interior Rep. 1
3145.03	09/24/91	27°43.38	91° 16.63	2149	GC-233	Bed South Interior Rep. 2
3145.04	09/24/91	27°43.38	91° 16.63	2149	GC-233	Bed North Edge Rep. 1
3145.05	09/24/91	27°43.38	91° 16.63	2149	GC-233	Bed North Edge Rep 2
3145.06	09/24/91	27°43.38	91° 16.63	2149	GC-233	Bed North Interior Rep. 1
3145.07	09/24/91	27°43.38	91° 16.63	2149	GC-233	Bed North Interior Rep. 2

Table 6.1 Continued

3265.04	08/09/92	27°44.76	91° 13.33	1770	GC-234	Bed 1 Edge Rep. 1
3265.06	08/09/92	27°44.76	91° 13.33	1770	GC-234	Bed 1 Interior Rep. 1
3265.07	08/09/92	27°44.76	91° 13.33	1770	GC-234	Bed 1 Edge Rep. 2
3265.08	08/09/92	27°44.76	91° 13.33	1770	GC-234	Bed 1 Interior Rep 2
3265.09	08/09/92	27°44.76	91° 13.33	1770	GC-234	Bed 2 Edge Rep. 1
3265.10	08/09/92	27°44.76	91° 13.33	1770	GC-234	Bed 2 Interior Rep. 1
3265.11	08/09/92	27°44.76	91° 13.33	1770	GC-234	Bed 2 Edge Rep. 2
3265.12	08/09/92	27°44.76	91° 13.33	1770	GC-234	Bed 2 Interior Rep.2
3268.05	08/10/92	27°44.78	91° 13.28	1771	GC-234	Bed 1 Interior Rep. 1
3268.06	08/10/92	27°44.78	91° 13.28	1771	GC-234	Bed 1 Interior Rep. 2
3268.07	08/10/92	27°44.78	91° 13.28	1771	GC-234	Bed 1 Edge Rep. 1
3268.08	08/10/92	27°44.78	91° 13.28	1771	GC-234	Bed 1 Edge Rep. 2
3269.01	08/11/92	27°47.00	91° 30.47	1825	GC-184	Bed 1 Edge Rep. 1
3269.02	08/11/92	27°47.00	91° 30.47	1825	GC-184	Bed 1 Edge Rep. 2
3269.11	08/11/92	27°47.00	91° 30.47	1825	GC-184	Bed 1 Interior Rep. 1
3269.12	08/11/92	27°47.00	91° 30.47	1825	GC-184	Bed 1 Interior Rep. 2
3274.12	08/14/92	27°46.99	91° 30.46	1785	CG-184	Bed 1 Edge Rep. 1
3274.01	08/14/92	27°46.99	91° 30.46	1785	CG-184	Bed 1 Edge Rep. 2
3274.02	08/14/92	27°46.99	91° 30.46	1785	CG-184	Bed 1 Interior Rep. 1
3274.03	08/14/92	27°46.99	91° 30.46	1785	CG-184	Bed 1 Interior Rep. 2

* Sample considered bad due to lack of seep fauna and omitted from analysis.

Final analysis was very much influenced by the results obtained. The faunal composition proved to be so monotonous site to site, bed to bed, and edge to inner, that simple graphics and descriptive statistics were used. The very high dominance of a few gastropods and the general lack of correlation among fauna eliminated the utility of multivariates and made description the most useful analytical tool.

6.3   Results

The mussel bed samples were dominated by only 13 species. Of these, only the mussels and the gastropods, *Bathynerites* and *Provanna,* were sufficiently abundant to support statistical analysis. The counts for the remaining species were

dominated by zeroes, introducing major sample-size artifacts into any analyses undertaken. There were no significant correlations among the faunal groups overall, thus eliminating multivariates as a useful analytical tool.

6.3.1 The Mytilid Substrate

A total of 1542 specimens of the seep mytilid Ia-type mussel were taken in 61 JSL grabs. Collectively, specimens between 3 and 8 cm predominated. Juveniles less than 1 cm were abundant, but restricted to only four samples (3265-11 and 3142-3 outer edge grabs at GC 234, and 3137-5 and 3137-6 inner area grabs at GC 272). Specimens from 8 to 13 cm were few in number, but predominated in 17 samples from all sites. There were distinct inter-sample differences in size structure of the population, but these did not correspond to the factors of the sampling scheme (inner versus edge, different patches at a site, differences in patches) in any consistent manner. Ten Bush Hill (GC 184) and GC 234 samples had a wide size range of individuals. Only one location showed an exclusive predominance of smaller forms, a clump at CG 234. All other samples, regardless of site, clump, or position were dominated by animals in the 5 cm and greater size classes.

At the Brine Pool (GC 233), with its assumed simple gradient geometry, size segregation with smaller specimens predominating at the inner edge was apparent in observation and reinforced by sampling. The results of sampling at other sites (as well as observation) indicated that a similar segregation was taking place at all sites, but over a much smaller and complex spatial scale. Approximately 33% of the areas are predominated by specimens larger than 5 cm with no, or very few, smaller specimens. Of the 67% of the area with a wider size range, including smallest forms, only 7%, or four, samples showed recent recruitment to the smallest size class. The GC 272 results are unique in that the outer edge samples proved to be

articulated dead shells with no living mussels, and the inner edge samples were bimodal, with a few large specimens and many in the 1 cm class.

When the size frequency data taken from the *Johnson Sea-Link* grabs is combined with diver observation, it is apparent that successful recruitment of juvenile mussels into the smallest size class is relatively uncommon and restricted to discrete small areas within existing mussel beds. Clumps of small mussels have been observed al all four dive sites, even though such a clump was actually sampled only once. Unfortunately, at our current level of understanding we can not ascribe this recruitment pattern to rare and aggregated larval settlement in chemically suitable habitats, spatially heterogeneous post-settlement survival, or size segregating post-settlement migration.

Due to the great size range in mussels, count is a poor expression of the extent to which the mussels provide a habitat for associated species. Biomass, being an expression of volume, is more informative. The average biomass was 24.21 g AFDW/ sample (SD = 20.39) with a maximum 85 grams. Only 11 (approx. 20%) of the samples had a mussel biomass greater than 40 grams, and these came from all four sites. Although extrapolation to a larger size area is of questionable validity, it facilitates comparisons. The average mussel biomass over all sites and samples was 710 g AFDW/M^2 with a maximum observed of 2491 grams.

6.3.2 Seep Mytilid - *Bathynerites* Relationships

Bathynerites naticoidea (Gastropoda) was the dominant heterotroph in mussel beds. Much smaller than the mussels, it was actually the numerically dominant animal collected in the mats; 2,571 specimens were collected in 50 out of 61 *Johnson Sea-Link* samples. While present at all four sites, there were distinctive inter-site differences. *Bathynerites naticoidea* was most abundant at Bush Hill and GC 234 sites, but was less abundant at the Brine Pool and GC 272. Both of these

low abundance sites contained relatively large specimens. Where *Bathynerites naticoidea* was numerous, there was a wide size range. The highest abundance (317 specimens) was predominated by small (<4mm) specimens. That sample (collected on JSL dive 3142) coincided with a bed of numerous smaller mussels at the GC 234 site.

One sample was dominated by many small mussels and many small *Bathynerites*; otherwise, correlation between mussel and snail abundance was low and indicated little direct dependence on the scale of the sampling. A changing relationship between Bathynerites populations and the Bathymodiolus substrate is suggested by the statistical summaries in Table 6.2. The variances of counts and biomass values are so great that all four sites may be viewed as values along a continuum from high densities of mixed size mussels down to low densities of a few older individuals. *Bathynerites* was distinctly less abundant at GC 272 and the Brine pool, both in samples and in observations, and no mussel-snail correlation exits. Where the snail is abundant, Bush Hill and GC 234, higher correlation suggest some relationship between mussel and snail abundance.

Table 6.2   Site-specific *Bathymodiolus-Bathynerites* relationships.

	Bush Hill, n=16	GC 234 n=20	GC 272 n=8	Brine Pool n=17
Mussel Count	68.06 ± 87.95	46.95 ± 51.67	13.37± 24.68	8.35 ± 4.84
Snail Count	26.50 ± 19.54	62.25 ± 85.26	3.00 ± 4.11	12.53 ± 11.95
Mussel Biomass	30.57 ± 21.96	15.95 ± 15.04	20.45 ± 30.12	28.34 ± 16.57
Correlation				
Count - Count	0.777	0.540	0.337	0.172
Biomass - Count	0.474	0.558	0.119	.0400

6.3.3 Relationships With *Provanna scuplta*

A total of 511 specimens of *Provanna scuplta* were taken in 37 out of 61 submersible grabs. On a site basis, *P. scuplta* appeared to be rare at the Brine Pool, but ubiquitous elsewhere. It showed no consistent relationship with either the extent of substrate, or with the abundance of *Bathynerites*, Table 6.3.

Table 6.3   Site-specific *Provanna-Bathymodiolus-Bathynerites* relationships.

	Bush Hill, n=16	GC-234 n=20	GC-272 n=8	Brine Pool n=17
Mussel Count	68.06 ± 87.95	46.95 ± 51.67	13.37± 24.68	8.35 ± 4.84
Provana Count	8.38 ± 15.80	4.71 ± 8.82	9.00 ± 11.8	0. 06 ± 0.24
Correlation				
Count - Count	0.107	-0.260	0.396	0.141
Biomass - Count	0.224	0.009	0.260	.090
Nerite-Provanna	0.122	-0.004	0.974	-0.19

6.3.4 Geographic Patterns of Subdominant Species

Species counts are presented in Appendices (Volume III). Except for the two most abundant gastropods (Bathynerites and Provanna), all other species occurred in half or fewer samples. Any discerned patterns are likely to be influenced by sampling artifacts. The highly mobile shrimp, *Alvinocaris stactophila*, and squat lobster, *Munidopsis*, n. sp. probably avoid capture and have been observed to flee from the sample during transfer. As such, they may be seriously under-sampled. As many as 15 of the former have been taken in a single sample, but *Alvinocaris stactophila* was only taken in 31 of the 61 JSL grabs. It was not found in the few samples at GC 272. *Munidopsis* n. sp. was taken 25 times, with a maximum count of five; it was collected at all sites. The large orbinnid polychaete now undergoing taxonomic study by R.E. Ruff was taken 18 times, most frequently at the Brine Pool. It was not found at GC 272. Due to its observed aggregating behavior, it mighty

easily go unsampled. The gastropod, *Cataegis*, was found at all sites, a maximum abundance of 24 per grab, and present in 21 samples. The chitin, *Ischnochiton*, was taken in only four samples, exclusively at GC 272. However, other species have been taken at all sites. Similarly, an unidentified nemertine, a sipunculid, a limpit, and a small crab, *Trichopeltarion nobile*, were collected four or fewer times with no obvious geographic pattern.

6.4   Discussion: The Origins and Significance of Monotony

Since all the mussel mat-associated fauna are mobile, it should be expected that parts of a bed and beds separated by a few meters should share a common fauna. It is the similarity between sites that is most puzzling. It has two interpretations. First, conditions for successful colonization of a bed by a heterotroph must be so restrictive that only a particular suite of species can inhabit them. Second, all sites must be roughly at the same stage of succession or non-successive immigration. This seems only feasible if all are relatively old — old enough for the faunal composition to have reached an equilibrium. The failure to find simple relationships among species is disappointing since it underscores this project's failure to identify population regulating mechanisms. From a management perspective, the monotony of the mussel bed fauna across sites suggests that local damage to populations would probably be mitigated by recolonization from adjacent sites. There is a pool of common inhabitants largely restricted to the mussel bed system, but site-specific endemics do not appear to exist among the heterotrophs.

6.5   Description and Natural History of the Megafaunal Organisms
6.5.1 Mollusca

The upper slope seep communities are mollusc-dominated with respect to both chemosynthetic and heterotrophic forms. Mussels of the *Bathymodiolus*

species complex form the primary biogenic substrate. On the basis of external morphology, all specimens collected in this component of the study were the same species, and may be referred to as the seep Mytilid Ia. All further reference to "mussel" in this section refers to this form. Resolution of specific subdivisions of the five or more forms in the Gulf of Mexico *Bathymodiolus* complex is under study by Lutz, Turner, and associates. Sediment dwelling chemosynthetic forms *Calyptogena ponderosa* and *Vesicomya cordata, Lucinoma atlantis, Lucinoma* sp., and *Thyasira oleophila* are also associated with the seeps (Callender et al. 1990). There is a marked absence of heterotrophic bivalves in the seep community. A limid bivalve, *Acesta bullisi*, appears to be heterotrophic, but in addition to being found attached by byssal fibers to the rocks, some specimens enclose the anterior opening of tube worms suggesting a complex mutualism (Kohl and Vokes 1994).

The mussel-shell habitat supports an abundant fauna of heterotrophic gastropods (summarized in Warén and Bouchet 1993). In approximate sequence of dominance, the most common species present are *Bathynerita naticoidea, Provana sculpta, Cataegis meroglypta*, and *Buccina canatae*. Less common gastropods include *Cancellaria rosewateri, Cantrainia macleani, Gymnobela extensa*, a chiton *Ichnochiton* sp., and a rarely-collected limpet. *Hyalorisia galea* and *Gaza fisheri* were reported from the Bush Hill site based on material collected prior to the current study. The former was not collected during subsequent sampling, and the latter was observed on the sediments in seep areas, but not in mussel mats.

The question of recognizing endemism is greatly complicated by uncertainty as to specific and generic identities of deep-sea gastropods. The two most abundant species *Bathynerites naticoidea* and *Provanna scuplta* appear to be true endemics. The former genus seems to be restricted to the upper slope Louisiana seeps. *Provanna* is a cosmopolitan seep/vent associate, with *P. scuplta* being restricted to the Louisiana seeps.

Bathynerites naticoidea (Clarke 1989) was the most abundant heterotrophic animal collected in association with mussel mats and sometimes exceeded even the mussels in abundance. The genus and species were new to science prior to the seep studies. Clarke (1989) produced the original description based on Bush Hill material; Warén and Bouchet (1993) extended the description based on additional material. *Naticoidea* seems to be endemic to the Louisiana slope seeps. It has not been found at either the Alaminos Canyon or the Florida Escarpment sites. A similar fossil nerite has been found at Miocene sites in Italy (Taviani, personnal communications), but Warren and Bouchet point out that a lack of traits in the fossil form makes equating the two species problematic.

Considerable information on the natural history was developed by Zande (1994). *Bathynerites naticoidea* is a radular browser consuming a mixture of mineral material, organic detritus, bacteria, and periostricum from mussel shells, tube worms, and the substrate in the vicinity of chemosynthetic assemblages. Egg cases of 100 or more larvae are laid on convenient substrates, with development to juvenile benthic forms taking place in the capsule. The size frequency distribution of collected specimens suggests episodic settlement. The largest specimens were associated with the brine pool site. Although closely associated with the chemosynthetic fauna, episodes of roaming beyond the bed edge were observed during the 1993 dives series.

Provanna sculpta (Warén and Ponder 1991) was new to science, with the type species coming from Bush Hill (Warén and Ponder 1991). Although the genus *Provanna* has been collected away from chemosynthetic communities, its association with these systems has lead to the view that it is primarily a seep and vent endemic (Warén and Ponder 1991). The genus has been placed in the family Abyssochrysidae, a relict of a largely extinct group (Houbrick 1979). *Provanna sculpta* lacks a planktotropic form, but it is not known if it has a dispersive

developmental stage or not. A comprehensive monograph of the genus *Provanna* has not yet be published, but Warren and associates have produced a series of papers describing new species from seep and vent systems and refining the description of the genus (Warén and Ponder 1991). Ten or more species exist associated with the chemosynthetic systems of the Pacific. *P. sculpta* seems to be the only member of the genus yet found in the Atlantic.

Provanna is a radular browser. Being small and matching mussel operculum in color, it is largely unobserved, but very numerous. Present at all sites sampled, it is notably rare at the Brine Pool site. The shell usually shows deep dissolution pits which are often the settlement site for juvenile mussels. Dissolution of the shell makes measurement of length difficult. In the present study, the maximum length of the shell opening was used as the most reliable indication of size. The size range of specimens is quite narrow with no indication of recruitment.

Cataegis meroglypta (McLean and Quinn 1989) - The genus *Cataegis* was erected for two species of continental slope trochid, *C. finkli* and *C. meroglypta* that are apparently opportunistic grazers (McLean and Qinn 1989). The former species was found at slope depths associated with seagrass falls, and the latter in the upper slope seep systems. Warén and Bouchet (1993) have reviewed current information about the species. Since *C. meroglypta* has not been reported from outside of a seep environment it may be endemic. However, the genus *Cataegis* seems to be a rare, but more widely distributed deep-sea form.

Cataegis meroglypta is a radular browser. There is a conflict between video/photo observation and the results of JSL grab sampling. Grab sampling indicates that *C. meroglypta* is consistently less abundant than *B. naticoidea*. However, some photographs and observations suggest that it is locally very abundant and dominant. This discrepancy may be due to aggregation of *C. meroglypta* or behavior during sampling. Aggregates on mussels or adjacent to

mussel beds may capture the attention of observers and give the false impression that *C. meroglypta* predominates over a larger area. Alternately, the species may readily drop from mussels during the disturbance of collecting, while *Bathynerites* holds on, thus biasing the estimates.

Buccina canatae - The genus *Buccina* is a cosmopolitan species complex common on continental slopes. *B. canatae,* a predatory neogastropod, has been collected from seep and non-seep environments in the Gulf of Mexico and Caribbean (Warén and Bouchet 1993). Initially observed on the sediment surface of clam areas, it appears to forage widely and in aggregates. Aggregation may be related to mating. One mound of specimens collected from the sediment contained 48 individuals. During the 1992 dive series *B. canatae* were conspicuous within mussel beds at Bush Hill. The species was found at all sites.

Ischnochiton mexicanus (Kaas 1993) - The chiton, *Ischnochiton mexicanus,* was encountered in four of the JSL grab samples and eight bulk collections of mussels. The species is externally unremarkable, but posses a distinctive radula used in feeding. The species may be endemic to the upper slope seep, but the genus is more widely distributed. Due to the relatively few specimens and the status as a species new to science, ash-free dry weights were not determined. The new species was examined and diagnosed (Kaas 1993) by Piet Kaas of the National Museum of Natural History, Leiden, The Netherlands.

Minor Gastropods - Six species of gastropods were also collected incidental to large samples of mussels for physiological study. Of these, only an unidentified limpit was seen in the grab sample series. The remaining five species are listed below:

1. *Cancellaria rosewateri* (Petit 1983) - It has been speculated (Warén and Bouchet 1993) that *C. rosewateri* is a suctorial feeder parasitizing other

organisms in the seep environment. It appears to inhabit seep and non-seep environments. The genus is cosmopolitan and most common at shelf depths.

2. *Cantrainea macleani* (Warén and Bouchet 1993) - The species was new to science, but occurred in samples from both in and remote from seep communities. Its range includes the continental slope in both the Gulf of Mexico and Caribbean.

3. *Gymnobela extensa* (Dall 1889) - The genus *Gymnobella* is a common deep-sea group of selective invertebrate predators. Since *G. extensa* was reported by Dall from the Yucatans straights, it is most likely to not be specific to the seep environment.

4. *Phymorhynchus* sp. (Bouchet and Warén 1980)

5. *Hyalorisia galaea* (Dall 1889)

6.5.2 <u>Crustacea</u>

Crustaceans are an abundant and highly mobile component of the upper slope seep heterotrophic biota. About four species have been encountered in the JSL grab samples and an additional six to eight observed or taken as incedental specimens. In addition to those collected, large forms (these include the decapods, *Paralomis cubensis*, *Rochina crassa*, *Chaceon quinquedens*, *Chaceon fenneri*, and the giant isopod, *Bathynomus giganteus*), smaller zooplankton, and crustacean nekton often swarmed around the submersible lights at the Bush Hill site suggesting some bentho-pelagic coupling. It is assumed that the ecological role of the seep crustaceans is that of predator/scavenger, the same as typical benthic crabs and shrimp. In mussel bed grab samples, the two most abundant species, *Alvinocaris stactophilia* and *Munidopsis* sp., nov., are endemic. Alvinocaris belongs to a cosmopolitan seep/vent family. The genus *Munidopsis* is a cosmopolitan form common in deep water that also inhabits seeps and vents.

Alvinocaris stactophilia (Williams 1988) - Hydrothermal and hydrocarbon chemosynthetic communities often have high populations of three or fewer caridean shrimp genera, *Alvinocaris*, *Rimicaris*, and *Chorocaris*. Since these genera are new to science, their taxonomic position is not well established. However, they appear to represent a distinct group with common phylogenetic affinities, originally placed in the family *Bresiliidae* (Williams and Chace 1982). Subsequently, the new family Alvinocarididae was proposed (Christoffersen 1989) to contain these forms.

Two species of *Alvinocaris* have been found in Gulf of Mexico chemosynthetic systems. The hydrocarbon seeps on the upper continental slope off Louisiana are populated by *A. stactophilia* and both known deeper Gulf systems are populated by *A. muricola*. A key to the three species of *Alvinocaris* has been developed by Williams (1988) and was the basis of identification of the specimens collected in this study. These species are easily distinguished by the form of the rostrum. That of *A. muricola* is longer and has numerous spines on both the dorsal and ventral surfaces. That of *A. stactophilia* is shorter and bears only one or no ventral spines.

It is especially noteworthy that none of the 42 benthic shrimps reported on the typical deep-sea floor are found in the seep community. This failure of the background fauna to exploit the seeps is most dramatic for the most abundant species. Pequegnat's (1983) inventory of carideans lists 33 species in the Gulf of Mexico, of which at least 25 are found below the shelf break. *Nematocarcinus rotundus* is dominant on the upper slope and *N. ensifer* dominant on the lower slope. Three species of *Glyphocrangon* are sub-dominant but common: *G. nobilis*, *G. aculeata*, and *G. alispina*. These three sub-dominants have overlapping ranges mostly above 2000 m. None of these five have been collected or observed in the seep sites. Pequegnat (1983) lists 22 penaid shrimp, with 17 found below the shelf break. *Benthysicymus carinatus* is only slightly less common than *N. rotundus* and shares an overlapping range on the continental slope.

Although *Alvinocaris stac tophilia* appears to have the typical caridean feeding habit of predator/scavenger, perhaps grazing upon free living chemosynthetic bacteria. One member of the Alvinocarididae, *Rimicaris exoculata*, is specially adapted to feed upon epibiotic chemosynthetic bacteria living on its own cuticle. This symbiosis involves epibiotic bacteria on the mouth parts (Van Dover et al. 1988) and in the prebranchial chamber (Gebruck et al. 1992; Segonzac et al. 1993). A general review and detailed examination of the feeding of three species of Alvinocarididae at a mid-Atlantic ridge site has been given by (Segonzac et al. 1993).

Munidopsis sp, nov. - Galatheid crabs are common in the deep benthos and have invaded most seep and vent communities. There is distinctive sexual dimorphism in the chelae. Larger males may have chelae longer than the rest of the body. These animals appear to be opportunistic scavengers/predates.

Low Abundance Crustacea - Due to loss of smaller and lighter weight material during the transfer from the JSL grab to the storage chambers of the submersible, retention of copepods, isopods, tanaiids, etc. was unlikely. Sieving washings from the mussel samples through a 250 micrometer screen did not produce a macrofauna size class of specimens. One juvenile decapod crab was collected in three grabs and could be seen in video images of the mussel mats. Tentatively identified as *Trichopeltarion nobile*, it is a member of the background fauna with massive claws suitable for shell crushing. Adults were not observed.

6.5.3 Worms

Although polychaetes are usually a very diverse component of the benthos, the mussel beds contained few forms. A large (up to 20 cm long) polychaete related to the Orbinnidae occurred in dense clumps of several 10's of specimens. At the brine pool, these worms were conspicuous waving the anterior end about above the

mussel substrate. They were assumed to be detrital feeders. Nereiids of similar size were encountered in the orbinnid clusters. As with the smaller crustaceans, a smaller worm fauna was absent or lost during sampling. When rock material is taken, it frequently contains an undescribed sipunculid. Nemertines were also encountered.

6.6   Gulf-Wide Patterns

Chemosynthetic communities afford both a complex biogenic habitat and a rich food source exploited by heterotrophic species. Unlike the chemosynthetic producers, these exploiters may not be geochemically restricted in distribution. Therefore, a primary question is to what extent those species are colonists from the typical deep-sea biota, or are specialists endemic to chemosynthetic systems. It is to be expected for cold seeps, that like hydrothermal systems (Tunnicliffe 1991; 1992), the associated heterotrophic species reflect mixed sources. Some may be truly endemic to chemosynthetic communities. Some may be colonists from the surrounding benthos, which have established resident seep populations, while others are vagrants making temporary use of the seep site but not developing resident populations. The tremendous difficulty in actually assigning species to these classifications lies in a lack of knowledge of the species composition of the surrounding benthos. That environment can be very species-rich and is inhabited by such an abundance of rare species that a complete inventory is virtually impossible. Apparent seep and vent endemics may just be colonists or vagrants whose more widely scattered kin simply have not made it into a museum collection.

Fortunately, the Gulf of Mexico has been extensively sampled and the bathymetric distribution of the larger normal (megafauna) benthos well documented. Therefore, it is possible for many species to determine which are colonists and vagrants. Absolute determination of endemics remains uncertain;

however, the bathymetric range of samples affords an indirect method of assessment. Should apparent endemics show a bathymetric species turnover akin to the normal fauna, then their endemism may be suspect.

A comparison of heterotrophic forms is presented in Table 6.4. The comparison is limited to larger organisms (greater than 0.5 cm) and the more common groups. The species listed were primarily collected by manipulator grabs from the *Johnson Sea-Link* submersible and retained on a 500 micrometer sieve. Large crabs and fishes were recorded in video or still camera images. A more complete discussion of the data can be found in MacDonald (1992). The faunal tables in Pequegnat (1983) were used to establish the preliminary classifications. Species that have never been recorded from outside a seep are classified as endemics. Colonists have been recorded outside seeps, but obtain high population levels only within seeps. Vagrants are those species which are found outside seeps and do not appear to achieve unusually high population levels within. An "unresolved" classification is applied to all species in which the taxonomic position is uncertain at this time. The list of dominant chemosynthetic species is restricted to molluscs, crustacea, echinoderms, and fishes. Other taxa occurred too rarely to be of use in the comparisons.

Several conclusions are readily apparent. First, the upper slope and Alaminos Canyon heterotrophic fauna are very dissimilar. If elements are shared, their relative abundance at the two sites must be so dramatically different as to have escaped detection at this level of sampling. Second, endemism is low at the species level — five endemics out of 39 species. At the level of genus, only the two coiled gastropods, *Bathynerita naticoidea* and *Provanna sculpta*, possibly the Alaminos Canyon limpet, and the shrimp, *Alvinocaris* are endemic to chemosynthetic systems. Third, the colonists and vagrants reflect only 1/10th of the surrounding species richness, 23 species in seeps at the upper slope sites versus 251

Table 6.4 Composition of upper and lower slope seep heterotrophic fauna with reported species richness and dominant species of the background fauna.

UPPER SLOPE SEEP SITES		UPPER SLOPE BACKGROUND	ALAMINOS CANYON SITES		LOWER SLOPE BACKGROUND
		400 - 1000m			2000-3000m
					32 species
GASTROPODS		102 species	**GASTROPODS**		Dominants
Bathynertia naticoidea	Endemic	*Gemmula periscelida*	limpets	Endemic	*Leucosyrix tenoceras*
Provanna scuplta	Endemic	*Leucosyrinx tenoceras*	*Buccina sp.*	Unresolved	*Gynobela bairdi*
Cataegis meroglypta	Colonist	*Gymnobela ipara*			
Buccina canatae	Colonist				
Ichnochiton sp	Colonist				
Cantrainia macleani	Colonist				
Gymnobela extensa	Colonist				
Cancellaria rosewateri	Vagrant				
Hyalorisia galea	Vagrant				
CRUSTACEA			**CRUSTACEA**		
Galatheiid Crabs		18 spp	**Galatheiid Crabs**		6 spp
Munidposis sp.	Endemic	*Munidopsa sigsbei*	*Munidopsis sp*	Unresolved	*Munidopsis bermudezi*
Eumunida picta	Vagrant	*Munida valida*			
		Munida longipes			
Other Crabs		33 spp	**Other Crabs**		1 spp
Paralomis cubensis	Vagrant	*Parapagurus sp.*	none		*Chaceon quinquedens*
Rochina crassa	Vagrant	*Bathyplax typhla*			
Chaceon quinquedens	Vagrant	*Chaceon quinquedens*			
Chaceon fenneri	Vagrant				
Trichopeltarion nobile	Vagrant				
Large Isopods		*1 spp.*	**Large Isopods**		*1 spp.*
Bathynomus giganteus	Vagrant	*Bathynomus giganteus*	none		*Bathynomus giganteus*
Shrimp-Like Forms		35 spp.	**Shrimp-Like Forms**		13 spp
Alvinocaris statophilus	Endemic	*Systellapsis pellucida*	*Alvinocaris muricola*	Colonist	*Nematocarcinus acanthitelsonis*
		Pasiphaea merriami			*Benthesicymus cereus*
		Glyphocrangon alispina			*Hemipenaues carpenteri*
		Glyphocrangon nobilis			
		Penaeopsis serrata			
		Parapenaeus longirostris			
		Benthesicymus bartletti			

Table 6.4   Continued.

ECHINODERMS			ECHINODERMS		
Asteroidea		25 species	**Asteroidea**		21 spp
Sclerasterias sp.	Colonist	*Plutonaster intermedius*	none		*Dytaster insignis*
		Nymphaster arenatus			*Ampheraster alaminos*
		Astropecten americanus			*Benthopecten simplex*
Ophiuroidea		26 spp	**Ophiuroidea**		13 spp
none		*Ophiernus adspersum*	*Ophiomusium sp*	Colonist	*Ophiomusium planum*
		Bathypectinura heros			*Bathyplectinura hero*
Fishes		111 spp.	**Fishes**		21 spp.
Eptatretus sp	Vagrant	*Gadomus longifilus*	Liparid	Unresolved	*Dicrolene intronigra*
Synaphobranchus sp	Vagrant	*Dibranchus atlanticus*			*Coryphaenoides macrocephalus*
Urophycis cirratus	Vagrant	*Nezumia aequalis*			
Hoplostethus sp.	Vagrant	*Dicrolene intronigra*			
Chaunax suttkusi	Vagrant	*Synaphobranchus sp.*			

species in the background fauna. Fourth, the distinction between vagrant and colonist seems to be related to size and mobility. Colonists tend to be smaller, slower, and subdominant in the background. Vagrants tend to be larger, highly mobile, and may include dominant elements from the background.

The low endemism and changing heterotrophic fauna of sites at 400-1000 m, and 2000 m are generally consistent with colonization from a vertically changing deep-sea fauna. However, the factors that limit successful colonization to such a small percent of the background species remain obscure. Purely random colonization can be ruled out, since all of the more than 10 locations sampled in this and other programs at the upper slope site had the same suite of colonizing species. Perhaps the species of this suite are the only ones of all the background fauna capable of persisting in the unique chemical environment of the seep sites. Or, they predominate locally due to contagious colonization in which the very high populations densities of initial successful colonists make subsequent colonization of nearby sites highly probable.

The observed distribution of apparent endemics is puzzling. The possible absence of the gastropods *Bathynerites* and *Provanna* from the deeper site would suggest that these abundant forms are actually colonists from the vertically zoned background fauna. However, other evidence points to true endemism. A nerite similar to *Bathynerites* appears to have had a long association with seeps, being found in Miocene deposits in Italy (Taviani, personal communications), but has been reported from no other sites. Other species of the genus *Provanna* are associated with vent and seep sites in the Pacific (Warén and Boucet 1993).

Deep-sea species richness with its many potential colonists makes it highly likely that colonization is a probable mechanism influencing the species composition of seep assemblage to some degree. If the heterotrophic component is predominantly colonists, then such fauna should parallel deep-sea community

changes bathymetrically, geographically, and in the fossil record. If, however, endemism is predominant then the heterotrophic component should not parallel the surrounding benthos, and may share with the taxa of the chemosynthetic assemblage common origins and convergent adaptations for colonization and persistence. It is even tempting to suggest that heterotrophic and chemotrophic endemics may have linked life histories. A possible example of this has been found in the upper slope sites. Juvenile *Bathymodiolus* are common on shells of *Bathynerities* and *Provanna*, and the cuticles of *Munidopsis* sp. Tube worms have been found growing from the shells of *Bathynerities*. Such epizootic associations provide the sessile members a post-settlement means of dispersion that may be important in maintaining viable populations as the chemical gradients of seeps and vents undergo local shifts.

The low endemism of the Gulf of Mexico sites, especially the upper slope, and the high degree of colonization by fauna from the surrounding seafloor is markedly different from that found for hydrothermal systems where 95% of the species are endemic. As noted by Tunnicliffe (1991; 1992) as much as 95% of hydrothermal vent fauna is endemic and with little taxonomic similarity to continental margin systems except the chemosynthetic of the assemblage. On the basis of the results presented herein, it can be proposed that the hydrothermal versus cold vent faunal distinction may be due to the geographic and bathymetric gradients of the surrounding benthos. Seep systems associated with continental margin geology exist within the biodiversity framework of the continental slope. High overall species richness at the base of the slope and increasing large predator diversity on the upper slope afford many opportunities for colonization and exploitation of seep systems. Displacement by colonists and extermination by predators may eliminate many hydrothermal vent endemics from continental slope communities. Hydrothermal systems, due to their association with spreading centers, tend to be

remote from continental margins. While overall surrounding species richness may be high, low overall abundance and substrate dissimilarity may limit opportunities for colonization. Large predators, especially decapod crustaceans are absent, thus reducing predation.

6.7   Potential for Adverse Impact

Now that we have some knowledge of the species composition of chemosynthetic mussel beds, it is possible to consider management issues with respect to the whole local community rather than just the chemosynthetic species.

In this regard the main findings are:

1.   that the associated fauna is monotonous in composition at the sites sampled;

2.   that the dominant associated species are seep specific and may be endemic;

3.   that the associated species consists mostly of larger and possibly older individuals;

4.   that the associated species at the sites studied differ from seeps elsewhere in the Gulf of Mexico;

5.   that large predators and scavengers from the normal benthos do exploit seep productivity.

In certain respects the heterotrophic component of mussel beds may be relatively robust. Sessile forms unique to mussel beds are virtually absent, and the mobile species are heavily shelled. Thus, acute physical disruption of a bed should have minimal effect so long as the chemosynthetic organisms survive. However, the ecology of the component species may make the assemblage fragile if exposed to chronic disturbances. This fragility stems from the facts that recruitment seems to be sporadic, and the whole community (mussels included) are subject to predation by at least one sea star and a variety of fish and invertebrates. Chronic disruption

might trip the balance in populations such that predators exterminate local populations faster than they can be resettled.

The Gulf-wide distribution of seep associates is difficult to interpret since the deeper sites are so poorly studied. However, it appears that mussel beds are locally monotonous on the scale a ten's of kilometers and hundreds of meters depth, but regionally different on a scale of one hundred meters distance and a thousand meters depth. Since there seems to be some degree of zoogeographic restriction for seep species, the question of how much disturbance can take place without extinction arises. At this time, we know that the upper slope seep associates occur at many sites giving them some protection from extinction. However, the extent of deeper sites (2000m +) in the Gulf of Mexico is unknown. If limited, the species at sites may be at greater extinction risk and warrant greater environmental protection than sites above 1000 meters.

7.0 Stability and Fluctuation in Chemosynthetic Communities Over Time Scale of ~1 Month to ~1 Year
Ian R. MacDonald and Robert S. Carney

7.1 Introduction

7.1.1 Need to Understand Time-Scales of Seepage

For management, the major question about hydrocarbon seep communities is how much regulation is required to protect them from the possibly detrimental activities of oil and gas development and production. Are these communities uniquely impervious to industrial impact due to their adaptation to oiled and otherwise chemically hostile environments, or do these same adaptations suggest the existence of an easily perturbed system occupying a very narrow and fragile geochemical niche? Although long-term monitoring and experimentation is needed for a definitive answer to the robust or sensitive question, the 5-year series of submersible observations of hydrocarbon seep communities between 1989 and 1993 provided an opportunity for initial observations as to how communities change naturally and in response to intentional perturbation.

7.1.2 Scope of the Work

Chemosynthetic communities generally occupy areas affected by hydrocarbon seepage that are a few hundred meters in width. Within these sites, tube worms form clusters a few meters to a few tens of meters across and mussels form clusters that are less that one meter to a few meters in width (MacDonald et al. 1990a). To test whether major faunal changes were occurring as a natural process within these communities and to make observations that would allow us repeatedly to examine the type and density of fauna at sub-meter scales, we needed to acquire measurements of variations in the seepage process that might affect the communities. Our approach was to photograph repetitively functional clusters of

typical chemosynthetic fauna at each of the Study sites, to deploy *in situ* monitoring devices to observe the seepage process, and to examine the geological record for evidence of events that would have changed the habitat structure of the seeps.

The repetitive photography operated at two scales. We assembled mosaics of faunal clusters from about 5 to 25 sq m in area and looked for changes at a 1 m scale. We also initiated disturbance (to mussel clusters) and monitored recovery. Two programs of controlled disturbance were initiated. The first simply placed marker rods at the edge of mussel mats to facilitate long-term observation, and the second consisted of placing recovery experiments at three locations. Mussel clusters were mechanically disturbed, a recovery cage placed over the disturbed portion of bottom, and re-population by mussels monitored over time.

In situ monitoring focused on gas hydrate mounds that we observed breaching the seafloor at GC 184 and elsewhere. Gas hydrate is an ice-like substance that forms, under pressure, at temperatures above the freezing point of water by inclusion of methane (and other gases) into a lattice of water molecules. Most often detected by seismic means as deeply buried layers in marine sediment (Singh et al. 1993), gas hydrate has also been collected from <5 m below the floor of the continental slope in the Gulf of Mexico (Brooks et al. 1984; 1986). Globally, subaquatic gas hydrate comprises a 10^{16} kg reservoir of organic carbon (Kvenvolden 1988) that may interact with the atmosphere to influence climate cycles. Regionally, they are potential energy resources as well as potential hazards to seafloor structures (Kvenvolden et al. 1993). The interplay of hydrate formation and community structure is significant and contributes a source of short-term fluctuation with measurable effects.

7.2   Materials and Methods

7.2.1   Photomosaics and Other Quantitative Photography

Both video and emulsion photographs were used to obtain images in which seep fauna could be identified and the aerial coverage of the image was known. Studio-quality videos were provided by the cameras on the *Johnson Sea-Link*. The emulsion camera used was either a Benthos® 35 mm camera with 28 mm lens or a Photosea® stereo camera, which took photographs stereo-paired as an aid to determining three-dimensional details in the communities. The cameras were oriented vertically and generally took pictures at altitudes of 1 to 3 m above the seafloor. Lasers, mounted on the cameras in parallel arrays of two or four, provided a reliable faducial mark for the photographs by projecting red dots at known distance apart in the final images. Additional analysis of video sequences was occasionally employed to obtain a qualitative characterization of the fauna at sampling stations. In all cases, the time and date were recorded on the imagery. This time tag, together with the navigation records of the support ship and the dive notes, provided a reliable means for determining where each image was taken. We also deployed durable markers at the sites to facilitate collection of abiotic samples and photographic survey from repeatable locations. During collection of the mosaic imagery, the operator traversed the area in the immediate vicinity of the marker in a series of short, overlapping tracks about 10 m in length.

Mosaics were assembled from a series of digital files made by either scanning the 35 mm photographs by use of a Nikon 3510AF slide scanner, or by "capturing" individual frames of video by use of a Targa 64 video capture board. Digital mosaicking was conducted using AGIS software. This involved a series of homologous transforms whereby daughter images were joined to an initial image after rotation, translation, and scale adjustment to render the daughter image equivalent to the

parent image. Rotation, etc. was performed on the basis of matching two points in the daughter image to two identical or nearly identical points in the parent. This process specifically did not adjust for error due to differences in look angle between successive images, nor did it adjust for parallax differences due to the topography of the seafloor features. This meant that as more and more images were added to a mosaic, errors tended to accrue in the scale and relative position of bottom features. However, for areas on the order of 10 to 20 sq m, the method provided a robust technique for determining the structure and stability of fine-scale faunal clusters.

Table 7.1 summarizes the locations of the study sites where mosaics were compiled in order to observe short-term change in community type. Table 7.2 lists the classification of community type used to evaluate photomosaics and video coverage. Percent coverage for these classifications and change in per cent coverage over time was determined using gridded (hard copy) mosaics and gridded video renderings of the same areas for all three years. Some grids were not covered completely by photomosaic elements, making occasional estimates necessary. Accuracy was achieved by simultaneously inspecting the hard copy(s) and on-screen views of the same grids for both the same and different years.

Table 7.1. Summary of locations at study sites where mosaics were compiled in order to observe short-term change in community type.

Study Site Sampling Location	Aerial Coverage (sq m)	Years	Data Sources
GC 184, *Bush Hill*			
1. Marker Bucket #1	38	1991	color mosaic
	22	1992	color mosaic
2. Marker Bucket #2	25	1993	B&W high-alt. mosaic
GC 272			
1. Milk-crate	6	1992	Hi8 video: JSL92 dive 3277
	6	1993	color mosaic
2. Aluminum frame	25	1991	color mosaic
	25	1992	Hi8 video: JSL92 dives 3276 and 3277
VK 826, *Viosca Knoll*			
1. Marker Bucket	8	1991	color mosaic
	8	1992	Hi8 video: JSL92 dive 3261
GC 234			
1. Site #1 (Milk-crate)	20	1991	Hi8 video: JSL91 dive 3142
	16	1992	color mosaic
2. Site #2 (Mussel bed)	4	1991	color mosaic
C-buoy	4	1992	Hi8 video: JSL92 dive 3268

Table 7.2. Classifications of community type used to evaluate photomosaics and video coverage.

1. Tube Worms (T_)

Density	Description	Code
Dense	Dome shaped bush; cannot see sediment	**Td**
Medium	Recumbent; cannot see sediment	**Tm**
Sparse	Isolated; sediment visible	**Ts**

2. Mussels — assumed to be Seep Mytilid Ia — (M_ _)

Second term describes the density of the mussels:

Dense	Solid mass; cannot see sediment.	**Md_**
Medium	Patchwork; some sediment is visible.	**Mm_**
Sparse	Scattered; sediment visible	**Ms_**

Third blank describes the color for *living* mussels:

Brown	Live mussels periostracum intact	**M_b**
White	Live mussels periostracum eroded	**M_w**

Hyphenate abbreviation describes *dead* mussels.

Dead	Dead; occur as scattered debris	**M-d**

(*Example*: Msb, Live, sparse, brown mussels)

3. Bacterial Mats (B_)

Second blank describes color of bacteria, when interpretable. Specific color discrimination cannot be reproduced, so a simplified approach is employed.

White	White bacteria	**Bw**
Colored	Orange, Pink, Yellow	**Bc**

4. Sediment (S_)

Second blank refers to surficial morphology

Featureless	No visible features; smooth	**Sf**
Bioturbated	Visible burrows; intense reworking of sediment	**Sb**

Hyphenated terms refer to "rocky" debris or fragments

Rubble	Scattered rocky debris; cm scale assumed	**S-r**
Boulders	Large (+20 cm) rocks	**S-B**

7.2.2 Controlled Disturbance

Plastic rods (3/4 in PVC pipe) were deployed at dive sites starting in 1987 to serve as simple reference scales. Of special interest is the deployment of both 0.5 m and 3 m rods at the NR-1 Brine Pool site (GC 233). This site has a simple overall geometry, making it an ideal study site. Seven 3 m rods were deployed along the long axis of the pool. Pole 2596 was laid horizontally across the mussel mat at the northern end of the pool on JSL dive 2597, Sept. 13, 1989. On dive 2598, 3 m rod 2598 was placed at the southern end on the mussel mat. On dive 2599, rod 2599-1 was inserted vertically at the northern edge of the pool and 2599-2 at the southern edge. These poles were within 20 cm of the inner edge of the mussel mat, but not touching it. A 2 m long rod was planted upright in the brine pool approximately 2 m from the mussel mat on the northern and southern ends of the pool. Approximately 2 m from the northern end, rod B was inserted in the bottom of the brine pool and rod C similarly placed at the southern end. A third rod sank from sight when placed in the center of the pool.

Outer Edge Markers - The edge markers were 50 cm 0.52-inch PVC rods painted with 10 cm wide white, red, blue, and yellow bands. These bands allowed for both scale and color balance. Edge markers were inserted more or less vertically into the sediments at the outer edge of the mussel mat. At the northern end of the pool, five rods were placed at 1 to 2 m intervals along the well-defined edge of the mat. At the southern end, where the solid mat was replaced by scattered clumps of mussels, four rods were placed at the edges of clumps.

Inner Edge Markers - A 2 m long 1.5 inch PVC pipe was inserted into the pool bottom within 10 cm of the mussel mat inner edge, but not touching the mat. Approximately 40 cm of rod remained above the surface of the brine.

Rectangular recovery frames were constructed of 21 mm outside diameter PVC water pipe. Fifty cm lengths were used to make 0.25 m^2 top and bottom

sections, and the remaining sides constructed of 20 cm lengths. Corners were fastened with 3-way right angle joints and commercial PVC pipe adhesive. The corners were drilled to allow for flooding of cavities. Half the interior of the cage was enclosed in 3.5 cm stretch mesh plastic fruit tree bird netting. The line of the netting was less than 1 mm in diameter, was easy to see through, and its black color limited obscuring of a video image. Nylon line was stretched across the diagonal of the cage, and then netting was secured with tie-wraps to these diagonal lines and adjacent sides. The 50 cm rods used had been sanded and painted white, blue, red, and yellow with an epoxy-based paint. The 10 cm long color bands provided visual scale, orientation, and color balance in subsequent image analysis.

Cages were deployed in conjunction with massive mussel sampling during the 1991 dive series. Two cages were deployed at Bush Hill on dives JSL-3129 (Sept. 5, 1991) and JSL-3139 (Sept. 20, 1991). Single cages were deployed at Green Canyon 272 on dive JSL-3137 (Sept. 19, 1991) and Green Canyon 234 on dive JSL-3144 (Sept. 24, 1991). Disturbance consisted of repeatedly grabbing mussels with the JSL manipulator until more than 100 individuals had been collected. Since the contiguous area denuded was typically less than 0.25 m^2, the cages were placed over the denuded area and adjacent bare substrate. The mussels collected were used in other shipboard studies. When marked mussels were returned to the site, they were deployed away from the recovery frames.

The cages were revisited during the August 1992 dive series, approximately one year after deployment. The cages were visually inspected and then surveyed with the JSL video camera. Still frames from this video were printed using a Mitsubishi CP210U video copy processor, and the content and position of biota within the frame recorded. The rods at NR-1 Brine Pool were video surveyed in 1991 and 1992.

7.2.3 Monitoring Seafloor Gas Hydrates

In 1991, we noticed a mound of gas hydrate that was breaching the seafloor near the bucket 1 sampling station at GC 184. In 1992, the feature was photographed to document its size and shape. In 1993, an intensive sampling effort was conducted to characterize this feature. All observations and sampling were conducted using the research submarines *NR-1* and *Johnson Sea-Link I*. Samples of bubbles were collected in an acrylic vessel fitted with a funnel, inlet and outlet valves, which allowed the gas to enter the vessel and the displaced water to escape, and a check valve to release excess pressure during ascent. Aliquots of the sample were released under pressure and stored chilled in glass containers. Inert and volatile components of the bubble samples were analyzed at sea using a gas chromatograph with a thermal conductivity detector (Childress et al. 1984).

Sediment samples were collected in 45 cm long by 6.5 cm diameter coring tubes that were pressed into the seafloor with the manipulator arm of the *Johnson Sea-Link*. The cores were cut into 15 cm sections, poisoned with sodium azide and stored frozen under nitrogen in sealed cans. Gaseous hydrocarbons were recovered from the head space of the cans for analysis. Hydrocarbon analysis for all gas samples was performed using a gas chromatograph with flame ionized detection (Kennicutt et al. 1988a).

Sediment temperatures under the hydrate mound were measured with a semi-autonomous temperature probe. The probe consisted of eight thermistors (YSI model 44006) mounted 20 cm apart along a 1.5 m long fiberglass tube. Thermistor readings were recorded at 30 s intervals by use of a Tattletale® data logger mounted inside a pressure housing at the handle end of the probe. The thermistors were calibrated by comparison to a Hewlett Packard quartz thermometer and recorded temperature to an accuracy of at least ±0.05°C. The probe was pushed into the sediment by the

mechanical arm of *NR-1* and was left in place for ~30 min to allow temperatures at the thermistors to stabilize.

To determine the influence of fluctuating water temperature upon gas hydrate stability, we deployed a bubblometer ~25 m away from the mound in a bed of mussels where we suspected that hydrate was present in the underlying sediment. This device, fitted with thermistors and a Tattletale® data logger, used a 50 cm by 50 cm hood to funnel gas bubbles into a four-chambered wheel. Rotation of the wheel was retarded by a sliding counterweight; at 540 m water depth, a buoyant volume of gas equivalent to ~3600 mL at standard temperature and pressure was required to lift the counterweight and rotate the wheel. Each chamber rotation tripped a magnetic switch; rotations and water temperatures were recorded at 5 min intervals. Deployment was accomplished with *NR-1,* and recovery was made with *Johnson Sea-Link.*

7.3   Results

7.3.1   Photomosaics at GC 184: Site 1

This site encompasses approximately 200 sq m that contained two beds of live mussels and a scattering of dead mussel shells. The entire region comprises a low knoll near the top of Bush Hill; minimum water depth is 540 m. The area covered by the photomosaic was surrounded three sides by tube worm bushes. Gas vents were evident in several sites within the mussel beds and the gas hydrate outcrop described in section 7.5 was situated approximately 10 m to the northwest. The site is marked with a white, weighted bucket (5 gal) inscribed with a large number one. Although photomosaics were collected over about 25 sq m of the site during 1991-1993, the effective overlap was limited to a 6 sq m area, which is designated grids A through F. The features observed in A through F for 1991 to 1993 were as follows:

Grid A.	1. Mdb		Grid B.	1. Mdb	4. M-d
	2. Mdb+Ts			2. Msb	
				3. Ts	
Grid C.	1. Msb		Grid D.	1. Tm	
	2. Ts			2. Bw	
	3. M-d			3. Sf	
	4. Sf			4. Ts	
Grid E.	1. Ts		Grid F.	1. Ts	
	2. M-d			2. Bw	
	3. Bw			3. Sf	
	4. Sf			4. M-d	

The assessment of aerial variation in feature coverage over 1991 to 1993 revealed no observable change. Evaluation of 1991 and 1992 data showed direct correlations for all grids. No observable change in population densities or distributions were seen for tube worms, mussels, or bacterial mats. The 1993 data was evaluated in a similar manner, but since it was a b/w mosaic, less accuracy in identifying color-dependent bacterial mats was obtained. Therefore, the 1993 mosaic was evaluated for the presence or change in those features, which are not color dependent for identification.

From 1991 through 1993, the 6 sq m area around Bucket #1 did not reveal any discernible change in the aerial distributions or densities for tube worms, living mussels, dead mussels, featureless sediment, or bacterial mats. It was evident that some individual mussels had died during the study period, a smaller (50 cm) grid may detect some slight variations, but none were evident at this scale.

7.3.2 Photomosaics at GC 184: Site 2

This site consist of a medium dense cluster of tube worms bordered by an expanse of uncolonized sediment. The sedimented area included several small patches of bacteria and a scattering of mussel shells. The area sampled by the

photomosaics encompassed a total of 8 sq m marked by a white weighted bucket (5 gal) inscribed with a large number two. Water depth at the site was 550 m.

The area evaluated was determined by the extent of video coverage available from 1992, as no usable photo coverage exists for that year. The area evaluated was 8 sq m extending southwards from the bucket. Grids are designated A though H. Features observed in A through H for 1991 and 1992 were as follows:

Grid A.   1. Sf   Grid B.   1. Sf
                                             2. M-d

Grid C.   1. Sf   Grid D.   1. Sf
                                             2. M-d
                                             3. Ts

Grid E.   1. Tm   Grid F.   1. M_b (density . . ?)
           2. Ts   2. Ts
           3. Sf   3. Sf
                                             4. M-d

Grid G.   1. Ts   Grid H   1. Sf
           2. Bc *1   2. M-d
           3. Sf *1   3. Ts *2
                                             4. Msb *2

*1 - Cannot discriminate Bc from Sf on video owing to the oblique view presented, and variable
      illumination conditions.
*2 - The "sparse" and "medium" descriptors are unclear on video for the same reasons as stated
      above.

Between 1991 and 1992, no signs of colonization of the open sediment area was observed. No visible changes in tube worm occurrence or density was observed. Mussels were more difficult to evaluate owing to their small size and scattered occurrence. Nonetheless, no variations in the mussel population was observed.

Video from *Johnson Sea-Link* dives 3270 and 3274 (1992) were examined for comparison to the color 1991 mosaic. It was not always possible to determine an accurate percent aerial coverage (distribution) for the desired features. Therefore, the video was examined to establish the presence or absence of features seen in 1991.

Wherever possible, percent change was estimated. Review of the data reveal no evidence for change in the distribution or density of any observed fauna.

The same features observed in 1991 were seen in 1992 with no noticeable change in distribution or density characteristics. Live video, which provided occasional (although accidental) close-ups, did not reveal any change in the character of the open sediment area or in fauna.

7.3.3 Photomosaics at GC 234: Site 1

This site was characterized by a large (approximately 8 sq m) mussel bed that graded into medium dense tube worms at the edges. These chemosynthetic fauna had colonized a broad terrace in a north-south slope. The site is marked by a green plastic milk crate and a 50 cm framework of pvc pipe. The water depth at the site is 535 m. The area defined by 1992 coverage was 16 sq m. Grids are labeled A through P. Features observed in A through P for 1991 and 1992 were as follows:

Grid A.	1. Tm	Grid B.	1. Tm	Grid C	1. Tm
					2. Msb
					3. Sf

Grid D.	1. Tm	Grid E.	1. Tm	Grid F	1. Tm
					2. Ts
					3. Msb
					4. M-d
					5. Sf

Grid G.	1. Tm	Grid H.	1. Tm	Grid I.	1. Msb
	2. Ts		2. Ts		2. M-d
	3. Msb		3. Sf		3. Sf
	4. M-d				
	5. Sf				

Grid J.	1. Tm	Grid K.	1. Tm	Grid L	1. Tm
	2. Ts		2. Ts		2. Ts
	3. Msb		3. Sf		3. Sf
	4. M-d				
	5. Sf				

Grid M.   1. Tm   Grid N.   1. Tm   Grid O   1. Tm
           2. Msb   2. Ts
           3. M-d   3. Sf

Grid P.   1. Ts
           2. Sf
           3. Tm

The mosaic and dive video provided sufficient quality and resolution to allow for accurate interpretation. In all 16 sq m evaluated for 1991 and 1992, identical features were observed. Tube worms revealed no visible change in density or distribution between 1991 and 1992. Here, were arranged in a ring, which forms a barrier around the open, central area of the bush. The center was dominated by open sediment and was colonized by mussels and sparse tube worms.

In all 16 sq m evaluated for 1991 and 1992, identical features were observed. Both live (sparse) brown mussels and dead mussels were evident. Some brown mussels were borderline in classification between "sparse" and "medium" in density. No detectable change between 1991 and 1992 was observed for density or distribution. Some re-arrangement of mussels was observed, though no large-scale movements are seen. Finally, no new colonization in the open sediment area was observed for any fauna type. Except for small scale movements of mussels within the central open area of the bush, no detectable changes in distribution or density for any fauna was observed.

7.3.4 Photomosaics at GC 234: Site 2

This site is a cluster of mussels that had colonized a gas chimney about 75 cm in diameter and 1.2 m high. A steady stream of gas bubbles was observed escaping through the mussel bed during observations in both 1991 and 1992. The chimney was surrounded on three sides by very dense tube worm bushes. The entire aggregation was perched on the edge of a steep dropoff to the south. The site is

marked by an orange float labeled with the letter C. Water depth at the site was 545 m. Because no scale controls (i.e., laser dots, beer cans, etc.) were included, the size of the grids was estimated. For convenience, the mosaic was divided into 4 grid areas that are easily assessed on the 1992 video. Grids are labeled A through D. Features observed in A through D for 1991 and 1992 were as follows:

Grid A.	1. Mdb	Grid B.	1. Mdb
	2. Mmb		2. Mdw *
	3. Ts		3. Ts
	4. Tm		4. Tm
	5. Sf		5. Sf

Grid C.	1. Tm	Grid D.	1. Tm
	2. Sf		2. Mdb
	3. Ts		3. M-d *

* It is difficult to separate dead mussels from live white mussels on the mosaic. This is also not possible on the live video.

All features observed in 1991 year were readily detected in 1992. The only noticeable change in faunal distribution occurred with sparse tube worms in Grid A. The 1991 mosaic revealed a small, isolated clump of brown mussels intermixed with sparse tube worms (and several stellaroids). In the 1992 video the sparse tube worms, though still present, appeared to be greatly reduced in number. Estimated reduction was approximately one half. Live brown mussels were easily seen in both years. However, the white mussels were only seen in the 1991 coverage. The same look angle was not available in the 1992 video, therefore, positive discrimination between Mdw and M-d was speculative. This reduced the confidence in interpretation for Grid B. The variation in look angle between coverage types limited our confidence in establishing a high degree of accuracy for the entire evaluation area. However, those areas that were well represented in both years of data coverage revealed no clear evidence for change in faunal distribution or density.

7.3.5 Photomosaics at GC 272: Site 1

This site consists of a mussel bed approximately 10 sq m in area and situated amidst a number of prominent carbonate outcrops. Tube worms were present in limited numbers around the western edge of the bed. Depth increases sharply to the south and west. Markers at the site include a Gas seeps were observed in 1991, but were absent or less evident in 1992. Water depth at the site is 719 m. The area photographed defined 9 sq m, but 1993 coverage was limited to 6 sq m. Grids evaluated were designated A through F Features observed in A through F for 1992 and 1993 were as follows:

Grid A.
1. Tm
2. Ts
3. MmW
4. Msb
5. Sf

Grid B.
1. Mdb
2. MdW
3. Sf

Grid C.
1. Tm
2. Sf
3. Mdb
4. MmW

Grid D.
1. Sf
2. M-d
3. MsW

Grid E.
1. Sf
2. Mdb
3. M-d

Grid F.
1. Sf
2. M-d
3. MsW
4. Msb

Numerical evaluation was performed on the 1993 mosaic and qualitative estimates (low, medium, high) were attributed to the features seen in the 1992 video. Correlation was interpreted by comparing the qualitative terms with the percentages between features. High quality of both the video and the mosaic permitted accurate assessments.

Tube worms showed no evidence of change in distribution or density. A minor variation for mussels was observed in Grid B. The Mbd (i.e., dense brown mussels) appeared to have 'rearranged' but with no discernible change in aerial distribution. It is probable that this change was due to disturbance during sample collection. The

percentage of "white" mussels (those in which the periostracum was eroded) did increase in this grid between 1992 and 1993. The percent change in white mussels was estimated at 100% (i.e., the number of w. mussels doubled) between 1992 and 1993. No tube worm or other mussel colonization was observed in the open sediment areas. Except for the white mussel variations, the lack of any perceptible change in distribution or density for any other features suggested that the GC 272 area observed was very stable. Mussels appeared to move about, but did not show any large-scale shifts in density or distribution, and their percent of aerial coverage remained essentially constant.

7.3.6 Photomosaics at GC 272: Site 2

This site is found within an extensive region of vesicomyid clams. The site consists of flat and relatively featureless sediment. It is marked by a "clam corral," a square aluminum frame measuring 3 m on a side and marked with a float labeled with the number three. Water depth at the site was 728 m. A high level of detail was observable for the sediment surface in both years of evaluation. Any changes were readily seen. Comparison of 1991 and 1992 revealed, however, no observable changes in fauna type, distribution, or density. In both years, only a few clams were observed outside the corral. No visible colonization of sediment was observed by any organisms. No significant signs of bioturbation were noted, although a few, rare trails were seen and a spider crab was observed at Corral #3. The area appeared 100% stable with no discernible changes between observational periods.

7.3.7 Photomosaics at VK 826

This site consisted of a carbonate hard-ground colonized by sparse tube worms and bacterial mats along two intersecting fractures. The site is marked with weighted, orange bucket (5 gal). Water depth at the site is 455 m. Grids were

designated labeled A through F. Features observed in A through F for 1991 and 1992 were as follows:

Grid A.	1. Bw 2. Sf	Grid B.	1. Mdb
Grid C.	1. Sf 2. M-d 3. Ts	Grid D.	1. Bw 2. M-d 3. Sf 4. Ts
Grid E.	1. Sf 2. Bw 3. Ts	Grid F.	1. Sf 2. Bw 3. Ts

We evaluated both mosaics simultaneously after inspecting each mosaic separately for greater accuracy. Numerical variation, when viewed in this manner, were seen as functions of estimates made where substantial areas of no coverage exist. One-to-one comparisons (made on screen) were more revealing and eliminated this problem.

Replication of percent cover were observed for all features. Tube worms revealed no change in distribution or density. One noteworthy observation was the appearance of the bacterial mats located in (and near to) the fracture set. In both years, bacteria was highly visible. In fact, individual, small (~ 6 - 84 cm diameter) patches of bacteria were specifically identifiable from 1991 and 1992. We initially suspected a change in bacteria from the mosaics alone; however, upon review of dive tape 3261, we observed exactly the same patches observed in 1991. Bacteria showed no signs whatsoever for change in distribution. We estimated the same bacteria at 50 cm grid scale, and again found no visible change. Viosca Knoll appeared to be very stable. No observable changes in any feature distributions were observed. As with bacteria mats, it was possible to identify specific tube worm individuals from 1991 in the 1992 coverage, further suggesting a very stable setting.

7.4   Disturbance

7.4.1   Bush Hill Site, GC 184/185

Two cages were deployed approximately 40 cm apart at a site of dense mussel and mussel-tube worm cover. The cages were placed on sediments that had been exposed by the collection of mussels for experimentation. In cage one, approximately 15 large (greater than 7 cm) mussels occurred as a cluster in the open area of the frame. Approximately 10 animals of similar size were attached to the frame of the cage on the open side. The netted side appeared to be devoid of mussels. The crustacean *Munidopsis* and *Alvinocaris* were present in both the open and netted area. The bottom in the open side not occupied by mussels was colored white, suggesting chemical and/or bacterial activity. The bottom on the netted side appeared to have no special coloration.

Cage two was quite noticeably different. The netted section was completely covered with white *Beggiatoa* film obscuring observation of any contents. The open side was devoid of mussels, and the bottom was covered with both white and red *Beggiatoa* mats. Approximately two large mussels were attached to the outer edge of the frame, but none were in the open area. *Munidopsis* and *Alvinocaris* could be seen adjacent to the frame, but not within it.

The area between the two cages contained a cluster of approximately 20 large mussel specimens both clumped and singly. This clump was an extension of a large mussel aggregation located adjacent to the cages. The bottom between the cages also had reddish *Beggiatoa* cover. Two specimens of the sea star *Sclerasterias* were near the to cages.

7.4.2 GC 234

A single cage was deployed on an area of mud and exposed low relief carbonates. The site contained both dense mussel aggregations and mussel-tube worm assemblages. The larger area around the cage was whitish due to bacteria or chemical activity. Two mussels were attached to the frame in this section. The netted section contained no mussels, but approximately three large specimens appeared to be attached to the exterior of the frame. The netted side contained numerous specimens of *Alvinocaris*, *Munidopsis*, and the gastropod, *Buccinium*.

7.4.3 Site Three GC 272

A single cage was deployed in a field of mussel clumps. Tube worm bushes were in the area, but greater than 2 m from the cage. The cage abutted two mussel clumps. The open side contained a single mussel attached to the inner side of the frame. The bottom of the open side was soft bottom with no distinctive features. The netted side contained two mussels attached to the frame, one under the netting on the bottom and the other attached to the outside of the frame. At the edge of the netting, nearly centered within the frame was a large burrow approximately 30 cm across. The legs of a large crustacean, possibly an anamuran crab, could be seen within the burrow. During the period of observation, both a hake and a hag fish swam through the open side of the cage.

7.4.4 Brine Pool

The rods in the brine had a coating of "fuzz" that appeared to be hydroids. No other organisms were visible by simple inspection. There were no juvenile mussels obvious at any position on the rods. Rods around the periphery of the mussel mat had little or no such fuzz covering. Rods lying horizontally on the mat appeared to be devoid of a covering.

7.4.5 Inner Edge Markers - Brine Pool

Only the southern edge marker was repeatedly surveyed in 1991, 1992, and 1993. With respect to the relationship with the mat edge, there was no major change between 1989 and 1993. The rods remained centered in a 10 cm radius indentation in the mussel mat with no noticeable advance in the mat edge. Faunsitically, two years after placement, the rod was covered with an unidentified tubiculous organism. Only in the 1993 survey were juvenile mussels, approximately 2 cm in maximum dimension observed. These were settled at the brine pool interface, where a reddish precipitate appeared to have formed. In addition to the tubicullous covering, limpets and sepulid worm tubes could be observed on the rod.

The rod at the northern end was never well surveyed since its emplacement. By 1991, it was covered by tubiculous organism and still stood approximately 10 cm from the mat edge. Video footage taken in 1993 showed the tubiculous organisms to still be present. The rod appeared to still be at the very edge of the mat, but resolution was insufficient to resolve its exact position.

7.4.6 Mat Surface Markers - Brine Pool

Only three edge markers remained upright and visible at the southern end. The surface rod had obviously moved since its deployment and rested against one of the vertical rods. Its ends lie upon living mussel clumps, while its central portion spans a mud channel. That is largely devoid of mussels and marked by dark chemical stains. No mussels, either juveniles or adults were observed on the rod in 1991, 1992, or 1993. Major movement of the rod from its deployment to its present location occurred between 1989 and 1991. Since then, there has been apparently progressive movement of the rod in the direction of its length. This movement was quite evident by monitoring the point at which the vertical edge marker touches the surface

marker. Between 1991 and 1992, this point of contact moved 20 cm. Between 1992 and 1993, there was an additional 10 cm movement in the same direction.

Already by 1991, adult mussels were moving on to the northern edge although only ~50% of the surface was obscured by mussels. In 1993, only the inner 1/2 of the rod was well surveyed. That end was ~80% covered with adult mussels, greatly obscuring the rod. Even the small bare spaces bore marks of abyssal attachment.

7.5   *In Situ* Observations

During submarine dives at Bush Hill in July 1991, we observed streams of bubbles issuing from a low mound at a depth of 540 m. Covered with bacterial mats and surrounded by chemoautotrophic tube worms and mussels, the mound was quite conspicuous. Although seismic and geochemical evidence (Kennicutt et al. 1988a) indicated that shallow gas hydrate was present throughout Bush Hill, we did not recognize the mound as gas hydrate until H. H. Roberts (1991 personal communication) described finding gas hydrate in bubbling mounds at a hydrocarbon seep ~10 km from Bush Hill. We now realize that hydrate mounds are common at hydrocarbon seeps in the Gulf of Mexico.

The size and shape of the mound altered significantly over the course of <1 year. On August 28, 1992, the hydrate mound comprised three distinct lobes protruding in a row that extended ~2.5 m along the crest of a low hillock (Figure 7.1 top). The central lobe, the most prominent, was lens shaped and ~50 cm in diameter. A deep undercut on its downslope side exposed yellow hydrate material (Figure 7.1 top right). A steady stream of tiny bubbles and occasional bursts of larger bubbles escaped along the edges of the central lobe. The right-hand and left-hand lobes had some fractured sediment at their bases but lacked the undercut of the central lobe. Small pieces of hydrate broke free and floated away when the right-hand lobe was probed. We returned to the mound in 1993 for a series of dives that began on May
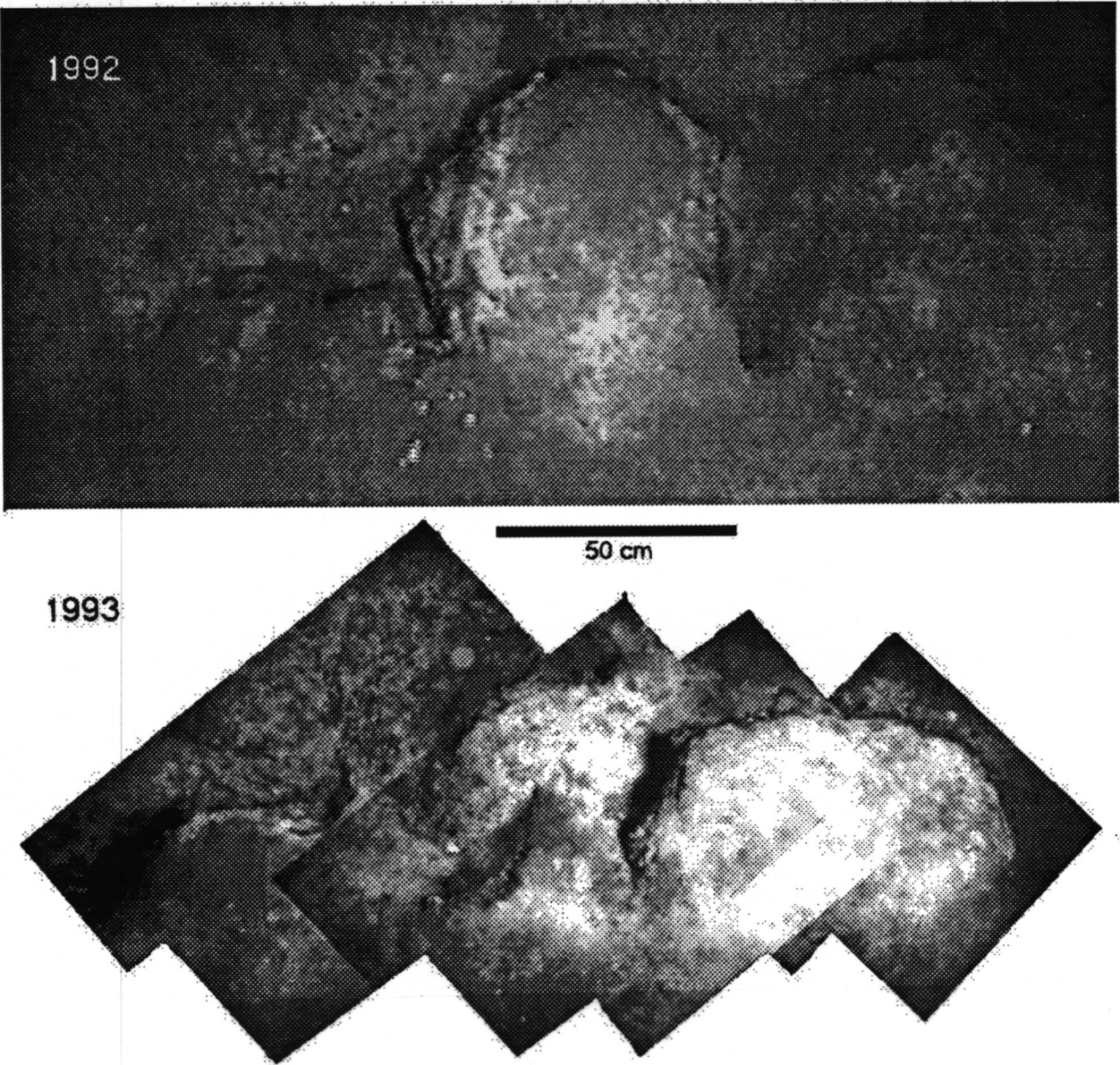
Figure 7.1   Gas hydrate at a depth of 540 m on the continental slope of the Gulf of Mexico (27°26.7'N and 91°30.4'W). A frame of video taken in 1992 (upper) shows a prominent central lobe of hydrate breaching the seafloor between two smaller lobes (scale bar is 50 cm). The yellow material in the color inset photograph shows gas hydrate exposed near the point of the arrow; similar material was visible around the entire edge of the lobe (scale bar is 10 cm). Note the small bubbles on the left side of the frame. A mosaic of four photographs taken in 1993 (lower) shows that the central lobe of gas hydrate observed in 1992 had disappeared in 1993, leaving an area of disturbed sediment and exposed gas hydrate. The right-hand lobe increased in volume and elevation above the surrounding sea floor during this period.

15th. Comparison of photographs and videotapes showed that the entire central lobe had disappeared between the 1992 and 1993 observations, leaving an area of disturbed sediment and patches of exposed gas hydrate (Figure 7.1 bottom). The left-hand lobe remained relatively unchanged, but the right-hand lobe had grown and had developed a deep undercut on its downslope margin.

The temperature probe was inserted under the down-slope side of the left-hand lobe (Figure 7.1 lower) on June 2, 1993. We were able to insert the bottom 60 cm of the probe before it grounded against an impenetrable layer. The angle of insertion was about 50° off vertical. So, the lower-most thermistor was buried beneath the hydrate lobe at a subsurface depth of ~26 cm; the middle thermistor was buried at ~13 cm; the third was at the seafloor; and the remaining thermistors were in the water column. After 26 min, the lower and middle thermistors had equilibrated to temperatures of 7.55°C and 7.41°C, respectively. The seafloor and water column temperatures were 7.35°C and 7.28°C, respectively. Insertion of the probe initiated a copious discharge of oil and gas that persisted for 30 min. Samples of the gas stream that vented continuously around the hydrate mound consisted of 0.2% O_2, 8% CO_2, 11.4% N_2, 69.6% methane, 6.3% ethane, 1.7% propane, 0.2% i-butane, 0.9% n-butane, 0.3% i-pentane, and < 0.1% n-pentane. The relative concentrations of C_{2+} gases in all samples collected at Bush Hill ranged from <0.5% to >12% (Table 7.3). Highest C_{2+} concentrations were found in samples of the bubble stream; lowest concentrations were recovered from sediment cores.

Table 7.3. Hydrocarbon composition (C_1-C_5) of gas samples from the study site.

Sample	Methane (%)	Ethane (%)	Propane (%)	Iso-Butane (%)	N-Butane (%)	Iso-Pentane (%)	N-Pentane (%)
Bubble	88.0	8.0	2.1	0.3	1.2	0.4	<0.1
Bubble	88.0	7.5	2.2	0.5	1.1	0.6	<0.1
Sediment	89.4	8.0	0.9	0.1	1.0	N.D.	0.3
Sediment	93.5	5.3	0.8	0.4	0.4	0.2	N.D.
Sediment	94.3	4.2	0.8	0.4	0.3	N.D.	N.D.
Sediment	99.5	0.5	N.D.	N.D.	N.D.	N.D.	N.D.

Note: N.D.–not detected

The bubblometer was deployed from May 15 to June 27, 1993. Over this 44 day period, spontaneous gas releases were only recorded during a 10 day interval when water temperatures exceeded 8.0°C (Figure 7.2). Small gas releases began when the water temperature first exceeded 8.0°C on May 19. The temperature remained >8.0°C and additional releases were recorded on May 21 and 23. Beginning on May 25, a series of major releases caused up to 23 rotations of the chamber per hour. Cessation of major releases coincided with a decline of water temperature to below 8.0°C. Temperatures remained <8.0°C for the subsequent 30 days, and no additional gas releases were recorded. The total volume of the gas release recorded by the bubblometer amounted to ~900 L at standard temperature and pressure.

7.6 Geological Interpretations

The near-surface geology of hydrocarbon seeps is described in detail elsewhere in this report. Our purpose here is to examine the geological record for evidence of sudden, localized processes that could disrupt or destroy portions of the chemosynthetic community. The tectonic history of a seep will clearly result in gradual changes as hydrate mounds — such as Bush Hill — increase in size, or as active faults separate to form grabbens or half-grabbens such as can be seen at the GC 234 site. The progression of these processes is probably sufficiently slow that the
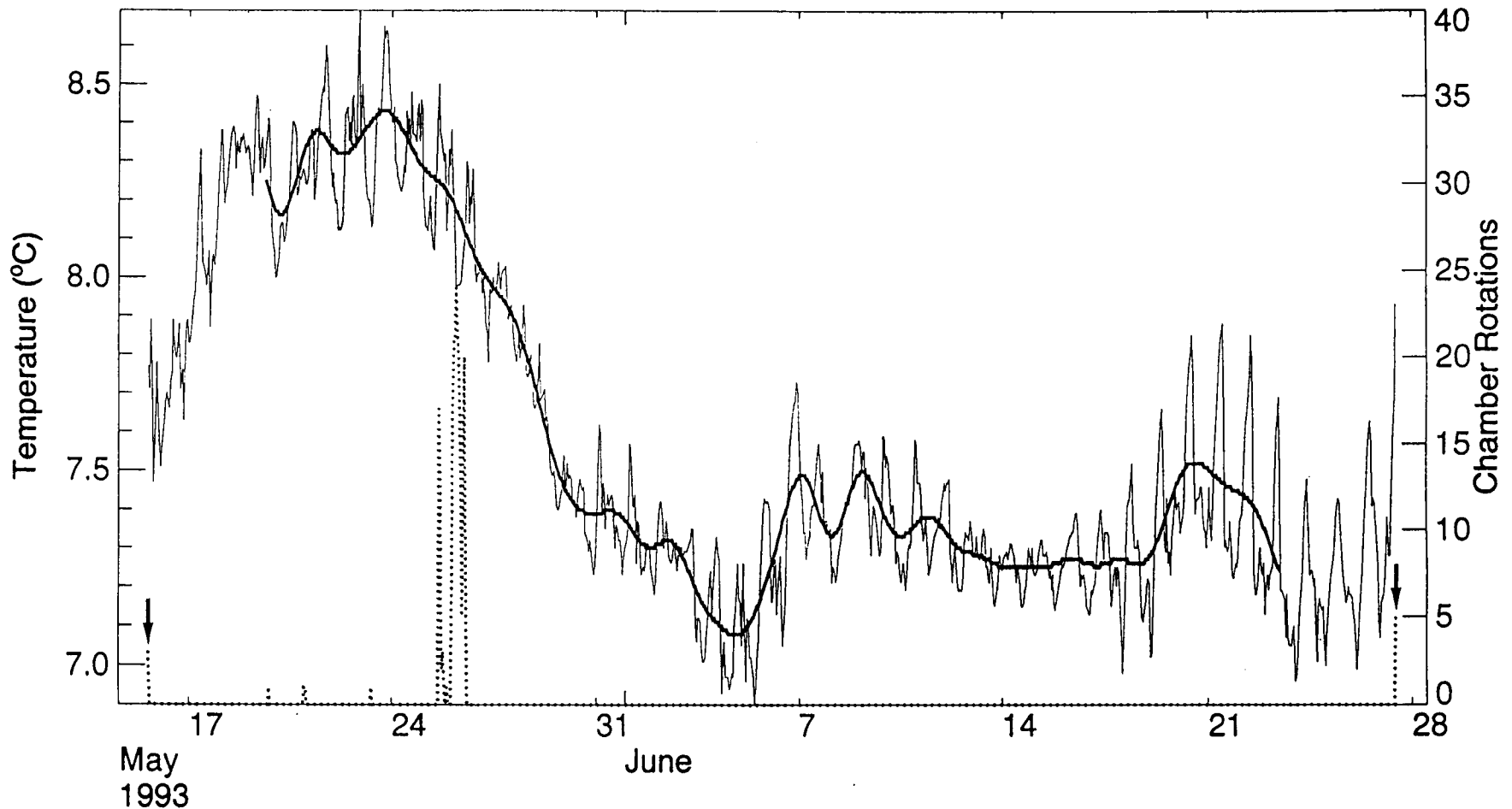
Figure 7.2   Data recorded by a bubblometer showing the release of gas and the water temperatures during a 44-day period in 1993. Temperatures detected by a thermistor resting in contact with the sea floor were recorded at 5-min intervals (solid line). The trends contained in the oscillations was determined with use of a 40-h low-pass filter (heavy line). The hourly rotation count (broken line) shows a series of intense gas releases interspersed with long periods of inactivity. Rotations at the beginning of the deployment (left arrow) resulted from gas released by our disturbance of the mussel bed. Five manual rotations were recorded upon recovery (right arrow) to check the system.

communities are able to persist in the face of the ongoing change. A disruptive event, in contrast, causes relative sudden changes in conditions that render a habitat uninhabitable or prevent colonization. Several distinct processes meet this criterion, which are related to active fluid migration through the sediment-water interface.

Active discharge of brine or brine and mud mixtures have been observed at numerous sites. The largest example of the latter was described by on the basis of observations made from Submarine NR-1 in May of 1993. The site is located the GB 425 lease block (near 27°33.6'N and 92°32.3'W) at a water depth of 590 m (Figure 2.1). It consists of a flat-topped, semicircular mound with a diameter of about 1100 m and a bathymetric relief of about 20 m above the surrounding seafloor. The top of the mound was covered with thin crusts of calcium carbonate. Extensive mud flows were evident on the southern and northeastern flanks of the mound. Active mud vents were found by following the traces of these flows onto the upper periphery of the mound. These vents were roughly circular pools of undetermined diameter from which liquefied mud was overflowing at the down-slope edges. Continual streams of gas bubbles and oil droplets were erupting from these pools, creating a localized cloud of suspended sediments. A temperature probe, lowered into the mud recorded a temperature of 19°C, about 12°C warmer than ambient sea water. Several clusters of mussels (SM Ia) were found at locations adjacent to the mud vents where the substratum had stabilized sufficiently to permit colonization. Notably, no tube worms colonies were observed on this feature.

The evidence of the mud volcano in GB 425 suggests that fluid discharge must stabilize before chemosynthetic fauna can make effective use of a seep site. Pockmarks offer a further example of this relationship. Formation of pockmarks has been attributed to vigorous discharge of gas through the seafloor (Hovland and Judd 1988). The brine-filled pockmark found in GC 233 is an example of the combination of pockmark formation and brine flow (MacDonald et al. 1990a,b). The very high

concentrations of dissolved methane in the brine provide favorable circumstances for seep mytilids, which have formed a contiguous mat around the edges of the pool. In the current status of the mussel bed surrounding this brine pool, we see a highly productive and evidently stable community, but earlier in the geologic history of this feature, the edges of the pool would have been untenable. Even in the present configuration, the anoxic, hypersaline brine is a potential hazard to mussels and to fish. A slight change in the level of the brine in the pool would inundate the mussels around the inner edge and cause high mortality.

The tendency for hydrate or authigenic carbonate to temporality cap active vents creates a potential instability in chemosynthetic habitats. Effects of pressure release due to failure of a hydrate plug is discussed earlier in this section; the geological record also provides evidence for eruptions that dislodged carbonate caps. Examples of disruptive or catastrophic events have been found at GC 184. Figure 7.3 shows a massive slab of mussel shells and carbonate cement that was upended in the floor of a large pockmark near the crest of Bush Hill. The combination of the cemented shells in what is essentially a debris field left by an eruptive event clearly demonstrates the potential for localized mortality in chemosynthetic communities due to catastrophic pressure releases.

7.7   Conclusions

Over periods of one to two years and at scales of 1 m we could not detect any change in the distribution or composition of the chemosynthetic fauna at seven sampling stations in four separate study sites. These stations included tube worm, mussel, and vesicomyid clam habitats, as well as areas of bacterial mat and uncolonized sediment. As a corollary, neither were we able to detect recovery of mussel clusters from artificial disturbances when patches of about 0.25 sq m were removed.

Figure 7.3   Photograph of a massive slab of mussel shells and carbonate cement that was up-ended in the floor of a large pockmark near the crest of Bush Hill.

On a larger scale, submarine observations at three of these site date to 1986 or 1987. Over this period as well, the character of the communities — the composition, the density, and the general distribution of the sessile chemosynthetic fauna has remained unaltered. That is to say that markers, both natural and artificial, that were associated in 1987 with clusters of tube worms or mussels, or with an area in which living vesicomyid clams could be found were in all cases associated with the equivalent fauna in 1993. No mass die-offs or large scale shifts in faunal composition have been documented during the 8-year history of investigation of hydrocarbon seep communities in the northern Gulf of Mexico. Unless a longer time series can be obtained to challenge these results, the conclusion must stand that hydrocarbon seep communities show fidelity of composition and distribution over time scales of at least 5 years and probably 10 years and over length scales of meters to tens of meters.

At the sub-meter scale, the surface markers at the brine pool (GC 233) indicate that there can be appreciable movement of mussels in some portions of the mat, while in other areas the mussels are much more sedentary. This can be interpreted in at least two ways. First, it might indicate that movement to maintain position on a gradient is more intensive at the northern end. Here, there is a low berm directly behind the mussel mat restricting the mat and the edge of the brine pool. Even slight vertical fluctuations in the brine layer would be easily manifest on the fauna, attempting to move up to avoid the brine or move down to obtain greater methane. By contrast, the southern end resembles an overflow plain in which any change in the surface level of the brine pool would simply flow through the outflow channels, and not create a major change in the vertical gradient experienced by the south end mussel clumps.

An alternate interpretation is that movement of mussels does not reflect repositioning to stay in a desired range of a moving gradient, but that it is due to

growth of individuals wedging themselves deeper into the mat. In this view, the apparent lack of movement onto the rod at the southern end may reflect lower growth rates and/or recruitment rates in that region.

The main conclusion that can be drawn from controlled disturbance observations is that recovery from the experimental disturbance does not proceed rapidly. Immigration of adult mussels into a disturbed area was minimal over a year, and there is no conspicuous recruitment of juveniles over the period of a year. These results are the same for all three sites with cages. The massive bacterial over-growth of cage two at Bush Hill indicates that development of bacterial mats can take place in less than a year.

The absence of apparent larval recruitment was the most interesting finding. However, the relatively short duration of the experiment coupled with the lack of any microscopic examination of the caged bottom limits the certainty of this observation. Mussels may have settled, but the field growth rates could be so slow that recruited individuals are still in the undetectable 1-2 mm size range. Alternatively, larvae may not have settled at all or, have recruited but failed to survive to a detectable size range.

The observation that mussels have not colonized the brine pool rods for three years supports the conclusion that larval recruitment is a slow, and possibly rare event. This is especially important in the case of rods crossing the brine/seawater interface just a few centimeters from dense mussel clumps. It may be safely assumed that the rods are situated in a chemically suitable environment, yet no mussel clumps have appeared on the rods.

In the introductory section, we mentioned that interspecies competition may be important. The hydroid cover on the brine pool rods is a hint that such processes are in operation. The vertical rods may provide an artificial refuge from predatory browsing by gastropods and crustacea. Isolated from the mussel mat's heterotrophic

fauna, the rods in the brine have escaped browsing by gastropods and crustacea and developed a dense hydroid cover. Rods lying horizontally on the mussel mat are exposed to browsing that crops back the hydroids. Similar dense hydroid cover is found on some tube worms in the Bush Hill area. It may be assumed that some peculiarities of local topography tend to restrict browsers on such bushes. Unfortunately, this grazer control explanation for the hydroids fails to explain the absence of new recruits from all rods at the brine pool.

Recovery of artificially displaced mussel clumps by migration of mature mussels had begun one year after disturbance. Except for cage 1 at Bush Hill, very few specimens participated in this migration. More important to recovery, after one year there was no obvious recruitment of juvenile mussels. At this preliminary stage, it appears that recovery from disturbance that denudes mussel cover will be slow with successful recruitment of juveniles taking more than 3 years.

Significant changes have occurred in these communities, however, within recent time. The animals are indisputably growing — albeit quite slowly, as we describe earlier in this volume. Presence of juvenile tube worms (Gardiner personal communication) and mussels demonstrates that spawning and settlement are on-going. Observational evidence documents the presence of defunct mussel clusters and of dead tube worms in the process of being buried by sediment. These are localized loss, however, probably tied to subsurface rechanneling of seepage or to catastrophic, but again local events such as mud flows, blow-outs, or development of hydrate mounds. Geological evidence that small scale catastrophes that punctuate overall stability is overwhelming. The upended pavements, pockmarks, mud-flows, brine flows, and hydrate formation and dissociation are all consequences of a environment in which the final few meters of the sediment column alternately channel, check, and release fluids migrating from much greater depths. Resulting disturbances are neither so pervasive, nor so devastating as the volcanism of the

mid-ocean ridges, but will clearly affect sessile animals that form part of the barrier to seepage.

The evidence from our observations of the outcropping hydrate at GC 184 suggests that shallow gas hydrate acts as a kind of pressure relief system, alternately checking and releasing the flow of hydrocarbons from localized vents. Gases accumulate as components of hydrate; gas and oil are also trapped beneath layers of hydrate. The accumulated volume escapes when the plug of gas hydrate either dislodges because of excess buoyant force, or dissociates because water temperature rises above the limit of stability. The range of stable temperature is defined by hydrostatic pressure and by the chemical composition of individual hydrate bodies. Under these circumstances, intermittent formation and loss of shallow gas hydrate occurs over periods of less than one year.

Shallow gas hydrate initially forms when gas, migrating from deep hydrocarbon reservoirs, encounters barriers such as authigenic carbonates and layers of biota near the seafloor. Lateral displacement of the flow of gas and temperature gradients such as we measured would contribute to the growth of gas hydrate layers. Observations indicate that these near-surface layers can be ~10 m in diameter; morphologically, they resemble pingos. The exposed gas hydrate lobe (Figure 7.1) is merely the edge of a larger formation. When a layer of gas hydrate breaches the seafloor, the flow of gas around its emergent edge will entrain fine sediment and undercut the base. The exposed lobe of gas hydrate is not a permanent feature. Eventually, its buoyant force and that of free gas trapped below will exceed the strength of its attachment; the hydrate lobe will then break free with a burst of gas and oil. A detached lump of gas hydrate will float upward in the water column for a considerable distance before dissociating completely in warm surface waters. Whether an entire layer of shallow gas hydrate could break free in a similar manner is

a matter for speculation, but clearly a catastrophic event of this type has the potential to affect local communities of chemosynthetic fauna.

Intermittent releases of gas during warming events are a second mechanism that can release pulses of hydrocarbon to the water column. The gas venting recorded by the bubblometer (Figure 7.2) was consistent with dissociation of methane hydrate and subsequent release of trapped gas caused by a temporary rise in water temperature. The brief lag observed between maximum temperature and maximum release would result from time required for the temperature wave to propagate downward into the sediment. No metabolic activity of the mussels or sediment bacteria could possibly produce a gas release of such magnitude or duration. To support this argument, we need to estimate the maximum stable temperature for hydrate that might form from the gases present in the shallow sediment of Bush Hill.

Maximum stable temperatures for gas hydrate depend upon its chemical composition. The C_2+ gases, particularly propane, are preferentially incorporated by the hydrate lattice and increase the dissociation temperature of gas hydrate. With the use of the program CSMHYD presented in Sloan (1990), we calculated that at a hydrostatic pressure of 5.4 MPa, the maximum temperature for a hydrate of pure methane is 7.5°C; whereas a hydrate formed at equilibrium with a gas mixture of 98% methane and 2% propane will contain 70% methane and 30% propane and remain stable to 14.5°C. Inert gases will also increase the stability temperature of gas hydrate.

Understanding gas hydrate formation and dissociation under these conditions is incomplete. It seems unlikely that natural gas hydrate at Bush Hill forms in equilibrium with its source gases. Preferential inclusion of C_2+ gases during hydrate formation, and methanogenesis caused by microbial degradation (James and Burns 1984), will increase the proportion of C_1 in gas trapped near the seafloor. The gases

sampled at Bush Hill have a range of compositions (Table 7.3). Dissociation temperatures for hydrates formed from these gases should, therefore, also vary.

Formation and loss of shallow gas hydrate is much more dynamic than is the case for deep gas hydrate. Generally, deep gas hydrate has probably been stable during recent geologic time. Dissociation of deeply buried gas hydrate over 10 ka cycles may result from sea level change and atmospheric warming and may influence climate cycles (Kvenvolden et al. 1993; McDonald 1990). More rapid dissociation might occur if large-scale slumping of marine sediments reduced overburden pressure. Our results indicate that formation and loss of shallow gas hydrate occurs at or near the seafloor within a year or less and that transient temperature increases can markedly influence this process. Warm cored eddies form in the northern Gulf of Mexico every 10-12 months, on the average (Sturges 1992); large eddies can reach 14°C at 500 m depth and can force warm water onto the continental slope (Walker et al. 1993). High temperatures could cause dissociation of gas hydrate in near-seafloor sediment. Free oil and gas trapped beneath the gas hydrate would then escape. Given the widespread occurrence of shallow gas hydrate in this region, normal water circulation processes may intermittently trigger pulses of hydrocarbon released into the water column over a large geographic area. It is, therefore, reasonable to consider the possible effect of prolonged warming upon the total input of hydrocarbon into the Gulf of Mexico and the World Ocean.

8.0 Evidence for Temporal Change at Seeps
Eric N. Powell

8.1 Perspective

As a population of benthic animals die, some fraction is buried and preserved in the sediments. This collection of dead remains is called a death assemblage. Because sediment is continually collecting, the death assemblage produces a more-or-less continuous record of the community. Unless long-term monitoring has been conducted, the death assemblage will be the only record of the history of the community. We have used the death assemblage to study the long-term history of petroleum seeps. Our primary objectives were to: (1) determine how stable or persistent seep communities are over long time spans; (2) document the types of temporal variability present in seep communities and to suggest reasons for that variability; and (3) examine the response of seep communities to disturbance and determine their resilience.

We utilize three measures of community structure to examine persistence, resilience, and temporal variability in seep communities: numerical abundance, paleoproduction, and paleoingestion. We evaluate persistence, resilience and temporal variability by using these measures to follow changes in guild and their structure and habitat optimally. Paleoproduction and paleoingestion are the paleontological analogues of biomass and energy flow through the consumer food chain in living communities (Powell and Stanton submitted a; b). Biomass and ingestion as preserved are lifetime attributes, as all preserved individuals have completed their life spans. The prefix "paleo" is used to distinguish time-averaged attributes of this kind from their ecological counterparts. Accordingly, we define paleoproduction, the paleontological analogue of biomass, as the net production of somatic tissue over the animal's lifetime. In the same vein, we define paleoingestion,

the paleontological analogue of energy demand or daily consumption, as the amount of energy required to maintain the animal's necessary physiological processes (respiration, reproduction, growth) over its life span. We use a hindcasting model to calculate paleoproduction and paleoingestion.

8.2 Flow Model

The hindcasting model is formulated as follows. Estimation of paleo-energetics followed the approach described by Powell and Stanton (1985):

$$A_{lt} = P_{glt} + P_{rlt} + R_{lt} \tag{1}$$

where A_{lt} is the energy assimilated (in calories) over the individual's life span, P_{glt}, paleoproduction, is the portion of net production devoted to somatic growth over the individual's life span, P_{rlt} is the portion of net production devoted to reproduction over the individual's life span, and R_{lt} is the amount of energy respired over the individual's life span. Paleoingestion, the amount of energy consumed (in calories) over the animal's life span is, then, the assimilated energy divided by the assimilation efficiency.

$$I_{lt} = A_{lt} (A/I)^{-1} \tag{2}$$

The parameters of equation (4) are estimated as from the study of recent bivalve species follows:

$$P_{glt} = \kappa B \tag{3}$$

where B is biomass-at-death in g ash-free dry weight (AFDW) and κ is a caloric conversion (5675 cal g AFDW-1 for gastropods, 4452 cal g AFDW-1 for bivalves). Biomass is calculated from biovolume (in mm^3) by

$$\log_{10}B = m_b\log_{10}V + b_b; \qquad (4)$$

where, for bivalves, $m_b = 0.9576$, $b_b = -4.8939$, and $V = L^3$ where L is the maximum anterior-posterior length (in mm); and, for gastropods, $m_b = 0.7708$, $b_b = -3.2421$, and V is an operational equivalent of shell volume derived, for most gastropods, from the equation for a cone, $V = 1/3\pi(W/2)^2L$, where W (in mm) is the maximum width and L (in mm) is the apex-adapical tip length. For some cylindrical species, alternative equations are used (Staff et al. 1985; Powell and Stanton 1985).

$$P_{rlt} = 18 \text{ or } 6.8\% \text{ of } \left[\int_{t_0}^{t_n} RdR - \int_{t_0}^{t_m} RdR \right] \qquad (5)$$

where t_0 is age at birth; t_m, age at maturity; and t_n, age at death. The values of 18% or 6.8% are for bivalves and gastropods, respectively.

$$R_{lt} = \int_{t_0}^{t_n} \left[\left(s_T^{3m_r m_b} \right) \left(10^{m_r b_b + b_r} \right) \left([\log_{10}(T+1)]^{3m_r m_b} \right) \right] dT \qquad (6)$$

The constants in equation (6) come from three equations: (a) biomass versus respiration at 10°C

$$\log_{10}R = m_r\log_{10}B + b_r; \qquad (7)$$

(b) size (biovolume) versus biomass [equation (4)]; and (c) size versus age.

$$V = S^3 = [s_T \log_{10}(T+1)]^2, \qquad (8)$$

where S (in mm) is a linear measurement of size. The values of b_b and m_b are those used in equation (4). The values of m_r and b_r were taken from the equation relating biomass to respiration at 10°C, $m_r = 0.8573$; $b_r = 1.4984$. The constant s_T was obtained by solving equation (8) using a known maximum size and maximum age for each species.

Maximum size was obtained from Odé (1975-1988) and our unpublished data. Maximum ages were obtained from Powell and Cummins (1985), Powell and Stanton (1985), Comfort (1957), Heller (1990), and Callender and Powell (in press). In cases where a maximum age could not be obtained from the literature either through reference to the species in question or a closely-related taxon, we assigned a maximum age of two years. This resulted in an underestimation of paleo-energetics for these species. Probably, the most egregious underestimate was setting lucinid maximum age at two years. No maximum age data are available for Lucinidae. This probably represents an underestimate of 400% or more. Consequently, estimates of energy flow derived from the model are also very conservative.

Trophic guilds and habitat tiers were assigned using information in Andrews (1977), Staff et al. (1985), Callender and Powell (in press) and Stanton and Nelson (1980) supplemented by our own observations and other references cited in Staff et al. (1985) and Callender and Powell (in press). The set of trophic guilds comprised the following six guilds: herbivores, chemosynthetic species, low-level suspension feeders, high-level suspension feeders, predators, and deposit feeders. Parasites and predators were combined into one feeding category. No deep subsurface deposit feeders, which might require a fifth guild, were present. We divided the fauna into four habitat tiers

based on consideration of the location of their body mass and also their feeding structure: infauna, semi-infauna, low-level epifauna, and high-level epifauna. Rather than distinguishing habitat by mobility [e.g., vagrant as used by Scott (1978) and Miller (1982)], we used the high and low-level epifaunal categories of Ausich and Bottjer (1982) to distinguish habitat type. Low-level epifauna include species whose bodies rest on or just off the sediment surface and whose feeding structures are confined to near sediment-surface water. Mussels are good examples. The high-level epifaunal tiers comprise species that can raise their feeding structures significantly above the surrounding sediment either by being erect forms, forms attached to other taxa, or mobile forms, which typically climb on top of other species. Most vagrant benthos were included among the high-level epifauna. Semi-infauna are those animals whose body mass straddles the sediment-water interface, such as the vesicomyids.

8.3   Size Frequency Distributions

We examined the size-frequency distribution in two ways depending upon how an individual's size was standardized with respect to the remainder of the assemblage. In one case, we standardized individual size relative to the maximum size of the species. In this case, all adults, regardless of size, are relatively large, but some juveniles, considered small by this definition, may be of the same size as adults of another species, themselves considered large. Stunting is frequently a result of local shortages in food supply, such individuals fail to reach the species' maximum size. The absence of adults can indicate a suboptimal environment. Accordingly, large, by this criterion, is an important population attribute. In the second case, we standardized size relative to the size of the largest shell found in the assemblage. We chose the individual attaining the maximum linear dimension measured in all of the biofacies to designate this maximum size. By this definition, some adults are small.

An assemblage comprised exclusively of small individuals may indicate a generalized impoverishment in food supply.

In both cases, the size-frequency distribution of each assemblage was divided into 10 size classes computed as the tenth percentiles of the chosen maximum size. We also calculated the fraction of the species' paleoproduction and paleoingestion contributed by the members of each size class. These plots are not frequency distributions where the size classes were redefined according to the biomass or energy flow parameter plotted. Rather, we retained the size of each linear size class in the species' or assemblage's total paleoproduction or paleoingestion. Accordingly, for paleoproduction and paleoingestion, the frequency spectra indicate the contribution by that linear size class to the whole assemblage. This follows the convention of Powell and Stanton (1985).

8.4 Effects of Taphonomy

Reconstruction of the long-term record of any community from its death assemblage requires an understanding of the processes that formed the preserved assemblage from the original community of living organisms. The processes that affect the organisms' remains after death are termed taphonomic processes. Taphonomic processes bias the death assemblage in several predictable ways. Not all species and individuals are preserved. Preservation is poor for species having few or no hardparts. Smaller individuals are generally less likely to be preserved even among the shelled biota, where preservation is better. Those that are preserved may be broken into fragments. Taphonomic processes are, therefore, an important bias that alters the death assemblage from its original composition.

A second important bias is called time averaging. Because the process of sedimentation gradually buries the older remains, death assemblages provide a record, not only of the organisms that were alive, but also the sequence in which they

were alive. The degree to which this temporal record of events is recorded depends upon the sedimentation rate, the rate of sediment resuspension and redeposition, and a suite of biological processes that homogenize the sediment or otherwise disrupt the sequential record. The gradual degradation of the temporal record by these processes is called time averaging. Interpretation of the preserved record requires an understanding of the degree to which time averaging biased the assemblage.

8.5   Taphonomy at Petroleum Seeps

Taphonomic information was obtained in two ways: the death assemblage was examined for evidence of taphonomy, called the taphonomic signature, using a semiquantitative method developed by Davies et al. (1990); and shells were deployed for extended periods to measure the rate of taphonomic processes and time averaging at Bush Hill only. The results of this research will be summarized here.

Dissolution and breakage are the principal taphonomic processes operating at petroleum seeps. Both processes occur in most death assemblages. However, petroleum seeps differ from most other environments of deposition by the severity of the taphonomic process. Dissolution, probably driven by sulfide oxidation that produces sulfuric acid, is of greater consequence at petroleum seeps than elsewhere on the Texas continental shelf, continental slope, or in most Texas estuaries and lagoons. Disarticulation and breakage is primarily caused by crabs or other animals and affects a significant fraction of the preserved biota. The resulting biases are of three kinds: (a) juvenile preservation is extremely poor; (b) small species are poorly preserved (unlike many environments, the bias against small individuals extends to the adults of small species); and (c) mussels are poorly preserved in comparison to the various clam species at all sizes. Thus the rarity of mussels in the death assemblage should not be taken as evidence of the rarity of mussel communities in the site's history. Little record of this biofacies is preserved under normal

sedimentary conditions. Catastrophic burial is required. A detailed discussion of the taphonomic data can be found in the Appendix.

8.6   Effects of Taphonomy on Seep Assemblages

We now consider the effect of taphonomy on species composition, guild and tier structure, and size-frequency distribution. We did this by recalculating each of the assemblage attributes under the assumption that taphonomy biased the assemblage against the lowest three size classes as defined by the assemblage's maximum size. We include, for comparison, a fossil analogue from Tepee Buttes, which represents the expected state after extensive taphonomic alteration. The Tepee Buttes of the Pierre Shale (middle late Campanian) near Pueblo, Colorado, are classic examples of cold seep deposits (Arthur et al. 1982 and Howe et al. 1986). The Buttes are aligned in quasi-linear group that represent fault traces along which hydrogen sulfide-rich fluids migrated from the underlying Pierre and Niobrara strata (Howe et al. 1986). Each linear group of buttes consists of asymmetrical conical carbonate mounds, ranging from 1 to 20 m tall and 4 to 60 m wide, surrounded by shale (Petta and Gerhard 1977). Portions of the limestone core contain a low diversity fauna dominated by lucinid bivalves. The low diversity and high density lucinid-dominated assemblages, stratigraphic relations between the carbonate mounds and adjacent shale, and the quasi-linear arrangement of the buttes suggest that the Tepee Buttes were formed by ancient hydrogen sulfide seeps, very similar to the Louisiana petroleum seep sites.

Species richness was relatively high in the vesicomyid and lucinid biofacies, but low in the thyasirid biofacies and the Tepee Buttes assemblage (Figure 8.1). Numerically, *Calyptogena ponderosa* dominated the vesicomyid biofacies; however, four additional taxa contributed at least 5% and 12 other taxa as much as 1% of the abundance. By paleoproduction or paleoingestion, *Calyptogena ponderosa* dominated
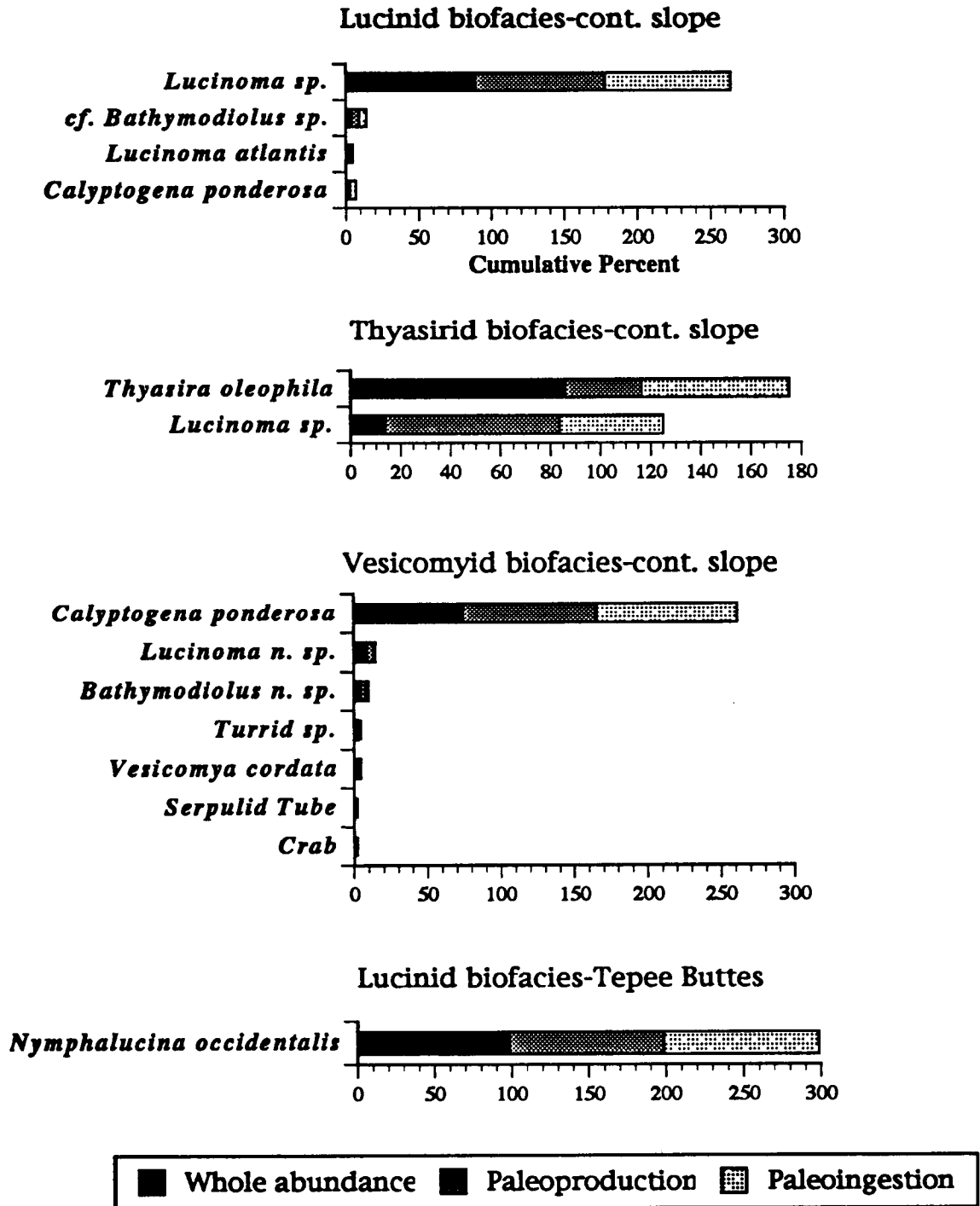
Figure 8.1 The species composition of the clam biofacies summed over all sites. Rank orders by numerical abundance, paleoproduction, and paleoingestion of taxa contributing 1% or more to the death assemblage.

all the other taxa, contributing over 90% of the total. The *Lucinoma* biofacies was dominated by a species of Lucinidae, *Lucinoma* sp., and by the vesicomyid, *Vesicomya cordata*. Typically three to four other taxa accounted for 1% or more of the numerical abundance. *V. cordata* frequently was more abundant than the lucinids. Both paleoproduction and paleoingestion were overwhelmingly dominated by *Lucinoma* sp. The thyasirid biofacies was dominated numerically by *Thyasira oleophila*; however, by paleoproduction or paleoingestion, *Lucinoma* sp. contributed over 60% to the assemblage's composition. Unlike the previous two biofacies, few other species were present. *Nymphalucina occidentalis* was the dominant species at Tepee Buttes in terms of numerical abundance, paleoproduction, and paleoingestion. The mactrid bivalve, *Cymbophora ashbunerii*, was the second most common species, but contributed only 2.3% of the individuals and less than 1% of the paleoproduction.

After taphonomic loss, species richness dropped precipitously in the lucinid and vesicomyid biofacies, but changed relatively little in the thyasirid biofacies and in the Tepee Buttes assemblage (Figure 8.2). The precipitous drop in species richness in the former two indicates the importance of size-selective taphonomic loss in assemblages numerically dominated by small species and juveniles of large species. In contrast, the presence and rankings of species by paleoproduction or paleoingestion was changed relatively little by taphonomic processes.

The guild structures of the lucinid and vesicomyid beds at petroleum seeps were dominated by chemoautotrophs, with minor contributions from the predator, suspension-feeder, and herbivore guilds, when evaluated by numerical abundance (Figure 8.3). Chemoautotrophs accounted for over 90% of the paleoproduction and paleoingestion. The thyasirid biofacies was somewhat unique in that the guild structure was exclusively chemoautotrophic, and thus the guild structure consisted exclusively of low-level suspension feeders. The guild structure of the fossil analogue from Tepee Buttes was almost identical to that of the thyasirid biofacies.

A. (chart, top)

Species (top to bottom), horizontal axis Percent (%), 0 to 90:

- Lucinoma n. sp.
- Vesicomya cordata
- Lucinoma atlantis
- Thyasira oleophila
- Gymnobela judithae
- Chama sp.
- Pleurotomella sp.
- Pleuromeris sp.
- Bathymodiolus n. sp.
- Alvania ceritanmus
- Cuspidaria obesa
- Lucinoma n. sp.
- Bathymodiolus n. sp.
- Calyptogena ponderosa
- Lucinoma atlantis
- Solemya sp.
- Vesicomya cordata
- Lucinoma n. sp.
- Bathymodiolus n. sp.
- Calyptogena ponderosa
- Vesicomya cordata
- Cantrainea sp.
- Lucinoma atlantis

Legend: Individuals, Biomass, PaleoIngestion

B. (chart, bottom)

Species (top to bottom), horizontal axis Percent (%), 0 to 100:

- Calyptogena ponderosa
- Thyasira oleophila
- Vesicomya cordata
- Cantrainea sp.
- Lucinoma n. sp.
- Bathymodiolus n. sp.
- Cataegis cf. meroglypta
- Pleurotomella sp.
- Turridae sp.
- Chama sp.
- Lucinoma atlantis
- Unidentified gastropod
- Unidentified gastropod
- Trochidae sp.
- Ervillia sp.
- Unidentified limpet
- Gymnobela sp.
- Calyptogena ponderosa
- Lucinoma n. sp.
- Bathymodiolus n. sp.
- Vesicomya cordata
- Calyptogena ponderosa
- Bathymodiolus n. sp.
- Lucinoma n. sp.

Legend: Individuals, Biomass, PaleoIngestion

Figure 8.2 A. The species composition of the lucinid biofacies summed over all sites. Rank orders by numerical abundance, paleoproduction, and paleoingestion of taxa contributing 1% or more to the death assemblage. B. The species composition of the vesicomyid biofacies. Rank orders by numerical abundance, paleoproduction, and paleoingestion of taxa contributing 1% or more to the death assemblage.
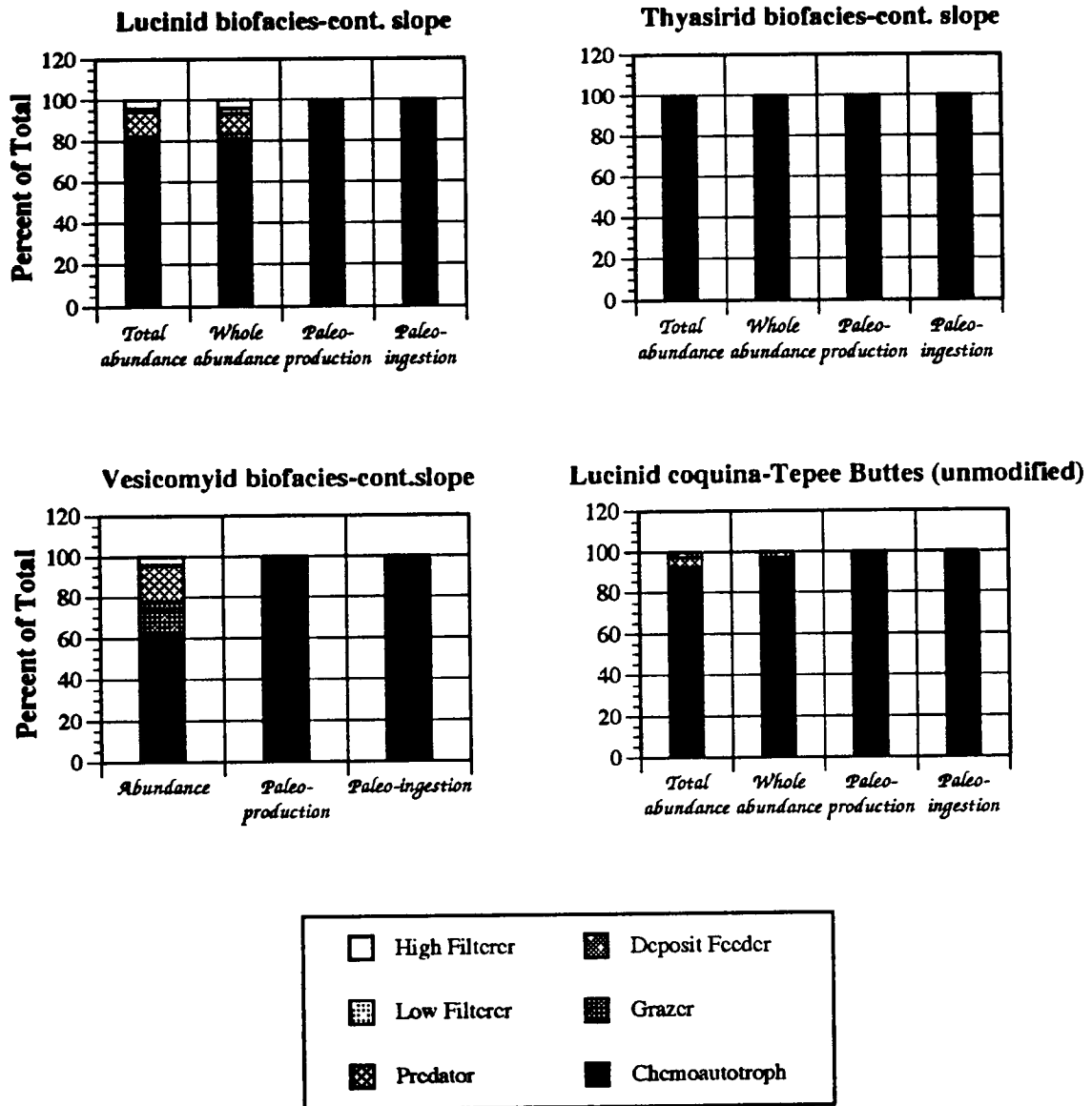
Figure 8.3   The cumulative feeding guild structure of the seep clam biofacies
summed over all sites, defined by total and whole abundance,
paleoproduction, and paleoingestion.

Following taphonomy, the guild structures of the lucinid and vesicomyid beds was overwhelmingly dominated by chemoautotrophs (Figure 8.4). Few of the remaining guilds were represented at all and none were important contributors. Chemoautotrophs accounted for over 99% of the paleoproduction and paleoingestion. Unlike the lucinid and vesicomyid biofacies, the guild structure of the thyasirid biofacies was unchanged and it remained exclusively chemoautotrophic.

The tier structures of lucinid and vesicomyid beds, when evaluated numerically, were a complex mixture of infauna, semi-infauna, and low-level epifauna (Figure 8.5). Infauna, however, dominated the tier structure of lucinid beds and semi-infauna the tier structure of vesicomyid beds when evaluated by paleoproduction or paleoingestion. Infauna dominated the tier structure of the thyasirid biofacies by any measure — numerical abundance, paleoproduction, or paleoingestion. The fossil analogue from Tepee Buttes, like the thyasirid assemblage from the continental slope, was dominated by infauna when evaluated numerically, by paleoproduction or by paleoingestion.

Following further taphonomic loss, infauna came to dominate the tier structure of lucinid beds numerically as well as by paleoproduction or paleoingestion (Figure 8.6). Semi-infauna came to dominate the tier structure of vesicomyid beds numerically as well as by paleoproduction and paleoingestion. Infauna dominated the tier structure of the thyasirid biofacies by any measure — numerical abundance, paleoproduction, or paleoingestion. Thus, like guild structure, the thyasirid biofacies was unchanged by further taphonomic loss.

The size-frequency distribution was divided into 10 size classes computed as the tenth percentiles of the chosen maximum size. We defined the assemblage's maximum size according to the largest shell collected in the assemblage. We also calculated the fraction of the species' paleoproduction and paleoingestion contributed by the members of each size class. These plots are not frequency distributions where
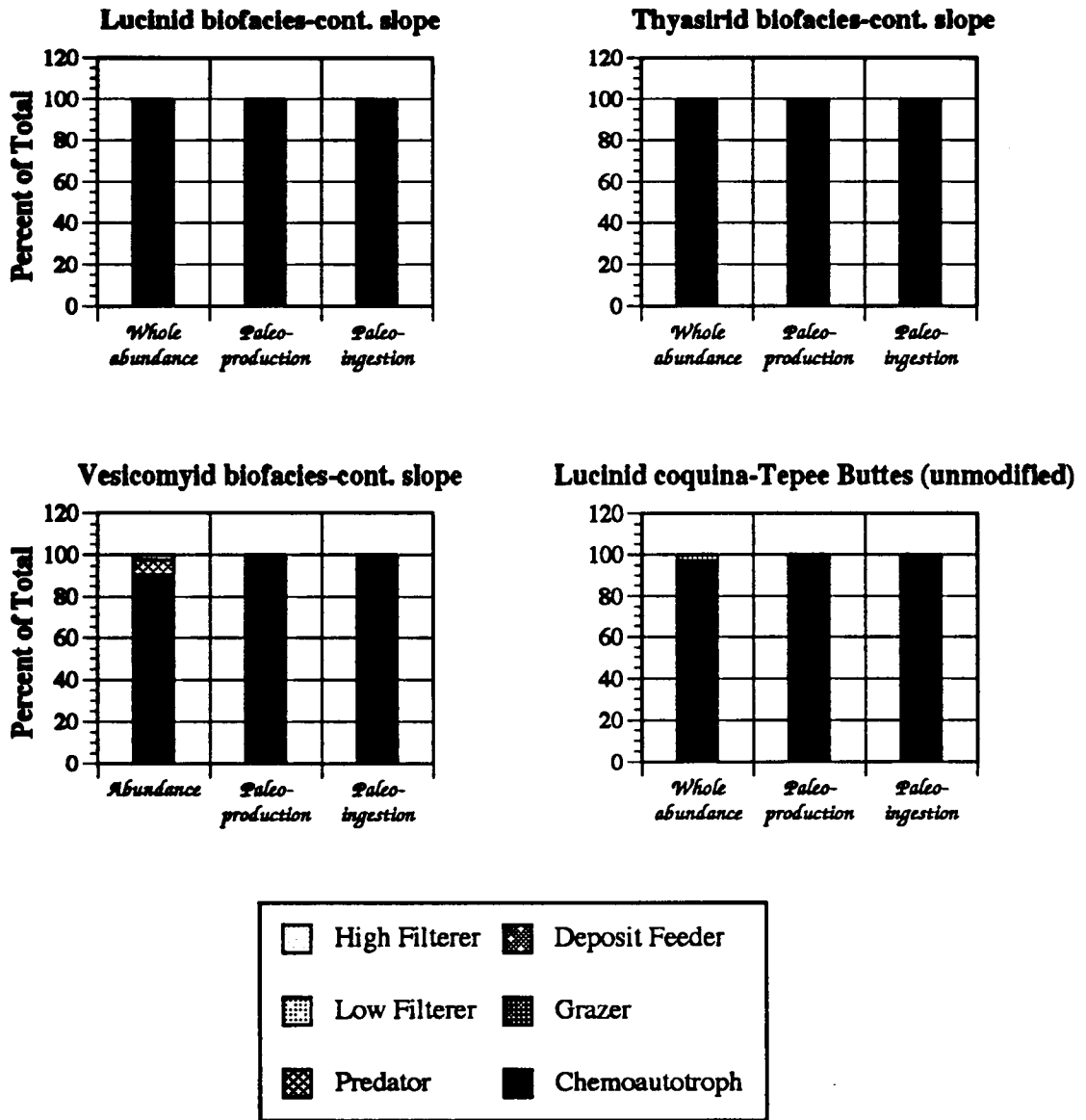
Figure 8.4   Predicted paleoguild structure of seep clam biofacies summed over all sites, defined by total and whole abundance, paleoproduction, and paleoingestion after taphonomic loss of all individuals in the lowermost three size classes.

Lucinid biofacies-cont.slope

Percent of Total

120
100
80
60
40
20
0

Total abundance Whole abundance Paleo-production Paleo-ingestion

Thyasirid biofacies-cont.slope

120
100
80
60
40
20
0

Total abundance Whole abundance Paleo-production Paleo-ingestion

Vesicomyid biofacies-cont.slope

Percent of Total

120
100
80
60
40
20
0

Abundance Paleo-production Paleo-ingestion

Lucinid biofacies-Tepee Buttes (unmodified)

120
100
80
60
40
20
0

Total abundance Whole abundance Paleo-production Paleo-ingestion

☐ High Epifauna

▦ Low Epifauna

▧ Semi-Infauna

■ Infauna
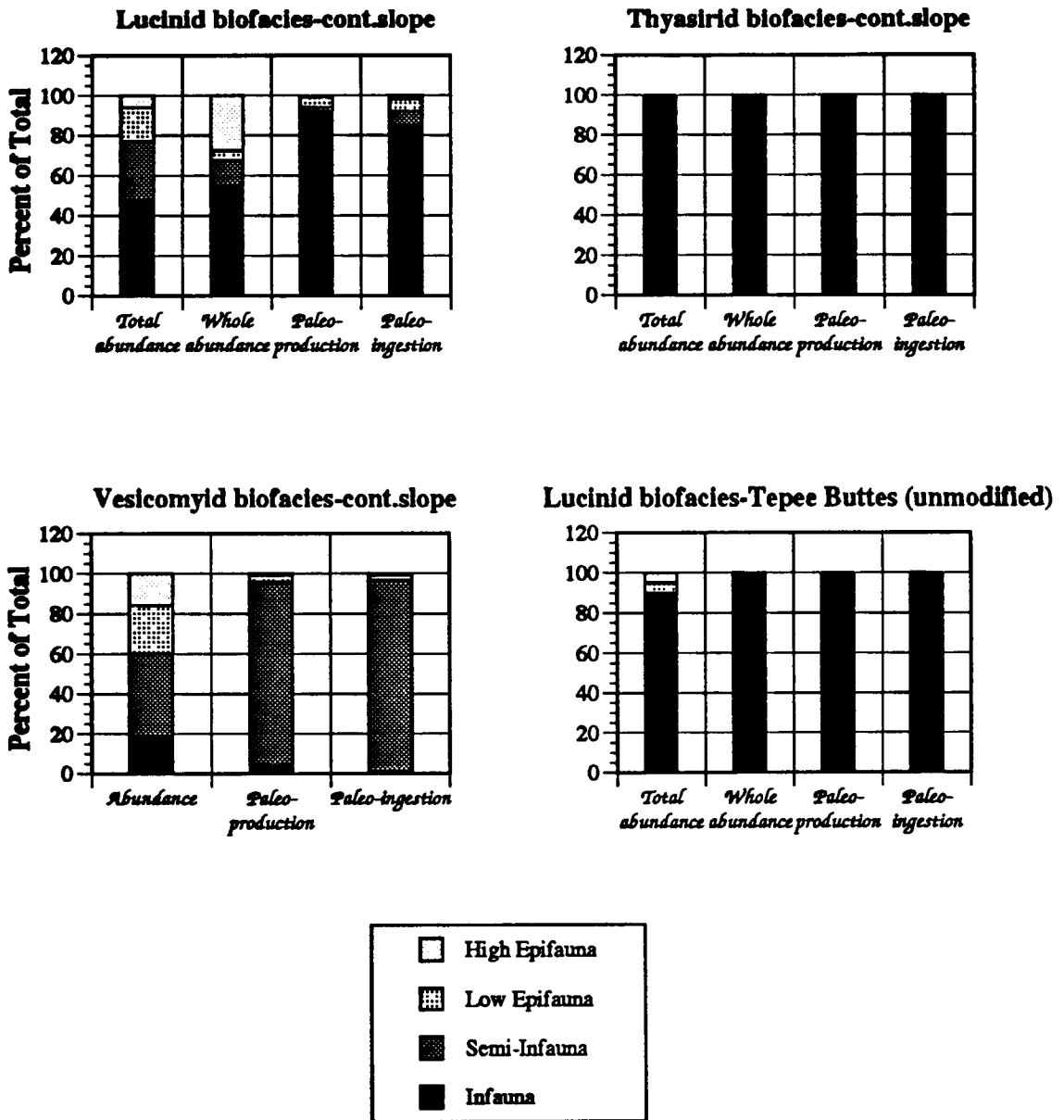
Figure 8.5   The cumulative habitat tier structure for seep clam biofacies summed over all sites, defined by total and whole abundance, paleoproduction, and paleoingestion.
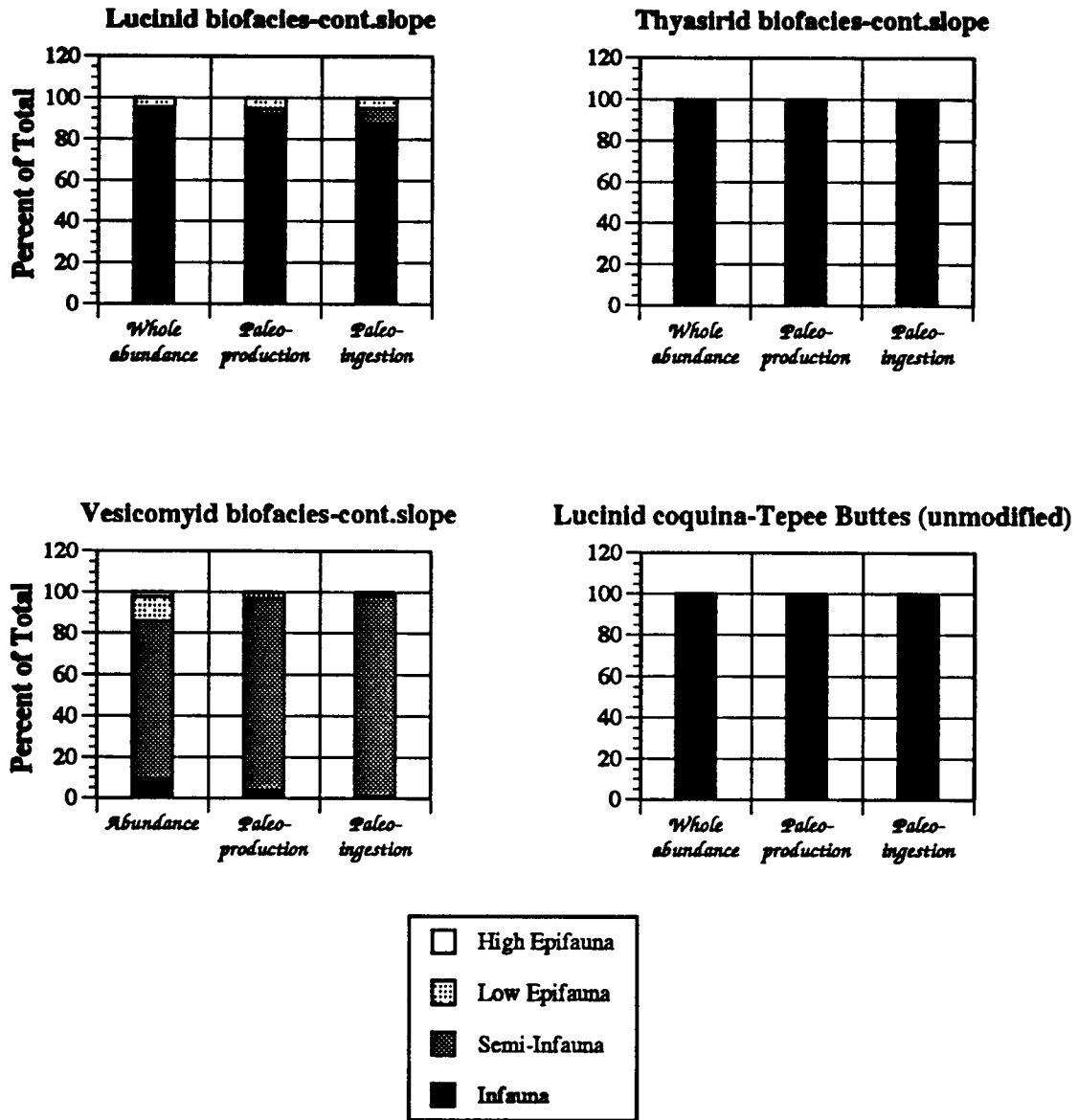
Figure 8.6   Predicted tier structure of seep clam biofacies summed over all sites, defined by total and whole abundance, paleoproduction, and paleoingestion after taphonomic loss of all individuals in the lowermost three size classes.

the size classes were redefined according to the biomass or energy flow parameter plotted. Rather, we retained the size classes defined by linear dimension to show the relative importance of each linear size class in the assemblage's total paleoproduction or paleoingestion. Accordingly, for biomass and paleoingestion, the frequency spectra indicate the contribution by that linear size class.

The size-frequency distributions for the vesicomyid, lucinid, and thyasirid assemblages were bimodal (Figures 8.7 to 8.9). The lucinid biofacies contained a mode in the smaller two size classes and a mode in the middle four size classes. Most of the paleoproduction was present in the central four size classes. Much of the paleoingestion was also, however, a significant component present in the uppermost size classes. The largest specimen in this assemblage was 92 mm. The largest specimen in the thyasirid assemblage was much smaller, 59 mm. This assemblage's size-frequency distribution was distinctly bimodal, with modes in size classes two to four and in the uppermost three. The two modes were produced by two chemosynthetic species of differing size, *Lucinoma* sp. and *Thyasira oleophila*. The larger individuals, all lucinids, were about the same size as those occupying the central mode in the lucinid assemblage. Both species were present primarily as adults. Consequently, the assemblage's paleoproduction and paleoingestion were distributed relatively evenly between the two modal size groupings. (Had the lower mode been dominantly by juveniles, it would have contributed little to the assemblage's paleoproduction and even less to the assemblage's paleoingestion.) The vesicomyid biofacies also contained two modes, one in the lower two size classes, and the other in the upper four. The upper three size classes contained most of the paleoproduction and paleoingestion. The largest specimen collected was 92 mm. The largest specimen from Tepee Buttes was 39 mm. The size-frequency distribution was monomodal; the mode occupied the central size classes. The single mode shifted to somewhat larger sizes for paleoproduction and took on a slightly bimodal

Numerical abundance by biofacies
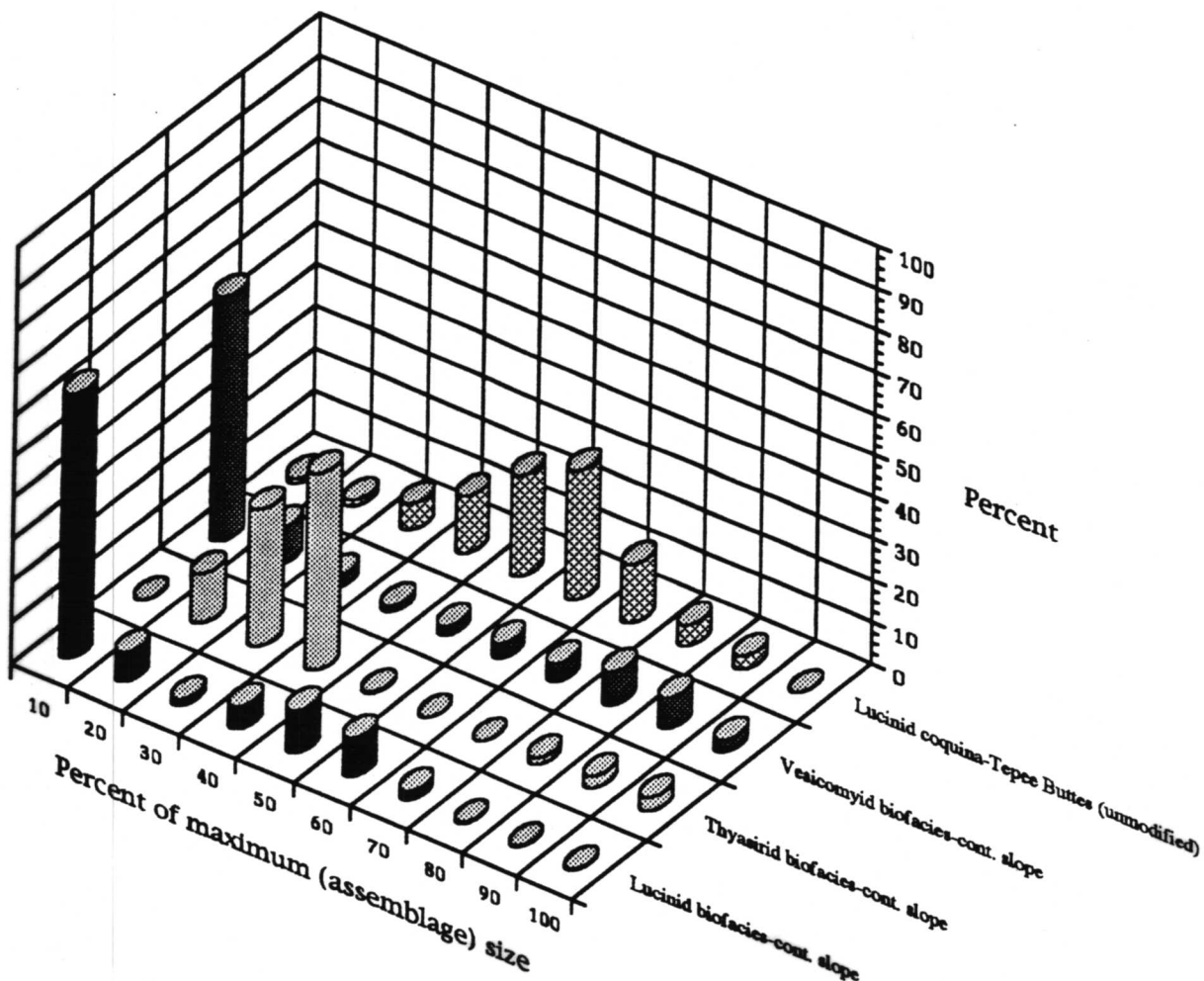
Figure 8.7   The size-frequency distribution for the clam biofacies summed over all sites. Size classes are defined as the tenth percentiles of the size of the largest individual in each assemblage. Listed values are the upper boundaries of the size classes. Numerical abundance represents the fraction of the total number of individuals is each size class. Each distribution is color coded for clarity.

Paleoproduction by biofacies
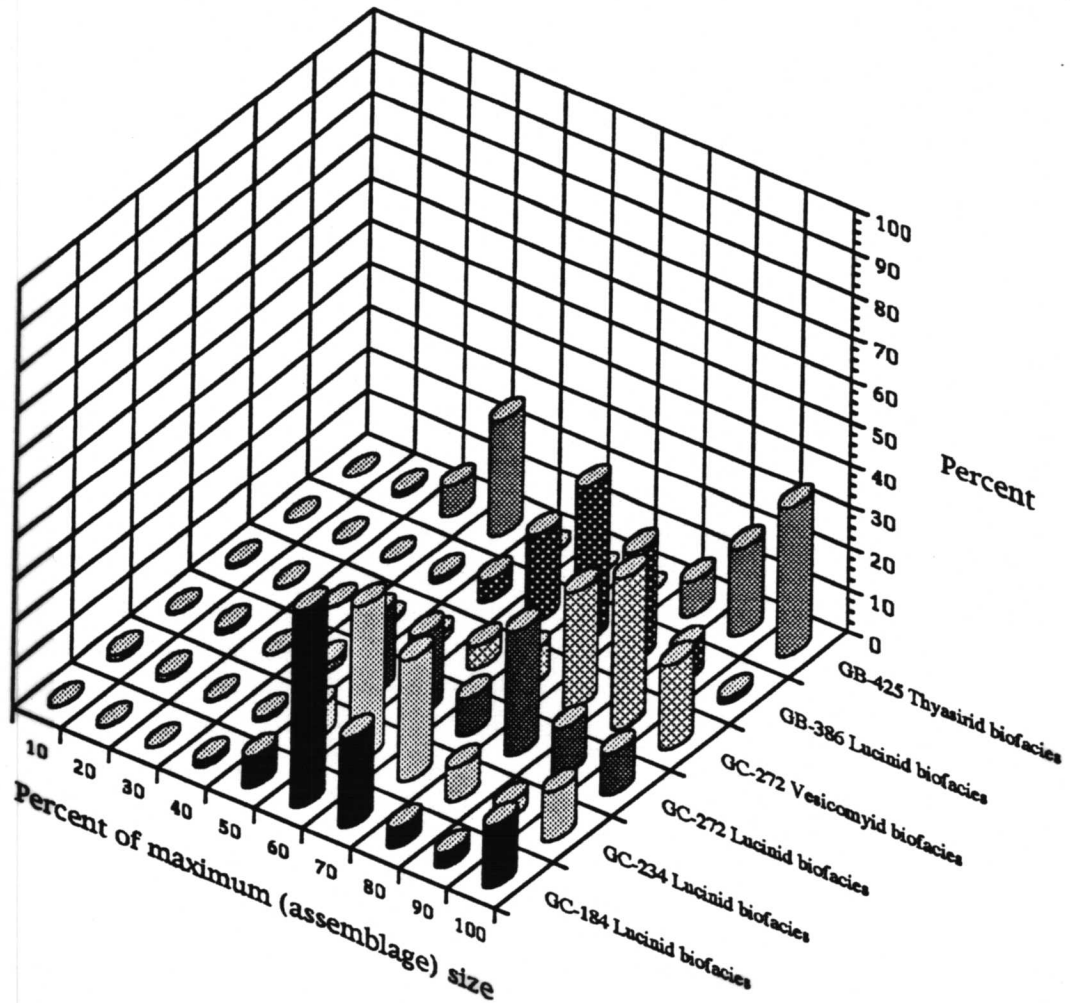
Figure 8.8 The apportionment of paleoproduction among the size classes for the clam biofacies summed over all sites. Size classes are defined as the tenth percentiles of the size of the largest individual in each assemblage. Listed values are the upper boundaries of the size classes. Paleoproduction represents the fraction of each assemblage total contributed by the individuals in each size class. Each distribution is color coded for clarity.

Paleoingestion by biofacies
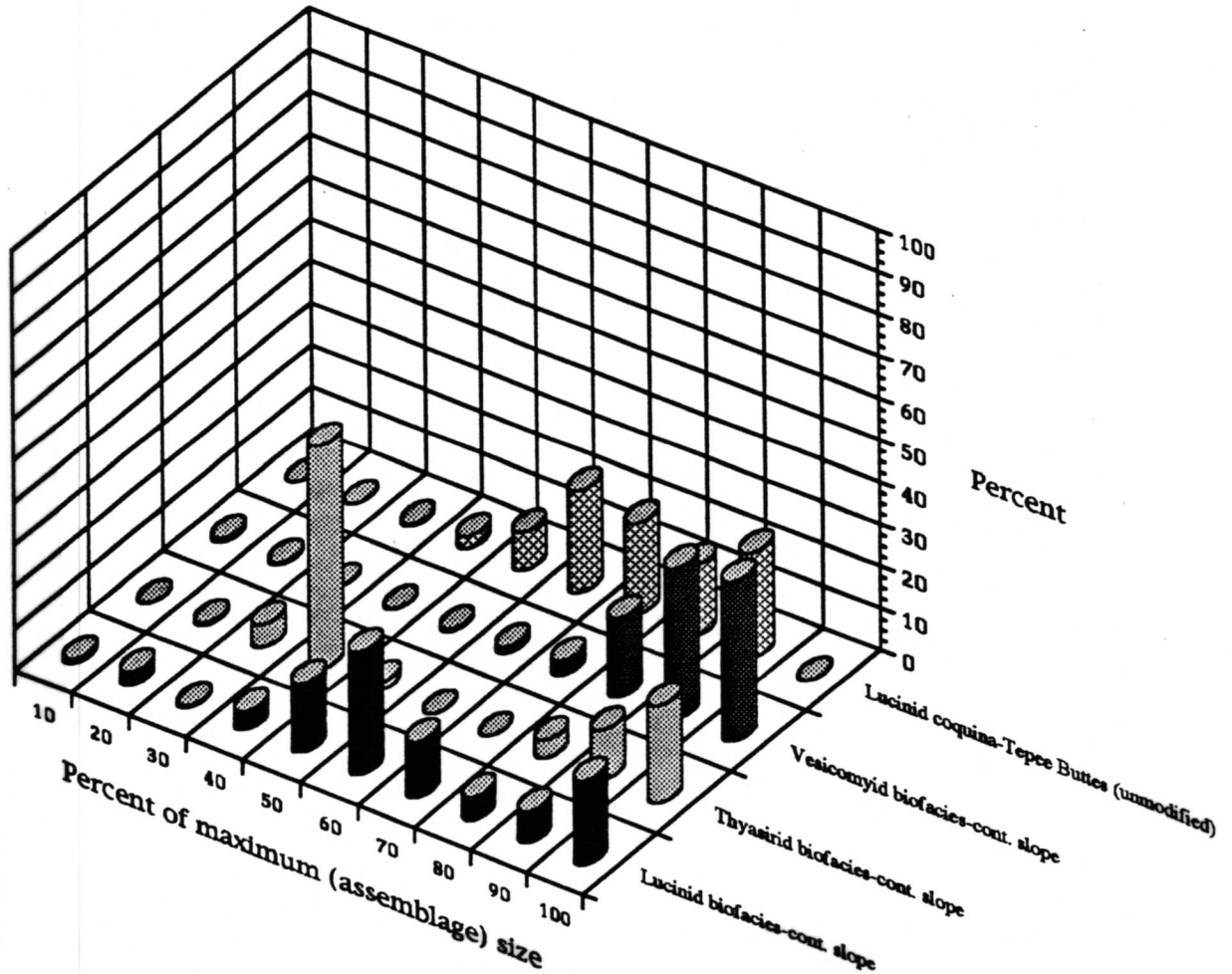
Figure 8.9   The apportionment of paleoingestion among the size classes for the clam biofacies summed over all sites. Size classes are defined as the tenth percentiles of the size of the largest individual in each assemblage. Listed values are the upper boundaries of the size classes. Paleoingestion represents the fraction of each assemblage total contributed by the individuals in each size class. Each distribution is color coded for clarity.

appearance for paleoingestion because some individuals of large species attained near-maximum size. Overall, the size-frequency distribution resembled the lucinid biofacies but lacked the smaller mode that was produced by the juvenile size classes.

After further taphonomic loss, only the large mode in the lucinid and vesicomyid biofacies' size-frequency distribution remained (Figures 8.10 to 8.12). In contrast, the thyasirid assemblage remained as distinctly bimodal after further taphonomic loss as it had been originally. Paleoproduction and paleoingestion remained distributed after further taphonomic loss as they had been in all original biofacies.

Thus, taphonomic loss modifies the guild, tier, and size-frequency structure of the lucinid and vesicomyid biofacies towards that observed in the fossil analogue from Tepee Buttes, and also toward the thyasirid biofacies at petroleum seeps. The latter is a recent analogue that evidently has not received significant living input in the near term. The thyasirid biofacies resembled the Tepee Buttes assemblage in most of the important attributes that are consistent with its taphonomic age. The taphonomic process uniformly resulted in simplification of tier and guild structure, a substantial decline in species richness, and a lesser, but important, change in size-frequency distribution (when evaluated by numerical abundance). Taphonomic loss affected the evaluation of community structure relatively little when paleoproduction and paleoingestion were used as the defining variables. These two variables, then, are robust indicators of community structure.

Time averaging, in assemblages deposited below storm wave base, occurs by one of four mechanisms: (1) sedimentation rate is so slow that individuals of widely different ages are deposited in effectively the same sampling interval; (2) bioturbation mixes the sedimentary column and reorients the contained shells; (3) physical processes of sediment degassing and seepage mix the sedimentary column and reorient the contained shells; and (4) infauna die at depth in sedimentary layers

Numerical abundance by biofacies
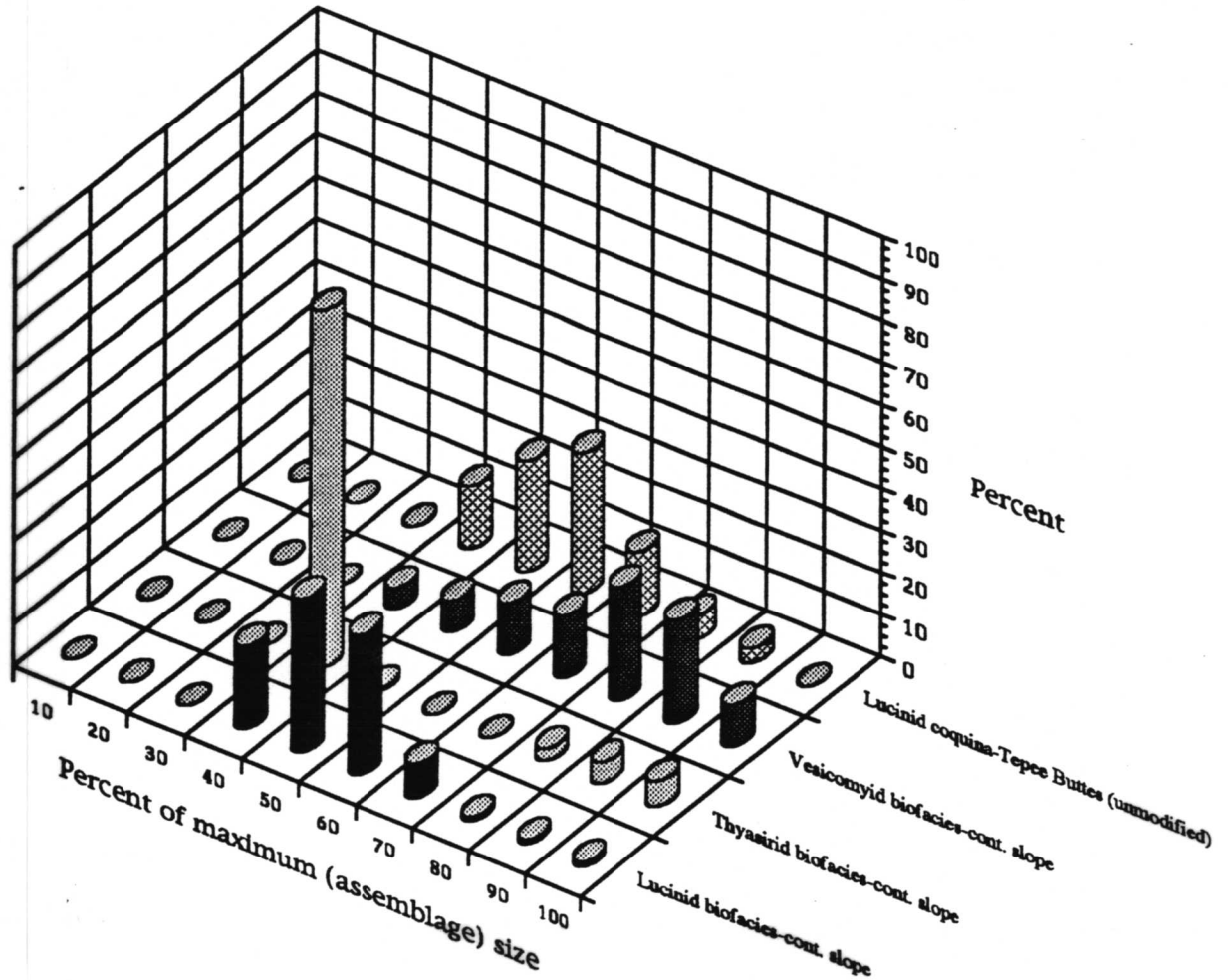
Figure 8.10   Predicted size-frequency distribution for the clam biofacies summed over all sites after taphonomic loss of all individuals in the lowermost three size classes. Size classes are defined as the tenth percentiles of the size of the largest individual in each assemblage. Listed values are the upper boundaries of the size classes. Numerical abundance represents the fraction of the total number of individuals is each size class. Each distribution is color coded for clarity.

Paleoproduction by biofacies
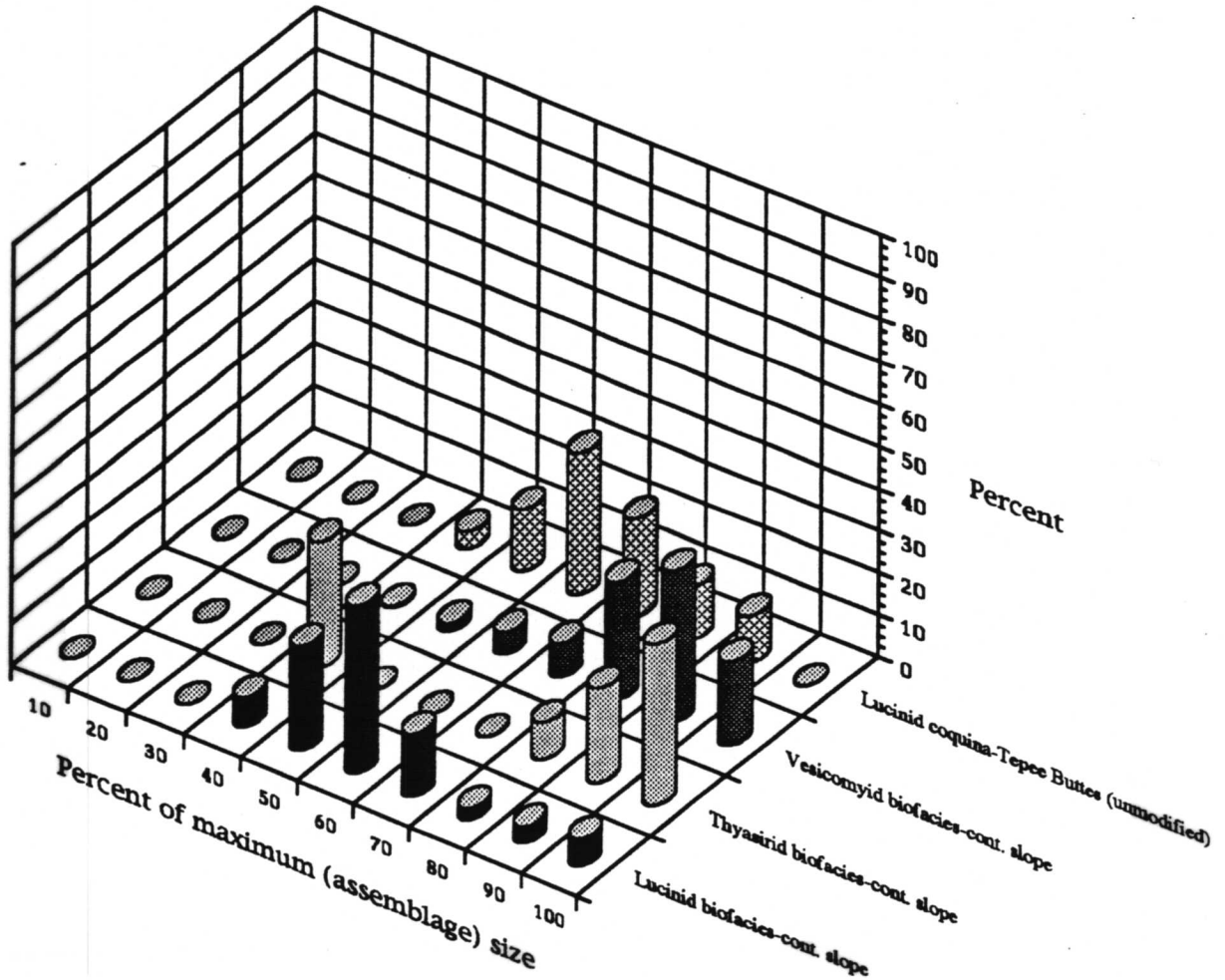
Figure 8.11   Predicted apportionment of paleoproduction among size classes for the clam biofacies summed over all sites after taphonomic loss of all individuals in the lowermost three size classes. Size classes are defined as the tenth percentiles of the size of the largest individual in each assemblage. Listed values are the upper boundaries of the size classes. Paleoproduction represents the fraction of each assemblage total contributed by the individuals in each size class. Each distribution is color coded for clarity.
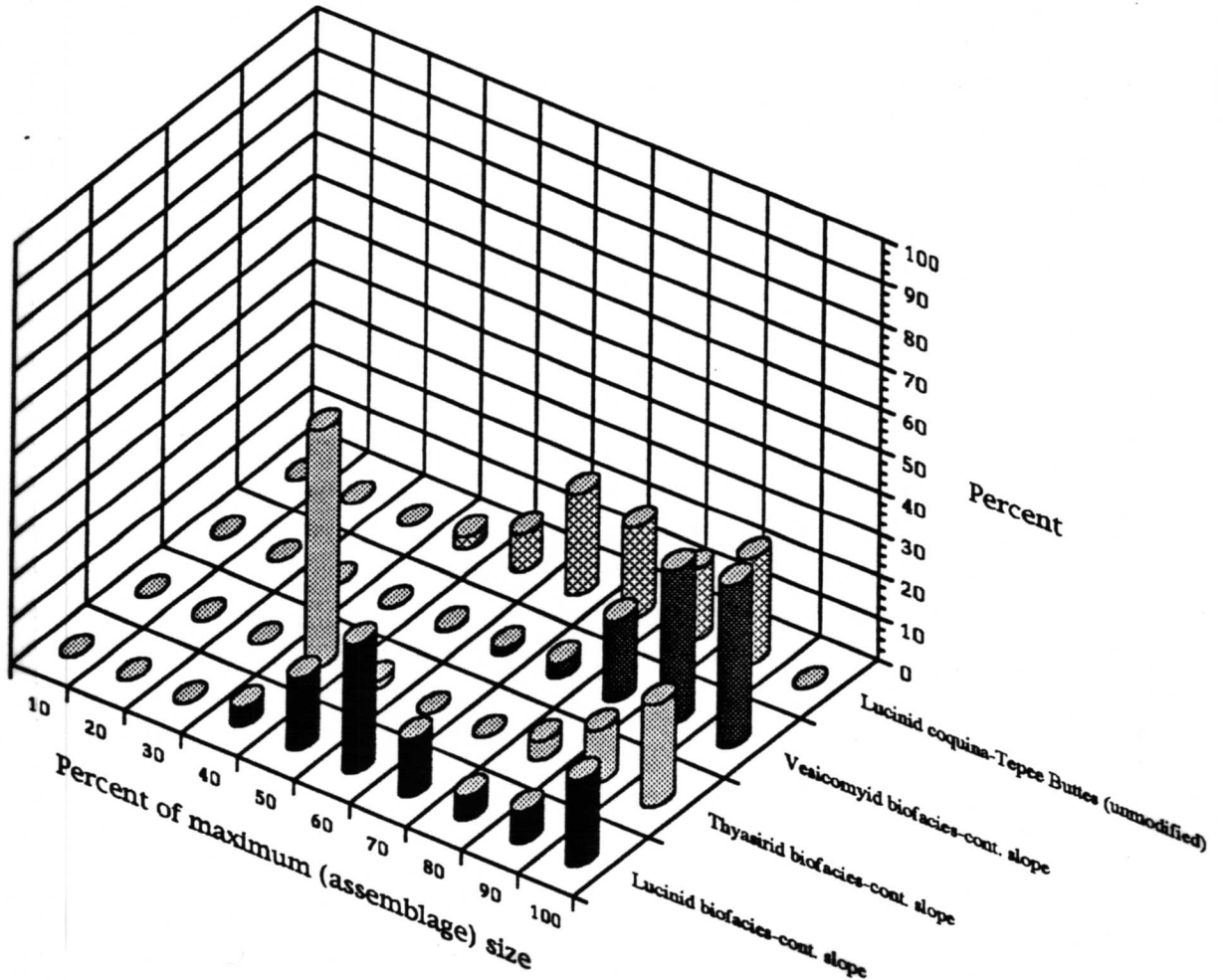
Figure 8.12   **Predicted apportionment of paleoingestion among size classes for the clam biofacies summed over all sites after taphonomic loss of all individuals in the lowermost three size classes. Size classes are defined as the tenth percentiles of the size of the largest individual in each assemblage. Listed values are the upper boundaries of the size classes. Paleoingestion represents the fraction of each assemblage total contributed by the individuals in each size class.   Each distribution is color coded for clarity.**

containing the remains of much older epifaunal species. Bioturbation is relatively unimportant at petroleum seeps. Physical processes capable of mixing shells have been observed. These include mud volcanoes and gas blowout craters. Their overall importance cannot yet be ascertained but clearly can have local significance. Measurements of time averaging, now available from single cores taken at four sites (GC 184, GC 272, GC 234, and GB 425) show no evidence of these processes. Infauna dying at depth is, however, a significant process, which, combined with a slow sedimentation rate, assures a certain degree of time averaging. Nevertheless, amino acid analyses show that individuals of single infaunal species gradually become older downcore, consistent with the expectation that time averaging occurs on a limited scale defined by the living depth of the adults of these species. Thus, a significant temporal record is present that would permit examination of temporal trends on the scale of about 300 years for lucinid beds and less that 300 years for the vesicomyid and mussel assemblages.

8.7   Site Descriptions

Site descriptions will be limited to clam beds, with one exception, because the keystone species of the other important chemosynthetic associations found in seep habitats, tubeworms and mussels, are rarely preserved in significant quantities.

8.7.1   Green Canyon 184 (Bush Hill)

Samples from Green Canyon 184 (Bush Hill) were dominated numerically by vesicomyids and lucinids (Figure 8.13). Although some *Lucinoma atlantis* and *Calyptogena ponderosa* were collected, *Lucinoma* sp. and *Vesicomya cordata* predominated. *Lucinoma* sp. accounted for the majority of the paleoproduction and paleoingestion. Samples were obtained by box coring, so penetration rarely exceeded 50 cm. The lucinid biofacies at GC 184 was typical of lucinid biofacies at all the sites

GC-184 Lucinid biofacies

Vesicomya cordata
Lucinoma n. sp.
Lucinoma atlantis
Bathymodiolus n. sp.
Calyptogena ponderosa
Alvania ceritanmus
Pleurotomella sp.
Thyasira oleophila
Vitrinella
Unknown Gastropod
Gymnobela judithae
Pleuromeris cf. armilla
Gymnobela sp.
Chama sp.

0 20 40 60 80 100 120 140 160 180 200
Cumulative Percent

GB-386 Lucinid biofacies

Lucinoma n. sp.
Lucinoma atlantis
Pleuromeris cf. armilla
Thyasira oleophila
Cantrainea sp.
Vesicomya cordata
Solemya sp.
Thyasira cf. exavata
Gymnobela judithae
Bathymodiolus n. sp.
Batrschia canatae
Unknown bivalve
Owenia sp. A

0 50 100 150 200 250 300
Cumulative Percent

■ Abundance ■ Paleoproduction ▦ Paleoingestion

Figure 8.13   The species composition of the lucinid biofacies at GC 184 and GB
386. Rank orders by numerical abundance, paleoproduction, and
paleoingestion of taxa contributing 1% or more to the death
assemblage.

in its size-frequency composition. Modes occurred in the lowermost two size classes and the middle four (Figure 8.14). The central mode and the largest two size classes accounted for the bulk of the paleoingestion and paleoproduction (Figures 8.15 and 8.16). These size frequencies were nearly identical to that observed at GC 234, very similar to GC 272, and somewhat different from GB 386 where the largest two size classes were not equivalently represented.

Categorizing the individuals by species' maximum size showed that the majority of the individuals were juveniles (Figure 8.17). Adults rarely exceeded 70% of the species' maximum size. Individuals greater than 70% of the species' maximum size were more abundant at GC 234, GC 272, GB 386 and GB 425 indicating that GC 184 was a less optimal site for lucinid growth than the other sampled sites. Those few large individuals did account for proportionately more paleoproduction and paleoingestion than at the other sites, however (Figures 8.18 and 8.19). One explanation for this oddity would be occasional periods near optimal for growth interspersed by periods of much longer duration that were marginal enough to limit survivorship to adulthood. The fraction of individuals of 10% maximum size was highest in the lucinid biofacies from GC 184 indicating that survivorship was probably lower here than at GC 272, GB 386, and GB 425, assuming that the taphonomic process was similar at all sites.

Guild structure at GC 184 was overwhelmingly chemosynthetic when evaluated numerically and almost exclusively chemosynthetic when evaluated by paleoproduction or paleoingestion. Comparison to lucinid biofacies at other sites shows that chemosynthetic dominance was this high only at GC 184 and GB 386 (Figure 8.20). Tier structure was complex, when evaluated numerically, because of the presence of vesicomyids and some true epifauna. Infauna dominated tier structure when evaluated by paleoproduction or paleoingestion. The infaunal

Numerical abundance by biofacies
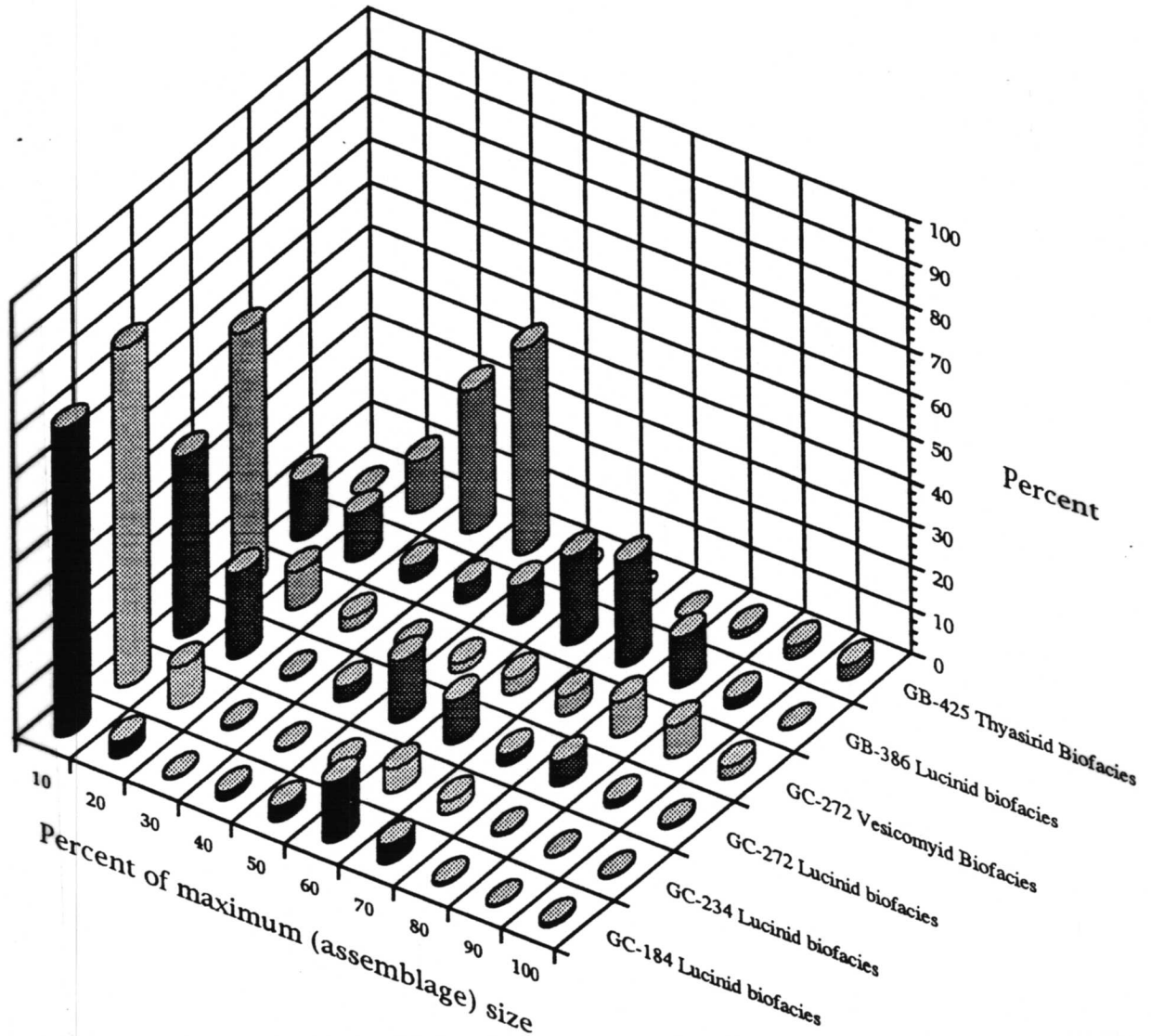
Figure 8.14   The size-frequency distribution for the clam biofacies at GC 184, GC 234, GC 272, GB 386 and GB 425. Size classes are defined as the tenth percentiles of the size of the largest individual in each assemblage. Listed values are the upper boundaries of the size classes. Numerical abundance represents the fraction of the total number of individuals is each size class. Each distribution is color coded for clarity.

Paleoproduction by biofacies
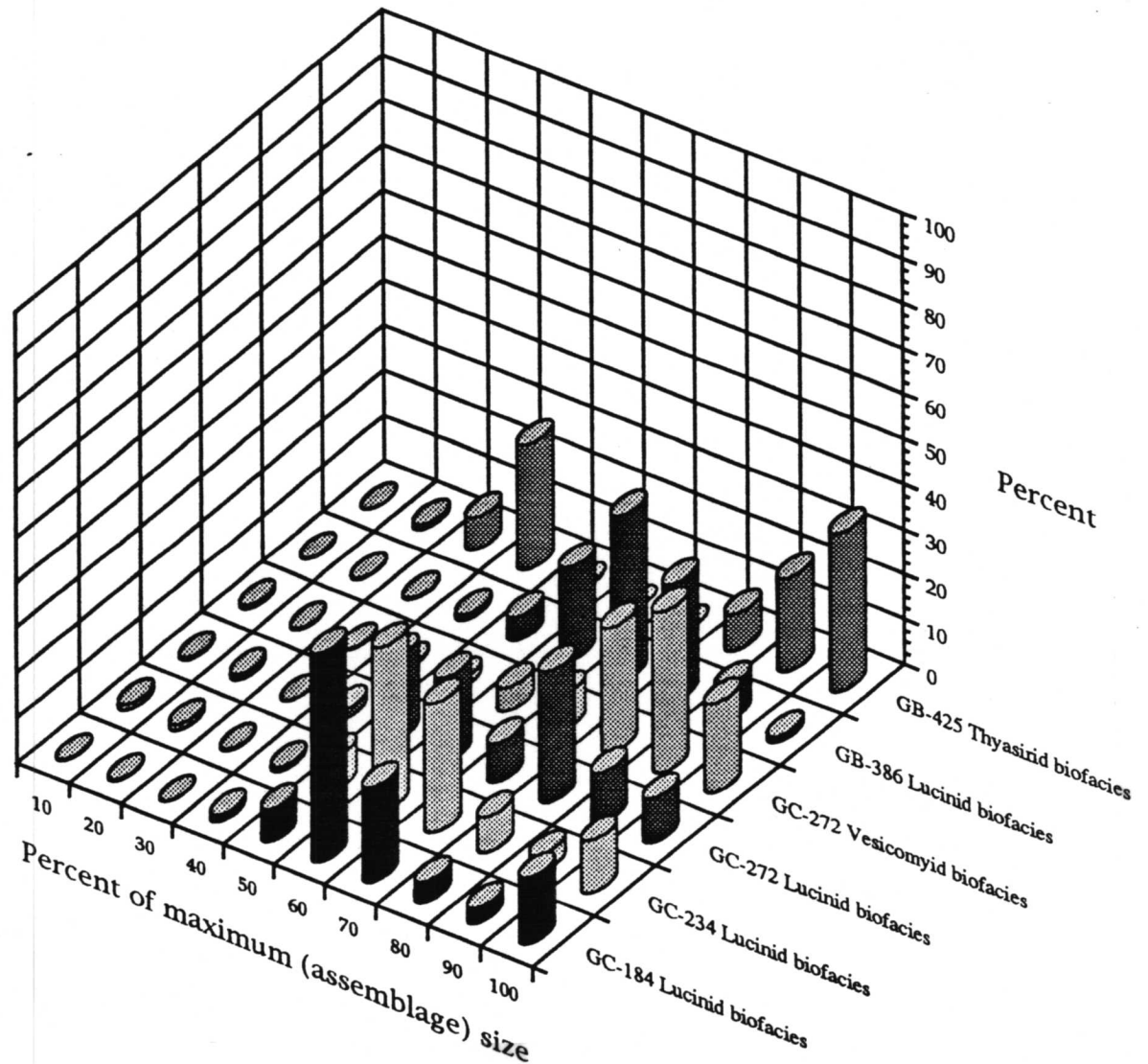
Figure 8.15   The apportionment of paleoproduction among the size classes for the clam biofacies at GC 184, GC 234, GC 272, GB 386 and GB 425. Size classes are defined as the tenth percentiles of the size of the largest individual in each assemblage. Listed values are the upper boundaries of the size classes. Paleoproduction represents the fraction of each assemblage total contributed by the individuals in each size class. Each distribution is color coded for clarity.

Paleoingestion by biofacies
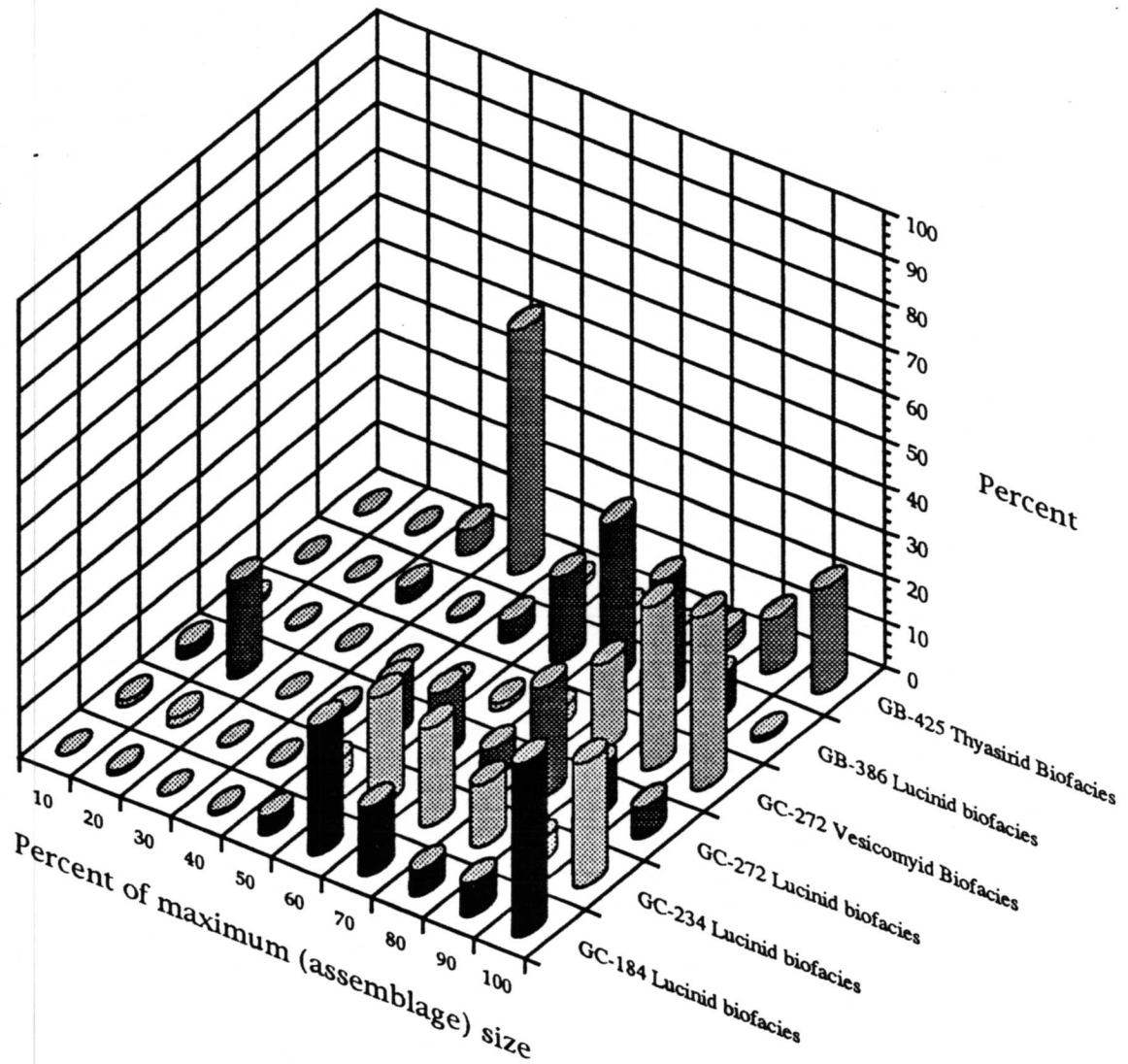
Figure 8.16   The apportionment of paleoingestion among the size classes for the
clam biofacies at GC 184, GC 234, GC 272, GB 386 and GB 425.
Size classes are defined as the tenth percentiles of the size of the
largest individual in each assemblage. Listed values are the upper
boundaries of the size classes. Paleoingestion represents the fraction
of each assemblage total contributed by the individuals in each size
class. Each distribution is color coded for clarity.

Numerical abundance by biofacies
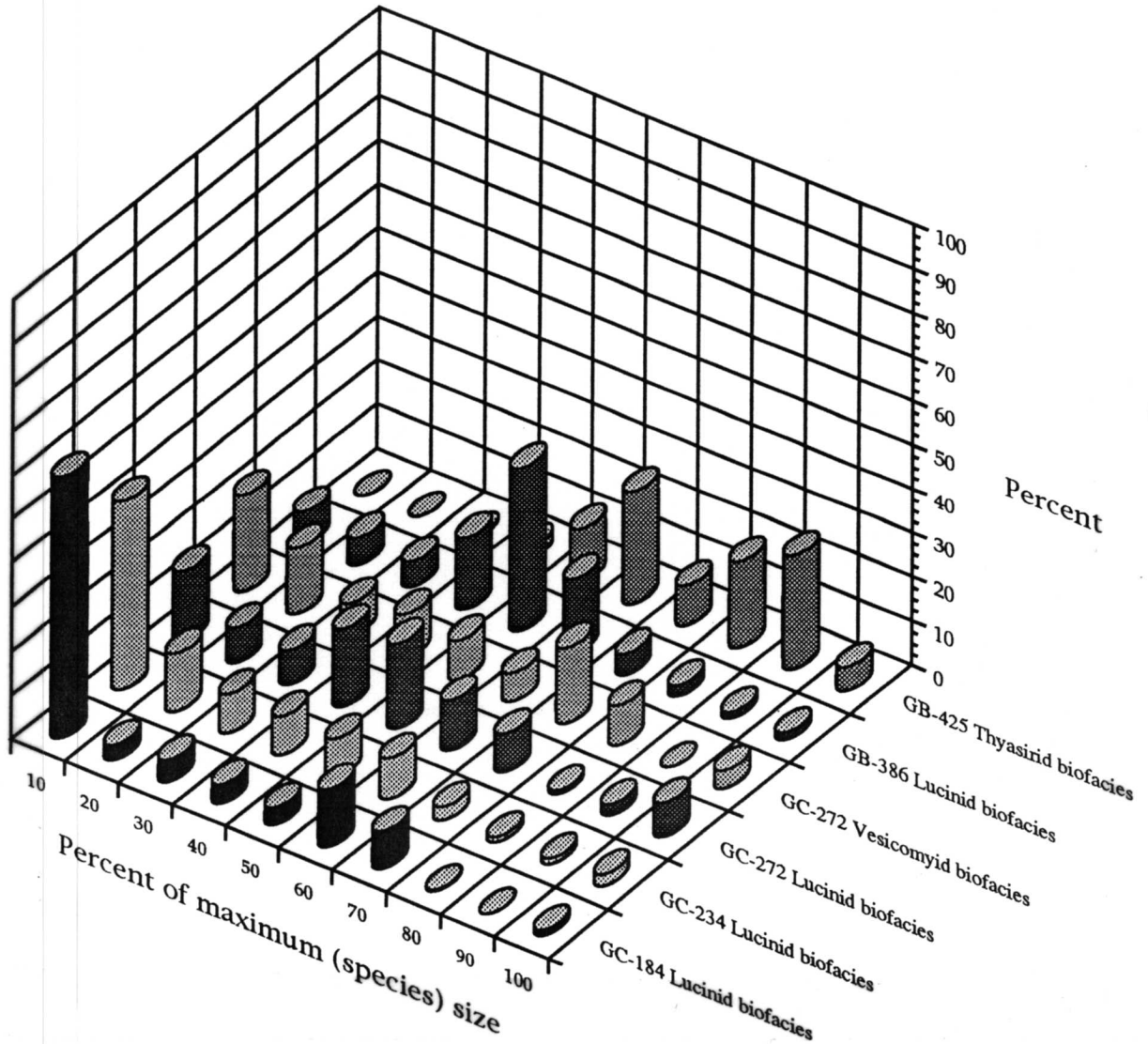
Figure 8.17   The size-frequency distribution for the clam biofacies at GC 184, GC 234, GC 272, GB 386 and GB 425. Size classes are defined as the tenth percentiles of the size of the largest individual for each species. Listed values are the upper boundaries of the size classes. Paleoingestion represents the fraction of each assemblage total contributed by the individuals in each size class. Each distribution is color coded for clarity.

Paleoproduction by biofacies
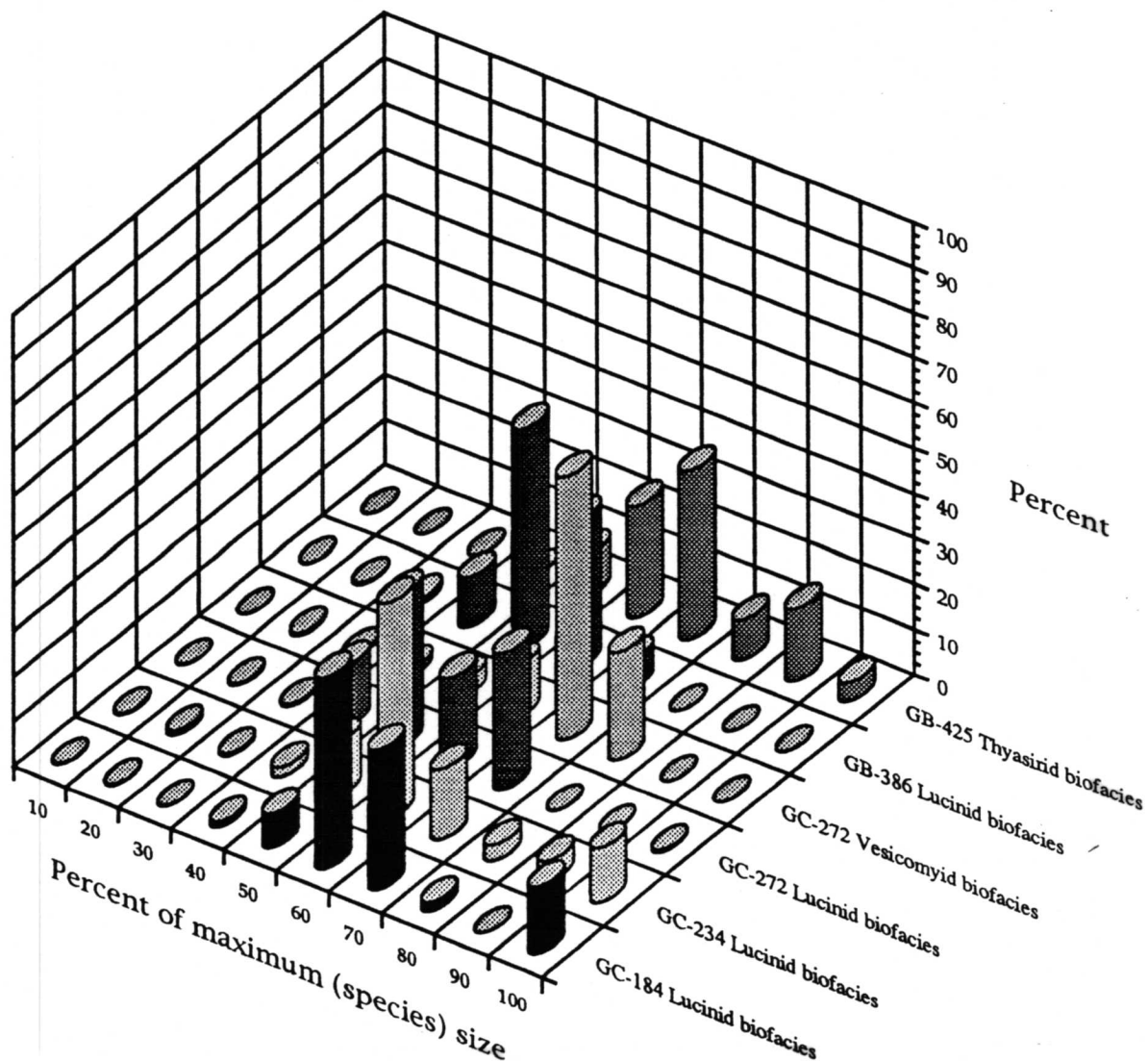
Figure 8.18   The apportionment of paleoproduction among the size classes for the clam biofacies at GC 184, GC 234, GC 272, GB 386, and GB 425. Size classes are defined as the tenth percentiles of the size of the largest individual for each species. Listed values are the upper boundaries of the size classes. Paleoproduction represents the fraction of each assemblage total contributed by the individuals in each size class. Each distribution is color coded for clarity.
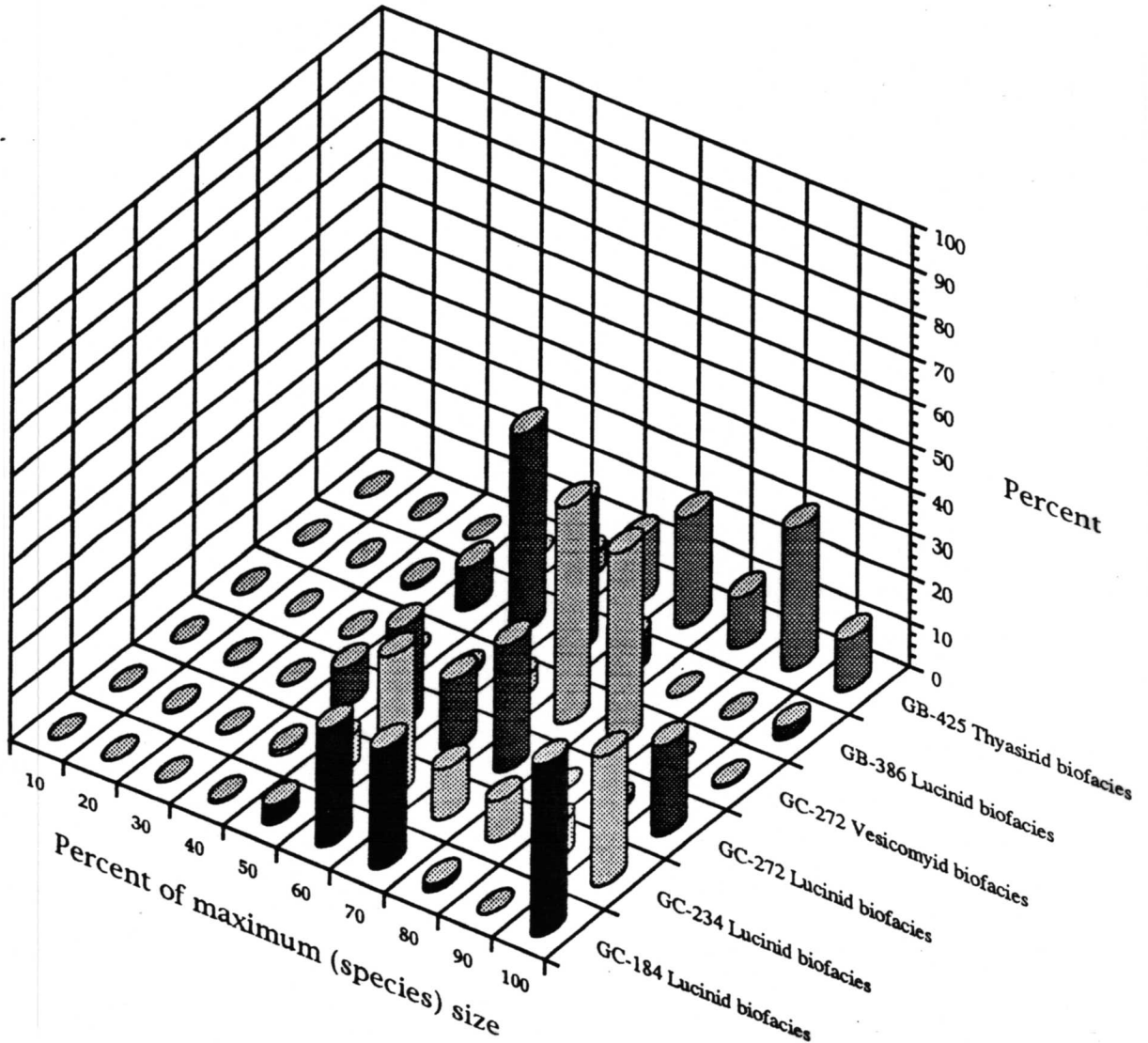
Figure 8.19 The apportionment of paleoingestion among the size classes for the clam biofacies at GC 184, GC 234, GC 272, GB 386, and GB 425. Size classes are defined as the tenth percentiles of the size of the largest individual for each species. Listed values are the upper boundaries of the size classes. Paleoproduction represents the fraction of each assemblage total contributed by the individuals in each size class. Each distribution is color coded for clarity.
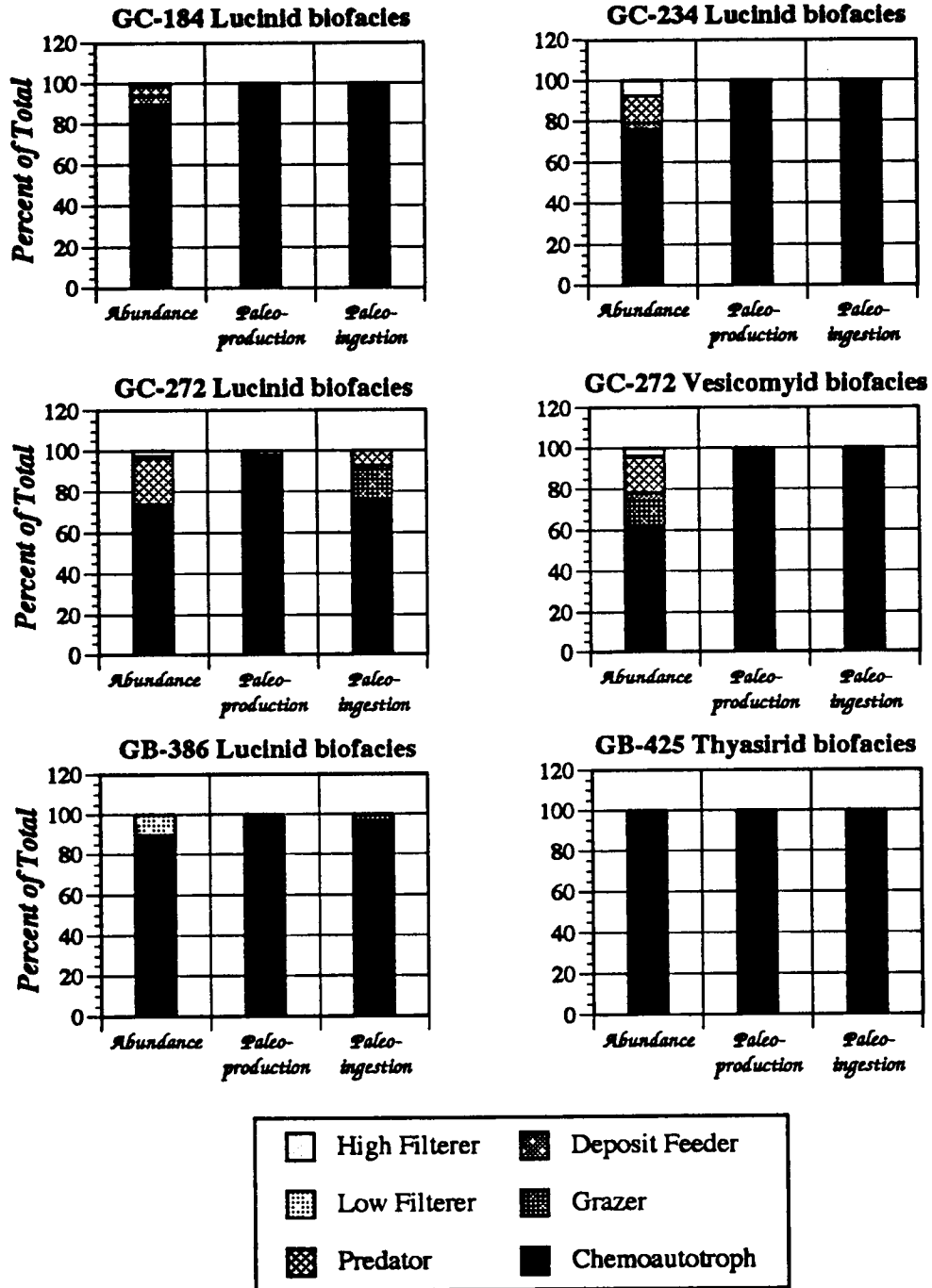
Figure 8.20   The cumulative feeding guild structure for the seep clam biofacies at
GC 184, GC 234, GC 272, GB 386, and GB 425, defined by numerical
abundance, paleoproduction, and paleoingestion.

contribution to tier structure, when evaluated by energy flow, was typical of most lucinid biofacies (Figure 8.21).

A number of cores were obtained with lucinids spanning the coring interval of 50 to 70 cm. We know from piston coring elsewhere that the accumulated remains extend much deeper than this at most, if not all, sites. Living lucinids rarely are found deeper than 5 cm. An estimation from sedimentation rate would give the lowermost lucinids an age of 667 to 4000 yr. given Behren's (1988) range in sedimentation rate. ^{14}C dates identified the oldest shell as 3,500 yr. old (Table 8.1). ^{13}C/^{12}C ratios for shell carbonate indicated that nearly all shell carbonate came from seawater bicarbonate and ^{14}C dates of living shells were effectively present day so that shell ages were not compromised by the inclusion of ^{14}C-dead carbon, obtained as interstitial or metabolic bicarbonate, into the shell. Amino acid dating showed that lucinid beds in this area have been gradually accumulating for many years. No evidence of catastrophic processes was present.

Figures 8.22 through 8.28 show an example of one core through a lucinid bed at GC 184. Juveniles accounted for the majority of the individuals in this core throughout its length (Figure 8.23). Large individuals were most frequent above 20 cm and below 35 cm. Large individuals were rare in-between. The largest shells were found primarily above 20 cm. Plots of paleoproduction and paleoingestion (Figures 8.24 and 8.25) show that community energy flow was dominated by small individuals from 20 to 35 cm (and at 5 cm). Categorizing size relative to species' maximum size (Figures 8.26 through 8.28) shows that adults were uncommon between 25 and 35 cm and that large adults were only common in the upper 10 cm of the core. Juveniles dominated the assemblage throughout the core. Thus, most small individuals were juveniles, not adults of small species. Plots of paleoproduction and paleoingestion show that the largest individuals accounted for the most energy flow (compare Figure

Table 8.1 ^{14}C dates of mussel, lucinid, and thyasirid beds.

Seep Site	Sample	Estimated Age (years)
GC-234	Mussel Bed 1 (95 cm)	2000 - 3000
GC-234	Mussel Bed 2 (195 cm)	3000 - 4000
GC-184	Lucinid Bed (68 cm)	> 3500
GB-425	Thyasirid Bed (40 cm)	500 - 1000
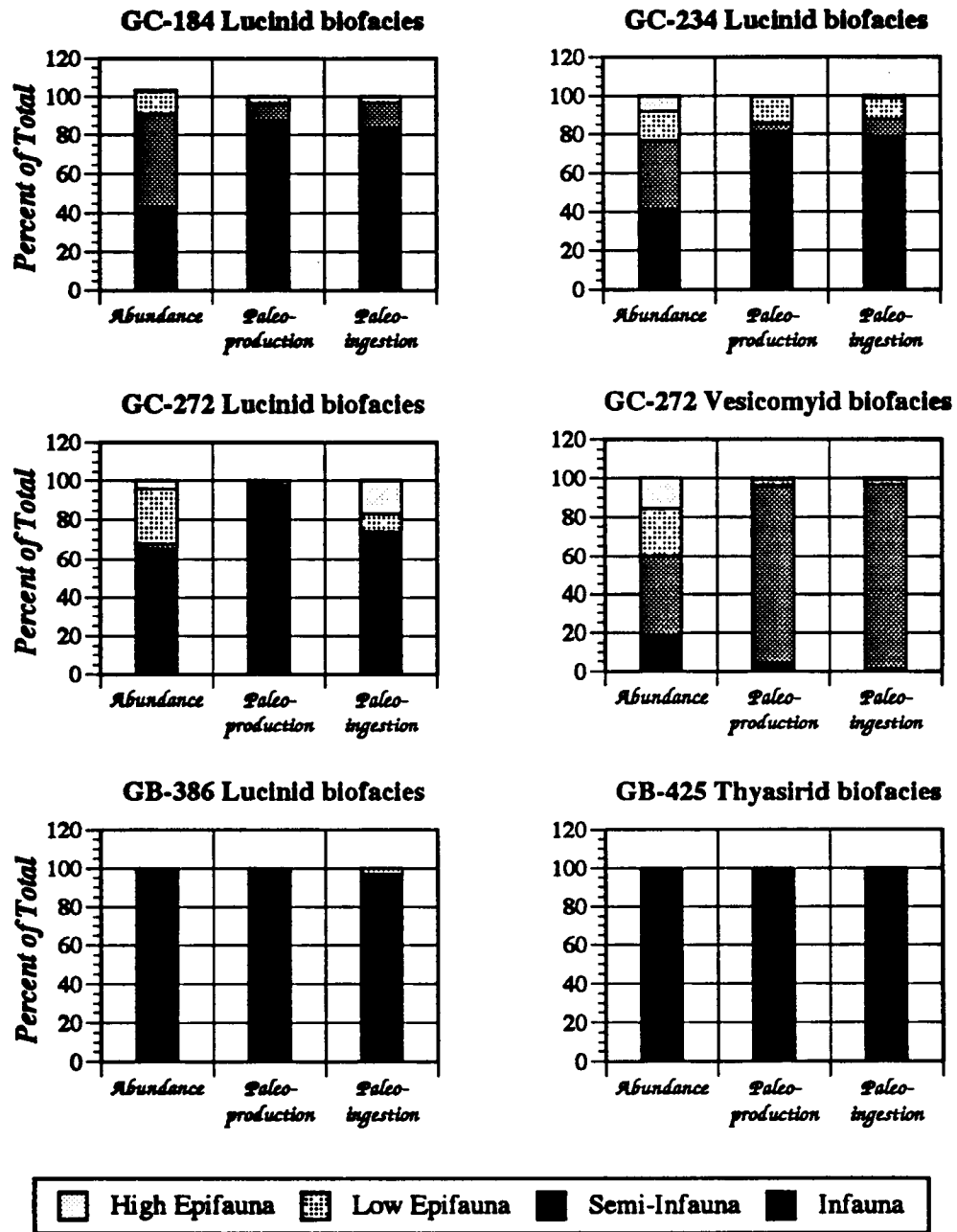
Figure 8.21 The cumulative habitat tier structure for the seep clam biofacies at GC 184, GC 234, GC 272, GB 386, and GB 425, defined by numerical abundance, paleoproduction, and paleoingestion.

GC-184 Lucinid biofacies-core 1

0 cm

Vesicomya cordata
Lucinoma n. sp.
Pleurotomella
Vitrinella

0   50   100   150   200   250
Cumulative Percent

10 cm

Vesicomya cordata
Pleurotomella
Vitrinella
Lucinoma n. sp.
Gymnobela judithae

0 20 40 60 80 100 120 140 160 180 200

25 cm

Vesicomya cordata
Gymnobela judithae

0   50   100   150   200   250

35 cm

Vesicomya cordata
Calyptogena ponderosa
Chama sp.

0   20   40   60   80   100   120   140   160

50 cm

Lucinoma n. sp.
Lucinoma atlantis
Vesicomya cordata
Alvania ceritanmus
Pleuromeris cf armilla

0   50   100   150   200   250

■ Abundance   ■ Paleoproduction   ▦ Paleoingestion

Figure 8.22   The species composition of the lucinid biofacies at GC 184 from Core 1. Rank orders by numerical abundance, paleoproduction, and paleoingestion of taxa contributing 1% of more to the death assemblage.

Numerical abundance by core interval
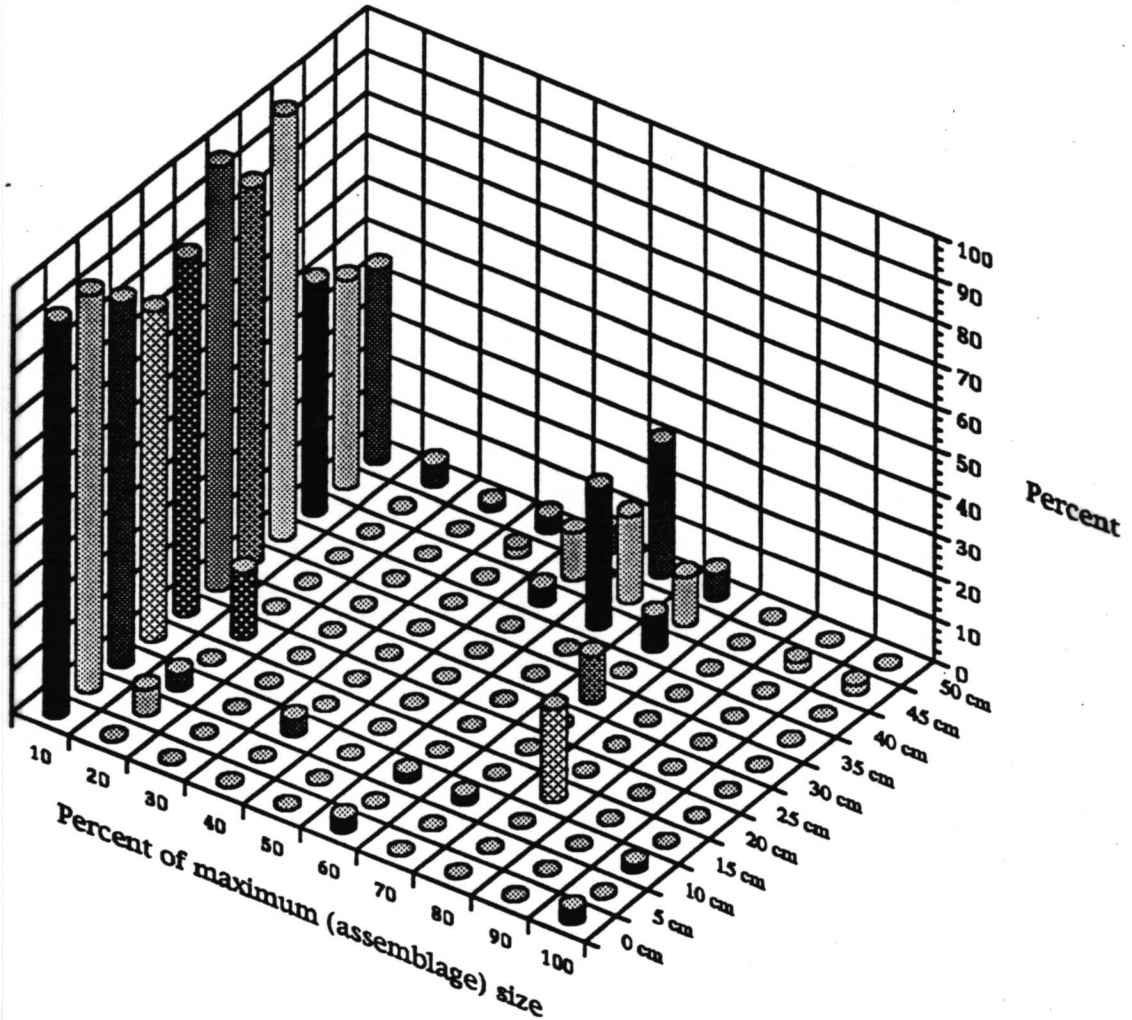
Green Canyon 184

Figure 8.23   The size-frequency distribution of 5 cm core intervals at GC 184
Core 1. Size classes are defined as the tenth percentiles of the size of
the largest individual in each assemblage. Listed values are the
upper boundaries of the size classes. Numerical abundance
represents the fraction of the total number of individuals is each size
class. Each distribution is color coded for clarity.

Paleoproduction by core interval
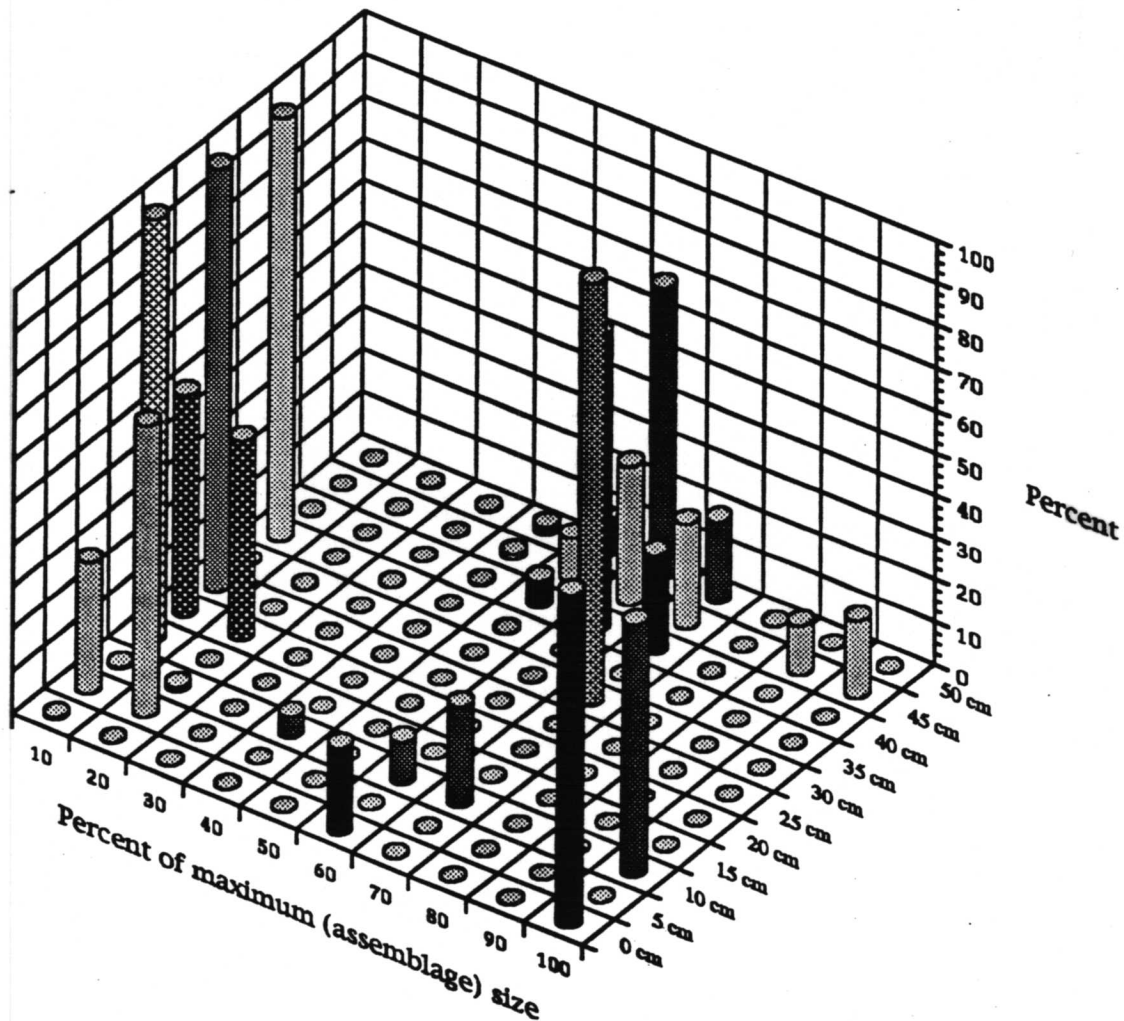
Green Canyon 184

Figure 8.24   The apportionment of paleoproduction among the size classes for 5 cm core intervals at GC 184 Core 1. Size classes are defined as the tenth percentiles of the size of the largest individual in each assemblage. Listed values are the upper boundaries of the size classes. Paleoproduction represents the fraction of each assemblage total contributed by the individuals in each size class. Each distribution is color coded for clarity.

Paleoingestion by core interval
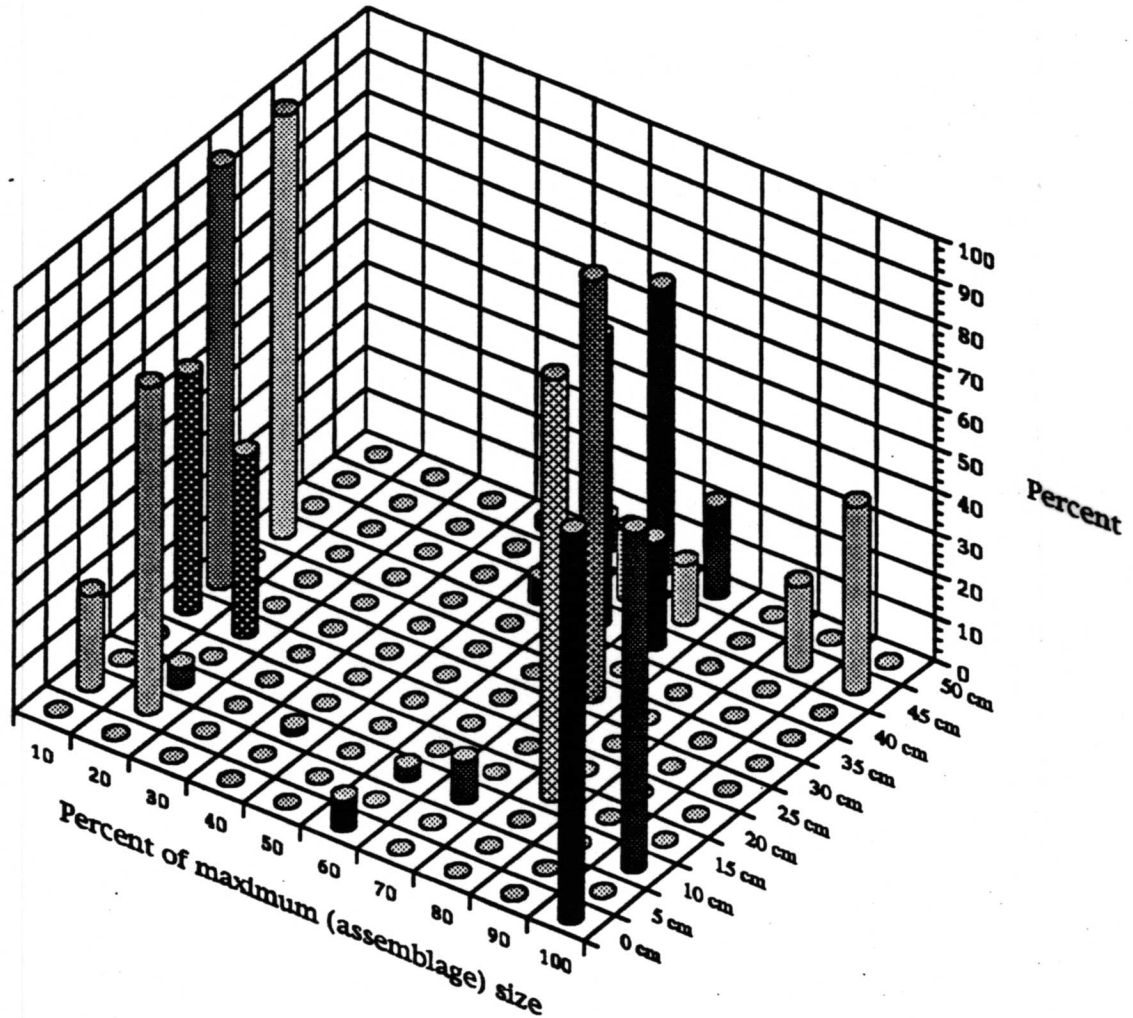
Green Canyon 184

Figure 8.25   The apportionment of paleoingestion among the size classes for 5 cm core intervals at GC 184 Core 1. Size classes are defined as the tenth percentiles of the size of the largest individual in each assemblage. Listed values are the upper boundaries of the size classes. Paleoproduction represents the fraction of each assemblage total contributed by the individuals in each size class. Each distribution is color coded for clarity.

Numerical abundance by core interval
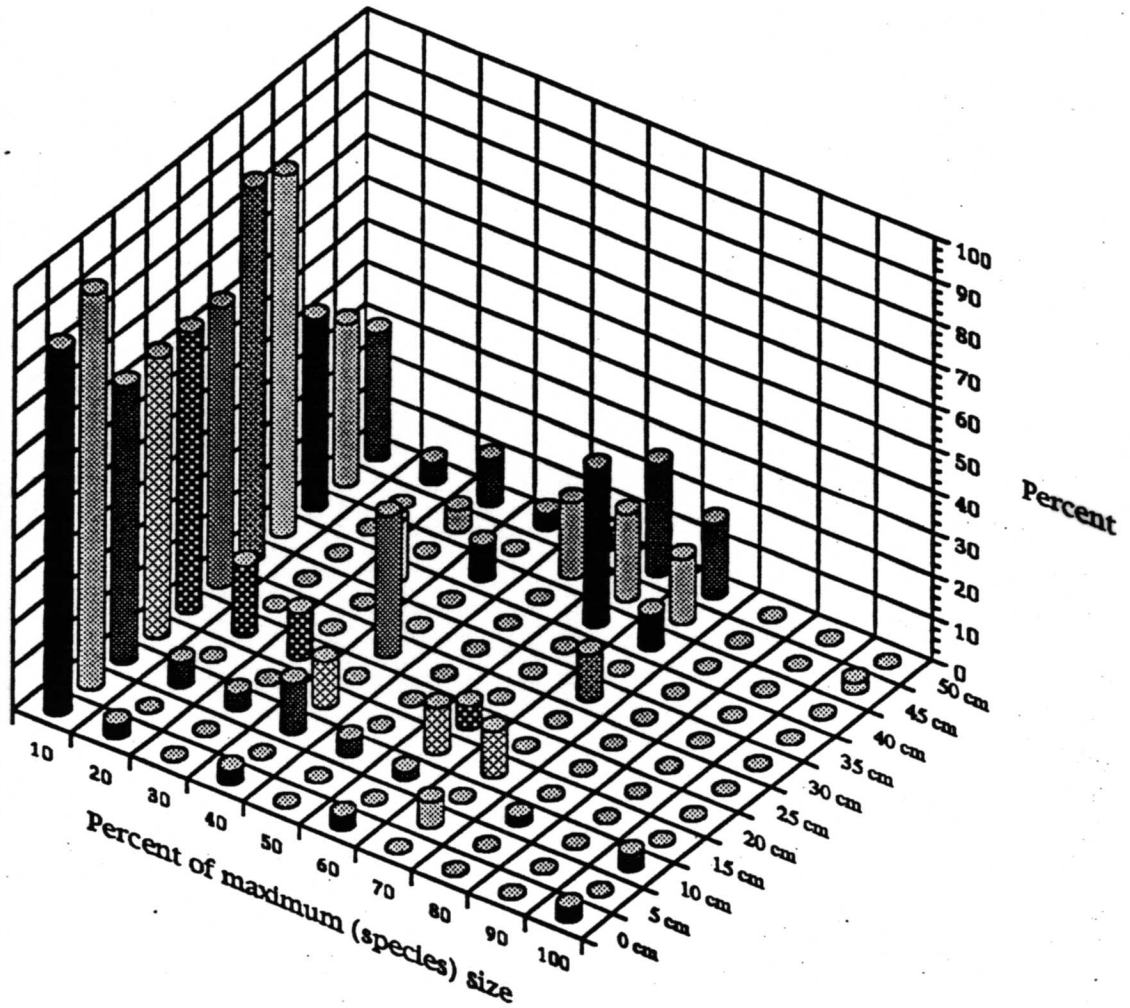
Green Canyon 184

Figure 8.26 The size frequency distribution for 5 cm core intervals at GC 184 Core 1. Size classes are defined as the tenth percentiles of the size of the largest individual for each species. Listed values are the upper boundaries of the size classes. Numerical abundance represents the fraction of the total number of individuals in each size class. Each distribution is color coded for clarity.

Paleoproduction by core interval
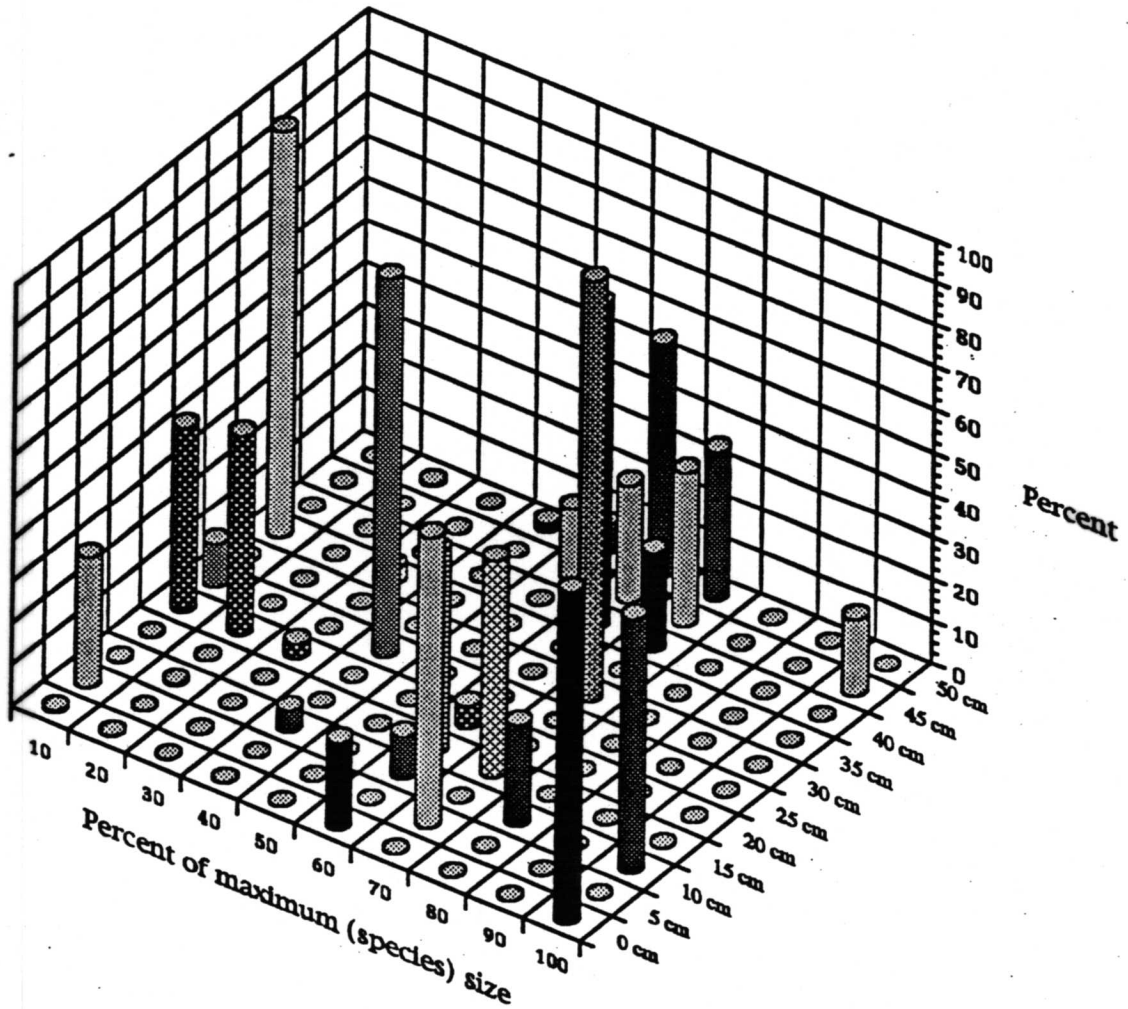
Green Canyon 184

Figure 8.27   The apportionment of paleoproduction among the size classes for 5 cm core intervals at GC 184 Core 1. Size classes are defined as the tenth percentiles of the size of the largest individual for each species. Listed values are the upper boundaries of the size classes. Paleoproduction represents the fraction of each assemblage total contributed by the individuals in each size class. Each distribution is color coded for clarity.

Paleoingestion by core interval
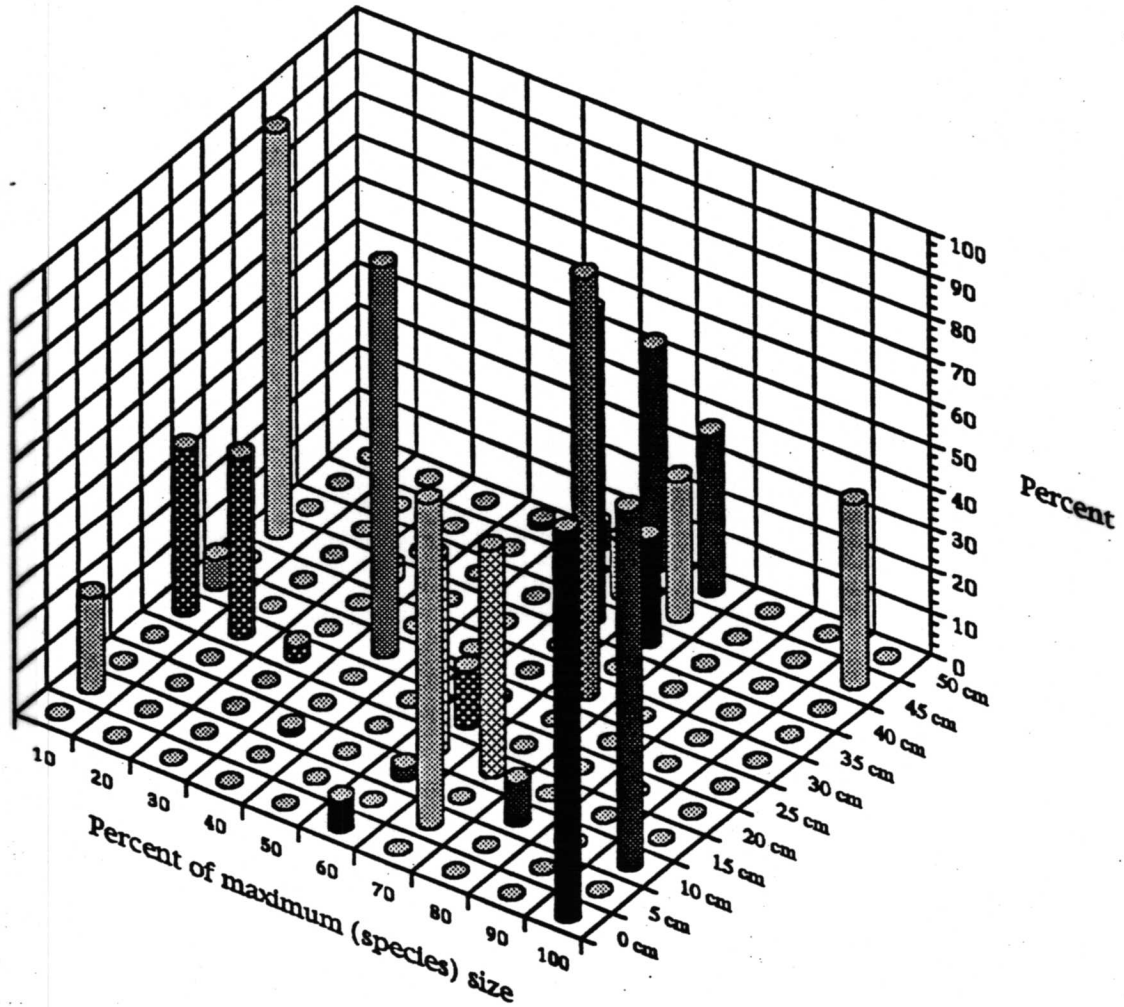
Green Canyon 184

Figure 8.28   The apportionment of paleoingestion among the size classes for 5 cm
core intervals at GC 184 Core 1. Size classes are defined as the tenth
percentiles of the size of the largest individual for each species. Listed
values are the upper boundaries of the size classes. Paleoproduction
represents the fraction of each assemblage total contributed by the
individuals in each size class. Each distribution is color coded for
clarity.

8.28 with Figure 8.25 for example). Long-lived small species were not important anywhere in the core.

Changes in species composition occurred coincident with changing optimality for the lucinaceans. Below 35 cm, habitat optimality was about average for Lucinidae. *Lucinoma* sp. was abundant and frequently reached 70% of the species' maximum size. The habitat became suboptimal for Lucinidae at about 30 cm and remained so to 20 cm. In this interval, vesicomyids dominated the community by number, paleoproduction and paleoingestion. However, few adults were found, so that the habitat was distinctly suboptimal for the vesicomyids. Interestingly, few juvenile lucinids were found, indicating that the reduction in habitat optimality for the lucinaceans included an essentially complete failure of settlement. *Lucinoma* sp. returned at 15 cm and again dominated the paleoproduction and paleoingestion of the assemblage, despite continuing settlement of vesicomyids, because this species routinely grew to 70% or larger of maximum size. Thus, the history of this site was defined by the disappearance and reappearance of lucinids and the persistent settlement of vesicomyids few of which, however, grew to adulthood. The lucinid assemblage was not persistent, but was resilient in this context. Although specific dates are unavailable, the 15 cm hiatus probably accounts for 500 to 1000 yr.

The changing structure of the biota at this site can also be visualized through guild and tier structure. Chemoautotrophs dominated in the upper and lower portions of the core and were overwhelmingly dominant in terms of paleoproduction and paleoingestion. In the central portion of the core, however, predators were dominant (Figure 8.29). This is one of the characteristics of the non-seep or normal slope fauna and indicates a transition from a chemosynthetic community where most of the primary consumers are shelled organisms to a community where most of the primary consumers are soft-bodied organisms. Changes in tier structure were complex. Infauna dominated deep in the core and, by paleoproduction and paleoingestion, at the

GC-184 Core 1 Lucinid biofacies
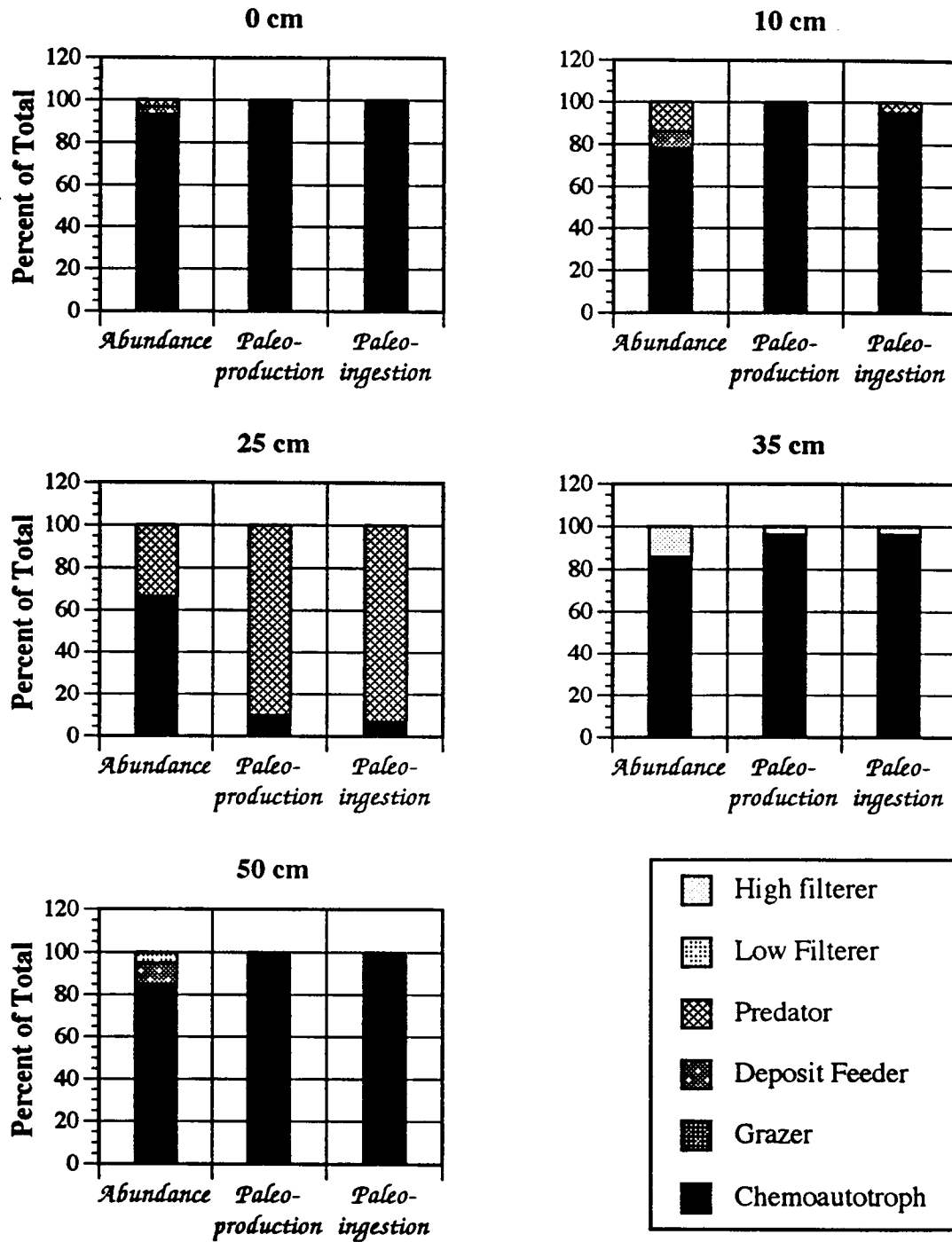
Figure 8.29   The cumulative feeding guild structure of several core intervals from the lucinid biofacies at GC 184 Core 1, defined by numerical abundance, paleoproduction, and paleoingestion.

top of the core. In-between, epifauna and semi-infauna were important. This, too, is a characteristic of the non-seep or normal slope fauna. The absence of a significant infaunal component in the shelled biota in the central region of this core is particularly significant because most chemosynthetic species that are preservable are also infaunal (Figure 8.30).

Figure 8.31 shows the downcore distribution of total faunal abundance, paleoproduction, and paleoingestion. The presence of a chemosynthetic biota coincides with high faunal abundances, paleoproduction, and paleoingestion. The presence of the non-seep biota coincides with low faunal abundance and extremely low paleoproduction and paleoingestion, in keeping with the dependency by the non-seep biota on planktonic production as the sole food supply. Faunal abundance, paleoproduction and paleoingestion were higher in the deeper chemosynthetic section of the core, even though the largest animals were found in the upper section, assuming roughly equivalent sedimentation rates. A second core at GC 184 sampled the background (non-seep) fauna for the region. Although the species composition varied downcore, no pattern could be discerned in the size-frequency distributions evaluated by any measure: numerical abundance, paleoproduction or paleoingestion. Most individuals were small, as is typical for the non-seep benthos. With a few spotty exceptions, these small individuals accounted for a large fraction of the paleoproduction and paleoingestion in each core interval because many of these were adults of small species. Categorizing the size classes by species' maximum size shows that adults were routinely collected in most core layers and some individuals normally attained 80% or more of species' maximum size. Juveniles of chemosynthetic species dominated the numerical abundance throughout the core indicating their persistent settlement but failure to survive. Thus, the absence of chemosynthetic adults was not due to settlement failure, but was due to poor survivorship. The standard slope fauna dominated energy flow at the site.
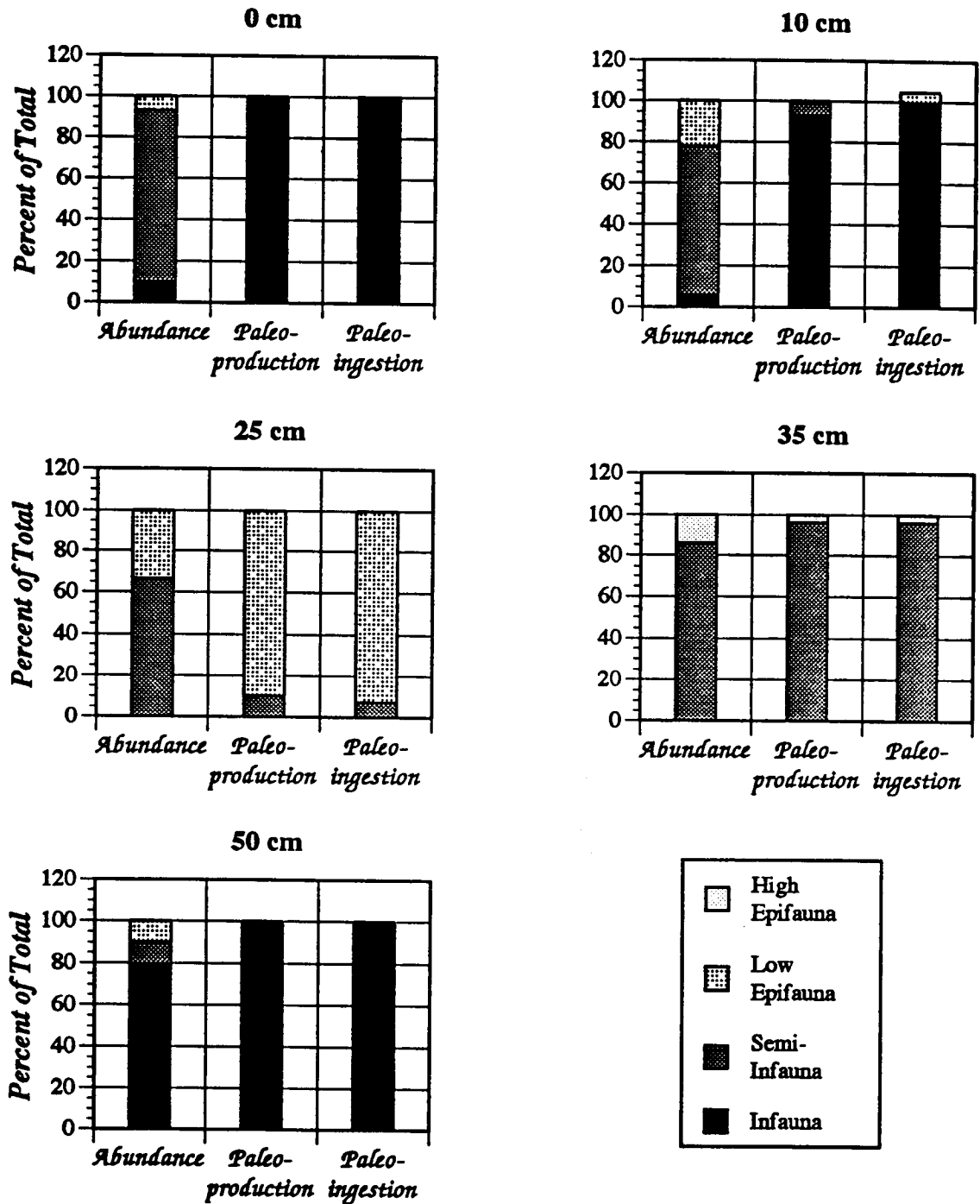
Figure 8.30   The cumulative habitat tier structure of several core intervals from the lucinid biofacies at GC 184 Core 1, defined by numerical abundance, paleoproduction, and paleoingestion.
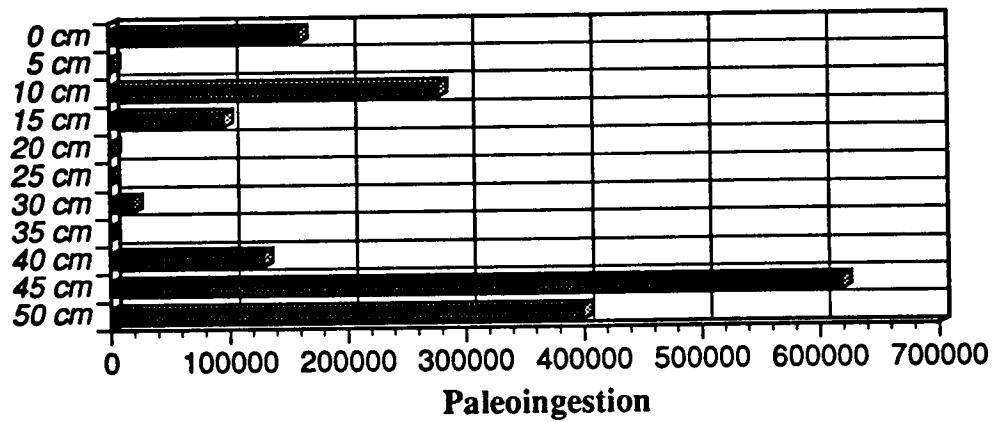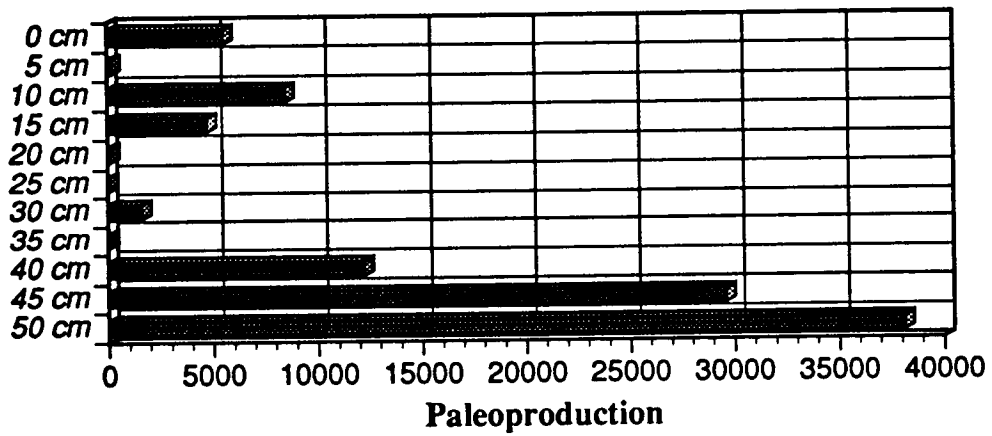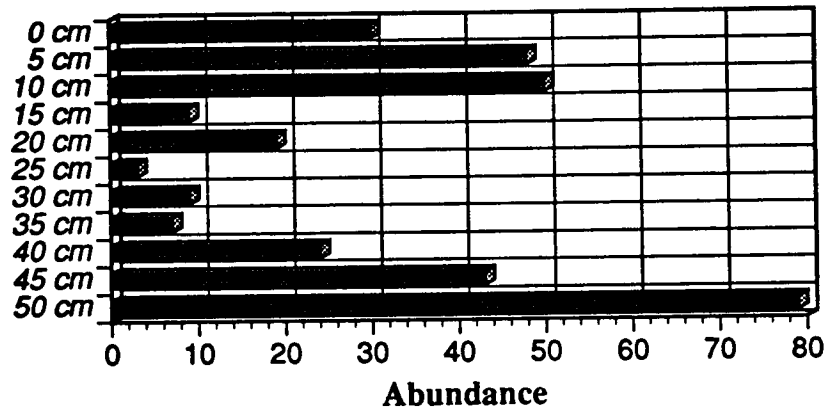
Figure 8.31 The numerical abundance, paleoproduction, and paleoingestion contributed by each 5 cm core interval from the lucinid biofacies at GC 184 Core 1.

Tier and guild structure provide a good example of the structure of the normal slope community. Most core intervals were dominated by predators. Predators are routinely over-represented in shelf and slope biofacies. This over-representation is particularly apparent in paleoproduction and paleoingestion. Chemoautotrophs are only important numerically, indicating their small size and insignificant contribution to community energy flow. Similarly, tier structure is weighted towards epifauna, as expected from the normal slope biota. Infauna were unimportant in community energy flow (as preserved).

The highest values of abundance, paleoproduction, and paleoingestion are low in comparison to the other core for GC 184 that included chemosynthetic faunas. A slight trend in increasing abundance was observed downcore. Paleoingestion and paleoproduction were highest in the upper section of the core and sporadically high lower in the core.

8.7.2 Green Canyon 272

Both lucinid (*Lucinoma* sp.) beds and vesicomyid (dominantly *Calyptogena ponderosa*) beds were sampled at GC 272. Samples were obtained exclusively by box core. Although penetration routinely exceeded 40 cm, the assemblage was always contained in the top 10 cm of the core. Evidence from piston cores obtained at other sites, discussed subsequently, prevent the unequivocal designation of GC 272 as a relatively new seep. Deeper samples would be required. Living vesicomyids were occasionally collected. Living lucinids were very rare. Lucinids in the top 10 cm, dated by amino acid dating using a ^{14}C calibration curve obtained from GC 184 samples, showed that most shells were no older than about 500 yr. Many specimens could not be distinguished from living individuals, indicating a very recent origin.

The lucinid biofacies at GC 272 was dominated numerically, by paleoproduction, and by paleoingestion by *Lucinoma* sp. The lucinid biofacies at GC

272 was nearly identical to that observed at GC 184 in most aspects. The size-frequency distribution was dominated by small individuals with a second smaller mode in the central 5 size classes (Figure 8.14). Larger individuals were proportionately somewhat more common that at GC 184. Unlike the lucinid beds at GC 184, GC 234, and GB 425, the smaller size classes accounted for a significant fraction of the assemblage's paleoingestion indicating that a suite of small species, represented by adult individuals, was also present at this site (Figure 8.16). These species accounted for little of the paleoproduction, however, because they were small (Figure 8.15). When the individuals were tallied according to the fraction of species' maximum size, the assemblage was characterized by a proportionately greater fraction of adult individuals than observed at GC 184 or GC 234. In this characteristic, the lucinid beds at GC 272 and GB 386 were similar (Figure 8.17). As in the other biofacies, the adult individuals accounted for the bulk of the paleoproduction and paleoingestion (Figures 8.18 and 8.19).

Guild structure at GC 272 was overwhelmingly chemosynthetic when evaluated numerically, by paleoproduction or by paleoingestion. Comparison to lucinid biofacies at other sites shows that chemosynthetic dominance was lower than at GC 184 and GB 386 (Figure 8.20). Tier structure was complex, when evaluated numerically, because of the presence of vesicomyids and some true epifauna. Infauna dominated tier structure when evaluated by paleoproduction or paleoingestion. The infaunal contribution to tier structure was typical of most lucinid biofacies (Figure 8.21).

The vesicomyid biofacies was dominated numerically, by paleoproduction, and by paleoingestion by *Calyptogena ponderosa*. Like the lucinid beds, the vesicomyid beds at GC 272 were characterized by a bimodal size-frequency distribution, one mode in the smallest size classes and another in the upper 4 size classes (Figure 8.14). A larger proportion of the shells collected were large (80% or better of the

assemblage's maximum size) than in the other clam biofacies. Like most of the other clam biofacies sampled, the upper five size classes accounted for the bulk of the paleoproduction and paleoingestion, indicating that most of the smaller individuals were juveniles (Figure 8.15, 16). When the individuals were tallied according to the fraction of species' maximum size, the assemblage was characterized by a proportionately greater fraction of adult individuals than observed in the lucinid beds at GC 184 or GC 234, but a similar proportion as observed in the lucinid beds at the same site and at GB 386 (Figure 8.17). As in the other biofacies, the adult individuals accounted for the bulk of the paleoproduction and paleoingestion (Figures 8.18 and 8.19).

Guild structure of the vesicomyid biofacies at GC 272 was overwhelmingly chemosynthetic when evaluated numerically and nearly exclusively chemosynthetic when evaluated by paleoproduction or by paleoingestion. Numerically, guild structure was somewhat more complete than observed in the lucinid biofacies (Figure 8.20). Tier structure was complex, when evaluated numerically, because of the presence of vesicomyids and some true epifauna. Semi-infauna dominated tier structure when evaluated by paleoproduction or paleoingestion (Figure 8.21).

The downcore trends in species composition and size-frequency distribution for the lucinid biofacies at GC 272 showed that the larger individuals were restricted to the upper 5 cm of the core. From 5 to 15 cm, only small individuals were found. No specimens were taken below 15 cm. Most of the assemblage's paleoproduction and paleoingestion in the top 5 cm of the core were contributed by the upper 5 size classes. Defining the size classes by the species' maximum size showed that most of the individuals in most core intervals were juveniles. However, some adults were present at 5 and 10 cm indicating that the intervals below the surface were characterized by small species, some of which reached a significant fraction of maximum size. Thus, in intervals down to 15 cm, adults accounted for most of the

paleoproduction and paleoingestion, even though, below the surface, these adults were of small species. The species composition of this core shows that lucinids were common down to 10 cm, however conditions were adequate to produce large individuals only in the upper 5 cm. Thus, below the top 5 cm, the habitat was suboptimal for chemosynthetic species. Below the top 5 cm, the assemblage was composed of a series of small species, many of which occurred in the central zone of the core described from GC 184 (Figure 8.22) and in the non-seep biofacies cored at the same site. Guild structure also documents the introduction of the chemosynthetic fauna at the top of this core. Predators dominate the lower core intervals as is typical of the normal slope biofacies. Chemoautotrophs dominate the upper portion of the core. Tier structure shows the transition from a dominantly epifaunal shelled biota to a dominantly infaunal shelled biota. Thus the assemblage below 5 cm at GC 272 contained those species characteristic of the non-seep biofacies. Whether this site is a new site, or whether the sampled horizons below 5 cm represent a period of time of suboptimal conditions for chemosynthesis such as recorded at GC 184, cannot presently be determined.

Six additional cores were taken from GC 272, none of which were subsectioned. These cores record the extent of local variability in conditions at this site. Small individuals are common in only three of the cores, both lucinid samples and one of the non-seep samples. The remaining two cores were composed of relatively large individuals (as compared to their respective biofacies elsewhere). Recalculation in terms of paleoproduction and paleoingestion show that the small individuals included a fair percentage of adults of small species in both lucinid samples. When examined according to species' maximum size, two of the lucinid cores contain a substantial proportion of juveniles. The other had fewer. Juveniles are important in only one of three of the sampled non-seep biofacies. Paleoproduction and paleoingestion show substantial variation in the size structure of the larger individuals. Nevertheless,

individuals routinely grew to 80% or more of species' maximum size in these biofacies, as they did in the one described previously from the subsectioned core indicating that this site has been characterized, at least recently, by near optimal conditions for chemosynthetic species. The absence of juveniles, however, suggests recruitment failure in most recent times (although severe taphonomic loss cannot be excluded as an alternative explanation).

In considering the guild and tier structures for these cores, only two cores are dominantly chemosynthetic. Two other cores containing chemosynthetic individuals retain significant non-chemosynthetic traits. Predators and deposit-feeders are common. Thus, local variability in guild structure is high, which might be indicative of a site recently colonized by chemosynthetic species. Analysis of tier structure supports these conclusions. In particular, infauna are uncommon.

Overall, then, GC 272 is characterized by substantial small scale variability in conditions. However, most locales conducive to chemosynthetic species provided near-optimal conditions in the recent past. Few living individuals and the paucity of preserved juveniles, however, suggests that optimal conditions may no longer be present for either the vesicomyids or the lucinids at this site. Moreover, examination of guild and tier structure suggests that this site has only recently harbored a chemosynthetic biota. Perhaps GC 272 is in transition between the normal slope and a well-developed seep habitat and so might be expected to contain a highly spatially variable biota and widely varying conditions of optimality for the various biotas.

8.7.3 Green Canyon 234

Samples from Green Canyon 234 "Mussel Beach" were of two types: lucinid dominated or mussel dominated. Samples were obtained by box core and piston core. Lucinid-dominated assemblages were generally upslope of the mussel beds and contained mostly *Lucinoma* sp. No dates are available for the lucinids. Several large

diameter piston cores were taken in the mussel bed locale at GC 234. Two of these cores recovered buried mussel beds. In one core, a buried mussel bed was found at 85 to 100 cm depth and another at 195 to 200 cm depth. The shell material was almost exclusively *Bathymodiolus* sp., with a few *Lucinoma* shells mixed in. In a second core, a buried mussel bed was also recovered at 85 to 100 cm. Like the former, most shell material was mussel. A few scattered lucinids and gastropods were recovered between and above these buried mussel beds in both cores, but no other significant shell accumulations were observed. In a third core, mussels were collected in the upper 10 cm, but few additional specimens were recovered in the remaining about 200 cm of core length. Thus, although mussel shells were not distributed continuously with depth, no other biofacies was present to take the place of the mussels in sedimentary units lacking them.

Both buried mussel beds had been killed catastrophically, probably by mud flows. [14]C dates indicate ages of about 2500 and 3500 years for these beds (± 500 yr. due to the variable amount of ^{14}C-dead carbon incorporated in their shells). Thus, this site has been inhabited, sporadically, by extensive mussel populations for at least 3500 yr.

The lucinid biofacies at GC 234 was similar to that observed at GC 184 in most respects (Figure 8.14 through 8.19). The size-frequency distribution was bimodal. Many small individuals were present and most of them were juveniles. Adults, also common, frequently lived to 80% or greater of maximum size. Adults accounted for most of the assemblage's paleoproduction and paleoingestion. The biofacies was unusual, however, in that the vesicomyids and thyasirids were dominant numerically, however *Lucinoma* sp. accounted for most of the assemblage's paleoproduction and paleoingestion. Thus, the vesicomyids and thyasirids were mostly juveniles that failed to reach adulthood. Five box cores from GC 234, three from lucinid beds and two from nearby non-seep habitats were analyzed. Of the three

lucinid beds, two are numerically dominated by *Lucinoma*, which also account for most of the paleoproduction and paleoingestion. One is numerically dominated by *Thyasira oleophila*, however *Lucinoma* and *Vesicomya cordata* dominate paleoproduction and paleoingestion. Each of these cores is characterized by a preponderance of small individuals. Large specimens are only abundant in core 342. Core 341, dominated by a mixture of chemosynthetic species, is composed exclusively of small individuals. Few of the individuals in any of the other cores were adults; core 341 contained only a few adult individuals and none approaching the species' maximum size. Accordingly, in core 341, unlike most others, juveniles accounted for a substantial fraction of paleoproduction and paleoingestion, an indicator of particularly poor survivorship. Accordingly, habitat optimality varied considerably among these three cores. The core containing the mixed chemosynthetic assemblage was distinctly suboptimal for all three species. Larval settlement, however, seemed to be an ongoing process, unlike at GC 272 (once again, this conclusion assumes an equivalent taphonomic milieu).

Guild structure in the lucinid biofacies at GC 234 was overwhelmingly chemosynthetic when evaluated numerically and nearly exclusively chemosynthetic when evaluated by paleoproduction or by paleoingestion. Comparison to lucinid biofacies at other sites shows that chemosynthetic dominance was lower than at GB 386, but about equivalent to GC 184 (Figure 8.20). Tier structure was complex, when evaluated numerically, because of the presence of semi-infauna and some true epifauna. Infauna dominated tier structure when evaluated by paleoproduction or paleoingestion. The infaunal contribution to tier structure was typical of most lucinid biofacies (Figure 8.21). Guild structure varied among the three cores examined. Core 341, unique for other reasons, had a much lower dominance by chemosynthetic species. Predators were more common, a normal slope characteristic. However, infauna were important contributors to all three cores. Thus these cores represent a

range of conditions from distinctly suboptimal to near-optimal for the lucinid biofacies.

Two non-seep biofacies were also sampled in the GC 234 area. Individuals were nearly or exclusively small. The two cores are, however, quite distinctive. Core 301, which was not subsectioned, shows a standard non-seep fauna with many adult individuals of small species, a significant number of which reached near-maximum size. This core, then represents an optimal normal slope habitat near the seep sites. The second core was taken in a suboptimal habitat for seep and non-seep species combined. This area has been suboptimal for an extended period of time. All individuals are small. Most are juveniles. Thus juveniles account for a substantial fraction of paleoproduction and paleoingestion throughout these cores. A look at species composition suggests that this site is gradually becoming more favorable for vesicomyids. The numerical contribution of vesicomyids increases upcore as the contribution of non-seep species declines. Moreover, the fraction of paleoproduction and paleoingestion contributed by chemosynthetic species increases substantially in the upper 5 cm. The core may document, then, the incipient colonization of the area by Vesicomyidae.

Guild and tier structure support these observations. Predators and deposit feeders dominate the guild structure at the two non-seep cores as is usual for the normal slope fauna. However, the upper section of one of these cores shows a significantly increased fraction of the paleoproduction coming from chemosynthesis. Chemosynthetic taxa dominate in the cores taken in the lucinid biofacies. The productivity of the biota increases upcore in the non-seep core. Abundance in the upper 10 cm is typical of chemosynthetic communities. Lower abundance downcore is typical of non-seep communities. Relatively low paleoingestion and paleoproduction throughout, however, indicate the preponderance of juveniles in the fauna, even at the nearsurface where these variables reach maximal values. Finally,

epifauna and semi-infauna dominate the tier structure of both non-seep cores, although infauna are increasingly important upcore, whereas infauna dominate the tier structure of cores taken in the lucinid biofacies. Thus, the incipient development of a chemosynthetic fauna is evident in the non-seep cores, suggesting an ongoing development of the chemosynthetic community.

8.7.4 Garden Banks 386

One piston core and one box core were taken from Garden Banks 386. The piston core contained a mixture of mostly *Lucinoma* with some thyasirids to a depth of 35 cm. No shell material was collected in deeper core intervals. The box core sampled to a depth of 35 cm and sampled lucinids throughout that depth range. The biofacies was dominated numerically, by paleoproduction, and by paleoingestion by *Lucinoma* sp. (Figure 8.13). *Lucinoma* sp. dominance persisted throughout the upper 35 cm of the sediment. The biofacies was bimodal containing a mode in the small size classes and one in the central 5 (Figure 8.14). This size distribution persisted throughout the core. Paleoproduction and paleoingestion were overwhelmingly contributed by the upper 5 size classes (Figures 8.15 and 8.16). This distribution persisted throughout the core. A substantial fraction of the assemblage consisted of large juveniles and adults (Figure 8.17). The proportion of adult individuals increased upcore, particularly in the upper 10 cm. Paleoproduction and paleoingestion were primarily contributed by large juveniles and small adults, however (Figures 8.18 and 8.19), a phenomenon that persisted throughout the core. Thus, the large adults found upcore were adults of small species. The site, though persistently conducive to dominance by chemosynthetic clams, was persistently suboptimal for them. Chemosynthetic clams rarely exceeded 60% of species' maximum size. Thus, this site sits in stark contrast to GC 184 where the habitat oscillated between near-optimal habitat and distinctly suboptimal habitat for the lucinids. At GB 386, the

habitat was invariantly suboptimal, but not sufficiently so to exclude the chemosynthetic clams from a dominant position in community energy flow.

The guild and tier structure of the lucinid biofacies at GB 386 was nearly exclusively chemoautotrophic and infaunal. This represents the extreme condition among the lucinid biofacies sampled. Guild and tier structure of the subsectioned core show that this site was nearly exclusively chemoautotrophic and infaunal throughout the sampled record of the site. Very little variation occurred downcore in guild and tier structure, in comparison to GC 184 for example. Very little variation occurred in numerical abundance, paleoingestion or paleoproduction as well, although the latter two reached highest values in the lowermost core section. The high values are typical of chemosynthetic faunas.

8.7.5 Garden Banks 425

Cores from GB 425 predominately contained thyasirids (*Thyasira oleophila*) and lucinids (*Lucinoma* sp.). Samples were obtained by box core and piston core. *Lucinoma* sp. was commonly encountered alive. *Thyasira* was not. One piston core recovered form GB 425 contained Thyasira, nearly exclusively, to a depth of 210 cm. Large accumulations were observed between 50 and 60 cm and again at 70 to 85 cm. A second piston core recovered a thyasirid layer at 70 to 75 cm depth with scattered thyasirid shells throughout the remainder of the core. A box core was sectioned into 5-cm intervals to a depth of 35 cm. This core resembles the piston cores in all significant respects. Thyasirids were numerically dominant in all intervals. Lucinids accounted for somewhat less than half to more than half of the paleoproduction and paleoingestion. However, juvenile thyasirids and lucinids were rare (Figures 8.14 and 8.17). This distribution persisted throughout the core. The size-frequency distribution of the assemblage was distinctly bimodal, the modes being produced by the smaller thyasirid and larger lucinid individuals (Figure 8.14). This trend persisted

throughout the core. The two species accounted for an equivalent share of the paleoproduction and paleoingestion (Figures 8.15 and 8.16). This trend occurred in most core intervals. Intervals at 10 cm and 20 cm, however, contained no large lucinids. Nearly all individuals were adults, a much higher fraction than any other biofacies or site (Figure 8.17). This was true in all core intervals. Individuals near 100% of maximum size were frequently encountered. In some cases, a near majority exceeded 80% of maximum size. Not surprisingly, large adults accounted for most of the paleoproduction and paleoingestion in all core intervals (Figure 8.20). Significantly, in core intervals where lucinids were not found, thyasirids still persistently reached near-maximum size.

This site, then, is unique in maintaining near-optimum conditions for two chemosynthetic species for a substantial length of time. Thyasirids at 30 cm depth dated as old as 1000 yr. (Table 1). The site was near-optimal for thyasirids throughout most of that time period. Optimality for lucinids varied. Lucinids disappeared from and reappeared in the assemblage twice over the 30 cm of core. At each reappearance, they attained adult size, however they rarely exceeded 70% of maximum size, indicating, along with their lower persistence, a distinctly less favorable habitat than was present for the thyasirids. Piston cores, as yet undated, indicate that this site has been conducive to thyasirids and lucinids for many thousands of years. Curiously, the absence of living thyasirids indicates a recent change in conditions unlike that present previously. Similarly, despite the number of adult lucinid clams, juveniles were not present in the death assemblage, although they were at most other sites. Although higher than normal taphonomic loss cannot be discounted, the suggestion is that this area is becoming less favorable for chemosynthetic clams than it has been over the last thousand or so years.

Guild and tier structure closely resembled that observed at GB 386 despite the difference in faunal composition. The biofacies was chemosynthetic and infaunal.

Guild and tier structure varied little downcore. This site and GB 386 are interestingly different from the Green Canyon sites in their simplified guild and tier structure evaluated by all three measures, numerical abundance, paleoproduction and paleoingestion. Very few heterotrophic individuals were preserved at this site and very few non-infaunal chemosynthetic individuals were present.

Abundance, paleoingestion and paleoproduction increased downcore, particularly below 10 cm. Values were typical of well-developed chemosynthetic faunas. The interval at 20 cm containing no lucinids was characterized by lower paleoingestion and paleoproduction than other core sections below 10 cm. The upper 10 cm were low in all three variables. Densities and energy flow variables, however, did not drop to unusually low values for chemosynthetic faunas. In fact, the values observed in the upper 10 cm were typical of most chemosynthetic faunas; the deeper densities and energy flow values were substantially higher than observed in most other cores, indicating periods of unusually high chemosynthetic productivity.

8.8   Community History, Persistence and Succession

Unlike mussel beds, clam beds may persist as a sediment surface phenomenon for extended periods without continual living input because taphonomic loss rate and sedimentation rate are low. Thus the proportion of small species and juveniles of large species in the assemblage can be used to evaluate whether recruitment is a continuing process in the assemblage or whether the clam bed represents an area no longer supporting chemosynthesis. Most clam beds were inactive. Living individuals were rarely encountered and only commonly encountered at GB 425. Juveniles were usually an important component of the death assemblage, however, so that larval settlement was a persistent feature at most sites. Like many shallower water habitats, however, larval survivorship varied greatly. Sites frequently failed to support adult individuals and only a few sites consistently supported individuals

larger than 70% of species' maximum size. Thus habitat optimality varied significantly amongst these clam beds and the widespread occurrence of clam beds, due to their high degree of preservability, belied the fact that thriving beds were probably no more common than were the less preservable mussel beds at most sites.

Some sites retained optimal habitat for some species continuously over geologically-long periods of time. More commonly, however, habitat optimality varied substantially over time scales of 300 to 500 yr. Local extinctions and recolonizations occurred and these seemed to occur fairly rapidly in the context of the time span represented by the entire core or a portion of the core recording times conducive to a selected fauna. These events, however, although occurring rapidly on a geological time scale, nevertheless occurred rarely over a human time scale. Over a 50 yr. time span, local extinctions and recolonizations should be gradual and exceedingly rare. Thresholds of optimality seem to be present. Thus, it is more typical for large adults to appear and vanish rather than for size to gradually increase or decrease. Triggering mechanisms producing the rapid (on a geological time scale) faunal changes are unknown, but could include small changes in sediment chemistry. Thresholds and triggers are important in most bivalve population dynamics.

In the case of the mussel beds, catastrophic burial was implicated in preservation, but the importance of catastrophic burial in fostering local extinctions seems to be minor. Most extinctions occurred quickly, but without hiatuses of faunally depauperate sediments that might be typical of catastrophic sedimentary events. Thus, one important characteristic of these sites was the degree of persistence of the chemosynthetic biota. A fauna typically was persistent over a time span of a few hundred years, but was typically not persistent over a time span of 300 to 500 yr.

Faunal succession was not observed. When local extinctions occurred in the chemosynthetic biota, the biota was replaced by a normal slope biota or a mixture of a normal slope biota and the juveniles of chemosynthetic species that failed to survive to adulthood. Thus the only faunal transitions were between chemosynthetic and non-chemosynthetic faunas. Not one distinctive faunal transition between two chemosynthetic species was observed. Sites were always recolonized by the chemosynthetic species that had previously become locally extinct. Accordingly, the chemosynthetic faunas were resilient over long time scales; time scales of geological importance. The inescapable conclusion is that sites are more or less permanently conducive to only one, or at most two, chemosynthetic species. Site specificity is retained over geologically-long time frames. This suggests that site chemistry remains within a narrow range for geologically-long times and that the local variations in chemistry are sufficient simply to control the presence or absence of the locally preferred chemosynthetic fauna at the expensive of the background heterotrophic fauna.

The relatively low persistence but high resilience of the seep faunas indicates that sites retain a degree of uniqueness in their capacity to support seep faunas over geologically-significant time periods. In this study, only the *Lucinoma* sp. biofacies was found at more than one site. Significantly, this species was rarely persistent over long time spans and rarely did a significant number of individuals attain near-maximum size, so that this species was simply more capable of surviving in a variety of suboptimal habitats than were the other species. At least as important was the failure to sample habitats optimal for several important chemosynthetic species, namely the solemyids (a few were taken at GB 386), *Lucinoma atlantis* (occasionally collected at GB 425) and *Vesicomya cordata*. We suggest that at least three additional unique habitats remain unsampled and unsurveyed. Given the uniqueness

of sites, we would expect these biofacies to dominate sites that are as yet unexplored rather than to be present but unsampled within already explored sites.

8.9   Summary and Management Implications

The purpose of this portion of the study was to evaluate the persistence of seep communities, their resilience and the frequency of disturbance, and successional relationships in recovery from disturbance.

Overall, seep communities were persistent on time scales of human life spans, but not over periods of 500 to 1,000 years. Although a substantial amount of variability existed, most sites maintained conditions conducive to the optimal growth of one or more seep species over periods of several hundred to over a thousand years. During these intervals, species composition, size-frequency distribution and productivity were relatively stable components in the community. Not all sites were characterized by optimal habitat during these intervals, however, if optimal is defined as promoting individual growth to ≥ 80% of species maximum size. Some sites clearly provided better conditions than others and did so for an extended period of time.

Despite this persistence, disturbances did occur in nearly every site. The mechanisms included catastrophic burial, but other more subtle mechanisms were also present. The results of disturbances were uniformly similar. For a time, a normal slope biota occupied no site. Chemosynthetic species normally recruited to these areas during this time, but failed to survive, so recruitment failure was generally not important in restricting recovery. Recovery normally took several hundreds of years, but, realistically, sampling intervals would have restricted observation of more rapid events, so short term episodes of disturbance and recovery might have been common but gone unnoticed in our analysis. Nevertheless, the time of recovery suggests that the natural cycle of disturbance and recovery will be very difficult to distinguish from a permanent loss due to anthropogenic impacts.

Recovery times are simply too long. Surprisingly, when recovery occurred, the same chemosynthetic species reoccupied the site. Species composition returned as before, but community productivity was often altered to some degree. No successional changes were observed, nor was replacement of one chemosynthetic species by another observed after the disturbance.

Accordingly, the singularly most significant observation in this study is the nearly-perpetual uniqueness of these sites. Sites seem to support only a restricted species complement for hundreds to thousands of years. Thus each site is relatively unique, and a management strategy whereby a certain number of sites are preserved unharmed while others are permitted to be impacted seems sensible until a wider range of sites can be studied to better assess the degree of uniqueness of each site over geologically-long time periods. Simply put, as of today, we have no site duplicates; that is, we have no sites that are sufficiently similar to be considered equivalent to each other for management purposes. Nor can we be sure that a site, once lost, will ever be replaced. Consequently, management policy should be formulated extremely conservatively based on the assumption that each site is unique and unreplaceable.

9.0 Age, Growth, and Reproduction in Deep Sea Gorgonian from Hydrocarbon Seep Sites in the Northern Gulf of Mexico
S.E. Beasley, W.W. Schroeder and M.R. Dardeau

9.1   Introduction

The purpose of this research element was to characterize the age and growth rate patterns, and reproductive strategy of a non-chemosynthetic faunal component of seep-sites. This effort was intended to provide input to two of the sections in Task 3 (Field Operations and Sampling) set forth in the RFP (Solicitation No. 3555). The first, task 3.c.5 (Chemosynthetic Epifauna and Associated Non-chemosynthetic Fauna), addresses estimating the biomass and size frequency of representative fauna at seep-sites while the second, Task 3.d (Temporal Variability), focuses on detecting differences over time in biomass, growth, numbers, and general health of representative fauna at seep-sites.

Octocorals have been acknowledged as a principal member of biological assemblages at numerous hydrocarbon seep sites in the Gulf of Mexico (e.g., Brooks et al. 1989; MacDonald et al. 1989; 1990a), but have not been the focus of any organized research to date. Although not represented in every seep community, they have been reported from at least thirteen seep sites (Table 9.1) and are considered non-chemosynthetic members of the assemblages. Their taxonomy is still being resolved. In this component of the study, two aspects of the basic life history of octocorals are examined; age and growth rate estimates, and reproductive characteristics.

The axial skeleton of sea whips is composed of gorgonian, which is deposited in concentric layers around a central canal (Wainwright et al. 1982). The degree to which these rings are visible varies from species to species. Little is known about growth rings, particularly their periodicity. Annual growth rings have been documented in *Muricea californica* and *M. fruticosa* (Grigg 1974), and have been

Table 9.1   Seep sites from which octocorals have been reported.

Lease Block	Source
East Break 376	2
Garden Banks 341	5
Garden Banks 382	5
Garden Banks 386	1
Garden Banks 388	2
Garden Banks 416	5
Green Canyon 53	4
Green Canyon 121	5
Green Canyon 166	5
Green Canyon 184/185	1,2,3
Green Canyon 232	5
Green Canyon 234	1,2
Viosca Knoll 826	1

1 - Present Study
2 - Brooks et al. 1989
3 - MacDonald et al 1989
4 - Roberts et al. 1989
5 - GERG Unpublished Data

proposed for *Leptogorgia hebes*, and *L. virgulata* (Mitchell et al. 1993). Nothing, however, is known about the periodicity of growth ring formation in deep-sea gorgonians. Information from analysis of growth rings can be used as a form of environmental hindcasting. The frequency of extinction events and recolonizing episodes can be estimated by determining population age structure. Further, comparative stability of different seep-sites can be evaluated by comparing growth rates of sessile organisms. When combined with a detailed examination of the physical processes impacting the various sites, these data may provide critical insight into the short- and long-term health of both the individual faunal components and the community at-large of these unique habitats. Reproductive cycles of these gorgonians are likewise undescribed. For example, it is not known if the deep-sea

communities are maintained by asexual and/or sexual means, when colonies become reproductively active, or if they exhibit a regular propagation cycle.

9.2 Year 1 Effort: Age and Growth Rate Estimates

9.2.1 Methods and Materials

In September 1991, 55 colonies were collected from the Green Canyon 234 (GC 234) study site using the *Johnson Sea-Link* submersible. They were identified as a new subspecies of an undescribed species of *Callogorgia* (Bayer personal communication). Upon return to the ship each colony was counted and corresponding height and basal diameter recorded. Seventeen of the colonies were randomly collected along a transect. These specimens were numbered, tagged, placed in Helly's fixative for eight hours, transferred to several washes of sea water over a 24 hr period and stored in 70% undenatured ethanol prior to laboratory analysis. The remaining 38 colonies were attached to rock samples and used only for measurements of height and basal diameter.

Ring morphology in the axial skeleton was determined by embedding a two centimeter-long basal section of each colony (n=17) in epoxy resin. A basal section was defined as the part of the colony between the basal plate and the first branch. A transverse thin section of the embedded base was made by using a Buehler low speed saw. The section was polished using 0.3 μm alumina paste to facilitate counting of growth rings under a binocular microscope.

9.2.2 Results and Discussion

Two types of layering were visible around the central axis of *Callogorgia* sp.; major bands and minor bands (Figure 9.1). Major bands are comprised of dense gorgonin material, burnt orange in color, which appears as either symmetrical or asymmetrical dark bands completely encircling the central axis. Major bands are

Figure 9.1   Major bands and minor bands are visible around the central axis of *Callogorgia* sp. The major bands shown here appear incomplete as the result of uneven polishing.

easily distinguished from each other. The number of major bands present in *Callogorgia* sp. (n=17) ranges from one to three. Minor bands, generally light brown in color, are made up of less dense gorgonin material and are located between the darker bands. Individual minor bands are often difficult to distinguish because of their abundance and proximity to one another. In addition, many of the minor bands do not appear to be completely concentric and therefore might more accurately be described as incomplete bands around the central axis. A comparison with the more uniform concentric ring structure observed in *Leptogorgia hebes* can be seen in Figure 9.2.

If major bands of *Callogorgia* sp. are annual, then the oldest colony could not exceed three to four years of age. If, however, the minor bands are laid down annually, then some colonies could be up to 70 years old. Although major bands probably represent periods of reduced growth, the large number of minor growth bands or layers make interpretation difficult and offer a poor scale against which occurrence of long term cycles could be verified. This is in contrast to two shallow water gorgonians of the northeastern Gulf of Mexico, *Leptogorgia hebes* and *L. virgulata*, whose axial skeletons are composed of concentric rings (e.g., see Figure 9.2) which appear to exhibit annual periodicity and whose population age structures suggest event-related (e.g., hurricane impacts) rather than biologically mediated mortality (Mitchell et al. 1993). It was concluded that the complex internal skeletal structure of *Callogorgia* sp. would not permit any meaningful estimates of age or growth rates. Therefore, the Year-2 field and laboratory research effort was modified to focus on the reproductive ecology of *Callogorgia* sp.

9.3   Year 2 Effort: Reproductive Cycle

9.3.1   Methods and Materials

In August 1992, additional *Callogorgia* sp. collections were made from the Viosca Knoll 826 (VK 826), Green Canyon 184 (GC 184) and GC 234 study sites,
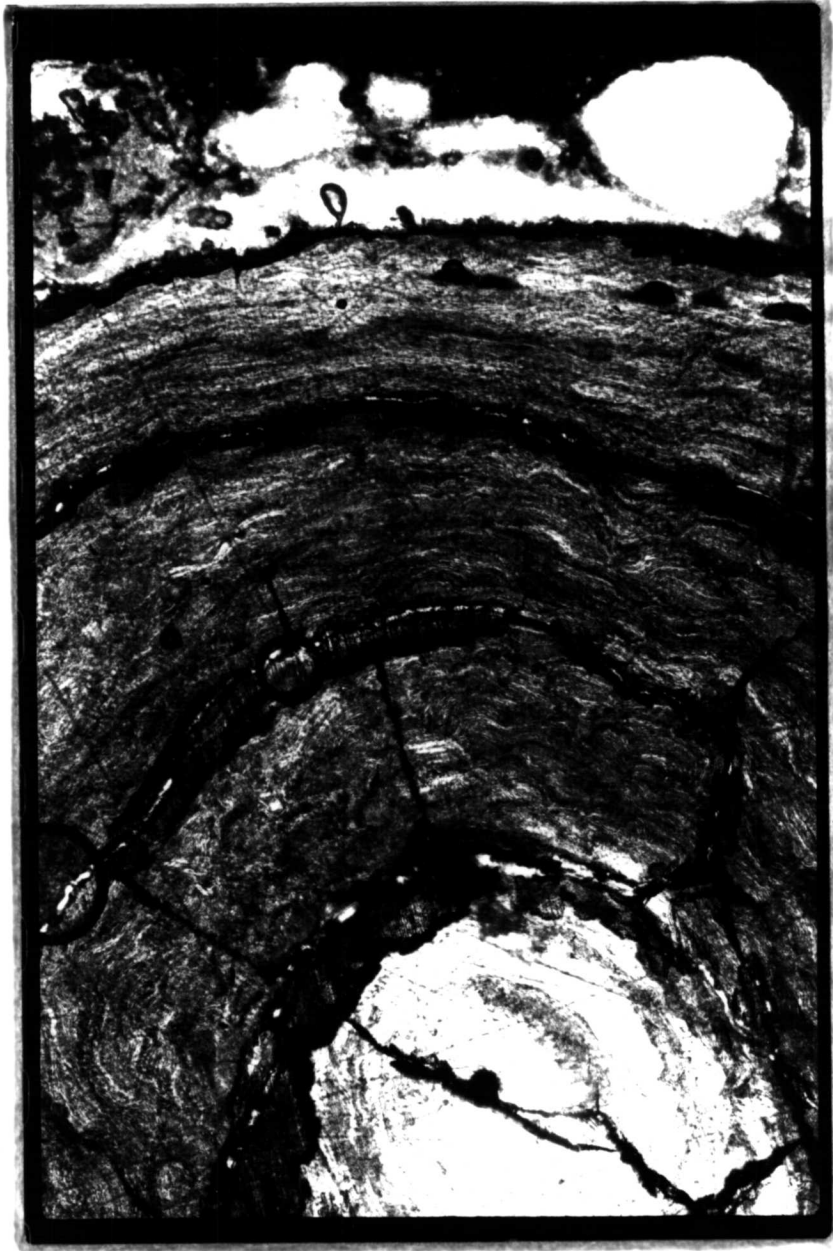
Figure 9.2   Cross section of axial rod showing concentric ring structure in *Leptogorgia hebes*.

again utilizing the *Johnson Sea-Link* submersible. Colony height and corresponding basal diameter were recorded for the colonies collected from VK 826 (n=6), GC 184 (n=10), and GC 234 (n=6). Of these colonies, four from VK 826 and five from GC 234 were tagged and preserved following the same procedures employed in 1991. No colonies from GC 184 were preserved for histological analysis.

Many corals are hermaphroditic; to determine if *Callogorgia* sp. is represented by separate sexes, the gametes present were examined to establish the gender of each colony. This was accomplished by randomly selecting 10 one centimeter long segments from the upper branches of each colony for sectioning. Once the one centimeter sections were selected, they were cut from the branch using a razor blade and subsequently stained using Cason's trichome stain technique (Cason 1950). Stained sections were infiltrated several times with Spurr's resin and absolute ethanol (1:1) to allow the resin to penetrate all soft tissue of the coral before embedding in 100% Spurr's resin. Embedded samples were polymerized in a dry heat oven at over 70°C. Using a Buehler Isomet slow speed saw, longitudinal thin sections were made of each branch sample and then mounted on petrographic slides, polished, and coverslipped. A Wild M-20 microscope was used to record presence and gender of gametes from each colony. Because sections do not expose polyps equally, each one centimeter segment was examined for polyps with the greatest number of gametes present. The mean maximum number of gametes per polyp is the mean of all polyps counted from 10 segments from each colony.

9.3.2 Results and Discussion

Total number of colonies examined for reproductive activity from collections made at VK 826 and GC 234 during September 1991 and August 1992 was 26; of these 13 were female and 13 were male. Of 17 colonies collected from GC 234 in September 1991, seven were female and ten were male. Four additional female

colonies and one male colony were obtained from the same site in August 1992 (n=5) and two female colonies and two male colonies were taken from VK 826 in August 1992 (n=4). In female colonies, oocytes are attached to sulcal septa of the gastric cavity by a short mesogleal stalk. The peripheral layer of a mature oocyte is made up of entoderm which encompasses a layer of mesoglea. Lying to the interior of the mesogleal layer is the vacuole and lipid enriched cytoplasm which surrounds the nucleolus and nucleus of the egg (Figure 9.3). The mean maximum number of oocytes per polyp for all female colonies was 3.5. Large oocytes, having a mean maximum diameter of 300 μm, occurred in colonies having a minimum height of 30 cm. Small gametes were present in the one colony < 30 cm in height but were too immature for gender to be determined. In male colonies, spermaries are attached to sulcal septa of the gastric cavity. Maturing spermaries contain thousands of sperm and are easily distinguished from yolk-laden eggs by the presence of spermatocytes which become mature sperm while converging into rows towards the center of the spermary where there is typically a hollow area (Figure 9.4). The mean maximum number of spermaries found in male colonies was 3.3 per polyp. A transmission electron micrograph of a colony collected from GC 234 in 1991 showed mature sperm present with a characteristic head and tail (Figure 9.5).

Regression analyses were performed to examine the relationship between 1) basal diameter and colony height, and 2) number of gametes in each polyp and colony height. Colony height increased significantly (P<0.001, r^2 =0.98) as the basal diameter of each colony increased (Figure 9.6). Number of oocytes per polyp also increased significantly (P=0.004) as colony height increased (Figure 9.7) for female colonies. However, no relationship (P=0.101) was found between number of spermaries present per polyp and colony height (Figure 9.7), although males did produce a maximum number of spermaries per polyp when a minimum height of 70 - 90 cm was reached.
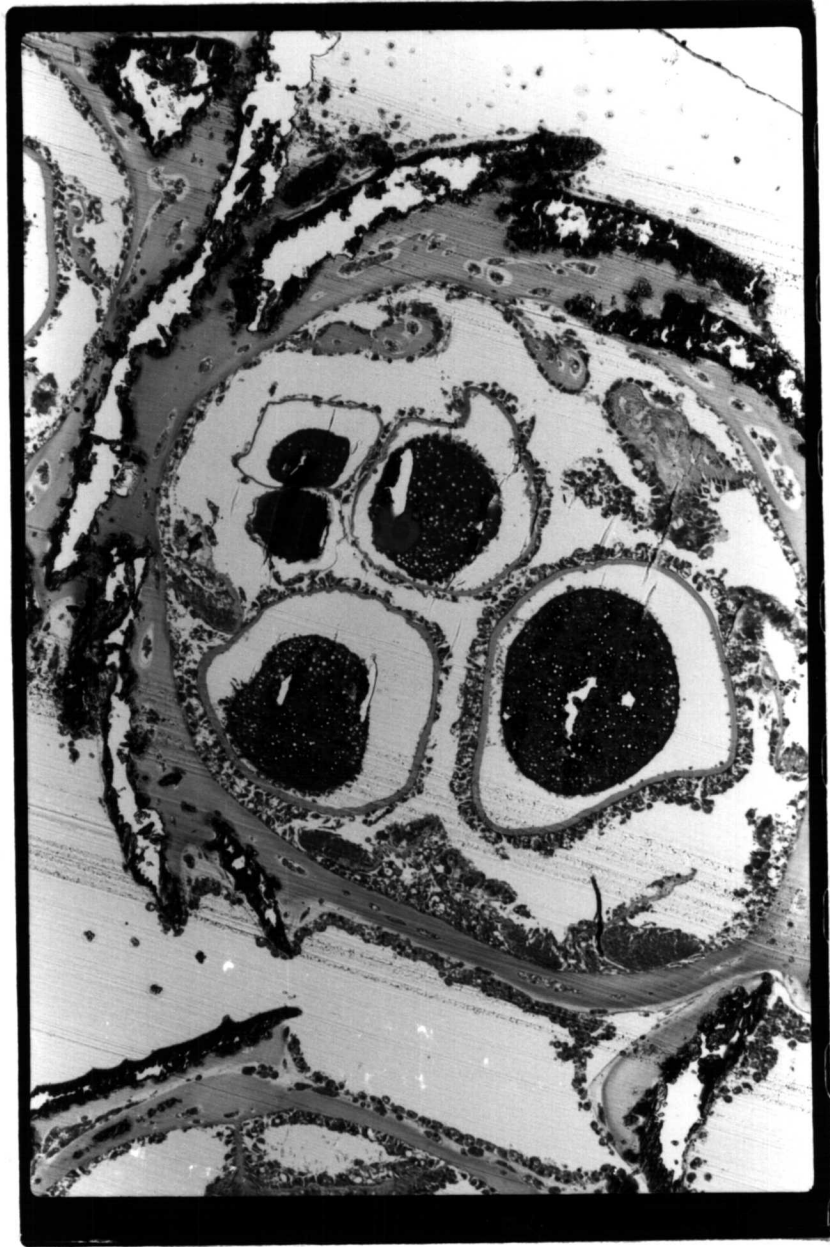
Figure 9.3   Vacuole and lipid enriched cytoplasm of an egg from GC 234 in 1991.
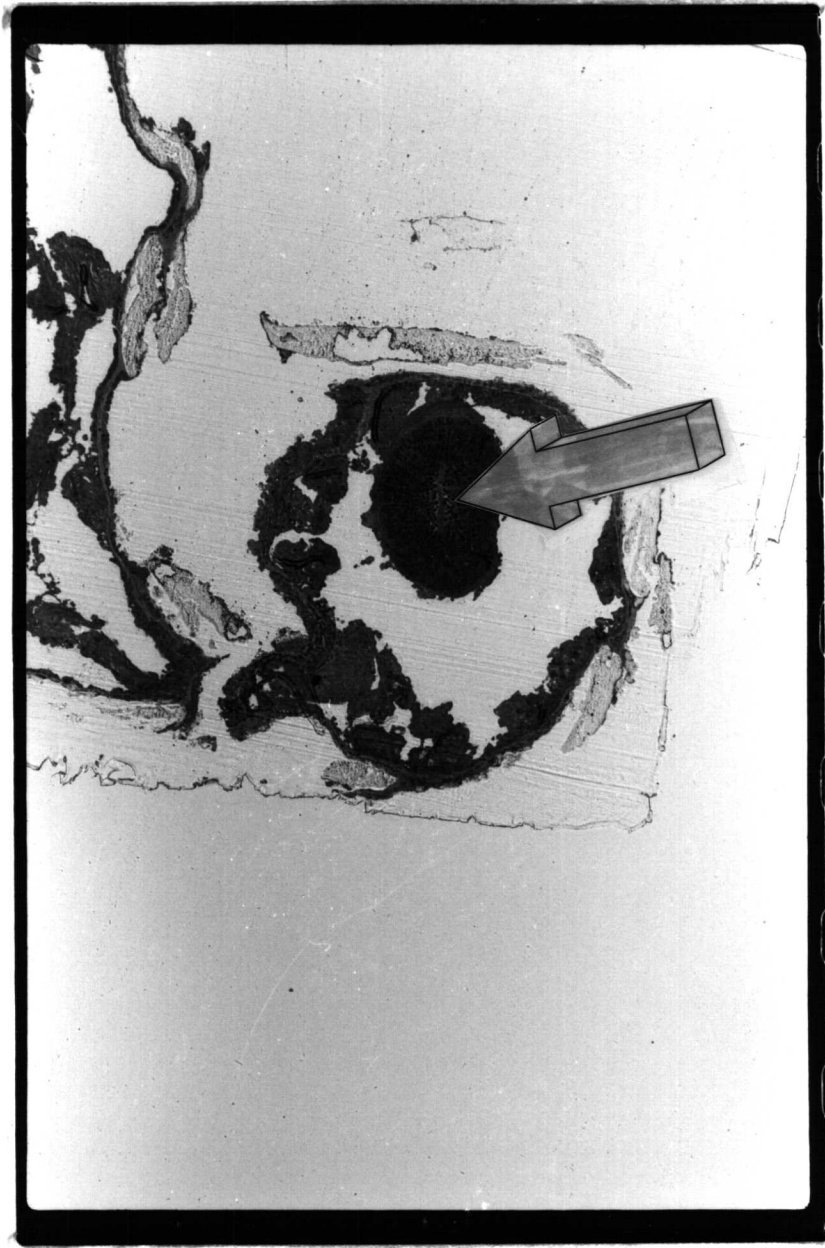
Figure 9.4 Rows of maturing sperm converge toward the center of a spermary from GC 234 in 1991.
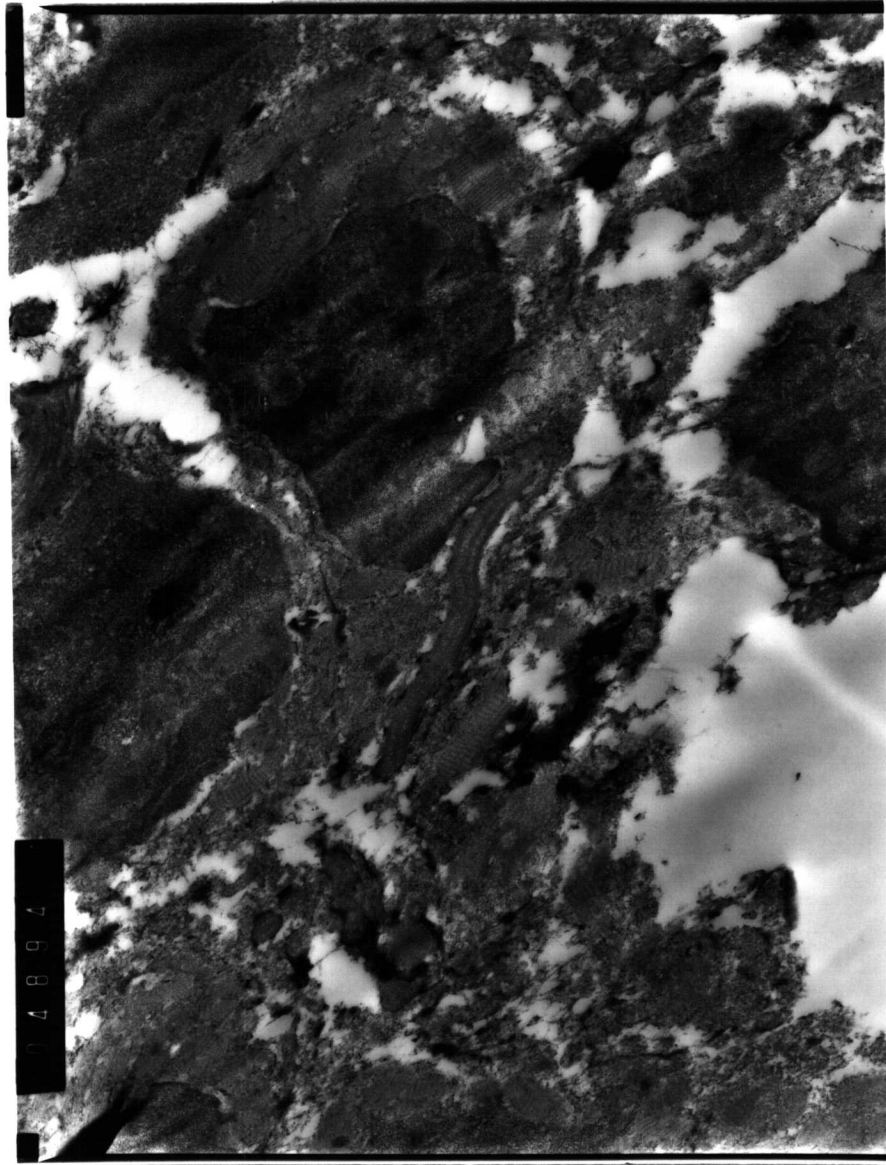
Figure 9.5 A mature sperm with a characteristic head and tail from GC 234 in 1991.
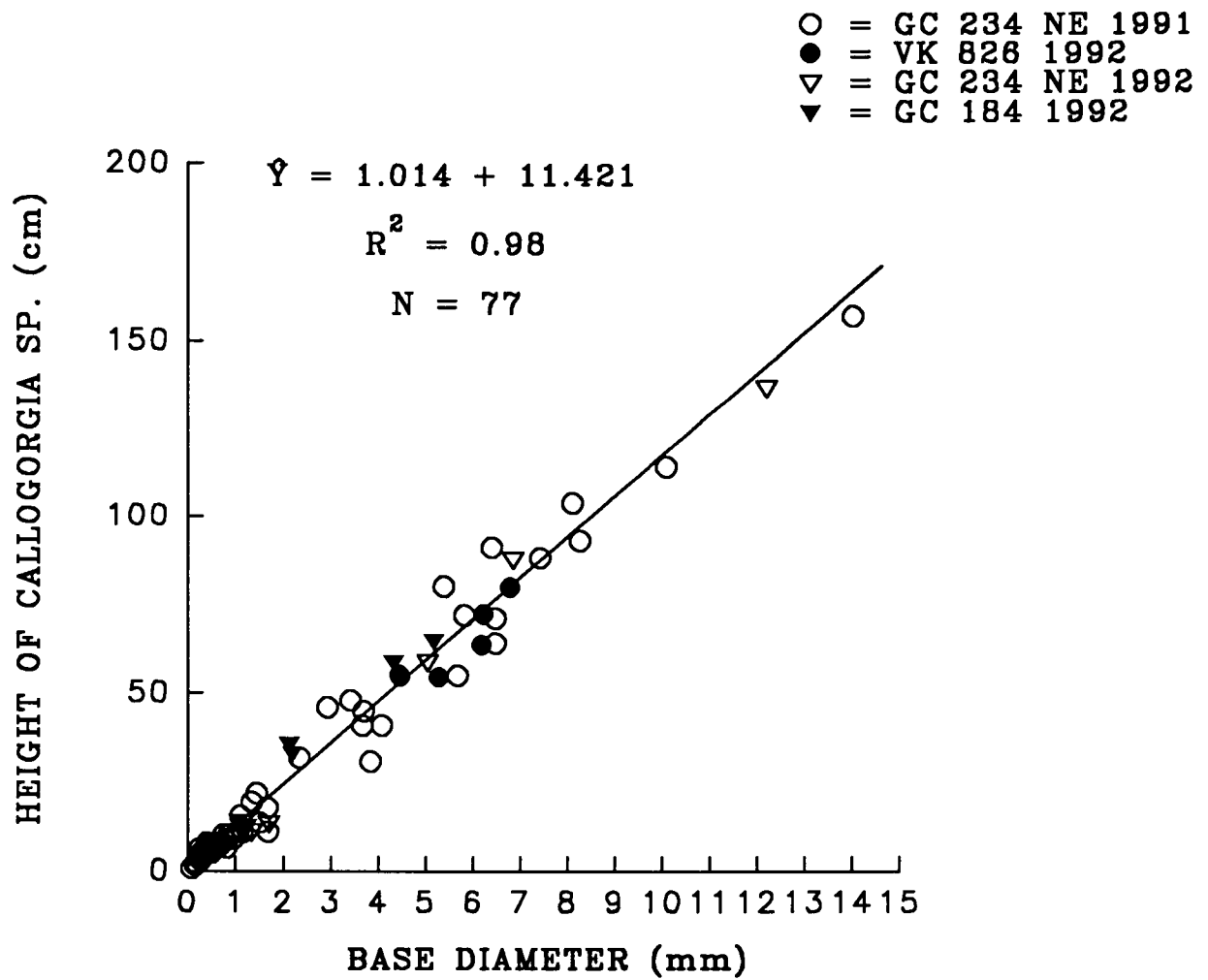
Figure 9.6   Relation of base diameter and height of *Callogorga* sp. colonies. The height of each colony tends to increase significantly (p<0.001) as the basal diameter of each colony increases.
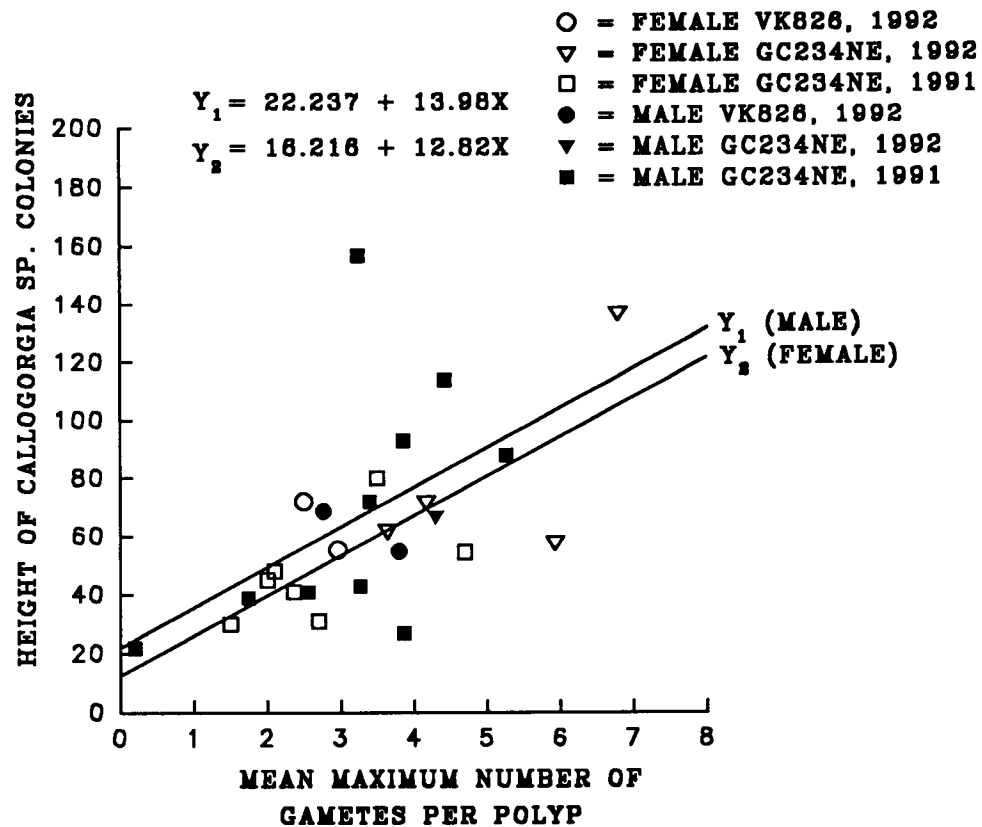
Figure 9.7 Relation between height and reproductive state of *Callogorgia* sp. colonies. Female colonies are reproductive by the time a height of 30 cm is reached. The number of oocytes per polyp tends to increase significantly (p=0.004) as the height of the colony increases. Male colonies are reproductive by the time a height of 20 cm is reached. The number of spermaries present per polyp does not tend to increase significantly (p=0.101) with increasing height.

One-way ANOVA's were performed to determine if: 1) height of reproductive colonies differed between study sites from September 1991 and August 1992; and 2) number of gametes per polyp differed significantly between study sites from September 1991 and August 1992. Mean height of reproductive colonies from GC 234 1992 (n=5) was greater than colonies from both GC 234 1991 (n=17) and VK 826 1992 (n=4). The differences, however, were not significant (P=0.271) (Figure 9.8). Colonies from GC 234 1992 (n=5) did have significantly more (P<0.05) gametes than GC 234 1991 (n=17) and VK 826 1992 (n=4) (Figure 9.9). Though sample size was to small for statistical analysis, the mean maximum number of oocytes per polyp for female colonies collected from GC 234 1991 (2.7; n=17) did not differ from VK 826 1992 (2.7; n=2). However, female colonies from study site GC 234 1992 (n=4) contained more oocytes per polyp (5.1) than earlier collections from GC 234 1991 and VK 826 1992 (Figure 9.4). Although size differences were not significant at Green Canyon between 1991 and 1992, colonies at GC 234 1992 were larger, which may have resulted in the increase in fecundity at GC 234 1992. Again, because of small sample size, statistical analysis could not be performed on mean maximum number of spermaries present per polyp in male colonies. However, there appeared to be no difference in the mean maximum number of spermaries present per polyp for male colonies collected from GC 234 1991 (3.2; n=10), GC 234 1992 (4.3; n=1), and VK 826 1992 (3.3; n=2). Caution must be taken in interpretation of differences in fecundity; it is difficult to draw conclusions based on the small number of specimens collected from Green Canyon and Viosca Knoll but differences in fecundity are consistent with colony size. Colonies from both GC 234 and VK 826 1992 were larger in overall height and possessed a greater number of gametes per polyp than colonies from GC 234 1991.

The possibility also exists that differences in fecundity resulted from the timing of our collections relative to spawning cues. Two distinct modes of sexual
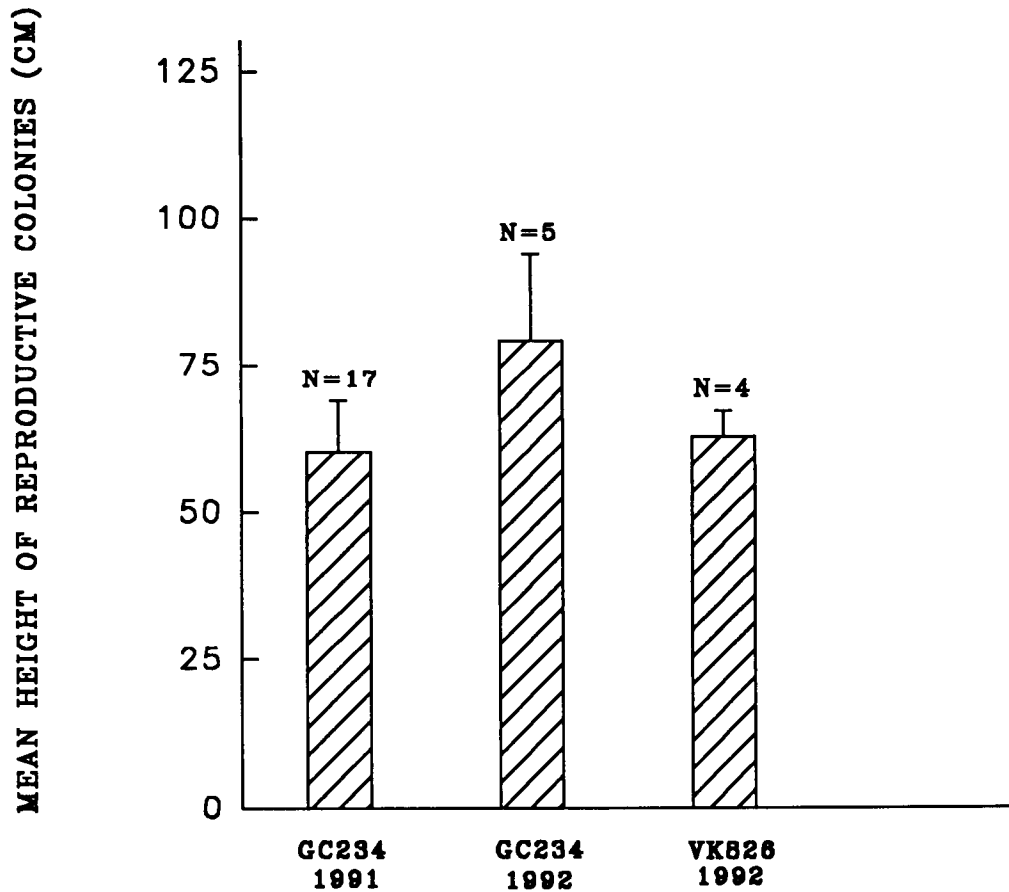
Figure 9.8   Relation of *Callogorgia* sp. colony height and collection site by year.
Mean height of reproductive colonies from GC 234 1991, GC 234 1992,
and VK 826 1992 did not differ significantly (p=0.271) from each other.
Error bars indicate standard error for each sample.
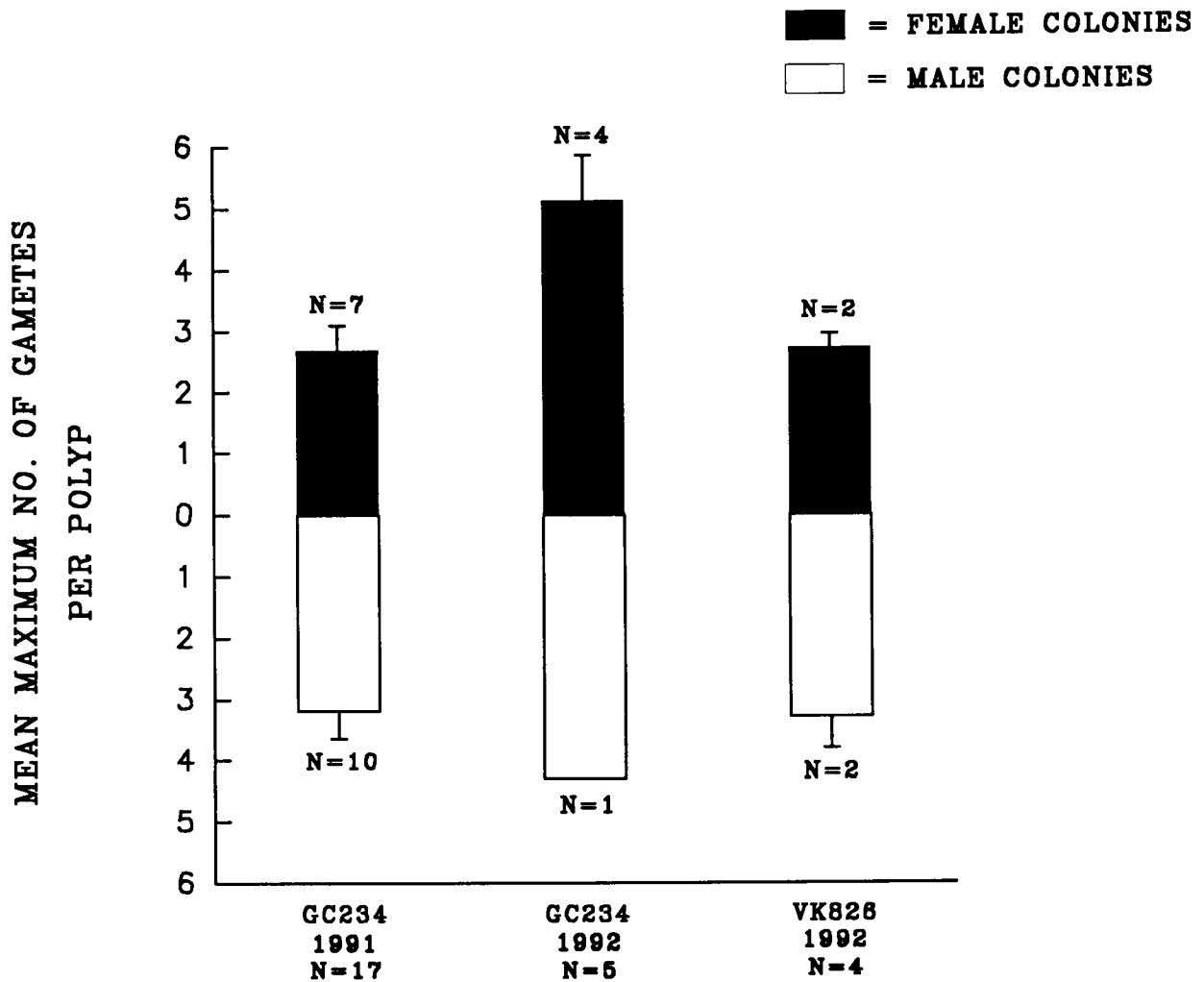
Figure 9.9   Relation between *Callogorgia* sp. gamete number and collection site by year. Colonies from GC 234 1992 have significantly more (p<0.05) gametes per polyp than GC 234 1991 and VK 826 1992. Error bars indicate standard error for each sample.

reproduction occur among gonochoric corals; internal fertilization followed by brooding and broadcast spawning followed by external fertilization. Dunn (1975) defined brooding in marine invertebrates as "the retention of offspring by a parent through the embryonic stages usually passed in the plankton." Corals exhibiting a brooding reproductive strategy produce small eggs (Rinkevich and Loya 1979), have an extended breeding season (Harrison and Wallace 1990) and facilitate localized recruitment (Stimson 1978). Broadcast-spawning corals contain large eggs, and have a distinct annual spawning period, either mass-spawning-spawning or minor, during which gametes are released from male and female colonies (Harrison and Wallace 1990). Mass broadcast-spawning occurs when gametes are released over one to several consecutive days (Babcock et al. 1986; Gittings et al. 1992), however, minor broadcast-spawns occur over an extended period of time lasting from one to several weeks (Hartnoll 1975; Gittings et al. 1992). Synchrony of spawning generates high gamete concentrations in the water column thus maximizing sperm-egg encounters and increasing the probability of successful fertilization (Oliver and Babcock 1992). Seasonal timing of broadcast-spawning events has been shown to coincide with lunar patterns. Mass spawning of hermatypic corals from the northwestern Gulf of Mexico (Gittings et al. 1992), Curaçao (Van Veghel 1993), and the Caribbean (Szmant 1991), occurring about a week following full moons in August and September, have been reported. In 1991, colonies were collected from Green Canyon on 24 September, one day after the September full moon and 29 days following the August full moon. In 1992, colonies from GC 234 were collected on 10 August, three days prior to the full moon which took place on 13 August. A minor spawning event occurring sometime after the full moon in August 1991 could have decreased the mean number of gametes present per polyp in colonies from GC 234 1991 relative to GC 234 1992. The possibility of participation in a region-wide

spawning event by these geographically isolated communities suggests a mechanism for gene flow.

9.3.3 Conclusions

Like many other octocorals, *Callogorgia* sp. is dioecious, with a sex ratio of 1:1. All colonies >20 cm were reproductive although mature gametes were observed only in colonies having a minimum height of 30 cm. Results of histological analysis from the same time of year for two consecutive years suggest that *Callogorgia* sp. exhibits an annual cycle of gonad development that are confirmed by the presence of mature sperm having fully developed head and tail regions. Presence of tails in sperm has been used to distinguish mature sperm and as an estimate of spawning period. Brazeau (personal communication) noted that spawning in the gorgonian *Plexaura* spp. occurred a couple of days after tails developed. Mature sperm present in *Callogorgia* sp. suggests that a broadcast-spawning event probably occurred within a few days after collecting in September 1991 and August 1992. Timing of sperm maturation in *Callogorgia* sp. coincides with the shallow water gorgonian *Leptogorgia hebes* (Beasley personal observation), as well as several hermatypic corals (Szmant 1991; Gittings et al. 1992; Van Veghel 1993), which spawn in late August or early September.

9.3.4 Management Implications

Reproductive fitness in benthic invertebrates results from successful recruitment. High fecundity and fertilization success lead to the availability of larvae for settlement. Fecundity is high in the populations of *Callogoria* sp. studied but broadcast-spawning puts an entire year class at risk to both natural (e.g. benthic storms) and anthropogenic (e.g. temporary burial of hard substrate surfaces as a result of oil/gas related drilling or construction activities) perturbations during a

relatively short period each year. On the other hand, the annual cycle ensures that, as long as the original population remains reproductively viable, the loss of one (and possibly more) year class to recruitment failure can be made up in successive years. Taller (older) colonies are clearly more fecund and should be given priority in any management considerations.

10.0 An Ecological Characterization of Hydrocarbon Seep Communities
Ian R. MacDonald

10.1 Introduction

Ecological theory proposes that every species occupies a niche uniquely defined by the organisms adaptation to a restrictive combination of geological space, physical and chemical tolerances, nutritional requirements, predators, feeding adaptations, prey, mobility, reproductive needs, etc. (Hutchinson 1953). By extension, an aggregate of niches forms an interdependent community of organisms; classes of communities, generally united by some more or less arbitrary theme form an ecosystem (the lake in Hutchinson's example). This study has the formal title: "The Chemosynthetic Ecosystem Study"; it is appropriate to consider the fauna of deep-sea hydrocarbon seeps in these terms.

In practice, species are described by their morphology rather than their ecological niche or function; and communities and ecosystems are often defined as convenient catchalls for organisms that seem to cluster together. We simply know too little about too many species to adequately explain why they are where we find them. For example, the fauna of the deep sea is characterized by a great abundance (numerical, not biomass) of highly diverse animals that burrow or crawl on the seafloor. Deep sea biologists are generally unable to explain why groups are found together, to predict what their geographic range will be, or how they will persist in the face of disturbance. In this context, the chemosynthetic communities found at cold seeps and hot vents offer the distinct opportunity for rigorous ecological definition. As Fisher (Chapter 5, this volume) has shown, these animals depend, directly or indirectly, upon chemoautotrophic production by bacteria and their metazoan hosts; the bacteria have well-defined chemical requirements that are met by a very narrow range of geological circumstances. We argue that chemosynthetic

communities at hydrocarbon seeps form a distinct subset of these communities; a subset which, to date, is known only from the northern Gulf of Mexico.

This section will attempt to identify deductively the factors that make the Gulf seep communities unique. The exercise progresses in steps from the regional to the local and from the general to the specific. At each level, we attempt to list key characteristics that distinguish a specific component of Gulf of Mexico seep ecosystem from its broader context.

10.1.1 The Gulf of Mexico Hydrocarbon System

The northern Gulf of Mexico is one of the most productive petroleum basins in the world. In contrast with other well-developed marine hydrocarbon systems, for example the North Slope of Alaska or the North Sea, the Gulf of Mexico has multiple hydrocarbon source rocks and appropriated reservoirs. Because of the timing of subsidence and Cenozoic salt tectonics, large amounts of liquid hydrocarbons have been preserved in the system instead of being cracked to gas. The circum-basin distribution of source rocks create wide-spread potential for natural seepage of hydrocarbon to shallow slope sediments.

10.1.2 Salt Structures and Faults

The continental slope in the Gulf of Mexico has been extensively modified in response to sediment loading and halokinesis resulting in the formation of extensional faults and tectonic uplift providing both a means of structural "focusing" of migrating hydrocarbons and the development of vertical conduits capable of delivering the reservoired hydrocarbons to the seafloor (Worrall and Snelson 1989; Kennicutt et al. 1988a). Absent the conduits for vertical migration, macroseepage of hydrocarbons could not persist. Therefore, deltaic hydrocarbon basins or basins

otherwise overlain by a less fractured sediment column are less likely to support extensive biological communities that are affected by seepage.

10.1.3 Seep Zones

Seeps zones are sub-sets of the hydrocarbon system and are generally less 1 km in extent. The entire extent of a seep zone is transformed by the hydrocarbons; however the most vigorous migration is localized in gas, brine, or mud vents, which are orifices 1 to 10 m wide. Thus, a seep is the entire zone affected by hydrocarbon migration, a vent is the most active portion of the seep. Chemical and thermal gradients are distinct. At least two styles of seep zone can be identified among the seeps studied; both are defined by the circumstances of migration. Salt-related seeps are regimes in which a salt piercement structure penetrates the shallow subbottom. The salt-related seeps studied have shown evidence for vigorous, localized, and intermittent migration, perhaps because authigenic carbonates and/or hydrate layers generate capping structures that deflect or retard migration such that the focus of venting evidently shifts in position across the area of the seep. Dissolution of the salt stock produces hypersaline fluids that generally contain high concentrations of biogenic methane. Migration of these briny fluids frequently entrains large volumes of fluid mud that can radically transform surficial sediment, producing such features as mud mounds, brine pools, and pockmarks. Fault-related seeps occur at kinks or intersections in faults, frequently the reliever or antithetic faults related to growth or transform faults. The zones studied have shown evidence for continual activity along the fault over recent geological time. When the fault remains active, the conduit for migration stays open, with the result that seepage is channelized along a distinct linear zone. Evidence for this includes massive (and old) colonies of seep fauna arrayed along faults and the lithification of the fault zones due to protracted precipitation of authigenic carbonates.

10.1.4 The Seep Hydrocarbon System

The fundamental property of the chemosynthetic habitat, i.e., a spatially contiguous source of reduced compounds and oxygenated water, is the same at hydrothermal vents and at hydrocarbon seeps; however, the secondary characteristics of the two environments are quite different. The following factors are particularly distinct: 1) the attachment substratum at hydrothermal vents is always litified, whether basalt or poly-metallic sulfide, whereas the substratum at seep habitats almost always has an unconsolidated sediment component; 2) the thermal gradients at hydrothermal vents are very strong, whereas at seeps they are generally slight or non-existent; and 3) the variability of fluid migration is on the order of months to years at vents, versus years to tens of years or more at seeps. Geochemical processes interact with the physical environment to create these differences.

Maintenance of the chemosynthetic habitat in the Gulf of Mexico relies on the delivery of biogenic and/or thermogenic hydrocarbons to the seafloor and the shallow subbottom in sufficient volumes and rates. The seep hydrocarbon system is a discrete region defined laterally by the extent of the migration conduit, vertically by sediment porosity and a complex of bacterially mediated geochemical transformations, and temporally by the persistence of migration. Qualitatively, the geochemical character of any portion of the seep zone is defined by the type and phase of migrating fluid, by the timing of migration, and by the history of migration at the particular locality.

The specific components of the chemosynthetic fauna are highly selective for geochemical properties. Sediments beneath isolated mats of H_2S-oxidizing bacteria (*Beggiatoa* sp.) generally contain thermogenic hydrocarbons that are altered by bacterial oxidation. Sediments near, but not immediately under the mats contain

lower concentrations of hydrocarbons. Bacterial oxidation of hydrocarbons depletes O_2, triggering bacterial sulfate reduction to produce the H_2S needed for mat development and creating an abrupt oxic-anoxic interface at, or very near, the seafloor. Moreover, CO_2 from the bacterial oxidation precipitates as authigenic carbonate rock, beginning a process that modifies the seafloor. Tube worm communities requiring H_2S occur at GC 185 where the seafloor has already been greatly modified since the Pleistocene by accumulations of oil, gas hydrate, and authigenic carbonate rock in sediments. Venting is thus suppressed over time, favoring slow development of complex communities that depend on abundant hydrocarbons in sediments. Sediment samples from an area with vesicomyid clams contain lower UCM (mean = 1,716 ppm) but C_1-C_5 concentrations are high (mean = 28,766 ppm). The clams appear to persist at relict thermogenic seeps where the rate of seepage has declined from past highs, or H_2S production is triggered by gas instead of oil. The sediment associated with the methanotrophic Seep Mytilid Ia is characterized by low infaunal diversity and by dominance of biogenic methane.

10.1.5 Seep Fauna

The life histories of the dominant seep species reflect the ecological characteristics of their habitat. Compared to their vent counterpart *Riftia pachyptils*, seep vestimentiferans (*Lamellibrachia* and *Escarpia*) are slow growing (probable life-span is 100+ years) and slender. The $\delta^{13}C$ values for seep tube worm tissues are -30 to -23‰ whereas vent tube worms are typically -12 to -8‰. The gas exchange organ, a very prominent plume in *Riftia*, is very reduced in both seep species, consistent with lower overall metabolic rates and growth. Although they require a hard attachment substratum as juveniles, adults are often rooted in soft sediment and circumstantial evidence suggests that they are able to acquire reduced compounds through their tube walls. The presence of large tube worm

aggregations probably tends to increase localized sedimentation (i.e. like dune vegetation).

Seep mytilids are hosts to methanotrophic symbionts and are able to satisfy their entire energy and carbon requirement from methane. No such symbionts have been described from vent mytilids. Seep mytilids are also slow growing; their probable life-span is 50+ years. Tissue $\delta^{13}C$ values are low and quite variable (-60 to -30‰), which reflects the variable mixture of biogenic (isotopically lighter) to thermogenic (isotopically heavier) methane available among the collection sites. Taxonomically, seep mytilids are quite speciose in the Gulf of Mexico with at least six probable species having been proposed (but not, as yet, described) by workers studying the group.

Less is known about the life history of the epifaunal seep clams (Vesicomyidae). Their reliance upon soft sediment clearly distinguishes them from the hydrothermal vent clams of the same family, which inhabit fissures in a basalt substrate. However, the family is quite cosmopolitan and has been found in sedimentary habitats in many other localities. The infaunal seep clams (Lucinacea) are little known in terms of life history. All of these bivalve species are presumed to be slow-growing and all are spatially less restricted in occurrence around seep zones. Hydrothermal vent communities contain high numbers of endermic species; in contrast, there is comparatively little endemism among seep heterotrophs. The infauna is depauperate compared to any sedimentary deep-sea habitat. However, the existence of any infaunal component is sufficient to distinguish the seep habitat from the hydrothermal vent habitat, where the absence of a sedimentary cover precludes survival of infauna.

10.1.6 Temporal Change

The paleontological record, which is primarily the shells of seep bivalves preserved in the sediment column and dating to about 4000 yr. before present, documents the stability of seep sites in terms of bivalve community composition and spatial location of the communities. In this regard, hydrocarbon seeps appear to be quite anomalous among soft-bottom bivalve communities. Generally, the paleo-record of bivalve communities on the continental slope and shelf shows marked shifts in the abundance and diversity of soft-bottom communities over time-scales of this order. The paleo-record also documents catastrophic burial events that repeatedly, but temporarily extirpated localized portions of a seep mytilid community.

The composition and distribution of living (and sessile) seep fauna shows equivalent stability during the course of the study. This is not unusual when compared to non-chemosynthetic analogs such as coral reef communities, but quite different from hydrothermal vent communities. Studies of vent communities show radical shifts in the composition, as well as marked declines in the abundance and apparent health of vent chemoautotrophs over one to five year time periods. Likewise, vent communities have been observed to recover completely from total extirpation (due to a volcanic eruption) in slightly over one year. The dynamic nature of the vent environment requires rapid colonization and growth. Seep fauna undoubtedly are more slow-growing and long-lived then their vent counterparts, but do not recover as rapidly from disturbance. The types of disturbance that are most common in seeps (blow-outs and mud or brine flows) are events that render portions of the habitat uninhabitable but lack the destructive force of a lava flow. In essence, seep communities can afford to recover slowly from disturbances because the seep environment is stable over comparatively long time and length scales. In

terms of human disturbance, this means that prospects for recovery from localized damage are good, but would require periods of years to tens of years to complete.

10.2   Recommendations for Future Study

The Chemosynthetic Ecosystem Study depended heavily upon the use of submarines for collection of samples and deployment of monitoring devices. The amount of submarine time available for the Study was very substantially augmented by grants to the principal investigators from agencies other than MMS. This augmentation was necessary to meet MMS's objectives. Even with this non-MMS funded submersible time, the sampling effort was necessarily restricted in time (both the duration of the program and the restriction to summer field work), in number of sites, and in water depths sampled. It is clear that the study of seep communities is an expensive and time-consuming undertaking. To be cost effective, future efforts should focus on aspects most pertinent to management objectives and should utilize approaches that minimize the need for submarine time and other resource-intensive field efforts. The following recommendations suggest several topics that have potential management relevance.

Archival and dissemination of imagery data collected during the Study - A substantial portion of the Study data takes the form of imagery. Image types include large format maps, video tapes, 35 mm color positives, and digital image data files. These data are an essential component of the geological, short-term change, and growth-rate investigations carried out under the Study. They should be available to MMS to investigate outside the program, and to the interested public; however, neither MMS nor the PIs fully anticipated the importance of these data sets at the outset of the Study. Consequently, there is no provision in the scope of work for dissemination of images in any format that approximates their

original resolution. A modest level of support would be adequate to provide for the archival of the data for future use.

An approach would be to reproduce and distribute a large selection of the images in a CD-ROM format. Using CD-ROM technology, it is possible to store up to 600 35 mm slides as high resolution digital files. Alternatively, a CD-ROM can store up to 30 min. of live video. The digital format are highly standardized and are readable by anyone with a desktop computer. Reproduction costs are modest.

Temporal change and growth rates of chemosynthetic fauna - Study results demonstrate that seep chemoautotrophs are slow-growing animals living in habitats that are generally stable; however, the period of observation has been short compared to the usual exploration and production cycle for offshore platforms. There is a need to better constrain processes that might tend to be confused with human impact on communities. Given the habitat stability and slow growth rates, near-term replication of the growth and change experiments is not indicated. Revisiting the mosaic sites after a period of three to five years to test whether local distribution of fauna has shifted is more likely to provide the needed information. Likewise, continued growth studies can be conducted with the marked mussels and tube worms currently deployed at the study sites.

Use of remote sensing methods for detection of seep communities - Although submarines offer investigators the capability of fine-scale sampling and manipulation, these studies target only a fraction of the total seeps on the Gulf of Mexico continental slope. The submarines used most often in the Gulf of Mexico, *Johnson Sea-Link* and NR-1, are limited in their operations to depths of 1000 m and 700 m, respectively; this artificially excludes a major portion of the potential habitat from consideration. Furthermore, submarine investigations proceed one site at a time, which will bias the results toward the characteristics of the small number of sites that can be investigated.

Satellite and airborne remote sensing have been used to determine distribution of seepage across parts of the continental slope and could provide a basin-wide estimate for the total number of active seep sites -- as well as an estimate for the total quantity of hydrocarbons entering the water column. The cost of image acquisition is significant for remote sensing, but cooperative research programs are underway that will compile complete coverage of the Gulf slope over at least two and possibly three time intervals. These programs are being carried out through the collaborative auspices of GOSAP (Gulf Offshore Satellite Applications Project), which is a consortium of industry and academic research institutions and under the sponsorship of the Environmental Task Force, which is a federal initiative convened by Vice President Gore. The Naval Research Laboratory has taken a lead role in providing interpretation of remote sensing data through the dual use of Navy remote sensing assets. Additional airborne remote sensing data are also being collected by the Marine Spill Response Corporation, with cooperation and participation of various state and federal agencies including the Texas General Land Office and the U.S. Coast Guard. Participation of MMS should, at a minimum, include consideration of these efforts to ascertain how data collected can be of use to MMS. Further participation could include supplementary programs to analyze or compile portions of the data set of most interest to MMS.

Laser line scan imaging of seep communities - The laser line scan system, which received it first trial at seep communities during the Study, offers a potential means for greatly decreasing the time and resources needed to map the dimensions and estimate the abundance of seep fauna. A program to test the system aboard the submarine NR-1 is scheduled for November 1994. Three of the study sites (GC 234, GC 233 and GC 184) may be mapped with the laser line scanner. MMS may wish to evaluate the results of this exercise and could commission a presentation of the data

in a format that would augment the results obtained in the present Study and provide a baseline for future efforts.

Study of gas hydrate and in situ monitoring devices for gas flux - One unexpected result of the Study was discovery of the potential for water circulation to influence seepage rates by regulating the formation and dissociation of gas hydrate. Catastrophic release of oil and gas due to loss of a hydrate seal under conditions of prolonged warming is a potential that should not be ignored. Studies of properties of gas hydrate under the conditions that prevail at seeps would help to constrain the possibility of such an occurrence. Methods available to conduct such studies include pressurized collection vessels that allow recovery of hydrate samples under near *in situ* conditions and the use of autonomous flux meters that can monitor gas release over protracted deployments. Both methods are designed around submarine deployment, but could be adapted to unmanned ROV applications.

Collaboration with on-going investigations - An noted above, the Study has been subsidized in part, by the willingness of the principal investigators to apply resources from other programs toward the goals that mutually benefit MMS and the principal investigators. Although the major collaboration ends with this program, prospects for future collaboration at a more modest scale continue. Two possible programs that would continue to develop Study results toward management concerns are outlined below.

Condition indices should be developed that will allow investigators to determine the relative health of chemoautotrophs from analysis of tissue samples. The method has application for ascertaining possible human impact to communities and for determining a baseline of condition among sites with different geochemical properties. On-going investigations of seep chemoautotrophs by Dr. Charles Fisher offers a source of material upon which development of these indices could be based.

Seep mussels are a major component of the chemosynthetic ecosystem, but the net productivity of these animals, and their subsequent contribution to the slope ecosystem, are difficult to determine because their productivity is a host-symbiont system. The productivity of the host is merged with productivity of the bacterial populations. Dr. Eric Powell has developed a host-parasite model for studying oyster populations. This simulation model could be readily adapted to the seep-mussel symbiont case and applied to predict productivity of mussel aggregations. Coupled with mapping data from seeps, such a model could be used to predict the contribution of seep mussel productivity -- and hence of methane flux -- to large portions of the Gulf continental slope ecosystem.

In conclusion, the Study has benefited from a broad agency and academic collaboration for submarine science. Numerous management-relevant programs are indicated by the Study results. The potential for on-going collaboration to improve our understanding of hydrocarbon seep ecology is stronger than ever.

11.0 Literature Cited

Allen, A.A., R.S. Schlueter, and P.G. Mikolaj. 1970. Natural oil seepage at Coal Oil Point, Santa Barbara, California. Science 170:974-977.

Almada-Villela, P.C. 1984. The effects of reduced salinity on the shell growth of small *Mytilus edulis*. J. Mar. Biol. Assoc. 64:171-182.

Anderson, A.L. and W.R. Bryant. 1990. Gassy sediment occurrence and properties; Northern Gulf of Mexico. Geo-Marine Letters 10:209-220.

Andrews, J. 1977. Shells and Shores of Texas. University of Texas Press, Austin, Texas, 365 pp.

Arp, A.J., J.J. Childress, and C.R. Fisher Jr. 1984. Metabolic and blood gas transport characteristics of the hydrothermal vent bivalve, *Calyptogena magnifica*. Physiol. Zool. 57:648-662.

Arthur, M.A., E.G. Kauffman, P.A. Scholle, and R. Richardson. 1982. Geochemical and paleobiological evidence for the submarine spring origin of carbonate mounds in the Pierre Shale (Cretaceous) of Colorado. Geol. Soc. of Am. Abstracts with Programs 14:435.

Ausich, W.I. and D.J. Bottjer. 1982. Tiering in suspension-feeding communities on soft substrata throughout the Phanerozoic. Science 216:173-174.

Babcock, R.C., G.D. Bull, P.L. Harrison, A.J. Heyward, J.K. Oliver, C.C. Wallace, and B.L. Willis. 1986. Synchronous spawnings of 105 scleractinian coral species on the Great Barrier Reef. Mar. Biol. 90:379-394

Bayne, B.L. (ed). 1976. Marine Mussels, Their Ecology and Physiology. Cambridge University Press, New York.

Bayne, B.L. and C.M. Worrall. 1980. Growth and production of mussels *Mytilus edulis* from two populations. Mar. Ecol. Prog. Ser. 3:317-328.

Bayne, B.L., J. Widdows, M.N. Moore, P. Salkild, C.M. Worrall, and P. Donkin. 1982. Some ecological consequences of the physiological and biochemical effects of petroleum compounds on marine molluscs. Phil. Trans. R. Soc. Lond. B 297:219-239.

Bayne, B.L. and R.C. Newell. 1983. Physiological energetics of marine molluscs. pp. 407-515. In A.S.M. Saleuddin and K.M. Wilbur. The Mollusca. Academic Press, New York.

Behrens, E.W. 1988. Geology of a continental slope oil seep, northern Gulf of Mexico. AAPG Bulletin 72:105-114.

Boland, G.S. 1986. Discovery of co-occurring bivalve *Acesta* sp. and chemosynthetic tube worms *Lamellibrachia*. Nature 323:759.

Boss, K.J. 1968. New species of *Vesicomyidae* from the Gulf of Darien, Caribbean Sea (Bivalvia; Mollusca). Bull. Mar. Sci. 18:731-748.

Bouchet, P. and A. Warén. 1980. Revision of the North-east Atlantic bathyal and abyssal Turridae (Mollusca, Gastropoda). J. Mol. Studies Supplement 8:1-119.

Brooks, J.M., M.C. Kennicutt II, R.R. Fay, T.J. McDonald, and R. Sassen. 1984. Thermogenic gas hydrates in the Gulf of Mexico. Science 226:965-967.

Brooks, J.M., H.B. Cox, W.R. Bryant, M.C. Kennicutt, R.G. Mann, and T.J. McDonald. 1986. Association of gas hydrates and oil seepage in the Gulf of Mexico. Org. Geochem. 10:221-234.

Brooks, J.M., M.C. Kennicutt, C.R. Fisher, S.A. Macko, K. Cole, J.J. Childress, R.R. Bidigare, and R.D. Vetter. 1987. Deep-sea hydrocarbon seep communities: evidence for energy and nutritional carbon sources. Science 20:1138-1142.

Brooks, J.M., M.C. Kennicutt II, I.R. Macdonald, D.L. Wilkinson, N.L. Guinasso, Jr., and R.R. Bidigare. 1989. Gulf of Mexico hydrocarbon seep communities: Part IV - Description of known chemosynthetic communities. Proc. 21st Offshore Technology Conference, OTC 5954, pp. 663-667.

Brooks, J.M., D.A. Wiesenburg, H. Roberts, R.S. Carney, I.R. MacDonald, C.R. Fisher, N.L. Guinasso, W.W. Sager, S.J. McDonald, R.A. Burke, P. Aharon, and T.J. Bright. 1990. Salt, seeps and symbiosis in the Gulf of Mexico. EOS 71:1772-1773.

Buffler, R.T., F.J. Schaub, R. Huerta, and A.K. Ibrahim. 1980. A model for the early evolution of the Gulf of Mexico basin. Proceedings 16th International Geologic Congress, Geology of Continental Margins Symposium, Paris, July, 1980, Ocean. Acta pp. 129-136.

Callender, W.R. and E.N. Powell. In press. Autochthonous death assemblages from chemosynthetic communities at petroleum seeps: biomass, energy flow and implications for the fossil record. Jo. Paleontology.

Callender, W.R., G.M. Staff, E.N. Powell, and I.R. MacDonald. 1990. Gulf of Mexico hydrocarbon seep communities; V. Biofacies and shell orientation of autochthonous shell beds below storm wave base. Palaios 5:2-14.

Carney, R.S., M.C. Kennicutt, I.R. MacDonald, and J.M. Brooks. Submitted. Chemosynthetic to heterotrophic linkages determined by stable carbon isotope ratios in upper continental slope hydrocarbon seep communities of the Gulf of Mexico. J. Geophys. Res.

Cason, J.E. 1950. A rapid one-step Mallory-Heidenhain stain for connective tissue. Stain Technology 25:225-226.

Cavanaugh, C.M., S.L. Gardiner, M.L. Jones, H.W. Jannasch, and J.B. Waterbury. 1981. Prokaryotic cells in the hydrothermal vent tube worm, *Rifita pachyptila*: possible chemoautotrophic symbionts. Science 213:340.

Childress, J.J., A.J. Arp, and C.R. Fisher, Jr. 1984. Metabolic and blood characteristics of the hydrothermal vent tube worm *Riftia pachyptila*. Mar. Biol. 83:109-124.

Childress, J.J. and T.J. Mickel. 1985. Metabolic rates of animals from the hydrothermal vents and other deep-sea habitats. Bull. Biol. Soc. Wash. 6:249-260.

Childress, J.J., C.R. Fisher, J.M. Brooks, M.C. Kennicutt II, R. Bidigare, and A. Anderson. 1986. A methanotrophic marine molluscan symbiosis: mussels fueled by gas. Science 233:1306-1308.

Childress, J.J. 1987. Uptake and transport of sulfide in marine invertebrates. pp. 231-238. In P. Dejours, L. Bolis, C. R. Taylor and E. R. Weibel. Comparative Physiology: Life in Water and on Land. Liviana Press, Padova.

Childress, J.J., C.R. Fisher, J.A. Favuzzi, R. Kochevar, N.K. Sanders, and A.M. Alayse. 1991. Sulfide-driven autotrophic balance in the bacterial symbiont-containing hydrothermal vent tubeworm, Riftia pachyptila Jones. Biol. Bull. 180:135-153.

Childress, J.J. and C.R. Fisher. 1992. The biology of hydrothermal vent animals: physiology, biochemistry and autotrophic symbiosis. Oceanogr. Mar. Biol. Annu. Rev. 30:337-441.

Christoffersen, M.L. 1989. Phylogenetic relationships between *Oplophoridae, Atyidae, Pasiphaeidae, Alvinocarididae* Fam. N., *Bresiliidae, Psalidopodidae* and *Disciadidae* (Crustacea *Caridea Atyoidea*). Bolm Zool. Univ. S. Paulo 10:273-281.

Clarke, A.H. 1989. New mollusks from undersea oil seep sites off Louisiana. Malacolgy Data Net 2:122-134.

Comfort, A. 1957. The duration of life in molluscs. Proceedings of the Malacological Society of London 32:219-241.

Cook, D. and P. D'Onfro. 1991. Jolliet Field thrust fault structure and stratigraphy Green Canyon Block 184, offshore Louisiana. Transactions-Gulf Coast Association of Geological Societies XLI:100-121.

Corliss, J.B., J. Dymond, L. Gordon, J.M. Edmond, R.P. von Herzen, R.D. Ballard, K. Green, D. Williams, A. Bainbridge, K. Crane, and T. H. van Andel. 1979. Submarine thermal springs on the Galapagos Rift. Science 203:1073-1083.

Cox, C. and W. Munk. 1954. Statistics of the sea surface derived from sun glitter. J. Mar. Res. 13:198-227.

Craddock, C., W.R. Hoeh, R.G. Gustafson, R.A. Lutz, J. Hashimoto, and R. C. Vrijenhoek. 1995. Evolutionary relationships among deep-sea mussels (*Bivalvia: Mytilidae*) from hydrothermal vents and cold-water methan/sulfide seeps. Mar. Biol. 121:In press.

Craeymeersch, J.A., P.M.J. Herman, and P.M. Meire. 1986. Secondary production of an intertidal mussel (*Mytilus edulis* L.) population in the Eastern Scheldt (S.W. Netherlands). Hydrobiologia 133:107-115.

Csandy, G.T. 1972. Turbulent diffusion in the environment. D Reidel, Boston.

Dall, W.H. 1889. A preliminary catalogue of the shell bearing mollusks and brachiopods of the southeastern coast of the United States. Bull. U.S. Natl. Museum. 37:1-221, Washington, D.C.

Damuth, J.E. 1975. Echo character of the western equatorial Atlantic floor and its relationship to the dispersal and distribution of terrigenous sediments. Marine Geology 18:17-45.

Damuth, J.E. and D.E. Hayes. 1977. Echo character of the east Brazilian continental margin and its relationship to sedimentary processes. Marine Geology 24:73-95.

Davies, D.J., G.M. Staff, W.R. Callender, and E.N. Powell. 1990. Description of a quantitative approach to taphonomy and taphofacies analysis: all dead things are not created equal. Special Publications (Paleontological Society) 5:328-350.

De Zwaan, A. and M. Mathieu. 1992. Cellular Biochemistry and Endocrinology. Developments in Aquaculture and Fisheries. Science 25:223-308.

Dobrin, M.B. and C.H. Savit. 1988. Introduction to Geophysical Prospecting, 4th ed. McGraw-Hill, New York, 867 pp.

Dunn, F.D. 1975. Reproduction of the externally brooding sea anemone *Epiactis prolifera* (Verrill, 1869). Biol. Bull. 148:199-218.

Estes, J.E., R.E. Crippen, and J.L. Star. 1985. Natural oil seep detection in the Santa Barbara Channel, California, with Shuttle Imaging Radar. Geol. 13:282-284.

Fallah, M.H. and R.M. Stark. 1976. Literature review: Movement of spilled oil at sea. Mar. Technol. Soc. 10(1):3-18.

Fisher, C.R., J.J. Childress, R.S. Oremland, and R.R. Bidigare. 1987. The importance of methane and thiosulphate in the metabolism of the symbionts of two deep-sea mussels. Mar. Biol. 96:59-71.

Fisher, C.R., J.J. Childress, A.J. Arp, J.M. Brooks, D. Distel, J.A. Favuzzi, H. Felbeck, L.W. Fritz, R. Hessler, K.S. Johnson, M.C. Kennicutt, R.A. Lutz, S.A. Macko,

A. Newton, M.A. Powell, G.N. Somero, and T. Soto. 1988. Microhabitat variation in the hydrothermal vent clam, *Calyptogena magnifica*, at Rose Garden vent on the Galapagos rift. Deep-Sea Res. 35:1811-1832.

Fisher, C.R. 1990. Chemoautotrophic and methanotrophic symbioses in marine invertebrates. Rev. Aquat. Sci. 2:399-436.

Fisher, C.R. 1993. Oxidation of methane by deep-sea mytilids in the Gulf of Mexico. pp. 606-618. In R.S. Oremland. Biogeochemistry of Global Change: Radiatively Active Trace Gases. Chapman and Hall Inc., New York.

Forster, G.R. 1981. A note on the growth of *Arctica islandica*. J. Mar. Biol. Assoc. 61:817.

Frenzel, P., B. Thebrath, and R. Conrad. 1990. Oxidation of methane in the oxic surface layer of a deep lake sediment (Lake Constance). FEMS Microbiol. Ecol. 73:149-158.

Gage, J.D. and P.A. Tyler. 1991. Deep-Sea Biology: A Natural History of Organisms at the Deep-Sea Floor. University Press, Cambridge.

Gallaway, B.J., L.R. Martin, and G.F. Hubbard. 1990. Characterization of the chemosynthetic fauna at Viosca Knoll Block 826. Unpublished report to Oryx Energy Inc. LGL Ecological Research Assoicates Inc., Dec. 1990. 35 pp., maps and photographs.

Gardiner, S.L. and M.L. Jones. 1993. Vestimentifera. In S.L. Gardiner (ed.), Microscopic Anatomy of Invertebrates, volume 12: Onychophora, Chilopoda, and Lesser Prostostomata. 12:371-460.

Garrett, W.D. 1986. Physiochemical effects of organic films at the sea surface and their role in the interpretation of remotely sensed imagery, pp. 1-18. In ONR Workshop Proceedings--Role of Surfactant Films on the Interfacial Properties of the Sea-Surface, Rep. C-11-86, Off. Nav. Res., Arlington, Virginia.

Gebruck, A.V., N.V. Pimenov, and A.S. Savvichev. 1992. Bacterial "farm" on the mouth parts of shrimps. Priroda (Moscow) 6:37-39. (In Russian).

Geyer, R.A. and C.P. Giammona. 1980. Naturally occurring hydrocarbons in the Gulf of Mexico and Caribbean Sea. pp. 37-106. Marine Environmental Pollution. I. Hydrocarbons. Elsevier Scientific, New York.

Gittings, S.R., G.S. Boland, K.J.P. Deslarzes, C.L. Combs, B.S. Holland, and T.J. Bright. 1992. Mass spawning and reproductive viability of reef corals at the East Flower Garden Bank, northwest Gulf of Mexico. Bulletin of Marine Science 51:420-428.

Grigg, R.W. 1974. Growth rings: Annual periodicity in two gorgonian corals. Ecol. 55:876-88.

Harrison, P.L. and C.C. Wallace. 1990. Reproduction, dispersal and recruitment of scleractinian corals. pp. 133-207. In Z. Dubinsky, Ecosystems of the World. Elsevier Scientific Publishing Co.

Hartnoll, R.G. 1975. The annual cycle of *Alcyonium digitatum*. Estuarine and Coastal Mar. Sci. 3:71-78.

Heller, J. 1990. Longevity in molluscs. Malacologia 31:259-295.

Hessler, R., P. Lonsdale, and J. Hawkins. 1988. Patterns on the ocean floor. New Scientist 24:47-51.

Hollinger, J.P. and R.A. Mennella. 1973. Oil Spills: measurements of their distributions and volumes by multifrequency microwave radiometry. Science 181:54-56.

Houbrick, J. 1979. Classification and systematic relationships of the Abysssochryssidae, a relict family of bathyal snails (Prosobranchia, Gastropoda). Smithsonian Contributions to Zoology 290:1-21.

Hovland, M. and A.G. Judd. 1988. Seabed pockmarks and seepages. Graham and Trotham, London.

Howe, B., E.G. Kauffman, and B.B. Sageman. 1986. Tepee Buttes, Late Campanian submarine springs and their biofacies: and shoreface biofacies of the Codell Sandstone Member ("Pugnellus Sandstone") at peak Greenhorn Cycle regression (Late Middle Turonian), in Huerfano Park, Colorado, pp. 150-198. In E.G. Kaufmann (ed.), Cretaceous biofacies of the central part of the Western Interior Seaway: a field guidebook. Fourth North American Paleontological Convention, Boulder, Colorado.

Huhnerfuss, H., W. Alpers, and F. Witte. 1989. Layers of different thicknesses in mineral-oil spills detected by grey level textures of real aperture radar images. International Journal of Remote Sensing 10:1093-1099.

Hummel, H., L.D. Wolf, W. Zurburg, L. Apon, R.H. Bogaards, and M.V. Ruitenburg. 1989. The glycogen content in stressed marine bivalves: the initial absence of a decrease. Comp. Biochem. Physiol. 94B:729-733.

Hutchinson, G.E. 1953. The concept of pattern in ecology. Proceedings of the Academy of Natural Sciences of Philadelphia 105:1-11.

Jackson, M.P.A. and S.J. Seni. 1983. Geometry and evolution of salt structures in a marginal rift basin in the Gulf of Mexico. Geology 11:131-135.

Jackson, M.P.A. and W.E. Galloway. 1984. Structural and depositional styles of Gulf Coast Tertiary continental margins: application to hydrocarbon exploration. AAPG, Continuing Education Course Note Series, no. 25, 226 pp.

Jackson, M.P.A. and C.J. Talbot. 1986. External shapes, strain rates, and dynamics of salt structures. GSA Bull. 97:305-323.

James, A.T. and B.J. Burns. 1984. Microbial alteration of subsurface gas accumulations. AAPG Bulletin 68:957-960.

Johnson, H.P. and M. Helferty. 1990. The geological interpretation of side-scan sonar. Rev. of Geophys. 28:357-380.

Johnson, K.S., C.M. Sakamoto-Arnold, J.J. Childress, and C.L. Beehler. 1988. The biogeochemistry of hydrothermal vent communities in the Galapagos Rift. EOS 69:1271.

Jones, M.L. 1985. On the Vestimentifera, new phylum: Six new species, and other taxa, from hydrothermal vents and elsewhere. Bull. Biol. Soc. Wash. 6:117.

Kaas, P. 1993. *Ischnochiton mexicanus*, a rare new chiton from the Gulf of Mexico (*Polyplacaphora Ischnochitonidae*). Basteria 57:4-6.

Kennicutt II, M.C., J.M. Brooks, R.R. Bidigare, R.R. Fay, T.L. Wade, and T.J. McDonald. 1985. Vent-type taxa in a hydrocarbon seep region on the Louisiana slope. Nature 317:351-353.

Kennicutt II, M.C., J.M. Brooks, and G.J. Denoux. 1988a. Leakage of deep, reservoired petroleum to the near surface on the Gulf of Mexico continental slope. Mar. Chem. 24:39-59.

Kennicutt II, M.C., J.M. Brooks, R.R. Bidigare, and G.J. Denoux. 1988b. Gulf of Mexico hydrocarbon seep communities-I. Regional distribution of hydrocarbon seepage and associated fauna. Deep-Sea Res. 35:1639-1651.

Kennicutt II, M.C. and J.M. Brooks. 1990. Recognition of areas affected by petroleum seepage: northern Gulf of Mexico continental slope. Geo-Mar. Lett. 10:221-224.

Kochevar, R., J.J. Childress, C.R. Fisher, and E. Minnich. 1992. The methane mussel: roles of symbiont and host in the metabolic utilization of methane. Mar. Biol. 112:389-401.

Kohl, B. and H.E. Vokes. 1994. On the living habitats of *Acesta bullisi* (Vokes) in chemosynthetic bottom communities, Gulf of Mexico. The Nautilus 108:9-14.

Kuivila, K.M., J.W. Murray, A.H. Devol, M.E. Lidstrom, and C.E. Reimers. 1988. Methane cycling in the sediments of Lake Washington. Limnol. Oceanogr. 33:571-578.

Kvenvolden, K.A. 1988. Methane hydrate -- a major reservoir of carbon in the shallow geosphere? Chem. Geol. 71:41-51.

Kvenvolden, K.A., G.D. Ginsburg, and V.A. Soloviev. 1993. Worldewide distribution of subaquatic gas hydrates. Geo-Mar. Lett. 13:32-40.

La Violette, P.E. and R.A. Arnone. 1988. A tidal-generated internal waveform in the western approaches to the Strait of Gibraltar. J. Geophys. Res. 93:15,653-15,667.

Laswell, J.S., W.W. Sager, W.W. Schroeder, R. Rezak, K.S. Davis, and E.G. Garrison. 1990. Mississippi-Alabama marine ecosystems study: Atlas of high-resolution geophysical data. OCS Study MMS 90-0045, U.S. Department of the Interior, Minerals Management Service, New Orleans, Louisiana, 42 pp.

Laswell, J.S., W.W. Schroeder, and W.W. Sager. 1994. Seafloor backscatter on the Mississippi-Alabama outer continental shelf. Trans. Gulf Coast Assoc. Geol. Soc.

Lowe, D.M. and R.K. Pipe. 1986. Hydrocarbon exposure in mussels: a quantitative study of the responses in the reproductive and nutrient storage cell systems. Aquat. Toxicol. 8:265-272.

Lutz, R.A., L.W. Fritz, and D.C. Rhoads. 1985. Molluscan growth at deep-sea hydrothermal vents. Biol. Soc. Wash. Bull. 199-210.

Lutz, R.A. and M.J. Kennish. 1993. Ecology of deep-sea hydrothermal vent communities: A review. Rev. Geophys. 31:211-242.

MacDonald, I.R., G.S. Boland, J.S. Baker, J.M. Brooks, M.C. Kennicutt II, and R.R. Bidigare. 1989. Gulf of Mexico hydrocarbon seep communities; II. Spatial distribution of seep organisms and hydrocarbons at Bush Hill. Mar. Biol. 101:235-247.

MacDonald, I.R., N.L. Guinasso Jr., J.F. Reilly, J.M. Brooks, W.R. Callender, and S.G. Gabrielle. 1990a. Gulf of Mexico hydrocarbon seep communities; VI. Patterns in community structure and habitat. Geo-Mar. Lett. 10:244-252.

MacDonald, I.R., J.F. Reilly, N.L. Guinasso Jr., J.M. Brooks, R.S. Carney, W.A. Bryant, and T.J. Bright. 1990b. Chemosynthetic mussels at a brine-filled pockmark in the northern Gulf of Mexico. Science 248:1096-1099.

MacDonald, I.R. and W.W. Schroeder. 1992. Chemosynthetic communities studies. Technical Report Submitted to Minerals Management Service, Gulf of Mexico OCS Region, New Orleans, Louisiana.

MacDonald, I.R. 1992. Sea-floor brine pools affect behavior, martality, and preservation of fishes in the Gulf of Mexico: Lagerstätten in the making? Palaios 7:383-387.

MacDonald, I.R., N.L. Guinasso Jr., S.G. Ackleson, J.F. Amos, R. Duckworth, R. Sassen, and J.M. Brooks. 1993. Natural oil slicks in the Gulf of Mexico visible from space. J. Geophys. Res. 98:16,351-16,364.

MacDonald, I.R., N.L. Guinasso, R. Sassen, J.M. Brooks, and L. Lee. 1994. Gas hydrate that breaches the sea floor on the continental slope of the Gulf of Mexico. Geol. 22:699-702.

McClean, J.H. and J.F. Quinn. 1989. *Cataegis*, a new genus of three new species from the continental slope (Trochidae: Cataeginae new subfamily). Nautilis 101:111-116.

McDonald, S.J. 1990. Benzo[a]pyrene metabolism in a deep sea mussel associated with natural petroleum seeps in the Gulf of Mexico. Texas A&M University. Dissertation.

Miller III, W. 1982. The paleoecological history of Late Pleistocene estuarine and marine fossil deposits in Dare County, North Carolina. Southeastern Geol. 23:1-13.

Minerals Management Service (MMS). 1988. Implementation of measures to detect and protect deep water chemosynthetic communities. MMS, Gulf of Mexico OCS Region, New Orleans, Louisiana. Notice to lessees and operators of federal oil and gas leases in the outer continental shelf Gulf of Mexico. 88-11:1-3.

Mitchell, N.D., M.R. Dardeau, and W.W. Schroeder. 1993. Colony morphology, age structure, and relative growth of two gorgonian corals, Leptogorgia hebes (Verrill) and Leptogorgia virgulata (Lamarck), from the northern Gulf of Mexico. Coral Reefs 12:65-70.

Neurauter, T.W. and W.R. Bryant. 1990. Seismic expression of sedimentary volcanism on the continental slope, northern Gulf of Mexico. Geo-Mar. Lett. 10:225-231.

Odé, H. 1975-1988. Distribution records of the marine Mollusca in the northwest Gulf of Mexico. Texas Conchologist 11:52-63; 12:40-56, 79-84, 108-124; 13:52-68, 74-81, 84-88, 106-107, 114-122; 14:10-11, 14-24, 41-52, 64-75, 93-104; 16:71-80; 19:54-63; 20:28-32; 24:59-82, 24:94-107.

Oliver, J. and R. Babcock. 1992. Aspects of the fertilization ecology of broadcast spawning corals: Sperm dilution effects and *in situ* measurements of fertilization. Biol. Bull. 183:409-417.

Peltzer, R.D., O.M. Griffin, W.R. Barger, and J.A.C. Kaiser. 1992. High-resolution measurement of surface-active film redistribution in ship wakes. Journal of Geophysical Research 97(C4):5231-5252.

Pequegnat, W. 1983. The ecological communities of the continental slope and adjacent regimens of the northern Gulf of Mexico. Prepared for Minerals Management Services under contract number AA851-CT1-12, 398 pp.

Petit, R.E. 1983. A new species of Cancellaria (Mollusca:Cancellariidae) from the northern Gulf of Mexico. Proc. Biol. Soc. Wash. 96:250-252.

Petta, T.J. and L.C. Gerhard. 1977. Marine grass banks - a possible explanation for carbonate lenses, Tepee Zone, Pierre Shale (Cretaceous) Colorado. J. Sed. Petrol. 47:1018-1026.

Powell, E.N. and H.C. Cummins. 1985. Are molluscan maximum life spans dominated by long-term cycles in benthic communities? Oecologia (Berlin) 67:177-182.

Powell, E.N. and R.J. Stanton Jr. 1985. Estimating biomass and energy flow of molluscs in palaeo-communities. Palaeontology (London) 28:1-34.

Powell, E.N. and R.J. Stanton, Jr. Submitted a. Size-frequency distributions and energy flow in parautochthonous death assemblages from a low salinity bay: the long-term record.

Powell, E.N. and R.J. Stanton Jr. Submitted b. Biomass and energy flow in parautochthonous death assemblages from a variable salinity bay: the long-term record.

Powell, M.A. and G.N. Somero. 1986. Adaptations to sulfide by hydrothermal vent animals: sites and mechanisms of detoxification and metabolism. Biol. Bull. 171:274-290.

Reiss, M.J. 1989. The allometry of growth and reproduction. Cambridge University Press, Cambridge.

Rhoads, D.C., R.A. Lutz, E.C. Revelas, and R.M. Cerrato. 1981. Growth of bivalves at deep-sea hydrothermal vents along the Galapagos Rift. Science 214:911-913.

Rinkevich, B. and Y. Loya. 1979. The reproduction of the Red Sea coral *Stylophora pistillata*. I. Gonads and planulae. Mar. Ecol. Progr. Ser. 1:133-144.

Ripmeester, J.A. and C.I. Ratcliffe (eds). 1991. Solid state NMR studies of inclusion compounds. pp. 37-85. In J.L. Atwood, J.E.D. Davis, and D.D. MacNicol. Inclusion Compounds, Inorganic and Physical Aspects of Inclusion, Oxford University Press.

Roberts, H.H., R. Sassen, R. Carney, and P. Aharon. 1989. Carbonate buildups on the continental slope off central Louisiana. Proc. 21st Offshore Technol. Conference, OTC 5953, pp. 655-662.

Roberts, H.H. and T.W. Neurauter. 1990. Direct observations of a large active mud vent on the Louisiana continental slope. AAPG Bulletin 74:1508.

Roberts, H.H., P. Aharon, R. Carney, J. Larkin, and R. Sassen. 1990. Sea floor responses to hydrocarbon seeps, Louisiana continental slope. Geo-Mar. Lett. 10(4):232-243.

Rosman, I., G.S. Boland, and J.S. Baker. 1987. Epifaunal aggregations of Vesicomyidae on the continental slope off Louisiana. Deep-Sea Res. 34:1811-1820.

Sassen, R, C. McCabe, J.R. Kyle, and E.W. Chinn. 1988. Deposition of magnetic pyrrhotite during alteration of crude oil and reduction of sulfate. Org. Geochem. 14:381-392.

Sassen, R., J.M. Brooks, M.C. Kennicutt II, I.R. MacDonald and N.L. Guinasso Jr. 1993a. How oil seeps, discoveries relate to deepwater Gulf of Mexico. Oil and Gas Journal, 19 April, pp. 64-69.

Sassen, R, H.H. Roberts, P. Aharon, J. Larkin, E.W. Chinn, and R. Carney. 1993b. Chemosynthetic bacterial mats at cold hydrocarbon seeps, Gulf of Mexico continental slope. Org. Geochem. 20:77-84.

Scott, J.C. 1986. Surface films in oceanography. pp. 19-40. In ONR Workshop Proceedings--Role of Surfactant Films on the Interfacial Properties of the Sea-Surface, Rep. C-11-86, Off. of Nav. Res., Arlington, Virginia.

Scott, K.M. and C.R. Fisher. Submitted. Physiological ecology of sulfide metabolism in hydrothermal vent and cold seep vesicomyid clams and vestimentiferan tube worms. Am. Zool.

Scott, R. 1978. Approaches to trophic analysis of paleocommunities. Lethaia 11:1-14.

Seed, R. and C.A. Richardson. 1990. Mytilus growth and its environmental responsiveness. Manchester University Press, Manchester, New York. Studies in Neuroscience 10:1-37.

Seed, R. and T. H. Suchanek. 1992. Population and community ecology of *Mytilus*. Developments in Aquaculture and Fisheries Science 25:87-170.

Segonzac, M., M. de Saint Laurent, et B. Casanova. 1993. L'enigme du comportement trophique des crevettes Alvinocarididae des sites hydrothermaux de la dorsale medio-atlantique. Chaiers des Biologie. Marine 34:535-571 (In French).

Seni, S.J. and M.P.A. Jackson. 1992. Segmentation of salt allocthons. Geol. 20:169-172.

Simmons, G.R. 1991. Regional distribution of salt in the northwestern Gulf of Mexico: styles of emplacement and implications for early tectonic history. Ph.D. dissertation, Texas A&M University, College Station, Texas, 185 pp.

Simpkins, M.A. 1994. Hydrocarbon seep vestimentiferans: growth and condition in a variable environment. Pennsylvania State University. Masters.

Singh, C., T.A. Minshull, and G.D. Spence. 1993. Velocity structure of a gas hydrate reflector. Science 260:204-207.

Sloan, E.D. 1990. Clathlate hydrates of natural gases. Marcel Drekker, New York.

Soules, S.D. 1970. Sun glitter viewed from space. Deep-Sea Res. 17:191-195.

Staff, G., E.N. Powell, R.J. Stanton, Jr., and H. Cummins. 1985. Biomass: is it a useful tool in paleocommunity reconstruction? Lethaia 18:209-232.

Stanton Jr., R.J. and P.C. Nelson. 1980. Reconstruction of the trophic web in paleontology: community structure in the Stone City Formation (Middle Eocene, Texas). J. Paleontology 54:118-135.

Stevenson, R.E., P.D. Scully-Power, and R.M. Nelson. 1988. Astronauts' Guide to Oceanographic Phenomena, NASA Johnson Space Center, Houston, Texas.

Stimson, J.S. 1978. Mode and timing of reproduction in some common hermatypic corals of Hawaii and Enewetak. Mar. Biol. 48:173-184.

Stromgren, T. and C. Cary. 1984. Growth in length of *Mytilus edulis* L. fed on different algal diets. J. Exp. Mar. Biol. Ecol. 76:23-34.

Stromgren, T., M.V. Nielsen, and K. Ueland. 1986. Short-term effect of microencapsulated hydrocarbons on shell growth of *Mytilus edulis*. Mar. Biol. 91:33-39.

Stromgren, T. and M. V. Nielsen. 1991. Spawning frequency, growth, and mortality of *Mytilus edulis* larvae, exposed to copper and diesel oil. Aquat. Toxicol. 21:171-180.

Sturges, W. 1992. The spectrum of loop current variability from gappy data. J. Phys. Oceangr. 22:1245-1256.

Sukhotin, A.A. and E.E. Kulakowski. 1992. Growth and population dynamics in mussels (*Mytilus edulis* L.) cultured in the White Sea. Aquaculture 101:59-73.

Szmant, A.M. 1991. Sexual reproduction by the Caribbean reef corals Montastrea annularis and M. cavernosa. Mar. Ecol. Progr. Ser. 74:13-25.

Theisen, B.F. 1973. The growth of *Mytilus edulis L.* (Bivalvia) from Disko and Thule District, Greenland. Ophelia 12:59-77.

Thompson, R.J. 1984. Production, reproductive effort, reproductive value and reproductive cost in a population of the blue mussel *Mytilus edulis* in a subartic environment. Mar. Ecol. Prog. Ser. 16:249-257.

Tunnicliffe, V. 1991. The biology of hydrothermal vents: Ecology and evolution. Oceanog. Mar. Biol. Ann. Rev. 29.

Tunnicliffe,V. 1992. The nature and origin of the modern hydrothermal vent fauna. Palaios 7:338-350.

Urick, R.J. 1975. Principles of underwater sound. McGraw-Hill, New York, 384 pp.

Van Dover, C.L., B. Fry, J.F. Grassle, S. Humphris, and P.A. Rona. 1988. Feeding biology of the shrimp Rimicaris exoculata at hydrothermal vents on the Middle-Atlantic Ridge. J. Mar. Biol. 98:209-216.

Van Veghel, M.L.J. 1993. Multiple species spawning on Curaao reefs. Bull. Mar. Sci. 52:1017-1021.

Volkes, H.E. 1963. Studies on tertiary and recent giant Limidae. Tulane Studies in Geology 1:75-92.

Wade, T.L., M.C. Kennicutt II, and J.M. Brooks. 1989. Gulf of Mexico hydrocarbon communities, III. Aromatic hydrocarbon concentrations in organisms, sediments, and water. Mar. Environ. Res. 27:19-30.

Wainwright, S.A., W.D. Biggs, J.D. Currey, and J.M. Gosline. 1982. Mechanical design in organisms. Princeton Univ. Press, Princeton. 436 pp.

Walker, N.H., O.K. Huh, L.J. Rouse, Jr. 1993. Warm-core eddy discovered in the Gulf of Mexico. EOS 74:337-338.

Warén, A. and W.F. Ponder. 1991. New species, anatomy, and systematics position of the hydrothermal vent and hydrocarbon seep gastropod family *Provaidae* fam.n (Caenogastropoda). Zoologica Scripta 20:27-56.

Warén, A. and P. Bouchet. 1993. New records, species, genera, and a new family of gastropods from hydrothermal vents and hydrocarbon seeps. Zool. Scripta 22:1-90.

Williams, A.B. and F. Chace, Jr. 1982. A new caridean shrimp of the family Bresiliidae from thermal vents of the Galapagos Rift. J. Crust. Biol. 2:136-147.

Williams, A.B. 1988. New Decapod crustaceans from waters influenced by hydrothermal discharge, brine, and hydrocarbon seepage. Fish. Bull. 86:263-287.

Winters, J.C. and J.A. Williams. 1969. Microbiological alteration of petroleum in the reservoir. American Chemical Society, Division of Petroleum Geochemistry. New York City Meeting, Preprints, pp. E22-E31.

Wootton, R.J. 1991. Ecology of Teleost Fishes. Fish and Fisheries Series 1 1:1-404. Chapman & Hall, London.

Worrall, D.M. and S. Snelson. 1989. Evolution of the northern Gulf of Mexico, with emphasis on Cenozoic growth faulting and the role of salt, pp. 97-138. In A.W.

Bally and A.R. Palmer. The Geology of North America - an overview. The Geology of North America Ser., Vol. A, GSA, Boulder, Colorado.

Wu, S., A.W. Bally, and C. Cramez. 1990a. Allocthonous salt, structure, and stratigraphy of the north-eastern Gulf of Mexico. Part I: stratigraphy. Mar. Petrol. Geol. 7:318-333.

Wu, S., A.W. Bally, and C. Cramez. 1990b. Allocthonous salt, structure, and stratigraphy of the north-eastern Gulf of Mexico. Part I: structure. Mar. Petrol. Geol. 7:334-370.

Zande, J.M. 1994. Feeding and life history of the gastropod Bathynerites naticoidea from the Gulf of Mexico hydrocarbon Seeps. A masters thesis, Dept. Oceanography and Coastal Sciences, Louisiana State University. 102 pp.

The Department of the Interior Mission

As the Nation's principal conservation agency, the Department of the Interior has responsibility for most of our nationally owned public lands and natural resources. This includes fostering sound use of our land and water resources; protecting our fish, wildlife, and biological diversity; preserving the environmental and cultural values of our national parks and historical places; and providing for the enjoyment of life through outdoor recreation. The Department assesses our energy and mineral resources and works to ensure that their development is in the best interests of all our people by encouraging stewardship and citizen participation in their care. The Department also has a major responsibility for American Indian reservation communities and for people who live in island territories under U.S. administration.

The Minerals Management Service Mission

As a bureau of the Department of the Interior, the Minerals Management Service's (MMS) primary responsibilities are to manage the mineral resources located on the Nation's Outer Continental Shelf (OCS), collect revenue from the Federal OCS and onshore Federal and Indian lands, and distribute those revenues.

Moreover, in working to meet its responsibilities, the **Offshore Minerals Management Program** administers the OCS competitive leasing program and oversees the safe and environmentally sound exploration and production of our Nation's offshore natural gas, oil and other mineral resources. The MMS **Royalty Management Program** meets its responsibilities by ensuring the efficient, timely and accurate collection and disbursement of revenue from mineral leasing and production due to Indian tribes and allottees, States and the U.S. Treasury.

The MMS strives to fulfill its responsibilities through the general guiding principles of: (1) being responsive to the public's concerns and interests by maintaining a dialogue with all potentially affected parties and (2) carrying out its programs with an emphasis on working to enhance the quality of life for all Americans by lending MMS assistance and expertise to economic development and environmental protection.